U.PORTO
INSTITUTO DE CIÊNCIAS BIOMÉDICAS ABEL SALAZAR
UNIVERSIDADE DO PORTO

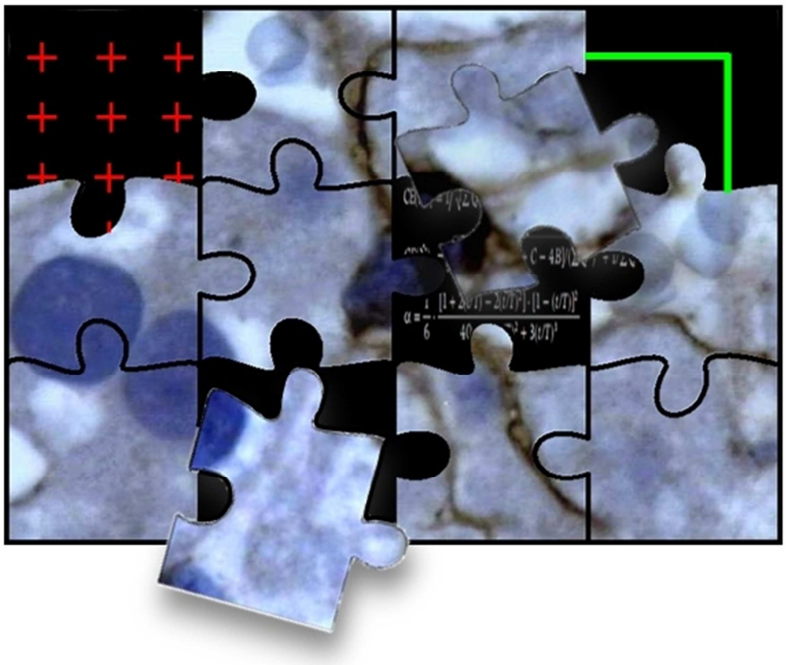

Age and gender influences on the rat liver model: quantitative morphological studies of hepatic stellate cells, hepatocytes and Kupffer cells and of related functional parameters

Ricardo Jorge Pereira Córdova Marcos

Tese de doutoramento em Ciências Veterinárias

2013

Ricardo Jorge Pereira Córdova Marcos

Age and gender influences on the rat liver model: quantitative morphological studies of hepatic stellate cells, hepatocytes and Kupffer cells and of related functional parameters

Tese de candidatura ao grau de Doutor em Ciências Veterinárias, submetida ao Instituto de Ciências Biomédicas Abel Salazar da Universidade do Porto.

Orientador – Doutor Eduardo Jorge Sousa da Rocha

Categoria – Professor catedrático

Afiliação – Instituto de Ciências Biomédicas Abel Salazar da Universidade do Porto.

Co-orientador – Doutor Rogério Alves Ferreira Monteiro

Categoria – Professor catedrático

Afiliação – Instituto de Ciências Biomédicas Abel Salazar da Universidade do Porto.

Preamble

Every line starts somewhere and an investigation line is no exception. In this case, the starting point was located twenty years ago at the Laboratory of Histology and Embryology of the Institute of Biomedical Sciences Abel Salazar. By that time Professor Rogério Monteiro and Professor Eduardo Rocha headed a research in liver quantitative morphology, first devoted to fishes. In the past ten years a bifurcation has emerged, with a branch devoted to mammals (rat model). It continues to evolve in, not giant, but consistent steps that produced results that have been published in scientific journals (ever since 2003) and presented in specialised meetings dedicated to the study of liver sinusoids (as organised by the International Society of the Hepatic Sinusoidal Research). This Thesis includes material that was already published in the following publications:

- **Marcos R, Monteiro RAF, Rocha E** (2004) Estimation of the number of stellate cells in a liver with the smooth fractionator. *Journal of Microscopy* 215, 174-182.
- **Marcos R, Monteiro RAF, Rocha E** (2006) Design-based stereological estimation of hepatocyte number, by combining the smooth optical fractionator and immunocytochemistry with anticarcinoembryonic antigen polyclonal antibodies. *Liver International* 26, 116-124.
- **Marcos R, Rocha E, Monteiro RAF** (2007) Determination of hepatocellularity. *Toxicology in Vitro* 21, 1692-1693.
- **Santos M*, Marcos R*, Santos N, Malhão F, Monteiro RAF, Rocha E** (2009) An unbiased stereological study on subpopulations of rat liver macrophages and on their numerical relation with the hepatocytes and stellate cells. *Journal of Anatomy* 214, 744-751 (*joint first authors).
- **Marcos R**, **Malhão F, Monteiro RAF, Rocha E** (2009) Gender and aging in the liver: preliminary data using design-based stereological methods. *Microscopy & Microanalysis* 15 (S3), 45-46.
- **Marcos R, Monteiro RAF, Rocha E** (2012) The use of design-based stereology to evaluate volumes and numbers in the liver: a review with practical guidelines. *Journal of Anatomy* 220, 303-317.

In addition to those listed above, other unpublished results contained in the Thesis will be organised as new manuscripts and submitted for publication in international journals devoted to ageing. The first manuscript of the series is under preparation, as follows:

- **Marcos R, Malhão F, Lopes C, Gomes C, Monteiro RAF, Rocha E** (2013) Male or female? Liver gender dimorphism revealed by design-based stereology (*in preparation*).

Acknowledgments

This is one of the most important sections in every Thesis (and eventually one of the most read). Herein, the help and work of those that made this Thesis possible is recognised and, for the sake of clarity, I will opt to express my sincere gratitude mainly in Portuguese.

Gostaria de expressar a minha gratidão e os sinceros agradecimentos a todos aqueles que direta ou indiretamente contribuíram para a realização deste trabalho, agradecendo especialmente:

Ao meu orientador, Professor Eduardo Rocha, e ao meu co-orientador, Professor Rogério Monteiro, por terem aceitado os respectivos cargos. Devo confessar que, ao longo de uma dezena de anos, já tive a oportunidade de acompanhar a evolução de alguns dos meus antigos alunos. Espero que essa evolução também tenha ocorrido comigo, e por isso acho que consigo imaginar o vosso contentamento. Já passaram mais de 15 anos desde que me sentei no antigo A0 nas aulas do Professor Rogério e sei hoje que deixei marcas (pelo menos as relativas ao slide dos anéis da traqueia…). Igualmente, na sala de aulas práticas (que depois veio a ser o armazém do antigo ICBAS) tive a oportunidade de abraçar pela primeira vez a Histologia, pela mão do Professor Eduardo.

Nesta linha não podia deixar de referir o Professor Rui Henrique, com quem partilhei os primeiros passos na estereologia, em longas tertúlias de fim-de-semana.

À Fernanda, pela ajuda constante nas colheitas, no processamento, nos cortes, nas imunohistoquímicas. Tenho a perfeita noção que só não fizeste mais porque não te foi possível. Igualmente o meu agradecimento especial à Célia: nestes últimos anos, a tua ajuda e mestria técnica (em especial a varinha de condão nas imunohistoquímicas) foram fundamentais. Igualmente gostava de agradecer à Vera, à Ana e aos técnicos que passaram pelo Laboratório de Histologia durante estes últimos 5 anos.

À Professora Margarida Lima e à Sónia, do Serviço de Hematologia Clínica do Hospital de Santo António pela ajuda na parte da citometria de fluxo. Conhecendo o empenho e dedicação de todos os que trabalham naquele Serviço, posso dizer que me sinto privilegiado.

À Professora Luísa Valente, ao Doutor Rodrigo Ozório e ao Doutor Carlos Gravato do Centro de Investigação Interdisciplinar Marinha e Ambiental (CIIMAR) pelo apoio incondicional e pela ajuda incansável na realização das análises de stress oxidativo.

Ao Professor José Lopes da Faculdade de Medicina da Universidade do Porto (FMUP) pela honra de me dispensar o seu microscópio (dos poucos que ainda têm polarizador!) para a observação das lâminas do *sirius red.*

Ao Professor Fernando Vanaclocha (Universidad San Pablo e Fundacion Hospital de Madrid) pelos comentários relativos a estes trabalhos, pelo intercâmbio de ideias e a disponibilidade na realização dos estudos de biologia molecular (ainda traídos pelo tempo e pela saúde).

À Professora Margarida Araújo e à Bárbara do biotério do ICBAS, assim como à Dra. Luísa Guardão do biotério da FMUP, pelos zelosos cuidados com os meus "hóspedes de longa duração".

À Professora Corália Vicente do ICBAS e à Dra. Carla Gomes da Scottish Agricultural College (Inverness), não só pela ajuda na análise estatística, mas principalmente pela amizade e pela disponibilidade constante.

Para terminar, não podia deixar de deixar de agradecer à Professora Fátima Gärtner, não só pela ajuda na imunohistoquímica mas principalmente pelo apoio muito para além da vertente institucional enquanto Diretora do Programa Doutoral em Ciências Veterinárias. Deixo aqui o meu enorme reconhecimento pelo trabalho realizado e o apreço pelos seus sábios conselhos.

"Last but definitely not least", um gigante obrigado à família. Todas as palavras serão pequenas para a Martinha, mas acima de tudo é um privilégio partilhar os bons momentos contigo e saber que existe um porto de abrigo. Muito mais difícil será deixar palavras para o Martinho…mas é para ti que este trabalho faz sentido (ainda que muito lamente as horas de ausência desde o teu primeiro dia de vida).

This work was financially supported by FEDER funds through the Competitiveness and Trade Expansion Program (COMPETE) and by national funds provided by the Fundação para a Ciência e Tecnologia (FCT) via a doctoral grant with reference SFRH/BD/38958/2007.

FCT Fundação para a Ciência e a Tecnologia

MINISTÉRIO DA CIÊNCIA, TECNOLOGIA E ENSINO SUPERIOR

COMPETE

QREN QUADRO DE REFERÊNCIA ESTRATÉGICO NACIONAL

UNIÃO EUROPEIA

Fundo Europeu de Desenvolvimento Regional

Abbreviations and symbols:

2D ..... Two-dimensional
3D ..... Three-dimensional
ALT ..... Alanine aminotransferase
ANOVA ..... Analysis of variance
ASMA..... α-smooth muscle actin
AST..... Aspartate aminotransferase
BCE .....Before the common era
BCV .....Biological relative variance
BnHEP .....Binuclear hepatocyte
CAT.....Catalase
CD .....Cluster defined
CE .....Coefficient of error
CEA ..... Carcinoembrionic antigen
CV..... Coefficient of variation
CYP ..... Cytochrome P450
DNA ..... Deoxyribonucleic acid
DTPA .....Diethylene triamine penta-acetic acid
ECM..... Extracellular matrix
ER ..... Oestrogen receptor
GFAP .....Glial fibrillary acidic protein
GPX ..... Glutathione peroxidase
GR ..... Glutathione disulfide reductase
GS ..... Glutamine synthetase
GSH..... Reduced glutathione
GSSG .....Oxidized glutathione
GST ..... Glutathione S-transferase
HBV ..... Hepatitis B virus
HCV .....Hepatitis C virus
HEP ..... Hepatocyte
HSC ..... Hepatic stellate cell
HSCI .....Hepatic stellate cell index
KC..... Kupffer cell
KCI.....Kupffer cell index
KPB.....Potassium phosphate buffer
LPO.....Lipid peroxidation

LSEC ..... Liver sinusoidal endothelial cell

MnHEP ..... Mononuclear hepatocyte

MMP ..... Metalloproteinases

N ..... Total number

NADPH ..... Nicotinamide adenine dinucleotide phosphate

NHC ..... Non-hepatocytic cells

N_V ..... Numerical density

OCV ..... Observed relative variance

P ..... Point

PSI ..... Point sampled intercepts

PBS ..... Phosphate buffered saline

RNA ..... Ribonucleic acid

ROS ..... Reactive oxygen species

SD ..... Standard deviation

SUR ..... Systematic uniform random

TBARS ..... Thiobarbituric acid reactive species

TBS ..... Tris-buffered saline

TIMP ..... Tissue inhibitor of metalloproteinase

USA ..... United States of America

V ..... Total volume

V_V ..... Volume density

$\overline{v}_N$ ..... Number-weighted mean volume

$\overline{v}_V$ ..... Volume-weighted mean volume

Contents I
Resumo VII
Summary IX

Chapter 1: Introduction

1.1- General introduction to the liver 1
1.2- Microanatomical organisation of the liver 3
1.3- Chronic liver diseases and fibrosis 5
1.4- The study of liver fibrosis 7
1.5- The study of ageing, gender and the liver 8
1.6- The use of stereological methods in liver research 12
1) Sampling liver fragments for stereological purposes 13
2) Fixation and processing liver pieces for stereological purposes 15
3) Estimation of volume by stereological methods 16
4) Estimation of number by stereological methods 24
1.7- Objectives 30
1.8- References 32

Chapter 2: Hepatic stellate cells

2.1- Introduction

1) Portrait of an intriguing cell 44
2) Quantification of HSC 47
3) Lobular heterogeneity and HSC 48
4) Ageing, gender dimorphism and HSC 49

2.2- Materials and Methods

2.2.1- Baseline study

1) Animals 51
2) Tissue preparation and sampling protocol 51
3) Immunohistochemistry for GFAP 52
4) Stereological analysis 53
5) Assessment of the optimum sampling 56
5) Statistical analysis 56

2.2.2- Age and gender study

1) Animals 56
2) Tissue preparation and sampling protocol 57
3) Immunohistochemistry for GFAP 58
4) Double immunohistochemistry for GFAP and GS 58
5) Immunohistochemistry for ASMA 58
6) Picro-sirius red staining 59
7) Electron microscopy 59
8) Stereological analysis 59
9) Statistical analysis 61

2.3- Results

2.3.1- Qualitative findings 62

2.3.2- Quantitative findings

2.3.2.1- Baseline study

1) Total number, number per gram and numerical density of HSC 67
2) Assessment of the optimum sampling 70

2.3.2.2- Age and gender study

1) Body, liver weight, liver-to-body weight ratio and liver volume 70
2) Hepatic transaminases and serum oestradiol levels 72
3) Section thickness and distribution of particles in the z-axis 73
4) Total number, number per gram and numerical density of HSC 73
5) Hepatic stellate cell index 76
6) Volume density and number-weighted mean volume 77
7) Lobular heterogeneity 79
9) Picro-sirius red staining 79

2.4- Discussion

2.4.1- Baseline study

1) About HSC quantification 81
2) The tagging of HSC 81
3) The sampling procedure 82

2.4.2- Age and gender study

1) About the obtained data 83
2) Ageing and the liver 84
3) Ageing and HSC 86
4) Ageing and liver collagen 89
5) Ageing and the hepatic stellate cell index 91

6) Ageing and the lobulation of HSC 92
7) Gender and HSC 94

2.5- References.....96

Chapter 3: Hepatocytes

3.1- Introduction

1) Quantification of HEP.....109
2) Ageing, gender and HEP 113

3.2- Materials and Methods

3.2.1- Baseline study

1) Animals, tissue preparation and sampling protocol 118
2) Immunohistochemistry for CEA.....118
3) Stereological analysis 118
4) Computer simulations to determine the optimum sampling 120
5) Statistical analysis.....120

3.2.2- Age and gender study

1) Animals, tissue preparation and sampling protocol 120
2) Immunohistochemistry for E-cadherin and stereological analysis.....121
3) Ploidy analysis by flow cytometry.....122
4) Biochemical analysis of oxidative stress.....122
5) Statistical analysis.....124

3.3- Results

3.3.1- Qualitative findings.....125

3.3.2- Quantitative findings

3.3.2.1- Baseline study

Total number, number per gram and numerical density.....127

3.3.2.2- Age and gender study

1) Porto-central distance 129
2) Total number, number per gram and numerical density of HEP 129
3) Number of BnHEP, their number per gram and percentage 132
4) Mean volume of HEP 133
5) Stereological analysis of young and old HEP nuclei.....134
6) Ploidy analysis of young and old liver by flow cytometry 136
7) Study of biomarkers throughout ageing and gender.....138

8) Number of all liver cells 141

3.4- Discussion

3.4.1- Baseline study

1) About the tagging of BnHEP and the stereological methods 142
2) About the quantification of HEP 142
3) The quantification of BnHEP 144
4) The sampling procedure 145

3.4.2- Age and gender study

1) About ageing and the liver 146
2) The lobular size 147
3) Total number and number per gram of HEP 149
4) BnHEP throughout ageing 150
5) Volume of HEP throughout ageing 151
6) Ploidy analysis in ageing 153
7) Oxidative stress analysis throughout ageing 155
8) HEP and gender 158
9) Ploidy, oxidative stress analysis and gender 160

3.5- References 164

Chapter 4: Kupffer cells

4.1- Introduction

1) Quantification of KC 179
2) Ageing, gender dimorphism and KC 182

4.2- Materials and Methods

4.2.1- Baseline study

1) Animals, tissue preparation and immunohistochemistry 184
2) Stereological analysis 184
3) Statistical analysis 185

4.2.2- Ageing and gender study

1) Animals and immunohistochemistry for ED2 186
2) Double immunohistochemistry for ED2 and GFAP 186
3) Stereological analysis 186
4) Statistical analysis 187

4.3- Results
4.3.1- Qualitative findings.....188
4.3.2- Quantitative findings
4.3.2.1- Baseline study
Total number, number per gram and numerical density of KC.....190
4.3.2.2- Age and gender study
1) Total number, number per gram and numerical density of KC.....191
2) Kupffer cell index 194
3) Co-localisation of KC and HSC 195
4.4- Discussion
4.4.1- Baseline study
1) KC quantification.....196
2) Subpopulations of liver macrophages 198
3) Relation between KC and other liver cells.....198
4.4.2- Age and gender study
1) About the obtained data.....199
2) Ageing and KC.....201
3) Gender and KC.....202
4.5- References 205

Chapter 5: Conclusion
5.1- Overview of cell populations and summary of the data.....213
5.2- Gender dimorphism: the Prometheus wife..... 216
5.3- Is there a functional liver lobule? 218
5.4- References.....222

Annex 1.....225

Resumo

O envelhecimento da população é uma realidade dos nossos dias. O fígado é visto como um órgão pouco afetado pelo envelhecimento, ainda que seja reconhecido que é mais sensível a hepatotóxicos e a cirrose no indivíduo idoso, e particularmente no sexo masculino. Esta mesma tendência também é constatada no fígado do rato. A diferença na fisiopatologia de machos *versus* fêmeas é conhecida como dimorfismo sexual. Apesar de se saber há muito que a actividade enzimática é diferente em fígados de machos e fêmeas, e mais recentemente, se ter mostrado que a expressão de genes varia com o sexo, não se sabe ainda se o dimorfismo sexual tem uma tradução morfológica. A literatura existente sobre dimorfismo e o processo de envelhecimento do fígado é relativamente escassa e por vezes contraditória. Os métodos estereológicos modernos, pela sua natureza não enviesada, são as ferramentas ideais para estudar diferenças quantitativas a nível microanatómico.

Assim, neste trabalho estudou-se um triunvirato de células (hepatócitos, células de Kupffer e células estreladas hepáticas) do fígado do rato, procurando diferenças numéricas e de ratios celulares que justificassem a tendência para a fibrose em machos. Foram usados ratos machos e fêmeas da estirpe Wistar com 2 meses (jovens), 6 meses (adultos), 12 meses (meia-idade) e 18 meses (velhos). Para garantir o reconhecimento adequado das células em estudo, foram empregues anticorpos contra a proteína ácido fibrilhar da glia, para marcar as células estreladas hepáticas, e contra o ED1 e ED2, para destacar as células de Kupffer. Adicionalmente, usaram-se anticorpos contra a E-caderina e o antigénio carcinoembrionário, para assegurar a diferenciação entre hepatócitos mono e binucleados. Primeiramente, as estratégias de quantificação foram testadas e otimizadas, em estudos preliminares. Seguidamente, o número total (do triunvirato de células) foi estimado através do fracionador ótico. O volume celular médio também foi estimado, quer através de técnicas indiretas (no caso das células estreladas hepáticas), quer através do “nucleator” (no caso dos hepatócitos); nestes últimos também se determinou o volume nuclear médio. Adicionalmente, a deposição de colagénio, lobular e intralobular, também foi quantificada, através de uma estratégia clássica de contagem de pontos. Finalmente, foram ainda realizados dois outros estudos: de citometria de fluxo (para avaliar diferenças de ploidia) e de stress oxidativo (uma vez que a fibrose é muitas vezes desencadeada pelos radicais livres de oxigénio).

Globalmente, a estrutura do fígado é mantida ao longo da idade em ambos os sexos (o diâmetro dos lóbulos mantém-se estável com a idade, uma vez que a distância entre os espaços porta e as vénulas centrolobulares não sofre alterações com a idade e com o sexo). De acordo com os nossos dados, o número total e o volume médio das células estreladas hepáticas são também mantidos ao longo da idade, em ambos os sexos,

ainda que existam diferenças a nível do corpo celular destas células (pelo aumento do conteúdo lipídico), na deposição de colagénio (neste caso apenas em machos) e na localização lobular das células. As células estreladas hepáticas (positivas para a proteína ácido fibrilhar da glia) predominam nas áreas periportais dos ratos velhos (machos e fêmeas). No caso dos hepatócitos, mostraram-se diferenças estatisticamente significativas em animais jovens (as fêmeas tinham um maior número de hepatócitos, de menores dimensões e menor ploidia, existindo um maior número de formas binucleadas). Estas diferenças foram-se esbatendo com a idade. A peroxidação lipídica aumentou com a idade, mas, em termos genéricos, as defesas antioxidantes de animais velhos eram comparáveis às dos novos. Já no que respeita às células de Kupffer, também foram encontradas diferenças entre sexos (maior número em fêmeas), que se atenuaram com a idade. Curiosamente, um terço das células estreladas hepáticas encontrava-se justaposta a células de Kupffer.

Esta tese mostrou que as três populações celulares estudadas se encontram correlacionadas ao longo da idade, em ambos os sexos (e.g., o número total de células estreladas hepáticas correlaciona-se com o de hepatócitos). Isto corrobora a complexidade do órgão e favorece a existência de lóbulos funcionais no fígado. Uma das nossas hipóteses iniciais (de que os machos e os animais mais velhos teriam maior número de células estreladas) foi negada. No entanto, foram destacadas diferenças a nível dos hepatócitos, em machos e fêmeas jovens, que podem justificar a maior capacidade regenerativa, normalmente atribuída às fêmeas. Adicionalmente, as diferenças entre sexos a nível das células de Kupffer podem justificar a maior suscetibilidade à hepatite alcoólica por parte das fêmeas. De acordo com o nosso trabalho, o dimorfismo sexual está patente no fígado, devendo ser tomado em consideração em investigações de âmbito biomédico e farmacêutico (e.g., desenvolvimento de medicamentos). Esta tese aumentou o conhecimento sobre o envelhecimento do fígado e sobre o dimorfismo sexual neste órgão, gerando novas hipóteses e caminhos que serão seguidos em estudos no futuro (estes recorrerão a técnicas estereológicas e de biologia molecular).

Summary

It is recognised that the human population is getting aged while being generally assumed that the liver endures time fairly well. Nevertheless, the aged liver is much more sensitive to hepatotoxicants and liver fibrosis/cirrhosis is typically a disease of the elders, being much more prevalent in the male gender; the same occurs in the rat. This inequality of pathophysiology is often called gender dimorphism. Despite it is known for long that the livers of male and female rats differ in enzyme activity, and more recently, also in gene expression, it is still unclear whether gender dimorphism may be traduced morphologically. The existing literature on this issue, as well as that on ageing effects in the liver, is scarce and often contradictory. At microanatomical level, design-based stereological methods, by their inherent unbiased nature, are the adequate tools to quantitatively disclose such structural differences.

In view of the above, a triumvirate of cells [hepatocytes (HEP), Kupffer cells (KC) and hepatic stellate cells (HSC)] were studied in the rat, seeking for differences in numbers or cell ratios that could underlie the fibrotic trend of males in the pathological setting. Male and female Wistar rats of 2 months (young), 6 months (adults), 12 months (middle-aged) and 18 months (old) were used. In order to guarantee that every cell would be properly recognised, we used immunohistochemistry tagging with antibodies against glial fibrillary acidic protein (GFAP), for HSC, and against ED1 and ED2, for KC. For assuring that mononucleated HEP could be separated from binucleated HEP (BnHEP), we used immunomarking against carcinoembryonic antigen and E-cadherin. Firstly, the quantification strategy was designed and tested, in baseline studies, and afterwards total numbers (N) were estimated throughout ageing, using the optical fractionator. The mean cell volume was also determined by an indirect technique (in the case of HSC) or directly by the use of the nucleator (in HEP); for HEP, the nuclear volume was also estimated. Lobular and interlobular collagen deposition was quantified by a classical point counting method. Finally, we conducted a flow cytometry study (to assess ploidy differences) and evaluated oxidative stress (as fibrosis is often triggered by reactive oxygen species).

Overall, the liver structure was preserved throughout ageing and gender (the diameter of lobules was maintained, since the distance from portal tracts to central venules did not vary with ageing, either in males or in females). According to our data, both the number and the mean volume of HSC were maintained throughout ageing in males and females, even if differences existed in the volume of the perikaryon (due to increase content of lipids), in the collagen deposition (only in males) and in the lobular location of cells; HSC (positive to GFAP) predominated in periportal areas in aged rats (both male and female). Regarding HEP, we showed that statistically significant gender differences existed in young rats (females had smaller but more numerous HEP, with more diploid nuclei, and

more binuclear cells); these gender differences were attenuated with ageing. The lipid peroxidation of liver homogenates increased with ageing, but, overall, antioxidant defences of old animals were comparable to that of young ones. Regarding KC, we also noted significant gender differences (higher number of KC in females), that were abolished in older animals. Interestingly, we found a co-localisation of cells types: indeed, one third of HSC had KC as their neighbours.

We showed in this Thesis that the three cell types studied were significantly correlated throughout ageing and gender (*e.g.*, the N of HSC and of HEP) — this substantiates the complexity of the liver and favours the existence of functional liver lobules. One of our initial hypotheses (that males and older animals could have more HSC under normal conditions) was not proved. However, we found previously undisclosed gender differences for HEP in young animals, that may well justify the greater regenerative potential generally attributed to females. Additionally, the gender differences in KC may underlie the increased sensitivity of females to alcoholic liver disease. According to our data, gender dimorphism exists in the rat liver and this should be considering in biomedical and drug development research. This study markedly enhances the (still meagre) knowledge on ageing and gender influences in the liver and points towards new research paths that will be followed with complementary stereological and molecular biology approaches.

Chapter 1 – Introduction

1 - Introduction

1.1- General introduction to the liver

The liver is located in the right side of the abdominal cavity being the largest gland of mammals. Ever since Hippocrates, several functions have been described in this organ. In all species of mammals, the liver is hematopoietic during embryonic development, and this capacity can be evoked later in life, in cases of chronic bone marrow disease. As to the liver of adults, it is comparable to a high-tech factory, specialised distribution centre and to an up-to-date sewage treatment plant. Indeed, the organ is the primary regulatory site for energy metabolism, taking up and processing ingested nutrients, for controlled distribution to extra-hepatic tissues. Moreover, it synthesises vital proteins, enzymes, and cofactors required for normal body function, and, like an up-to-date sewage treatment plant, the liver is responsible for the detoxification and elimination of a variety of compounds. Anatomically, the number of liver lobes diverges between species of mammals. In the rat four lobes can be considered: 1) the middle or median lobe (*lobus medialis*), which is the largest, accounting for 38% of the liver weight, being fixed to the diaphragm and abdominal wall by the falciform ligament; 2) the right lobe (*lobus lateralis dexter*), which comprises around one fourth of the liver weight and is located in the posterior hypochondrium; 3) the left lobe (*lobus lateralis sinister*), accounting for about one third of the liver weight, located in the epigastric and left hypochondriac regions; 4) the caudate lobe (*lobus caudatus*), recognised by their smaller size (8 to 10% of the liver weight) and the two processes, *papilaris* and *caudatus*, also known as Spiegel lobe and paracaval portion, respectively (Martins and Neuhaus, 2007). Except for the left one, all those lobes are subdivided in two or more parts, since a considerable individual variation exists (Kongure *et al*, 1999; Martins and Neuhaus, 2007). In contrast to most mammals, a quadrate lobe (*lobus quadratus*) is not present in the rat and the liver has no gallbladder, meaning that the organ is directly connected to the duodenum by the common bile duct (*ductus choleducus*); despite this anatomical feature is not exclusive of the rat, its functional implications are still unknown (Martins and Neuhaus, 2007). In rats, the liver mass can represent up to 5% of total body weight in young animals, standing for ≈ 3% in adults (Martins and Neuhaus, 2007). This feature is fairly similar to humans: in adults the organ weight is 1.3-1.7 kg depending on the sex and body size and it stands for 2-2.5% of the total human body weight (Grisham, 2009). Interestingly, the liver lobes of the rat are equivalent to the liver segments of humans defined by Couinaud (the median lobe, for instance, corresponds to segments III, IV, V and VIII) (Kongure *et al*, 1999).

Regarding the vascular organisation, it was first described by Babylonians during hepatoscopy practices, as far back as 2000-3000 before the common era (BCE) (Veiga,

2011)! The organisation of the liver is well adapted to all its functions, as the organ receives 25% of the cardiac output. Around 70% of blood goes through the portal vein, bringing blood with low oxygen content but highly enriched with nutrients. The remaining 30% of blood is oxygen-rich blood, brought by the hepatic artery (Roskams *et al*, 2007). Blood from these two sources joins in the organ, but the mixture actually differs between lobes and this underlies the lobar heterogeneity of the liver. In fact, blood from stomach and spleen tends to go for the left side of the liver, and this pattern is seen in liver metastasis from those organs (Roskams *et al*, 2007). This heterogeneity has been observed in normal as well as in pathological conditions, such as acetaminophen hepatotoxicity, chemical carcinogenesis and cirrhosis (Matsuzaki *et al*, 1997; Malarkey *et al*, 2005). Even the regenerative potential differs between lobes, since 5-fold differences in the number of proliferating hepatocytes (HEP) were recently reported (Deng *et al*, 2009)

Like in all other glands, the liver can be subdivided in parenchyma and stroma. The latter is relatively scarce, when compared with most glands, but it includes many components: the dense connective tissue of the Glisson's capsule, the smooth connective tissue of portal tracts, as well as reticular fibres that support all the parenchymal cells. In addition, the stroma also includes blood vessels and biliary tracts present in the connective tissue. The parenchyma represents ≈ 95% of the hepatic volume (Weibel *et al*, 1969; Hashimoto and Watanabe, 2000), being composed of cells with different, but complementary, functions. HEP, often called parenchymal cells, are the most abundant occupying ≈ 80% of the hepatic volume (Blouin *et al*, 1977; Grisham, 2009). In all adult mammals those cells are aligned in hepatic cords of one-cell thickness (Beresford and Henninger, 1986). The parenchyma also comprises the littoral or non-parenchymal or sinusoidal cells. Whilst the former terms are more frequent in biochemical studies (Bouwens *et al*, 1992), the latter designation is the most common, and it has even been used to name a society entirely devoted to their study (International Society of the Hepatic Sinusoidal Research). These cells stand for ≈ 6% of the hepatic volume (Blouin *et al*, 1977; Grisham, 2009) and include (Figure 1.1): 1) pit cells, which are liver specific natural killer lymphocytes that circulate within the sinusoids; 2) Kupffer cells (KC) that are liver specific macrophages, attached to the sinusoidal walls; 3) liver sinusoidal endothelial cells (LSEC), known for their typical *fenestrae*; and 4) hepatic stellate cells (HSC), with characteristic lipid droplets.

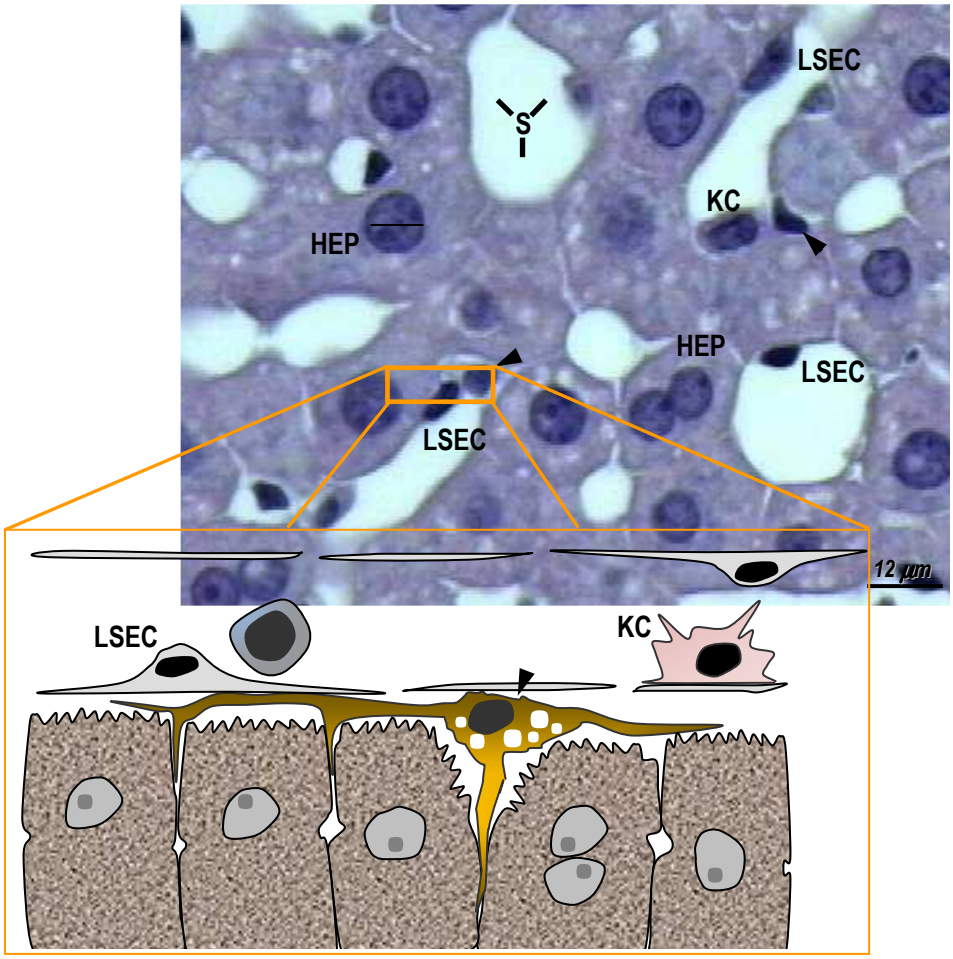

Figure 1.1 - Light micrograph of the liver parenchyma, with hepatic cords and sinusoids. Their microanatomy is represented in the schematic drawing. LSEC: liver sinusoidal endothelial cells; HEP: hepatocytes; KC: Kupffer cells; S: sinusoid; arrowhead: hepatic stellate cells.

1.2- Microanatomical organisation of the liver

The liver has lobules like many other glands, but, except for the pig and few other species of mammals (Ekataksin and Wake, 1991), their morphological recognition is feeble and their functional organisation has generated controversy for more than 400 years (Malarkey *et al*, 2005; Teutsch, 2005; Grisham 2009). The current conception is that the liver has a continuous network of parenchymal and non-parenchymal cells, lacking true lobules even in swine (Grisham, 2009). The first lobular concept to be proposed was defined by Kiernan, after studies with pig livers (Kiernan, 1833). The classical hepatic lobule was characterised by central venules, at the centre, and portal tracts at the periphery (Figure 1.2). Despite being often described as hexagonal (Fawcett, 1994), Kiernan originally referred his lobule as polygonal and, in the case of the pig, pentagonal lobules predominate (Ekataksin and Wake, 1991). In contrast, in humans, rats, and other species of mammals, the shape of lobules is hardly definable, since interlobular connective tissue

(that connects portal tracts) is scarce or absent (Kmiec, 2001). The second concept to be described was based in studies with the liver of rabbits and dogs — the portal lobule of Mall (1906) was triangular, bearing central venules at the corners and the portal tract in the centre. In contrast with this interpretation, Rappaport *et al* (1954) described a third lobular concept after studying the vascular perfusion and the biliary secretion in the liver of rabbits, rats and humans. The liver acinus is diamond-shaped, with a central line that connects two portal tracts and having peripheral terminal hepatic venules (the central venules of the classic lobules) (Rappaport *et al*, 1954). Meanwhile, other concepts continued to be added, like the primary lobule (Matsumoto and Kawakami, 1982). This latter is a cone-shaped unit, which extends the classical lobule to a three dimensional perspective. Matsumoto and Kawakami (1982) additionally defined a vascular septum, caused by blood flow adjacent terminal portal venules into sinusoids of two neighbouring classical lobules (Matsumoto and Kawakami, 1982; Grisham, 2009). All these concepts have been debated in the rat and most studies support that the primary lobule exists in this species (Teutsch *et al*, 1999; Malarkey *et al*, 2005; Teutsch, 2005; McCuskey, 2008). After studies with India ink injections and pig-serum induced fibrosis, Bhunchet and Wake (1998) concluded the rat liver has central venules located at the periphery of the liver, whilst portal venules and their branches are always located inside the organ. Those authors proposed the portal lobule for the rat (Bhunchet and Wake, 1998), but it did not gain much acceptance, as well as the liver acinus, which is considered unsuited for this species (Teutsch *et al*, 1999; Malarkey *et al*, 2005). It is noteworthy that in recent years, instead of morphological units, many authors have proposed functional organisations, which are gaining some acceptance (Roskams *et al*, 2007). Such concepts include: 1) the hepatic microcirculatory unit (McCuskey, 1993; 2008), which consists of a group of sinusoids supplied by a single inlet venule; 2) the choleohepaton (Ekataksin and Wake, 1997), defined as a group of liver cells that drain bile to a single Hering canal and share the same blood supply; and more recently 3) the stellate cell unit or stellon (Wake, 2006), consisting of overlapping groups of HEP and LSEC that have cell-to-cell contacts with HSC.

In geometrical terms, the classical lobule (as well as the primary lobule) can be characterised by a porto-central distance (or radius), which has been determined in different species (Ruijter *et al*, 2004). After sophisticated graphical reconstructions, such distance has been estimated as 350 to 420 μm in humans, encompassing 16 to 18 HEP, whereas in rats this measures from 300 to 450 μm (Wagenaar *et al*, 1993; Lamers *et al*, 1997; Ruijter *et al*, 2004).

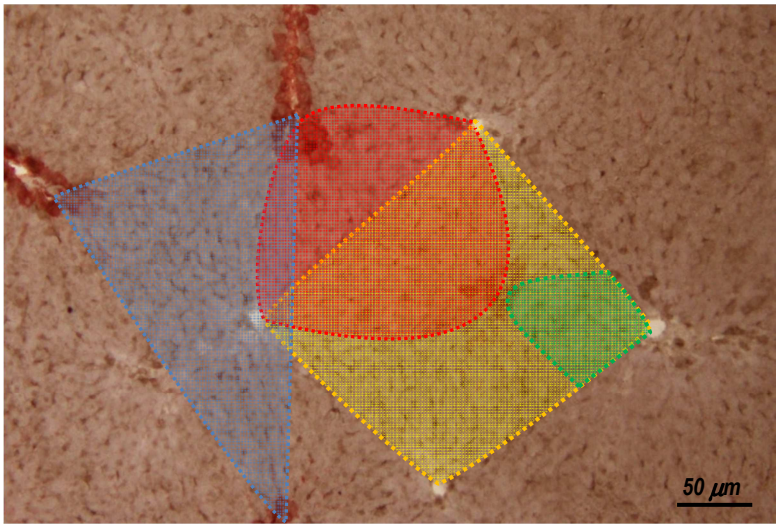

Figure 1.2 - Light micrograph of the liver parenchyma immunostained against glutamine synthetase, a marker of centrilobular hepatocytes (details of the immunostaining procedure will be given in Chapter 2). The different lobular concepts are highlighted: classical lobule (yellow), portal lobule (blue), acinus (red), primary lobule (green).

1.3- Chronic liver diseases and fibrosis

The first record of fibrosis dates back to 260 BCE, when Erasistratos, the founder of the Alexandrian School of Medicine, recognised that ascites was caused by induration of the liver due to fibrosis (Desmet, 1992). Obviously, science has evolved extensively and nowadays liver fibrosis is defined as a wound healing response, in which an excessive accumulation of extracellular matrix (ECM) takes place — especially collagen type I (Moreira, 2007). Chronic liver disease (*i.e.*, a disease with persistent symptoms and/or laboratory signs for more than 6 months) often has liver fibrosis as their terminal end-point. It is expected to occur in 25-30% of human patients (Povero *et al*, 2010). The scar tissue disrupts the blood flow and compromises the free passage of substances from blood to HEP, and fibrotic bands can be seen between different parts of the liver. Living cells try to regenerate within these fibrotic bands, through an erratic and disorganised response, forming small nodules that further disturb the blood flow in the organ. The coexistence of widespread nodules and fibrosis are the hallmarks of cirrhosis. This term comes from the Greek *kirrhos*, meaning tawny yellow, and it was coined by Laënnec, the inventor of the stethoscope and a recognised pneumologist (Desmet, 1992). The importance of liver fibrosis and cirrhosis is rising: nowadays, over 21 million people in the world are estimated to live with chronic liver disease and about 800000 die each year. In fact, cirrhosis is the most common non-neoplastic cause of death in Europe and United States of America (USA), being the 7th most common cause of death in western countries (World Health Organization, 2008). In Portugal, around 2000 people die per year due to liver cirrhosis, meaning that it is the 10th cause of death in adults (although it may rank to

the 4th cause of premature death, before the age of 70) (World Health Organization, 2008). The mortality is further increased via malignant transformation to hepatocellular carcinoma, which is strictly associated. Indeed, the risk of developing hepatocellular carcinoma in cirrhotic patients is 1 to 4% per year, meaning that this carcinoma is one of the most rapidly increasing neoplasms in the USA and Western Europe (Bruix *et al*, 2004).

Chronic liver disease can be due to different causes, which can be grouped in: viral, alcoholic, metabolic, hepatotoxic, autoimmune, genetic, and, finally, vascular causes. In developed countries more than half of the cases are due to chronic hepatitis C virus (HCV) and alcoholic liver disease. In Portugal, the latter is the leading cause, immediately followed by HCV and hepatitis B virus (HBV) (World Health Organization, 2008). Among metabolic causes of liver disease, the non-alcoholic steatohepatitis (NASH) is increasingly recognised as another major cause of fibrosis, which is gaining importance in more recent years, due to the current epidemics of obesity in more developed countries (Bataller and Brenner, 2009).

As mentioned above, viruses are common causes of liver fibrosis. HCV was first defined in 1989 as a single-stranded RNA virus that can be subdivided into groups depending upon the virus genotype. It has been estimated that more than 170 million people worldwide are chronically affected by HCV (Bataller and Brenner, 2009). It is transmitted via blood and blood products and so the use of unscreened blood in transfusions and re-use of needles have been major routes of transmission. Although much less common, transmission can also occur sexually, vertically, via tattooing and ear-piercing or acupuncture (Featherstone, 2008). The natural history of HCV differs from HBV because: 1) most cases of acute infection are clinically undetectable; 2) up to 85% of those will become chronically infected; 3) cirrhosis may develop after an average of 20-30 years (Featherstone, 2008; Bataller and Brenner, 2009). It should be noted that the peak for HCV associated liver disease has been predicted for the first decades of this century (Lim and Kim, 2008). This may have devastating consequences because a reduction of livers available for transplantation (which is the most effective treatment option) has been also forecasted (Povero *et al*, 2010).

Distinct patterns of fibrosis can be described, depending on the underlying cause of chronic liver disease. The bridging fibrosis has septa, that in most cases connects portal and central areas, and is typical of HCV and HBV-related hepatitis, whereas the perisinusoidal fibrosis corresponds to ECM deposition in the space of Disse, being related to alcohol abuse or NASH (Moreira, 2007). Fibrotic septa can also be seen in centrilobular fibrosis, but in this case they develop between central venules and occur in patients affected by chronic heart failure and liver stasis (Roskams *et al*, 2007).

Hence, the liver is characterised by a slow progression of liver fibrosis, in contrast with other organs. Fibrosis may progress more rapidly, over weeks to months, in a few conditions, but in most cases it progresses over years (Bataller and Brenner, 2009). This progression is influenced by a number of clinical features, like the hepatic iron content, daily alcohol intake, obesity, diabetes mellitus, as well as individual factors, like age and male gender. In fact, older age at the time of infection is particularly relevant for HCV-related fibrosis progression. Patients aged over 50 years have a progression of fibrosis twice as high as people under that age (Kage *et al*, 1997). This applies for both genders, since after menopause the progression of fibrosis in man and women is virtually identical (Di Martino *et al*, 2004). In fact, as it was recently reviewed by Hoare *et al* (2010), studies over the last 20 years have linked age with the clinical outcome of a variety of liver diseases besides HCV, like HBV, primary biliary cirrhosis, alcoholic liver disease, autoimmune hepatitis, NASH, alpha-1 anti-trypsin deficiency, hemochromatosis and Budd-Chiari syndrome.

Regarding gender, females not only have a slower progression of fibrosis, but also a lower evolution towards hepatocellular carcinoma; this results in two thirds reduction of risk for women comparing to men (Shimizu *et al*, 2007). This slower progression of fibrosis applies for HCV and HBV-related disease, as well as for NASH. Except for autoimmune liver diseases, cirrhosis is largely a disease of men (Harrison *et al*, 2002; Shimizu *et al*, 2007). This stands for most countries in Europe — in Portugal, deaths from chronic liver diseases and cirrhosis are 3.4 times more frequent in men than in women (World Health Organization, 2008).

In the rat, the same progressive trends appear to exist (Pinzani, 2004). Although some contradictory data has been reported (Zivna *et al*, 2001), classical studies by Reuber and Glover (1968) with hepatic fibrosis induced by subcutaneous CCl_4 injection described less severe cirrhosis in females. While Blain *et al* (1999) argued that females were more susceptible to the fibrotic drive produced by this substance another group confirmed the stronger fibrosis in males using the CCl_4 model (Xu *et al*, 2002). Additionally, this was also showed in fibrosis induced by dimethylnitrosamine (Yasuda *et al*, 1999) and by pig-serum (Shimizu *et al*, 1999). Sex steroids play some role, as exogenous and endogenous oestradiol has been shown to suppress the induction of both fibrosis and chemical hepatocarcinogenesis in the rat (Shimizu *et al*, 1998).

1.4- The study of liver fibrosis

The understanding of liver fibrosis has progressed markedly in the last decades. Obviously, most of the studies were performed in animal models, in order to overcome the issues involved in studying the human liver (like ethical constrains and scarcity of

material). Hepatic fibrosis has been induced by several methods that can be categorised by their aetiology: (1) hepatotoxins, which includes the CCl_4 administration or the injection of thioacetamide or dimethylnitrosamine; (2) nutritional, like the use of a choline deficient diet; (3) immunologic, in which heterologous serum, usually from pig, is injected; (4) biliary, by ligating the bile duct. All these methods have their advantages and disadvantages and it should be noted that no model replicates exactly the human fibrosis (Tsukamoto *et al*, 1990; Wasser and Tan, 1999; Li *et al*, 2002). The most used methods have been the CCl_4 and thioacetamide administration (Natarajan *et al*, 2006). The former depends on the conversion of CCl_4 into trichloromethyl free radical ($CCl_3\bullet$). This occurs by the cytochrome P450 (CYP) of HEP, which leads to lipid peroxidation and membrane damage (Natarajan *et al*, 2006). After fatty change and central necrosis, fibrotic septa develop, linking two central venules and crossing a mid-point between portal-portal connecting lines (Roskams *et al*, 2007). Regarding other hepatocarcinogens, the most used have been dimethylnitrosamine and thioacetamide (Natarajan *et al*, 2006). They do not cause fatty change, and cirrhosis is stable several months after the discontinuation of drugs (Wasser and Tan, 1999). It is considered that those models best replicate human cirrhosis and the associated liver cancer (Wasser and Tan, 1999; Passos *et al*, 2010).

The knowledge about the mechanisms underlying fibrosis has also increased substantially over the last 40 years: it was initially thought to be a passive process of hepatocellular damage with condensation of the pre-existing stroma, but nowadays it is viewed as a dynamic process of continuous ECM remodelling. The eighties had an important milestone in the study of liver fibrosis, since it was then established that HSC were the main collagen producing cells, regardless of the underlying aetiology (Martinez-Hernandez, 1985; Friedman *et al*, 1985). These cells are pivotal, but it should be stressed that, except for pit cells, all liver cells produce one or more components of ECM (Moreira, 2007). After a liver injury, HSC are firstly stimulated by damaged HEP that release reactive oxygen species (ROS) (Gressner *et al*, 1995) and afterwards by KC (and also leucocytes) that accumulate locally (Geerts, 2001). All these cells produce a number of factors that drive to the activation of HSC and to the deposition of ECM, typical of liver fibrosis (Greenwell *et al*, 1994). It should be noted that liver fibrosis can occur unrelated with HSC activation; indeed, biliary fibrosis is characterised by proliferative bile ductules and ECM production by portal fibroblasts (Povero *et al*, 2010).

1.5- The study of ageing, gender and the liver

Gerontology research involves the study of normal ageing processes and age related diseases. This research has increased in the last decades and several journals are strictly devoted to the subject (*e.g.*, *Mechanisms of Ageing and Development*, *Journal of*

Gerontology, and the more recent *Current Gerontology and Geriatrics Research*); this is certainly driven by the fact that the human population is getting aged. It is estimated that the number of persons aged over 85 years will increase by 40% in the next decades (Schmucker and Sanchez, 2011). It has been established for long that normal ageing presents a loss of cells and/or functions in many organs, including bone, muscle and brain.

The laboratory rat has been the main species used in gerontology research. The short lifespan, moderate size, low maintenance costs of this species allied to a good temperament, permitting easy handling, and a wealth of published physiological and biochemical data (at least in young animals) makes the rat a good model to study the changes of ageing (Sharp and La Regina, 1998; Nadon, 2006). Some countries even have specialised facilities that support gerontology research, either by grants, or by providing a constant number of aged rodents throughout the year. The National Institute on Ageing in USA, for instance, supplies three strains for ageing studies: the Fischer 344, the Brown-Norway rat and the Fischer 344-Brown-Norway F1 hybrid. The Fischer 344 (or simply named Fischer) is the most popular strain in ageing studies in that country (Nadon, 2006). However, Long Evans, Sprague-Dawley and Wistar rats are also frequently used in ageing studies in Europe and also in USA (Sharp and LaRegina, 1998). Whatever the rat strain chosen, the animals must be free of infectious diseases, the water and food should be given *ad-libitum*, using a nutritionally complete rodent chow. Regarding husbandry, the animals should remain active and environmental stresses (such as noise and animal density) should be minimal throughout all the duration of study (Nadon, 2006).

The maximum lifespan of wild rats is about 600 days (≈ 19 months) and 700 days (≈ 22 months) for males and females, respectively, but their median lifespan (in which there is a 50% survival) is considerably shorter (Nadon, 2006). The laboratory rat usually lives longer than its wild relative. For Wistar rats, for instance, the maximum lifespan is about 3 years and their median lifespan has been reported to vary from 19 months (Porta *et al*, 1980; Sawada and Carlson, 1987) to 24 months (Porta *et al*, 1980; Manikonda and Jagota, 2012); female Wistar rats live 2 months more, in average (Ghirardi *et al,* 1995). In the rat, full adulthood is generally attained at 4 to 6 months of age, and animals older than the median lifespan are usually considered as senescent (Nadon, 2006). This term refers to the presence of age related dysfunctions and diseases that typically begin during middle-age and exponentially accelerate mortality rates. As to reproductive parameters, puberty occurs at 40 to 60 days of age (Quinn, 2005), when a 4-5 days oestrous cycle is established. These cycles tend to be lengthened after 12 months, whilst reproductive senescence [*i.e.*, the existence of oestrous cycle abnormalities (anestrous, chronic oestrous and pseudopregnancy)] usually occurs between 15-24 months (Vom Saal *et al*,

1994; Quinn, 2005). Comparing rats to humans, the 2 months old Wistar rat can be considered equivalent to an adolescent (aged ≈ 15-16 years), whilst 12 and 18 months old rats can be viewed as comparable to humans aged ≈ 40 years and ≈ 55 years, respectively (Collier and Coleman, 1991; Quinn 2005).

The liver, unlike most other organs, does not exhibit marked changes in either the structure or function during the ageing process. Nevertheless, there is a loss of hepatic volume and a decline in perfusion, which affects the clearance of some drugs, as well as their sensitivity to toxins (Vollmar *et al*, 2002; Schmucker and Sanchez, 2011). Some evidence exists that liver regeneration tends to be compromised in the elder and this is mirrored in the number of deaths by liver diseases: they increase 3 to 5-fold after 65 years of age (Regev and Schiff, 2001). As earlier mentioned, the number of patients in the waiting list for liver transplantation does not cease to increase (Figure 1.3). To cope with the increasing demand for organs to be used in transplantation it is tempting to increase the age of liver donors (nowadays only patients younger than 60 years are included in this list). Since there is some evidence that livers from older donors may be less viable than those from younger ones (Washburn *et al*, 1996; Busquets *et al*, 2001), it is important to have an in-depth knowledge about the ageing liver.

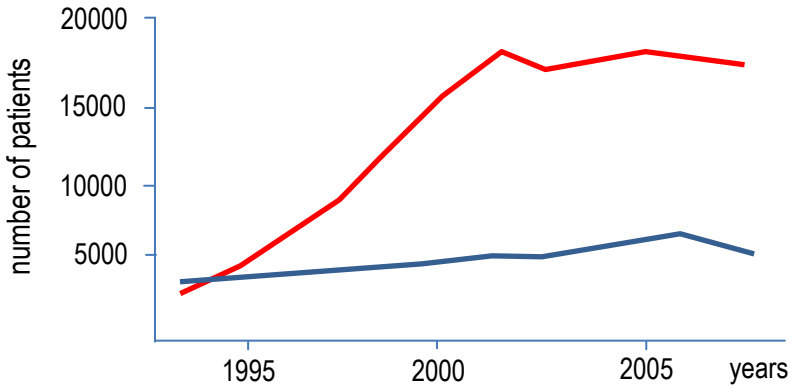

Figure 1.3 - Number of patients in the waiting list (red line) *versus* number of transplanted livers (blue line) in the millennium transition in USA [adapted from Thuluvath *et al* (2010)].

However, studies in human aged livers are rare, since they suffer from dependence on *post-mortem* samples or on samples from subjects diagnosed with liver disease (Schmucker and Sanchez, 2011). The livers of most rat strains are fairly similar to humans, either microscopically or functionally. Moreover, they are not affected by any specific age-related disease and the rat liver functions are fairly maintained in aged animals. Nevertheless, studies using ageing rat liver have been mostly qualitative (Schmucker and Sanchez, 2011) and conflicting results have been reported, for instance, regarding the number of HSC, volume of HEP or even the size of liver lobules (Vollmar *et*

al, 2002; Schmucker and Sanchez, 2011). It is generally accepted that the liver of aged rodents shows some reduction in perfusion, variations in the size of HEP and that these cells tend to increase their nuclear ploidy (Schmucker and Sanchez, 2011). This may affect certain functions, like the clearance of drugs that undergo phase I hepatic metabolism, because the activity of CYP seems to be reduced in old rats (Popper, 1985). Additionally, as in humans, there is a marked decline in the rate of hepatic regeneration after a chemical injury, or after partial hepatectomy (Schmucker and Sanchez, 2011). It should be emphasised that there have been few detailed and comprehensive quantitative studies on liver morphology during ageing and that those used the typical "ageing strains", like Fischer (Schmucker *et al*, 1978). It should be kept in mind that those strains are rarely used in hepatic fibrosis research and that differences between strains (as well as with gender) probably exist in this regard (Popper, 1985). For instance, strain differences in serum-induced fibrosis have been reported: Brown-Norway, Sprague-Dawley and Wistar rats differed not only in the severity of fibrosis, but also at the level of cellular infiltrations (Baba *et al*, 2004). Most studies in liver fibrosis currently use Wistar and Sprague-Dawley strains, and in most cases only males (Figure 1.4). By searching for "liver fibrosis" and "Wistar rat", "Sprague-Dawley rat" or "Fischer rat" in the Web of Knowledge^{SM} it can be perceived that: 1) the typical "ageing strains" (Fischer, Brown-Norway) are marginally employed; 2) female animals were used (with or without males) in less than 20% of the studies published over the last two decades (Figure 1.4). It is noteworthy that this "male bias" is a current concern in many fields of biology: in neurosciences, the ratio of male to female studies is 5.5 to 1 and there is a recent call for considering gender differences in biomedical research and in drug development studies (Kim *et al*, 2010; Scotland *et al*, 2011).

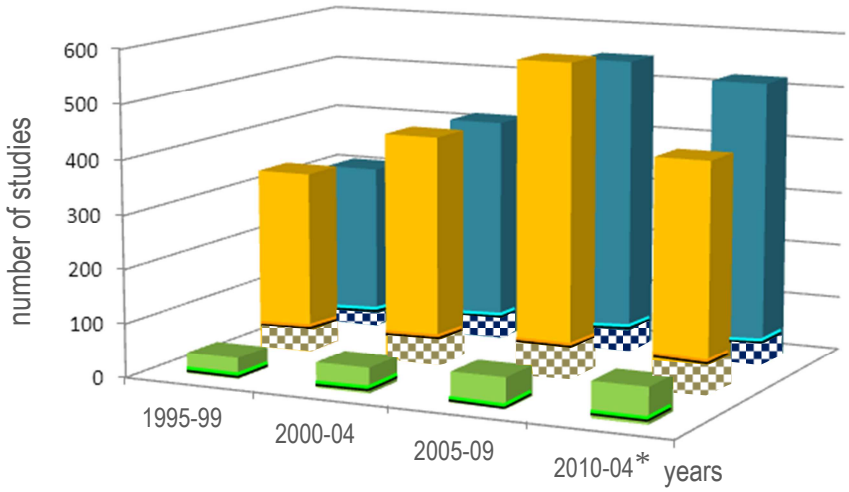

Figure 1.4 - Number of studies in the Web of Knowledge^{SM} devoted to liver fibrosis using Fischer (green columns), Wistar (yellow) and Sprague-Dawley rat strains (blue columns). The stippled part of the columns corresponds to studies that included females; (*) estimated from data concerning the years of 2010-12.

Ageing effects are not restricted to HEP, since the phagocytosis of KC as well as endocytosis of LSEC have also been reported to be reduced (Brouwer *et al*, 1985; Hilmer *et al*, 2007). In addition, the immune response and number of mast cells after acute liver injury have been shown to be reduced in older rats (Grizzi *et al*, 2002). More recently, the effects of age in HSC begun to be highlighted (Warren *et al*, 2011). However, in all those studies, the information was much more qualitative than quantitative (simplistic "numbers per area" were reported) and the special techniques devoted to quantification of cells in histological slides (that will be developed in following sections) were never used. Moreover, those studies included only males; none evaluated if gender differences were relevant for the course of ageing in the liver.

1.6- The use of stereological methods in liver research

Histological evaluation of the liver is often required for several purposes, such as the diagnosis of drug-induced hepatitis and non-alcoholic fatty liver disease, or to assess the severity of damage in chronic hepatitis. Liver biopsy continues to be the gold standard for grading liver fibrosis and diagnosing hepatocellular carcinoma. Regarding the former, a precise quantification of fibrotic tissue, both in clinical studies and in experimental models, has been pursued over the last decade (Dahab *et al*, 2004). It was shown that the relative volume, determined by point counting, is undoubtedly useful in the evaluation of hepatic fibrosis (Vertemati *et al*, 2004), in the diagnosis of hepatocellular carcinoma (Vertemati *et al*, 2008), and in assessing hepatic steatosis in liver biopsies (Catta-Preta *et al*, 2011).

Stereological methods are nowadays viewed as essential to quantify cells or other type of structures embedded in 3D universes, in an unbiased and reproducible manner. A quarter of century has passed since the milestone that marked the beginning of the so-called "design-based" generation of stereological methods (Sterio, 1984). These continue to be updated with the advent of new tools (Gundersen *et al*, 1988; Gardi *et al*, 2008; Stark *et al*, 2011) and applications in different fields of knowledge, with a traditionally special emphasis to neurosciences (Mayhew and Gundersen, 1996; Mouton, 2002). Nowadays, this generation of methods coexists with the old "model-based" strategies, but differences exist between the two methodologies: the "design-based" approach typically implies that no strict assumptions (about shape, size, orientation or distribution) are made about the objects under study and, instead, that a system of sampling rules is designed in order to ensure that all objects, in the targeted space, have the same probability of being sampled and hit by the desired probe (Geuna, 2005). Although some controversy still exists regarding the best suited methodology, it should be noted that the choice of method for each case should rely on the nature of the material under study, the type of object being quantified and on the level of accuracy required (Guillery, 2002). The latter is quite

important since it is recognised that assumptions inherent to “model-based” strategies cause an uncontrolled amount of bias, which only emerge when estimations by “model” and “design-based” techniques are compared in detail (West, 1993; Von Bartheld, 2002). To the best of our knowledge, this has never been performed in liver research.

It is curious that in terms of structural and functional complexity the brain is said to be immediately followed by the liver (Malarkey *et al*, 2005), but in the use of stereology these organs are ranked far apart. A search in Web of Knowledge^{SM} using the keywords “stereology/stereological” and “brain” renders around 3 times more results comparing with “stereology/stereological” and “liver”. The number of studies in both rodents and humans is still relatively low: apart from data gathered in normal conditions, at least for the rat model (Marcos *et al*, 2004; 2006; Santos *et al*, 2009), stereological tools already enabled detailed analyses of the effects of few substances (Valenca *et al*, 2008; Halici *et al*, 2009; Karbalay-Doust and Noorafshan, 2009; Odaci *et al*, 2009) and specific diets (Aguila *et al*, 2003; Souza-Mello *et al*, 2007; Altunkaynak and Özbek, 2009) in selected hepatic cells. However, those technical tools have never been used to disclose morphological features of the ageing process in the liver, and the eventual gender dimorphism that may be present during that course.

1.6.1- Sampling liver fragments for stereological purposes

The sampling strategy is often overlooked outside the stereology field (Ochs, 2006). In stereology, the minimum workload should be always balanced with the aimed precision of the quantitative information, considering the natural biological variability. The two pillars of the current strategies are the principles of both random and systematic samplings, in order to give each particle (*e.g.*, a cell) being studied an equal opportunity to be sampled (Kordower, 2000). In other words, the entire structure is sampled with equal probability — meaning that two or three presumably “representative” sections from the middle of the organ may be unacceptable in the light of stereology, since they produce an undetermined amount of bias if cells are unequally distributed in the organ (Dorph-Petersen *et al*, 2001), or if they contain regional differences (intrinsic or derived from local factors such as differential vascular supply in a disease). Thus, using a fragment of a single liver lobe is inherently unrepresentative, since lobar heterogeneities have been described in normal and pathological conditions (as discussed in the beginning of this Chapter).

In a detailed and correct approach, the whole liver volume is first estimated and then a sampling cascade is applied, in order to obtain truly representative samples of all parts of the organ. Usually, around 5-10 pieces are analysed per animal to offer sufficiently precise and accurate estimates across a group (Marcos *et al*, 2004). Basically, two types of sampling have been applied in rodents to obtain liver pieces for fixation and processing

(Figure 1.5): 1) independent random sampling; 2) systematic uniform random (SUR) sampling. In the latter, the sampling variance is always reduced by a (natural or artificial) "smooth" arrangement of fragments: in the so-called "smooth fractionator", the fragments obtained from macroscopically slicing an organ (preferably with a constant slice thickness) are placed in a diamond-shaped pattern so that the size increases from each end to the middle (Nyengaard, 1999; Gundersen, 2002).

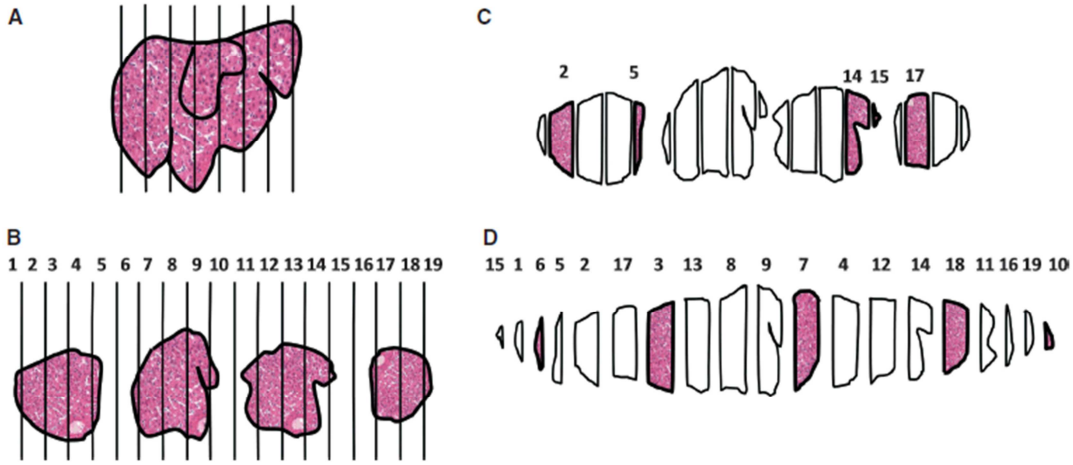

Figure 1.5 - Sampling cascade that can be applied in the liver: the liver is cut in slices (A), which are chopped in small fragments (B). Afterwards, the pieces can be selected by: (C) independent random sampling; in this case, five random numbers are taken from 1 to 19; (D) systematic uniform random sampling, meaning that the first fragment is taken at random (from 1 to 4, in this example) and then fragments are systematically sampled (every 4th fragment). In (D) a smooth fractionator was performed, as the pieces were rearranged smoothly, in a diamond shape pattern (with larger pieces in the middle and smaller ones at the periphery). (Image published in *Marcos et al, Journal of Anatomy, 2012.*)

In some species (*e.g.*, many fishes), the liver is naturally smooth arranged after sectioning, but, for instance in the rat, it is irregular (as described in the beginning of this Chapter), and the liver slices have to be reordered in the desired smooth distribution (Figure 1.5D). This will add an extra (but easy) step while sampling liver pieces, but considering the gain in sampling efficiency it is worth doing, as already illustrated by us in rats (Marcos *et al*, 2004). The use of SUR sampling has a consequence in terms of determining the coefficient of error (CE): the conventional formula ($CE = CV / \sqrt{n}$, where CV and *n* refer to the coefficient of variation and number of objects measured or counted, respectively) often does not apply, because fragments are not completely independent from each other (for instance in Figure 1.5D, the 6th fragment [#17] is only sampled if fragment #1 was sampled, *i.e.*, if 2 was the random number picked and the sampling period was 4). For this reason, special formulas for estimating the CE have been developed and tuned up over time, for instance, for the V estimation with the Cavalieri-point counting method (Gundersen *et al*, 1999) or for the N estimation with the fractionator

(Schmitz and Hof, 2000); these newer *formulae* incorporate the systematic sampling variation, which comes from the variation of the targeted stereological parameter between each section (Howard and Reed, 2005).

It is opportune to mention that, recently, a non-uniform random sampling method was developed: the proportionator (Gardi *et al*, 2008) is said to increase the efficiency for up to 25%, when compared with SUR sampling (Boyce *et al*, 2010). Although never used in the liver, it may be useful in studies with histochemical or immunohistochemical staining [*e.g.*, after centrilobular staining with antibodies against glutamine synthetase (GS)]. In that case the sampling of all fields would be proportional to the staining intensity, determined by image analysis (Boyce *et al*, 2010).

1.6.2- Fixation and processing of liver pieces for stereological purposes

Fixation and processing for microscopy always produces artefacts in tissues and the liver is not an exception. The choice of fixative depends mainly on the type of analysis, if light and/or transmission electron microscopy (or other) are being considered, and on the targeted cell; eventually requiring specific tagging for proper identification, for instance by immunohistochemistry. Fixation delay, the type of fixative and its acidity have been reported to play a role (Baak *et al*, 1989, Wisse *et al*, 2010). In optical microscopy, most studies use buffered formalin, because it is reported to produce fewer artefacts. Bouin's fixative and mercury formalin, for instance, have been reported to reduce the nuclear profile area of HEP by 25% (Baak *et al*, 1989). Moreover, the fixation route may also be important: perfusion fixation (through the portal vein or transcardiacally) always renders the best fixation (Wisse *et al*, 2010) but, by flushing the vascular bed, it was reported as providing estimates of volume fraction of sinusoids that are greater when compared with immersion fixed livers (Blouin *et al*, 1977). Even the dehydration step can influence stereological estimations, since it was proved that the numerical density of nuclei in acetone dehydrated liver pieces is larger than in ethanol dehydrated ones (Baak *et al*, 1989). Ultimately, it is the embedding medium that will majorly affect the stereological estimations and, consequently, several issues have to be considered when choosing the best embedding medium for a particular study.

Paraffin embedding is usually sufficient for routine diagnosis and may be adequate for most clinical applications of quantitative histopathology, if bias is controlled by careful standardisation (Laderkarl, 1998). Optimal processing is crucial in paraffin embedding, because relatively subtle changes in procedures may have a dramatic influence in the measurement results (Laderkarl, 1998). With paraffin, serial sectioning is easy, good morphology is achieved and nowadays it is compatible with most antibodies used in hepatology. Although differential z-axis compression along the section and shrinkage can

undermine the estimations, it has been commonly recommended for counting particles (Von Bartheld, 2002; Geuna, 2005). Some authors still recommend frozen cryostat sections for counting procedures (Baryshnikova *et al*, 2006), but it should be noted that the morphology is generally poor and serial sectioning (often required in stereological procedures) is not easy (in our experience), being even reported as extremely difficult (Von Bartheld, 2002). On the other hand, the (much more expensive) methacrylate and epoxy resins provide excellent preservation of structural details with very little shrinkage and distortion; although embedding is more cumbersome than with paraffin, they provide very thin sections and are generally recommended for volume estimations (Laderkarl, 1998); methacrylate can actually provide a broader range (0.5-40 µm) of section thickness when compared to paraffin. Shrinkage and unequivocal cell identification are the two factors to keep in mind when processing tissues for stereological studies, particularly those targeting cell sizes. It is unanimously agreed that shrinkage is relevant in volume and area estimations in cryostat and paraffin sections, but not in methacrylate or epoxy ones (Laderkarl, 1998; Mouton, 2002). Due to shrinkage, cells appear smaller and closer to each other in paraffin and cryostat sections. Shrinkage is less pronounced in the latter: the nuclear area of guinea-pig HEP in cryostat sections was 16% larger when comparing with paraffin (Baak *et al*, 1989). Since cells appear closer to each other, shrinkage also influences number estimations (*viz*., the numerical density). In all these cases, it must be measured in order to correct final estimations. A simple way to do this is to photograph a liver fragment before fixation and processing and after sectioning and mounting; a comparison of the fragment area in the 2 images estimates the two-dimensional (2D) shrinkage (Mouton, 2002), which can then be used to correct the three-dimensional (3D) estimates.

Unambiguous cell identification is essential for all stereological estimations: if only a fraction of cells are identified and counted/measured the estimation will not (or only by chance) represent the whole cell population. In the liver this is of particular importance since the routine haematoxylin-eosin staining does not allow a reproducibly accurate identification of some cells — like virtually all HSC and some KC (Malarkey *et al*, 2005; Roskams *et al*, 2007). In this vein, the need for special tagging procedures like immunohistochemistry will have to be weighed: if most antibodies work equally well in cryostat and paraffin sections, they do not in methacrylate ones (in this case, a special glycol methacrylate for immunohistochemistry will have to be considered).

1.6.3- Estimation of volume by stereological methods

With the liver tiers in mind, various volumes can be estimated: whole liver volume (V), the volume density of each structural component (V_V) and the local volumes, which include

the number-weighted volume ($\overline{v}_N$) and the volume-weighted volume ($\overline{v}_V$) of any structurally definable “particle”, such as the nucleus or the cell.

In hepatology, the $V_{(liver)}$ is often required in animal experimentation, namely for assessing hepatomegaly in toxicological studies in the rat (Carthew *et al*, 1996) and in clinical medicine in humans, as an indicator of therapeutic effectiveness or in the evaluation of liver cirrhosis (Sahin *et al*, 2003). In addition, this estimation is crucial in liver transplantation, especially with living donors, since the volume of the graft and of the remaining liver have to be (ideally) precisely estimated preoperatively to avoid postoperative complications (Duran *et al*, 2007). In humans, accurate information about the liver volume can neither be obtained by routine physical examination nor from biopsy material (Sahin *et al*, 2003).

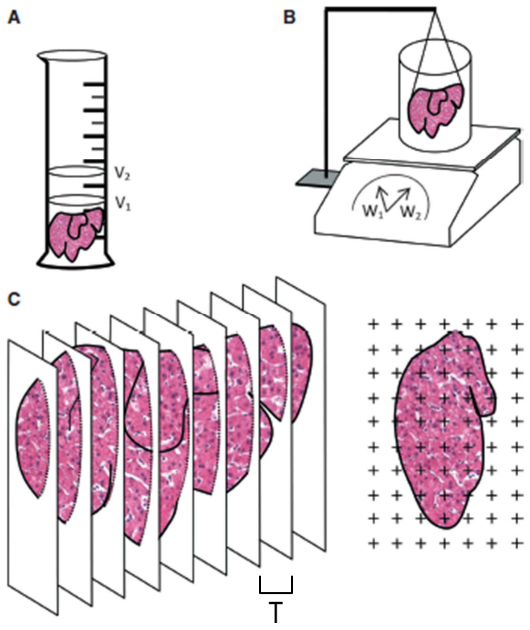

Figure 1.6 - Methods to estimate total volume (V) of liver. (A) Fluid displacement, in which the liver is immersed in graduated cylinder and $V = V_2 - V_1$ (corresponding, respectively, to the volume after and before immersion). (B) The Scherle’s method consists of a container with isotonic saline, placed on a precision weighing balance. The liver is fully immersed but suspended by a thin thread and $V = (W_2 - W_1) / \sigma$, in which W_2 and W_1 correspond to the weight after immersion and weight of the container with water, respectively, and σ is the specific gravity of isotonic saline; as $\sigma = 1.0048$, in practice $V = W_2 - W_1$. (C) In Cavalieri point-counting the whole organ must be cut, from end to end, in a series of parallel planes constantly distanced by (T); to avoid bias, the first section must be uniform random in an interval 0-T. A point grid is used, with an area associated with each point (a/p). By counting the number of points (P), the areas of the cut surfaces (Σareas) are determined, and finally V is estimated as $V = T \times a/p \times \Sigma P$. (Image published in *Marcos et al, Journal of Anatomy, 2012.*)

Presently, three methods exist for estimation of the liver volume (Figure 1.6): 1) direct fluid displacement; 2) Scherle's method; and the 3) Cavalieri's principle, which is most often associated with point counting and can be applied to microscopy or radiological images.

The fluid displacement approach is based on Archimedes' principle, in which the whole organ is immersed in a suitable liquid and the displaced fluid volume is directly measured in a graduated cylinder. It is more suitable for small livers, like in the rat (Altunkaynak and Özbek, 2009), tending to be less practical and precise in large organs that do not fit well in a graduated cylinder or beaker (Sahin *et al*, 2003); it should be noted that the sensitivity of the estimation depends directly on how finely the container is calibrated (Mouton, 2002).

The second method is a modification introduced by Scherle (1970) over forty years ago. It has been used in mouse (Karbalay-Doust and Noorafshan, 2009) and rat liver (Aguila *et al*, 2003; Souza-Mello *et al*, 2007; Valenca *et al*, 2008; Halici *et al*, 2009). In the Scherle's method, the organ is also fully immersed in fluid (of known density), but now suspended by a thin thread (care must be taken so that the liver does not touch the side or bottom of the container) — because the density of the used fluid is typically 1 (*e.g.*, for the common isotonic saline, 0.90% w/v of NaCl, the density is 1.0048), in practical terms the V corresponds to the weight increase after immersion (Scherle, 1970; Mandarim-de-Lacerda, 2003). It is more precise than water displacement, being recommended for larger organs (Mandarim-de-Lacerda, 2003; Howard and Reed, 2005). The most used technique nowadays is that of the Cavalieri. Paradoxically, this method was developed in the seventeenth century by the mathematician Bonaventura Cavalieri (1598–1647). Its implementation requires that the whole organ must be cut from end to end in a series of parallel planes distanced by (T); to avoid bias, the first section must be uniform random in an interval 0-T. The areas of the cut surfaces are typically estimated by a point grid (but other type of measurements, even automated, can be used), that has a known area associated with each point (*a*/*p*). By counting the number of points (P) falling on the liver surface in every section, the V is then calculated as:

$$V = T \times a/p \times \Sigma P$$

In practical terms, only a few hundred points (around 200) on 10-15 sections need to be counted per organ, in order to get an acceptable CE around 5-10% (Howard and Reed, 2005). It should be stressed that point-counting is actually a very fast process. In mouse and rat, the liver is easily embeddable but in the case of large organs other strategies exist: 1) it can be embedded in agar, sectioned, and the Cavalieri directly applied to the slices — this is a common approach in brain studies (Mouton, 2002); 2) the liver can be trimmed and then sampled into a small known organ fraction, using the fractionator (Gundersen, 1986), embedded in plastic resin (methacrylate) or in paraffin and the

Cavalieri-point counting applied to microscopy images — this so-called “volumetric fractionator” was originally developed for the lung (Geiser *et al*, 1990), but was applied recently in the liver (Altunkaynak and Özbek, 2009); 3) quantitative radiology may be used (Roberts *et al*, 2000). In the latter method, virtual “slices” are produced by computer tomography (Sahin *et al*, 2003; Mazonakis *et al*, 2004; Aydinli *et al*, 2006; Duran *et al*, 2007) or magnetic resonance (Sahin and Ergur, 2006), and point counting is then straightforward. In the liver, the three methodologies produced similar and correlated results (Sahin *et al*, 2003; Altunkaynak and Özbek, 2009), although it may be argued that fluid displacement and Scherle’s method are simpler and have the advantage of generating estimations closest to the *in vivo* reality, when compared with the Cavalieri-point counting after embedding and cutting (which generates estimations closer to the final dimensions of the tissue). Nevertheless, this issue may be obviated with radiology images, in which the Cavalieri-point counting estimates the volume of a fully blood perfused organ (Duran *et al*, 2007). The Cavalieri-point counting has one interesting advantage of allowing the estimation of subcomponent volumes — *e.g.*, volume of the parenchyma and sinusoids (Howard and Reed, 2005; Altunkaynak and Özbek, 2009) — whereas it may not require much additional effort when integrated into the sampling scheme for light microscopy (Marcos *et al*, 2003, Howard and Reed, 2005).

The volume density (also named relative volume or volume fraction) is a ratio between volumes — for instance, the V_V(HEP, liver) stands for the volume occupied by HEP in the whole liver. This is an intuitive parameter, unbiasedly estimated by overlaying a test-system of points (Figure 1.7) and then counting those falling over the HEP and those over the reference space (the whole liver in this case). The ratio of points (P), gives the estimation of volume:

$$V_V(\text{HEP, liver}) = P_P(\text{HEP, liver}) = P(\text{HEP}) / P(\text{liver})$$

According to the Delesse’s principle — dating from 1843 but only used in the biology field from 1963 on (Mouton, 2002) — the volume fraction of an object also varies proportionally to their area fraction as measured in random 2D sections or planes, thus meaning that V_V(HEP, liver) = A_A(HEP, liver) = P_P(HEP, liver). In other words, this means that each point controls an area in a 2D liver section, which is related to a defined volume in the 3D organ (Howard and Reed, 2005). The volume fraction is one of the oldest stereological parameters and virtually every liver structure has already been point-counted, either in optical and/or electron microscopy. Most of the gathered information refers to the rat; in other species the data is relatively scarce, but curiously points to the same figures, since for example the mean V_V(HEP, liver) in mouse ranges from 70.9 % (Karbalay-Doust and Noorafshan, 2009) to 78.0% (Neves *et al*, 2006), whereas in man it was estimated as

79.3% (Rohr *et al*, 1976). It is noteworthy that in recent years point counting (incorporated in image analysis software) has been also used in pathological conditions, namely for evaluating the degree of cirrhosis (Vizzotto *et al*, 2002; Vertemati *et al*, 2004), the outcome of liver transplants (Vertemati *et al*, 2005), and the diagnosis of hepatocellular carcinoma (Vertemati *et al*, 2008).

Point counting can be used jointly at different resolution levels, such as at light and electron microscopy. For instance, the volume fraction of the HEP in the parenchyma is determined by the former and the volume fraction of mitochondria in HEP determined by the latter (Blouin *et al*, 1977). When determining the volume fraction of rare or small structures, a grid with at least two sets of points with different densities is recommended. Volume fraction estimations are granted unbiasedness if some conditions are met: 1) the objects (cells or organelles) must be cut at random, following a randomised sampling design; 2) over-projection has to be negligible — this occurs when the section thickness is less than one-tenth of the height of the particle being studied (Weibel and Paumgartner, 1978). A third potential pitfall is the differential shrinkage, *i.e.*, uneven shrinkage throughout the organ due to processing (Dorph-Petersen *et al*, 2001); however, in contrast with the lung (Ochs, 2006), this is not considered relevant in the liver, since it is a homogeneous organ. This does not mean that differences in the volume ratios do not occur due to processing — as already mentioned, the volume fraction of sinusoids is higher in organs fixed by perfusion than those fixed by immersion (Blouin *et al*, 1977). Volume estimations also include the so-called local volumes, typically applied to cells or more often to their nuclei — *i.e.*, the nuclear $\overline{v}_V$ and $\overline{v}_N$. The $\overline{v}_V$ is not an intuitive parameter as it involves sampling the particle (say the nucleus) in proportion to their volume, therefore traducing the nuclear size variation and pleomorphism (Sørensen, 1992). It is mostly used in histopathology, since the parameter quantitatively grades malignancy, being correlated with prognosis in different neoplasms (Binder *et al*, 1992; Sørensen, 1992; Fujikawa *et al*, 1995; Ladekarl, 1998; Yörükoglu *et al*, 1998). The nuclear $\overline{v}_V$ of HEP was determined only once in preneoplastic lesions in the rat (Jack *et al*, 1989), but this parameter may be useful for differentiating regenerative nodules from well differentiated hepatocarcinomas.

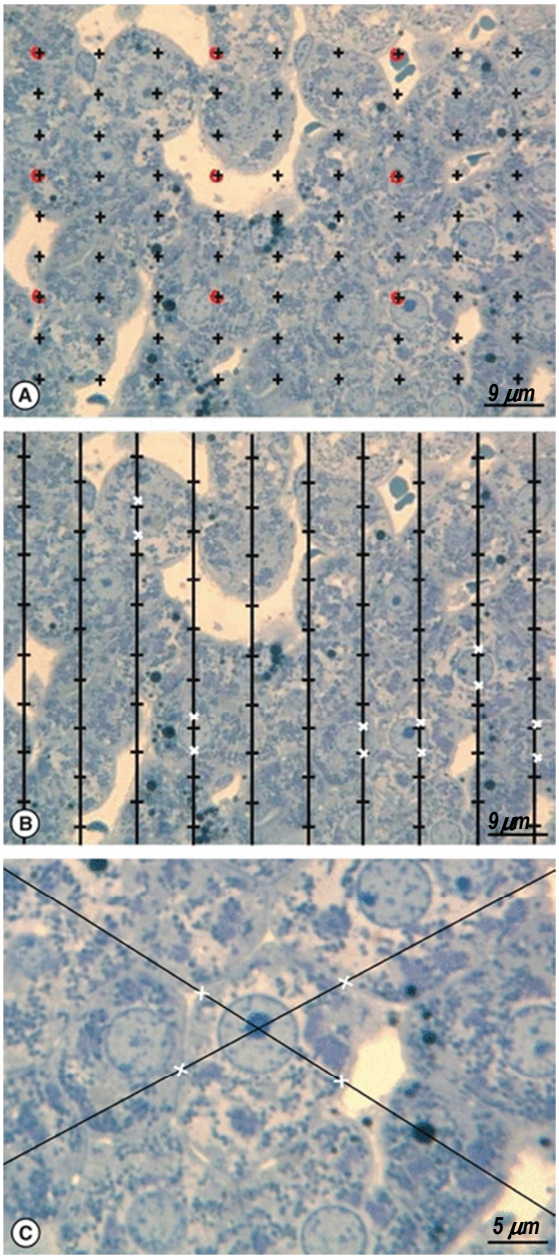

Figure 1.7 - (A) The relative volume of hepatocytes (HEP), V_V(HEP, liver) is estimated by counting those points falling on HEP and those in the reference space (the whole liver in this case). In order to avoid counting an excessive number of points, two different point densities can be used: the sparser ones (here in red) quantify larger structures. The V_V (HEP, liver) = P(HEP)/[P(liver) x κ], in which κ is a constant, representing the number of denser points "controlled" by sparser ones (here κ = 9). (B) Estimation of the volume-weighted mean nuclear volume ($\overline{v}_V$) according to the point sampled intercepts. The nuclei are sampled according to their volume, by overlaying a grid of points at random and, for each nucleus hit by a point, the distance between both ends of the nuclei (white crosses) is measured. (C) Nucleator method for estimating number-weighted mean cell volume ($\overline{v}_N$) of HEP. After applying the disector to sample cells and selecting their nucleolus (when visible) the stereological system generates two lines passing through it; the operator then marks the intersections between the lines and cell borders (in this example). The average distance from the intersections to the nucleolus is used to estimate the ($\overline{v}_N$). (Image published in *Marcos et al, Journal of Anatomy, 2012.*)

The unbiased estimation of the nuclear $\overline{v}_V$ is based on measurements of point sampled intercepts (PSI) in isotropic uniform random oriented sections (Jensen and Gundersen, 1985). The PSI method is a two-step procedure that involves: 1) sampling the particles (cells or nuclei) according to their volume, by overlaying a grid of points at random; 2) for each particle hit by a point, a line is drawn from the point to the particle border, in an isotropic direction (*i.e.*, all directions to the border are possible and equally probable); 3) a second line is drawn in the opposite direction and both distances are measured using a rule, with a linear or a non-linear scale (Figure 1.7). The $\overline{v}_V$ is then derived by applying the formula:

$$\overline{v}_V = (\pi / 3) \text{ x } \overline{l}_0^3$$

The procedure is tedious and time consuming if done manually — nowadays most studies use stereological packages (*e.g.*, newCast, Stereo Investigator, Stereologer). In the liver, the PSI was applied only to HEP of the rat, leading to a mean estimation of 5390 μm^3 and 8280 μm^3 in mono- and binucleated cells, respectively (Jack *et al*, 1989). In theory, to apply the PSI an isotropic or vertical uniform random design must be followed (Howard and Reed, 2005), as recently Karbalay-Doust and Noorafshan (2009) did, by using the orientator. However, for practical purposes the liver can be considered not oriented, in the sense that it is not possible to infer the orientation of a section by observing its histological appearance, because, overall, liver cells are randomly oriented, following all possible directions in 3D (Mandarim-de-Lacerda, 2003). Moreover, HEP nuclei are quite roundish, and virtually isotropic in 3D, meaning they have practically the same structural properties irrespective of orientation. Therefore, for most practical purposes, if liver biopsies are cut at random and thin sections are used, the PSI can be applied straightforwardly to all liver cells (Mouton, 2002).

The number-weighted mean volume ($\overline{v}_N$) can be related to the $\overline{v}_V$ by the formula:

$$\overline{v}_V = \overline{v}_N \text{ x } (1 + CV_n^2(V))$$

This means that $\overline{v}_v$ is always higher or, at least, similar to the $\overline{v}_N$ namely when the $CV_n^2(V)$ is small — in other words, when the cell volume is homogeneous, having low anisocytosis or anisokaryosis, the $\overline{v}_V \cong \overline{v}_N$. To estimate the $\overline{v}_N$ several direct and indirect approaches exist, and the so-called direct methods include the: 1) selector; 2) nucleator; and 3) rotator. These methods are actually ordered by their efficiency and chronological appearance (Nyengaard, 1999). The selector (Cruz-Orive, 1987) is more laborious and uses a random point inside the cell, whereas the nucleator (Gundersen, 1988) uses a fixed point, like the nucleolus. So far, only the nucleator has been used in the liver (Jack *et al*, 1989; 1990; Karbalay-Doust and Noorafshan, 2009). Although this method was

originally designed for mononucleated cells (Gundersen, 1988), it can also be used in binuclear hepatocytes (BnHEP); the sole adaptation is that the first nucleus with the nucleolus that appears in focus is considered for the measurements (Jack *et al*, 1989). Like the PSI, the nucleator is also a two-step procedure (Figure 1.7 C), but it does not require a grid of points to sample whatever targeted cells or particles — instead, these are sampled by either the optical or the physical disector, both of which sample cells in proportion to their number. Afterwards, one or two isotropic lines are drawn from the nucleolus to the nuclear or cellular border. The rotator (Jensen and Gundersen, 1993) can also be applied either to isotropic or to vertical uniform random sections. In this case, the vertical axis of the particle is first defined and then a grid of three or four lines is oriented perpendicularly to that axis, and the distances between these lines and the nuclear or the cellular borders are measured. It is often viewed as the most efficient method, because in each sampled particle six or more measurements can be recorded (Mouton, 2002; Tandrup, 2004). In either case, the mean distance (from the nucleolus or from the vertical axis) to the particle border, from a series of measurements, is used for estimating the number-weighted mean volume ($\overline{v}_N$):

$$\overline{v}_N = (4\pi / 3) \times \overline{l}_n^3$$

It must be stressed that for estimating the local volumes ($\overline{v}_N$ and $\overline{v}_V$) the borders must be unambiguously recognised. This is easy with nuclei, but problems may exist with cell borders; in HEP, these can be sometimes sufficiently well recognised in semithin epoxy sections (used in the PSI and the physical disector), but definitely not in routinely haematoxylin-eosin stained thick sections (used in the optical disector). In that case, an immunohistochemistry staining for the membranes would be needed (Marcos *et al*, 2003; 2006), as will be detailed in Chapter 3. Note that if paraffin is used, shrinkage effects must be accounted for and corrected at the end. If a plastic resin is used for optical sections, the need for immunotagging remains, and so a special methacrylate (*e.g.*, Technovit 1900, Heraeus-Kulzer, USA) must be used. In KC and HSC recognition of cell borders is also difficult, because cells are highly irregular. To overcome this problem, it would be preferable to embed liver fragments in suitable methacrylate-based resins and perform immunohistochemistry with appropriate antibodies.

It is noteworthy that another approach for estimating $\overline{v}_N$ exists, being called indirect because it results from the ratio of two other estimations:

$$\overline{v}_N = V_V / N_V$$

where V_V and N_V are obtained by point-counting and by the disector, respectively. In this case, care must be taken to avoid bias from overprojection and shrinkage. This is

especially true if different types of embedding media and sections are used for the two estimations. For example, if the V_V would be determined in epoxy and the N_V in paraffin sections, the shrinkage would have to be estimated; namely to correct the N_V. Alternatively, if epoxy sections are used for both estimations, the shrinkage influence would be cancelled in the formula. Finally, if both the V_V and the N_V were estimated in paraffin sections, and even assuming homogenous shrinkage, the N_V would have to be corrected again for retraction, as the N_V would always be overestimated. Note also that if estimated in paraffin the V_V of a cell/nucleus is prone to over-projection effects.

1.6.4- Estimation of number by stereological methods

In many fields of hepatology, it is common to find the number of cells reported as "number per mm^2" or "number per high power field". These are actually cell profile numbers that do not provide a meaningful estimate of real number, because all cells will not have the same probability of being counted (Boyce *et al*, 2010). In fact, this has been recognised for almost a century — in a single section, cells will be counted in proportion to their size, shape, orientation, and spatial distribution, in addition to their number; therefore larger cells, irregular or those normal to the section plane will be more often counted (Mouton, 2002). This also occurs in the liver: HSC and KC are particularly known for their irregularity, but size heterogeneity has been reported for almost all liver cells (Malarkey *et al*, 2005). In this vein, a precise and accurate estimation of cell number must call for the new generation of stereological methods, as introduced in the past 25 years (Boyce *et al*, 2010).

The quantification of liver cells is important in different scenarios. By knowing the total number of HEP it is possible to evaluate whether hepatomegaly is due to hypertrophy or to hyperplasia, and this is relevant, for instance, in toxicological assays in rodents (Carthew *et al*, 1998), as well as in hepatocarcinogenesis studies, both in rodents (Bannasch, 1976) and humans (Kondo *et al*, 1988). Like in volume estimation, the use of stereology tools can generate absolute and relative parameters — *i.e.*, the total number (N) and the relative number or numerical density (N_V), respectively. The latter refers to the number of cells per unit of volume and is directly estimated by the disector (Sterio, 1984). This method was first introduced in neurosciences, but soon found applications in many other organs (Mayhew and Gundersen, 1996).

The disector can be viewed as a 3D counting box with inclusion and exclusion surfaces, in order to count cells as they appear in the probe. Instead of simply counting cell profiles (subjected to all the above cited inherent biases), this box enables counting cells in proportion to their real number. In the box, we can either analyse its full interior, in the

case of the optical disector, or the analysis can be restricted to the top and bottom of the box, being the middle part deduced — this is the case of the physical disector (Figure 1.8).

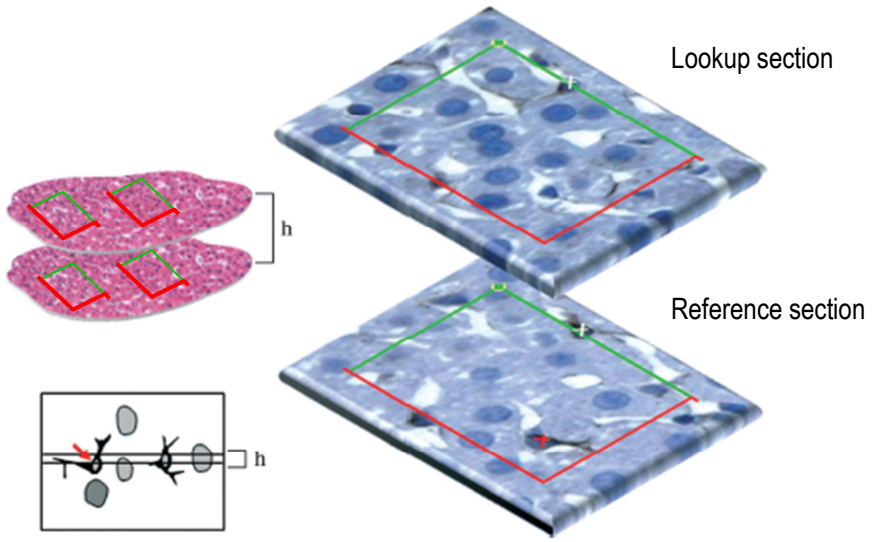

Figure 1.8 - The physical disector uses two thin sections, perfectly aligned and distanced by *h* (height of the disector). Then a counting grid is used (with exclusion and inclusion lines in red and green, respectively); here the procedure is illustrated for counting hepatic stellate cells marked with immunohistochemistry against glial fibrillary acidic protein. A cell is counted (here marked with a red cross) if present in the reference section but not in the lookup section. (Image published in *Marcos et al, Journal of Anatomy, 2012.*)

The physical disector was the first to be described (Sterio, 1984) and has been applied in liver, both to count HEP (Carthew *et al*, 1998; Aguila *et al*, 2003; Souza-Mello *et al*, 2007; Valenca *et al*, 2008; Altunkaynak and Özbek, 2009) and HSC (Marcos and Rocha, 2001). It consists of two thin sections separated by a fixed height (*h*), which has varied from 2 µm in HSC counting (Marcos and Rocha, 2001) to 3-5 µm height in HEP counting (Carthew *et al*, 1998; Aguila *et al*, 2003; Souza-Mello *et al*, 2007; Valenca *et al*, 2008; Altunkaynak and Özbek, 2009). This *h* is critical: 1) if it is too large the smallest cells to be counted can be missed in-between sections (*i.e.*, in the deduced middle part of the box), and the necessary alignment of the two sections will be cumbersome; 2) if it is too small, only a few or no cells will be counted, and the process will be inefficient. Our own experiences with physical disectors confirm those difficulties and the need to optimally adjust the *h* (Marcos and Rocha, 2001; Rocha *et al*, 2001); generally, it is recommended to be a third to a quarter of the height of the particles to be counted (Nyengaard, 1999).

In the physical disector, a cell is counted if present in the reference section but not in the lookup one. In order to avoid edge effects, an unbiased counting frame is used (with

inclusion and exclusion lines) in those sections (Gundersen, 1977). The counting procedure is actually easy, but the alignment of the liver sections can be a limiting step — due to the high cellularity and tortuous sinusoids. In our experience it tends to be time-consuming, particularly in paraffin sections. This may be partially overcome by using recent stereology workstations that integrate digital image recognition software for allowing a kind of "auto-alignment" or by using the optical disector probe.

In contrast to the physical disector, its counterpart optical method uses thick sections (Figure 1.9), which are most often observed with oil-immersion objectives that ideally should have the highest possible numerical-apertures, so that a thin focal plane actually scans the entire counting box. Naturally, the thinnest optical planes (matching the z-resolution) are obtained using a confocal microscope (Lemmens *et al*, 2010). Whatever the microscopy strategy, a built-in solution or additional equipment is needed, for instance a length gauge (microcator), to exactly determine the z distance between up and down planes of the disector (Howard and Reed, 2005). Anyway, the optical disector method is much faster than its physical form; in the liver, it has been used to count HEP (Marcos *et al*, 2006; Halici *et al*, 2008; Karbalay-Doust and Noorafshan, 2009; Odaci *et al*, 2009), HSC (Marcos *et al*, 2004) and KC (Kiki *et al*, 2007; Santos *et al*, 2009). In all these, paraffin thick sections were used and their thickness ranged from 15 µm (Karbalay-Doust and Noorafshan, 2009) to 40 µm (Odaci *et al*, 2009), whereas the optical disector height varied from 5 µm (Karbalay-Doust and Noorafshan, 2009) to 20 µm (Marcos *et al*, 2004; 2006; Santos *et al*, 2009).

The optical disector has been considered the standard of efficient unbiased number estimation for the past two decades, but over the years potential pitfalls in the method have been debated (Dorph-Petersen *et al*, 2001; Von Bartheld, 2002; Geuna, 2005; Baryshnikova *et al*, 2006). An issue that should be addressed is the so-called "z-axis compression": as a rule of thumb, the section thickness should be measured in every 5th field of vision and the intra- and intersectional coefficient of variation (CV) calculated (Dorph-Petersen *et al*, 2001). In our experience with thick liver sections, this variation is low, but if large variations do occur, the section thickness should be measured more frequently and a stratified fractionator (with larger disector heights in the thicker areas) should be considered (Dorph-Petersen *et al*, 2001).

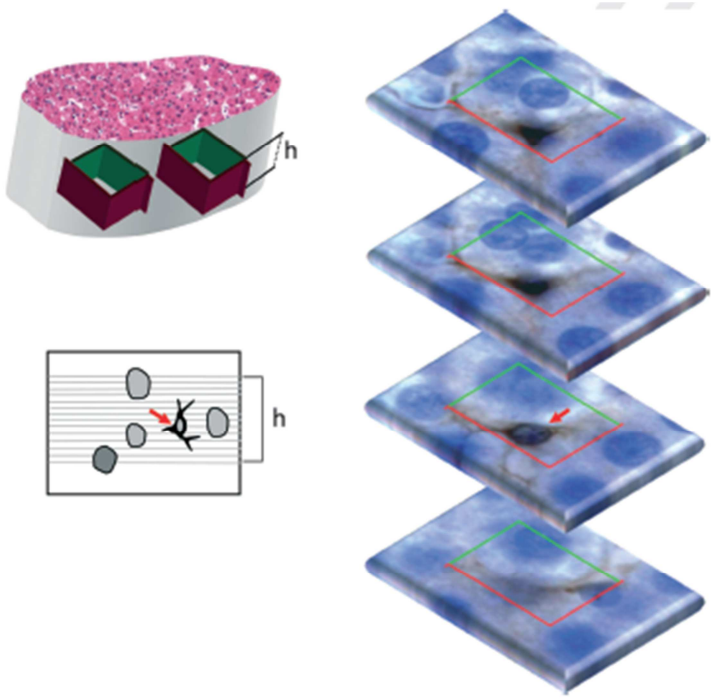

Figure 1.9 - The optical disector uses thick sections, which are optically scanned. The procedure is illustrated for counting hepatic stellate cells marked with immunohistochemistry against glial fibrillary acidic protein: a cell is counted (here marked with a red arrow) as it appears in focus within the disector height (*h*) and is within or touches the inclusion lines (green) but not the exclusion ones (red). (Image published in *Marcos et al, Journal of Anatomy, 2012.*)

Another potential pitfall refers to the loss of nuclear fragments dragged by the knife during sectioning — the so-called lost caps (Mayhew and Gundersen, 1996). In paraffin sections, it has been shown to affect up to one-third of the sectioned nuclei (Helander, 1983). To cope with this, guard spaces (or guard heights) in the upper and lower surfaces of the thick sections have been recommended, ever since the beginning of the implementation of the method, thus restricting the analysis to the central core of the thick section (Gundersen, 1986). In the liver, all studies have included minimal guard spaces of 4-5 µm, but their use is nowadays controversial because some authors argue that it may produce a 10% underestimation of particles (Gardella *et al*, 2003; Baryshnikova *et al*, 2006). At least in the nervous tissue, it has been shown that particles appear to move along the z-axis as they are sectioned and stained, thus generating a bimodal distribution of particles — *i.e.*, particles are more abundant in the upper and lower surfaces of the thick sections, inducing a central core depletion (Hatton and Von Bartheld, 1999; Von Bartheld, 2002; Baryshnikova *et al*, 2006). This distribution affects mainly paraffin and methacrylate sections and is influenced by delayed fixation, tissue processing and even knife cutting angles — which is considered the most relevant factor (Baryshnikova *et al*, 2006). Since it

is uncertain whether the bimodal distribution occurs in all tissues, it is generally recommended to check it before starting every new experiment, by recording the z-axis position of 250-350 particles in different sections (Baryshnikova *et al*, 2006). This procedure is also useful to assess that the staining (especially in immunohistochemistry slides) encompasses all tissue thickness, thus ensuring that all existing cells can be recognised and counted with the optical disector. In this way, a fundamental prerequisite of the method is fulfilled. In the case of the liver, this eventual bimodal distribution was not observed when counting HEP nuclei in our in-house trials with the rat liver (Annex 1).

It is noteworthy that the disector directly provides relative numbers (N_V), which are strongly influenced by the embedding medium, namely by paraffin shrinkage (Mouton, 2002). When using paraffin or cryostat sections for this method, the obtained figures are necessarily overestimations that should be corrected for the shrinkage to be directly meaningful in 3D (Marcos *et al*, 2006) — only estimations in glycolmethacrylate or in epoxy resin will tend to approach and practically match the real values. So far, estimations in the rat with paraffin thick sections (and "design-based" methods) and with epoxy sections (and "model-based" stereological techniques) have been of the same order of magnitude, ranging ≈ 1.6-folds (Loud, 1968; Marcos *et al*, 2006).

Two unbiased approaches are available for obtaining N (Figure 1.10): the fraction-based optical fractionator (West *et al*, 1991), and the volume-based ratio-technique (Pakkenberg and Gundersen, 1988). The latter is a two step analysis, since it results from the product of the N_V and the respective reference volume (V), which is usually the whole organ ($N = N_V \times V$). This strategy has been used in the liver to estimate the N of HEP, for example when evaluating different types of diet in rats (Souza-Mello *et al*, 2007; Altunkaynak and Özbek, 2009) and the N of KC in rats fed with a high fat diet (Kiki *et al*, 2007). Nevertheless, the ratio-technique may be influenced by eventual volume-related deformations during processing, and it may produce biases when the N_V and V cannot be measured in the same sections (Dorph-Petersen *et al*, 2001). Additionally, it is generally more time consuming than the optical fractionator (Tandrup, 2004) and, according to computer simulations, the existing methods to predict the CE of N do not seem to generate adequate predictions (Schmitz and Hof, 2000). Even so, the ratio-technique is valuable in many occasions, namely in studies combining light and electron microscopy and when it is unpractical to section the entire organ (Howard and Reed, 2005); in these cases, the V is estimated by one of the previously discussed methods.

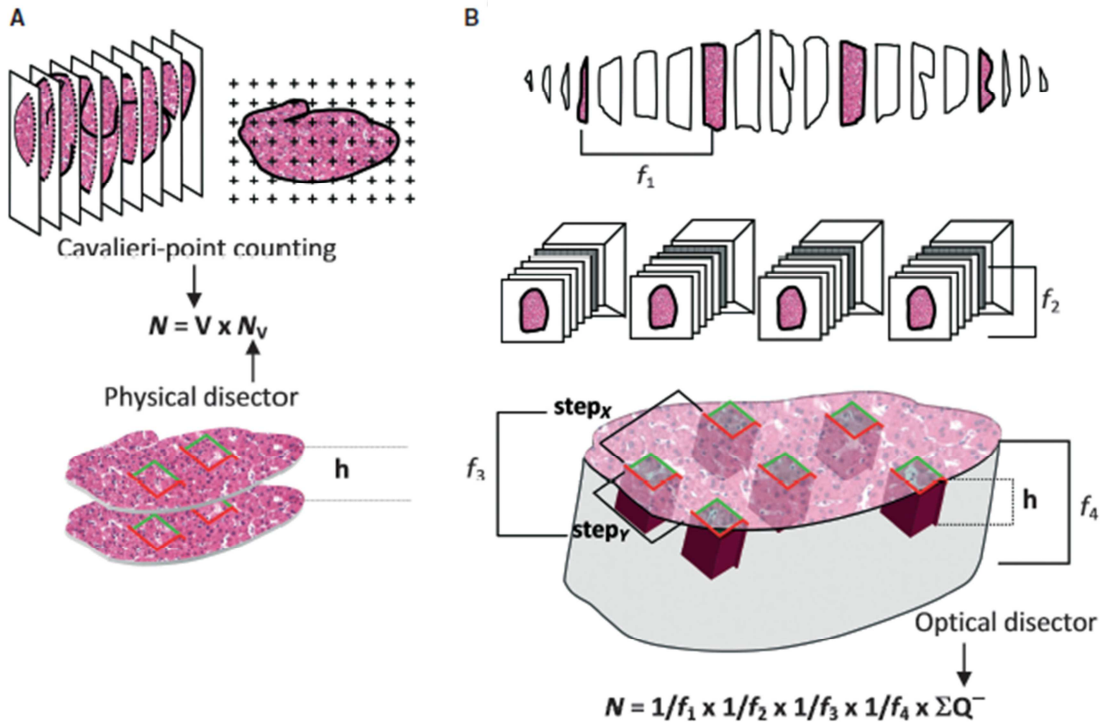

Figure 1.10 - Strategies to determine the total number (N). (A) Ratio-technique, here exemplified by Cavalieri point-counting and the physical disector. (B) Optical fractionator, in which a fraction of liver fragments is sampled (f_1); the paraffin blocks are exhaustively sectioned (thick sections) and a fraction of these are sampled (f_2). Sections are analysed and the stage performs step movements in x-y, so that a fraction of the area is sampled (f_3). Finally, in the optical disector, only a fraction (f_4) of the tissue thickness is analysed (f_4). In this latter procedure, all the cells are counted (ΣQ^-); *h*: disector height. (Image published in *Marcos et al, Journal of Anatomy, 2012.*)

In contrast to this, the optical fractionator estimates N in a more direct and consequently more efficient way (West *et al,* 1991). It selects cells based on their existence, since it combines the optical disector (Gundersen, 1986), that samples cells in proportion to their number, with the fractionator principle (Gundersen, 1986). A modification of this sampling technique is called the smooth fractionator (Gundersen, 2002), discussed previously. So far, the optical fractionator has been used to estimate the N of HEP (Marcos *et al*, 2006; Odaci *et al*, 2009), of HSC (Marcos *et al*, 2004) and of KC (Santos *et al*, 2009).

It is opportune to inform that there is also the possibility of using physical disectors instead of optical ones, and the method is called the physical fractionator. To our knowledge, there is yet no published paper with this approach on the liver of rodents. Usually the method is much more laborious than the optical fractionator, namely due to the already mentioned continuous need to align the two sections/planes under analysis. To overcome this, a recent advance entitled AutoDisector™, included in a stereological package

(newCast, Visiopharm), offers automation and thus better efficiency. It can be an option, especially considering that the physical disector is less sensible to shrinkage than the optical counterpart and the immunohistochemical protocol is much more straightforward.

1.7- Objectives

Keeping in mind that understanding and dealing with medical problems greatly benefits from the so-called fundamental scientific knowledge, and, in view of our hypothesis, that intrinsic structural differences in the liver may justify (at least partially) the increased fibrosis progression seen in males and elders, we intended to study (with cutting-edge quantitative morphology and immunohistochemistry):

1 - The HSC pool, for which we hypothesise that males and elders should have more HSC per unit of liver weight/volume. Within this context, and considering the liver heterogeneity, possible differences in the lobular distribution of cells were evaluated.

2 - The BnHEP pool, because these constitute the immediate response of liver cell loss by injury. Consequently, we hypothesised that males and elders should have relatively less BnHEP.

3 - The KC pool, since such cells boost the proliferation of HSC, and so changes in the HSC/KC numerical ratios with ageing and gender could influence the fibrotic processes.

Additionally, we wanted to investigate two other complementary hypotheses, namely by the study of antioxidant defence systems and by a flow cytometry approach:

4 – Since the first fibrotic stimulus is often triggered the release of ROS, we hypothesised that females should have more antioxidant enzymes, at least in the young age. The antioxidant defence systems of the liver are suspected to diminish with ageing and eventually, this dimorphism may be lost throughout ageing.

5 – Because fibrosis ultimately results from the inability of HEP to regenerate, and polyploidy nuclei delays this process, we further hypothesised that females would have a lower ploidy level of their HEP nuclei, which could promote or at least facilitate an higher regenerative potential.

In conclusion, in this Chapter we presented a general overview of the liver structure and emphasised the importance of rat models for the study of liver fibrosis and ageing in humans. It is now clear that this process involves a cellular interplay between liver cells, in which HSC, HEP and KC play important roles. The knowledge in the paracrine modulation within this triumvirate has increased substantially in the last years, due to advances in cell isolation procedures and molecular biology. Nevertheless the *in vitro* scenario often misses the functional cooperation between cells and much less is known about the

coordinate behaviour of liver cells *in vivo*. Recently, it has been emphasised that the microarchitecture of the liver is tightly regulated and that the establishment of wrong cell-cell (or cell-matrix) interactions drives the organ towards fibrosis (Hoehme *et al*, 2010). It has been hypothesised that a functional unit with a specific number of HEP and sinusoidal cells may exist in the liver (Rojkind *et al*, 2011). However, the ratios between different liver cells are largely unknown. Seminal studies in the sixties and seventies described the quantitative morphology of the liver, but this subject was never revisited. Moreover, it is unknown how the microarchitecture of the liver is affected by ageing and gender (two factors that have a major influence fibrosis progression). In the remaining sections of this Chapter, we detailed the most updated strategies for the quantification of numbers and volumes using stereological techniques, which will be the main foundations of this study.

In the following Chapters we will address the microarchitecture of the liver throughout ageing and gender, focusing in HSC, HEP and KC (respectively in Chapters 2, 3 and 4). For the sake of clarity, in each of these Chapters we will first detail the initial adaptations of the quantitative methods, under the heading “Baseline study”, and then report the age and gender data, under the heading “Age and gender study”. Finally, in Chapter 5 we intend to summarise all the collected data and define new paths for future research by our group.

1.8- References

Aguila MB, Pinheiro AR, Parente LB, Mandarim-de-Lacerda CA (2003) Dietary effect of different high-fat diet on rat liver stereology. *Liver International* 23, 363-370.

Altunkaynak BZ, Özbek E (2009) Overweight and structural alterations of the liver in female rats fed a high-fat diet: A stereological and histological study. *Turkish Journal of Gastroenterology* 20, 93-103.

Aydinli B, Kantarci M, Polat KY, Unal B, Atamanalp SS, Durur I, Unal D, Akgun M (2006) Stereological evaluation of treatment response in patients with non-resectable hepatic alveolar echinococcosis using computed tomography via the Cavalieri method. *Liver International* 26, 1234-1240.

Baak JPA, Noteboom E, Kovoets JJM (1989) The influence of fixatives and other variations in tissue processing on nuclear morphometrics features. *Analytical Quantitative Cytology and Histology* 11, 219-224.

Baba Y, Uetsuka K, Nakayama H, Dot K (2004) Rat strain differences in the early stage of porcine-serum-induced hepatic fibrosis *Experimental Toxicology and Pathology* 55, 325-330.

Bannasch P (1976) Cytology and cytogenesis of neoplastic (hyperplastic) hepatic nodules. *Cancer Research* 36, 2555–2562.

Baryshnikova LM, Halbach O, Kaplan S, Von Bartheld CV (2006) Two distinct events, section compression and loss of particles ("lost caps"), contribute to z-axis distortion and bias in optical disector counting. *Microscopy Research and Technique* 69, 738-756.

Bataller R, Brenner DA (2009) Hepatic fibrosis. In: *The liver: biology and pathobiology, 5th edition* (Arias IM, Alter HJ, Boyer JL, Cohen DE, Fausto N, Shafritz DA, Wolkoff AW eds), pp. 433-451. John Wiley & Sons Ltd.

Beresford WA, Henninger JM (1986) A tabular comparative histology of the liver. *Archivum Histologicum Japonicum* 49, 267-281.

Bhunchet E, Wake K (1998) The portal lobule in rat liver fibrosis: a re-evaluation of the liver unit. *Hepatology* 27, 481-487.

Blain RB, Reeves R, Ewald KA, Leonard D, Calabrese EJ (1999) Susceptibility to chlordecone-carbon tetrachloride induced hepatotoxicity and lethality is both age and sex dependent. *Toxicological Sciences* 50, 280-286.

Binder M, Dolezal I, Wolff K, Pehamberger H (1992) Stereologic estimation of volume weighted mean nuclear volume as a predictor of prognosis in "thin" malignant melanoma. *The Journal of Investigative Dermatology* 99, 180-183.

Blouin A, Bolender RP, Weibel ER (1977) Distribution of organelles and membranes between hepatocytes and nonhepatocytes in rat liver parenchyma – a stereological study. *Journal of Cell Biology* 72, 441–455.

Bouwens L, De Bleser P, Vanderkerken K, Geerts B, Wisse E (1992) Liver cell heterogeneity: functions of non-parenchymal cells. *Enzyme* 46, 155-168.

Boyce RW, Dorph-Petersen KA, Lyck L, Gundersen HJ (2010) Design-based stereology: introduction to basic concepts and practical approaches for estimating cell number. *Toxicologic Pathology* 38, 1011-1025.

Brouwer A, Barelds RJ, Knook DL (1985) Age-related changes in the endocytic capacity of rat liver Kupffer and endothelial cells. *Hepatology* 5, 362-366.

Bruix J, Boix L, Sala M, Llovet JM (2004) Focus on hepatocellular cancer. *Cancer Cell* 5, 351-372.

Busquets J, Xiol X, Figueras J, Jaurrieta E, Torras J, Ramos E, Rafecas A, Fabregat J, Lama C, Ibañez L, Llado L, Ramon JM (2001) The impact of donor age on liver transplantation: influence of donor age on early liver function and on subsequent patient and graft survival. *Transplantation* 71, 1765-1771.

Carthew P, Maronpot RR, Foley JF, Edwards RE, Nolan BM (1996) Method for determining whether the number of hepatocytes in rat liver is increased after treatment with peroxisome proliferator Gembrozil. *Journal of Applied Toxicology* 17, 47–51.

Carthew P, Edwards RE, Nolan BM (1998) New approaches to the quantitation of hypertrophy and hyperplasia in hepatomegaly. *Toxicology Letters* 102-103, 411-415.

Catta-Preta M, Mendonca LS, Fraulob-Aquino J, Aguila MB, Mandarim-de-Lacerda CA (2011) A critical analysis of three quantitative methods of assessment of hepatic steatosis in liver biopsies. *Virchows Archives* 459, 477-485.

Collier TJ, Coleman PD (1991) Divergence of biological and chronological aging: evidence from in rodent models. *Neurobiology of Aging* 12, 685-693.

Cruz-Orive LM (1987) Particle number can be estimated using a disector of unknown thickness: the selector. *Journal of Microscopy* 145, 121-142.

Dahab GM, Kheriza MM, El-Beltagi HM, Fouda AM, El-Din O (2004) Digital quantification of fibrosis in liver biopsy sections: description of a new method by Photoshop software. *Journal of Gastroenterology and Hepatology* 19**,** 78–85.

Deng M, Kleinert R, Huang H, He Q, Madrahimova F, Dirsch O, Dahmen U (2009) Statistical and economical efficiency in assessment of liver regeneration using defined sample size and selection in combination with a fully automated image analysis system. *Journal of Histochemistry & Cytochemistry* 57, 1075-1085.

Desmet V (1992) Liver cirrhosis: evolving aspects of an old problem. In: *Cellular and Molecular aspects of Cirrohsis* (Clément B, Guillouzo A eds), pp. 1-9. Coloque INSERM / John Libbey Eurotext Ltd.

Di Martino V, Lebray P, Myers RP, Pannier E, Paradis V, Charlotte F, Moussalli J, Thabut D, Buffet C, Poynard T (2004) Progression of liver fibrosis in women infected with hepatitis C: long-term benefit of estrogen exposure. *Hepatology* 40, 1426-1433.

Dorph-Petersen KA, Nyengaard JR, Gundersen HJ (2001) Tissue shrinkage and unbiased stereological estimation of particle number and size. *Journal of Microscopy* 204, 232-246.

Duran C, Aydinli B, Tokat Y, Yuzer Y, Kantarci M, Akgun M, Polat KY, Unal B, Killi R, Atamanalp SS (2007) Stereological evaluation of liver volume in living donor liver transplantation using MDCT via the Cavalieri method. *Liver Transplantation* 13, 693-698.

Ekataksin W, Wake K (1991) Liver units in three dimensions: I. Organization of argyrophilic connective tissue skeleton in porcine liver with particular reference to the "compound hepatic lobule". *American Journal of Anatomy* 191, 113-153.

Ekataksin W, Wake K (1997) New concepts in biliary and vascular anatomy of the liver. In: *Progress in liver diseases. Volume XV* (Boyer JL, Ockner RK eds), pp. 1-30. WB Saunders.

Fawcett DH (1994) Liver and gallbladder. In: *Bloom and Fawcett. A textbook of Histology, 12th edition*, pp. 652-688. Chapman and Hall.

Featherstone B (2008) Causes of liver disease and dysfunction. In: *Drugs and the liver. A guide to drug handling in liver dysfunction* (North-Lewis P ed), pp. 49-72. Pharmaceutical Press.

Friedman SL, Roll FJ, Boyles J, Bissell DM (1985) Hepatic lipocytes: the principal collagen-producing cells of normal rat liver. *Proceedings of the National Academy of Sciences of the United States of America* 82, 8681-8685.

Fujikawa K, Sasaki M, Aoyama T, Itoh T, Yoshida O (1995) Prognostic criteria in patients with prostate cancer: correlation with volume weighted mean nuclear volume. *Journal of Urology* 154, 2123-2137.

Gardella D, Hatton WJ, Rind HB, Rosen GD, Von Bartheld CS (2003) Differential tissue shrinkage and compression in the z-axis: implications for optical disector counting in vibratome-, plastic and cryosections. *Journal of Neuroscience Methods* 124, 45-59.

Gardi JE, Nyengaard JR, Gundersen HJ (2008) The proportionator: unbiased stereological estimation using biased automatic image analysis and non-uniform probability proportional to size sampling. *Computers in Biology and Medicine* 38, 313-328.

Geerts A (2001) History, heterogeneity, developmental biology, and functions of quiescent Hepatic stellate cells. *Seminars in Liver Disease* 21, 311-335.

Geiser M, Cruz-Orive LM, Im Hof V, Gehr P (1990) Assessment of particle retention and clearance in the intrapulmonary conducting airways of hamster lungs with the fractionator. *Journal of Microscopy* 160, 75-88.

Geuna S (2005) The revolution of counting “tops”: two decades of the disector principle in morphological research. *Microscopy Research and Technique* 66, 270-274.

Ghirardi O, Cozzolino R, Guaraldi D, Giuliani A (1995) Within- and between-strain variability in longevity of inbred and outbred rats under the same environmental conditions. *Experimental Gerontology* 30, 485-494.

Greenwell P, Geerts A, Ogata I, Solis-Herruzo JA, Rojkind M (1994) Liver Fibrosis. In: *The liver: biology and pathobiology, 3rd edition* (Arias IM, Boyer JL, Fausto N, Jakoby WB, Schachter DA, Shafritzed DA eds), pp. 1367-1381. Raven Press Ltd.

Gressner AM, Lahme B, Brenzel A (1995) Molecular dissection of the mitogenic effect of hepatocytes on cultured hepatic stellate cells. *Hepatology* 22, 1507-1518.

Grisham JW (2009) Organizational principles of the liver. In: *The liver: biology and pathobiology, 5th edition* (Arias IM, Alter HJ, Boyer JL, Cohen DE, Fausto N, Shafritz DA, Wolkoff AW eds), pp. 3-15. John Wiley & Sons Ltd.

Grizzi F, Franceschini B, Barbieri B, Gagliano N, Arosio B, Chiriva-Internati M, Annoni G, Dioguardi N (2002) Mast cell density: a quantitative index of acute liver inflammation. *Analytical and Quantitative Cytology and Histology* 24, 63-69.

Guillery RW (2002) On counting and counting errors. *Journal of Comparative Neurology* 447, 1-7.

Gundersen HJG (1977) Notes on the estimation of numerical density of arbitrary particles: the edge effect. *Journal of Microscopy* 111, 219-223.

Gundersen HJG (1986) Stereology of arbitrary particles: a review of unbiased number and size estimators and the presentation of some new ones, in memory of William R. Thompson. *Journal of Microscopy* 143, 3-45.

Gundersen HJ (1988) The nucleator. *Journal of Microscopy* 151, 3-21.

Gundersen HJ, Bagger P, Bendtsen TF, Evans SM, Korbo L, Marcussen N, Møller A, Nielsen K, Nyengaard JR, Pakkenberg B, Sørensen FB, Vesterby A, West MJ (1988) The new stereological tools: disector, fractionator, nucleator and point-sampled intercepts and their use in pathological research and diagnosis. *APMIS* 96, 857-881.

Gundersen HJ, Jensen EBV, Kiêu K, Nielsen J (1999) The efficiency of systematic sampling in stereology – reconsidered. *Journal of Microscopy* 193, 199-211.

Gundersen HJ (2002) The smooth fractionator. *Journal of Microscopy* 207, 191-210.

Halici Z, Dursun H, Keles ON, Odaci E, Suleyman H, Aydin N, Cadirci E, Kalkan Y, Unal B (2009) Effect of chronic treatment of haloperidol on the rat liver: a stereological and histopathological study. *Naunyn Schmiedebergs Archives of Pharmacology* 379, 253-261.

Harrison SA, Kadakia S, Lang KA, Schenker S (2002) Nonalcoholic steatohepatitis: what we know in the new millennium. *American Journal of Gastroenterology* 97, 2714-2724.

Hashimoto M, Watanabe G (2000) Hepatic parenchymal cell volume and the indocyanine green tolerance test. *Journal of Surgical Research* 92, 222-227.

Hatton WJ, Von Bartheld CS (1999) Analysis of cell death in the trochlear nucleus of the chick embryo: calibration of the optical disector counting method reveals systematic bias. *Journal of Comparative Neurology* 409, 149-169.

Helander KG (1983) Thickness variation within individual paraffin and glycol methacrylate sections. *Journal of Microscopy* 132, 223-227.

Hilmer SN, Cogger VC, Le Couteur DG (2007) Basal activity of Kupffer cells increases with old age. *The Journals of Gerontology. Series A, Biological Sciences and Medical Sciences* 62, 973-978.

Hoare M, Das T, Alexander G (2010) Ageing, telomeres, senescence, and liver injury. *Journal of Hepatology* 53, 950-961.

Hoehme S, Brulport M, Bauer A, Bedawy E, Schormann W, Hermes M, Puppe V, Gebhardt R, Zellmer S, Schwarz M, Bockamp E, Timmel T, Hengstler JG, Drasdo D (2010) Prediction and validation of cell alignment along microvessels as order principle to restore tissue architecture in liver regeneration. *Proceedings of the National Academy of Sciences of the United States of America* 107, 10371-10376.

Howard CV, Reed MG (2005) *Unbiased stereology. Three-dimensional measurements in microscopy*, *2nd edition*. Garland Science/Bios Scientific Publishers.

Jack EM, Cruz-Orive LM, Waechter F, Stäubli W (1989) Unbiased estimation of cell and nuclear volume in preneoplastic and uninvolved tissue from the same rat liver using the nucleator. *Acta Stereologica* 8, 257-262.

Jack EM, Bentley P, Bieri F, Muakkassah-Kelly SF, Stäubli W, Suter J, Waechter F, Cruz-Orive LM (1990) Increase in hepatocyte and nuclear volume and decrease in the population of binucleated cells in preneoplastic foci of rat liver: a stereological study using the nucleator method. *Hepatology* 11, 286-297.

Jensen EB, Gundersen HJ (1993) The rotator. *Journal of Microscopy* 170, 35-44.

Kage M, Shimamatu K, Nakashima E, Kojiro M, Inoue O, Yano M (1997) Long-term evolution of fibrosis from chronic hepatitis to cirrhosis in patients with hepatitis C: morphometric analysis of repeated biopsies. *Hepatology* 25, 1028-1031.

Karbalay-Doust S, Noorafshan A (2009) Stereological study of the effects of nandrolone decanoate on the mouse liver. *Micron* 40, 471–475.

Kiernan F (1833) The anatomy and physiology of the liver. *Philosophical Transactions of the Royal Society of London* 123, 711-770.

Kiki I, Altunkaynak B Z, Altunkaynak M E, Vuraler O, Unal D, Kaplan S (2007) Effect of high fat diet on the volume of liver and quantitative features of Kupffer cells in the female rat: a stereological and ultrastructural study. *Obesity Surgery* 17, 1381-1388.

Kim AM, Tingen CM, Woodruff TK (2010) Sex bias in trials and treatment must end. *Nature* 465, 688-689.

Kmiec Z (2001) Cooperation of liver cells in health and disease. *Advances in Anatomy Embryology and Cell Biology* 161, 1-151.

Kondo F, Wada K, Kondo Y (1988) Morphometric analysis of hepatocellular carcinoma. *Virchows Archives [A]: Pathology, Anatomy and Histology* 413, 425-430.

Kongure K, Ishizaki M, Nemoto M, Kuwano H, Makuuchi M (1999) A comparative study of the anatomy of rat and human livers. *Journal of Hepatobiliary and Pancreatic Surgery* 6, 171-175.

Kordower JH (2000) Making the counts count: the stereology revolution. *Journal of Chemical Neuroanatomy* 20, 1-2.

Ladekarl M (1998) Objective malignancy grading: a review emphasizing unbiased stereology applied to breast tumors. *APMIS* 79, 1-34.

Lamers WH, Geerts WJ, Jonker A, Verbeek FJ, Wagenaar GT, Moorman AF (1997) Quantitative graphical description of portocentral gradients in hepatic gene expression by image analysis. *Hepatology* 26, 398-406.

Lemmens MAM, Steinbusch HWM, Rutten BPF, Schmitz C (2010) Advanced microscopy techniques for quantitative analysis in neuromorphology and neuropathology research: current status and requirements for the future. *Journal of Chemical Neuroanatomy* 40, 199-209.

Li X, Benjamin IS, Alexander B (2002) Reproducible production of thioacetamide-induced macronodular cirrhosis in the rat with no mortality. *Journal of Hepatology* 36, 488-493.

Lim Y-S, Kim RW (2008) The global impact of hepatic fibrosis and end-stage liver disease. *Clinics in Liver Disease* 12, 733-746.

Loud AV (1968) A quantitative stereological description of the ultrastructure of normal rat liver parenchymal cells. *Journal of Cell Biology* 37, 27-46.

Malarkey DE, Johnson K, Ryan L, Boorman G, Maronpot RR (2005) New insights into functional aspects of liver morphology. *Toxicologic Pathology* 33, 27–34.

Mall FP (1906) A study of the structural unit of the liver. *American Journal of Anatomy* 5, 227-308.

Mandarim-de-Lacerda CA (2003) Stereological tools in biomedical research. *Anais da Academia Brasileira de Ciências* 75, 469-486.

Manikonda PK, Jagota A (2012) Melatonin administration differentially affects age-induced alterations in daily rhythms of lipid peroxidation and oxidant enzymes in male rat liver. *Biogerontology* 13, 511-524.

Marcos R, Rocha E (2001) Counting GFAP-marked Ito cells using the unbiased disector principle. In: *Cells of the hepatic sinusoid*. Volume 8 (Wisse E, Knook DL, Zanger R, Arthur MJP eds), pp. 203-204. Kupffer Cell Foundation.

Marcos R, Rocha E, Henrique R, Monteiro RA (2003) A new approach to an unbiased estimate of the hepatic stellate cell index in the rat liver: an example in healthy conditions. *Journal of Histochemistry & Cytochemistry* 51, 1101-1104.

Marcos R, Monteiro RAF, Rocha E (2004) Estimation of the number of stellate cells in a liver with the smooth fractionator. *Journal of Microscopy* 215, 174-182.

Marcos R, Monteiro RAF, Rocha E (2006) Design-based stereological estimation of hepatocyte number, by combining the smooth optical fractionator and immunocytochemistry with anticarcinoembryonic antigen polyclonal antibodies. *Liver International* 26, 116-124.

Marcos R, Monteiro RAF, Rocha E (2012) The use of design-based stereology to evaluate volumes and numbers in the liver: a review with practical guidelines. *Journal of Anatomy* 220, 303-317.

Martinez-Hernandez A (1985) The hepatic extracellular matrix. II. Electron immunohistochemical studies in rats with CCl_4-induced cirrhosis. *Laboratory Investigation* 53, 166-186.

Martins PNA, Neuhaus P (2007) Surgical anatomy of the liver, hepatic vasculature and bile ducts in the rat. *Liver International* 27, 384-392.

Matsumoto T, Kawakami M (1982) The unit-concept of the hepatic parenchyma — a re-examination based on angioarchitectural studies. *Acta Pathologica Japonica* 32, 285-314.

Matsuzaki S, Onda M, Tajiri T, Kim DY (1997) Hepatic lobar differences in progression of chronic liver disease: correlation of asialoglycoprotein scintigraphy and hepatic functional reserve. *Hepatology* 25, 828-832.

Mayhew TM, Gundersen HJG (1996) If you assume, you can make an ass out of u and me: a decade of the disector for stereological counting of particles in 3D space. *Journal of Anatomy* 188, 1-15.

Mazonakis M, Damilakis J, Mantatzis M, Prassopoulos P, Maris T, Varveris H, Gourtsoyiannis N (2004) Stereology *versus* planimetry to estimate the volume of malignant liver lesions on MR imaging. *Magnetic Resonance Imaging* 22, 1011-1016.

McCuskey (1993) Functional morphology of the liver with emphasis on its microvasculature. In: *Hepatic anion transport and bile secretion: physiology and pathophysiology* (Tavoloni N, Berk P eds), pp. 1-10. Raven Press.

McCuskey (2008) The hepatic microvascular system in health and in response to toxicants. *The Anatomical Record* 291, 661-671.

Moreira RK (2007) Hepatic stellate cells and liver fibrosis. *Archives of Pathology and Laboratory Medicine* 131, 1728-1734.

Mouton PR (2002) *Principles and practices of unbiased stereology. An introduction for bioscientists*. John Hopkins University Press.

Natarajan SK, Thomas S, Ramamoorthy P, Basivireddy J, Pulimood AB, Ramachandran A, Balasubramanian KA (2006) Oxidative stress in the development of liver cirrhosis: a comparison of two different experimental models. *Journal of Gastroenterology and Hepatology* 21, 947-957.

Nadon NL (2006) Gerontology and Age-associated Lesions. In: *The Laboratory rat*, *2nd edition*, pp. 761-772. Elsevier.

Neves RH, Alencar AC, Aguila MB, Mandarim-de-Lacerda CA, Machado-Silva JR, Gomes DC (2006) Hepatic stereology of Schistosomiasis mansoni infected-mice fed a high-fat diet. *Memories of the Institute Oswaldo da Cruz* 101, 253-260.

Nyengaard JR (1999) Stereologic methods and their application in kidney research. *Journal of the American Society of Nephrology* 10, 1100-1123.

Ochs M (2006) A brief update on lung stereology. *Journal of Microscopy* 222, 188-200.

Odaci E, Bilen H, Hacimuftuoglu A, Keles ON, Can I, Bilici M (2009) Hepatocyte numbers in rats. A stereological and histopathological study. *Archives of Medical Research* 40, 139-145.

Pakkenberg B, Gundersen HJ (1988) Total number of neurons and glial cells in human brain nuclei estimated by the disector and the fractionator. *Journal of Microscopy* 150, 1-20.

Passos CC, Ferreira AO, Blazquez FJH, Guerra RR (2010) Modelos experimentais para indução da cirrose hepática em animais: revisão de literatura. *Biotemas* 23, 183-190.

Pinzani M (2004) Therapies for hepatic fibrosis: real hope or just academic exercise. *Digestive and Liver Diseases* 36, 714-716.

Popper H (1985) Coming of age. *Hepatology* 5, 1224-1226.

Porta E, Joun N, Nitta R (1980) Effects of the type on dietary fat at two levels of vitamin E in Wistar male rats during development and aging. I. Life span, serum biochemical parameters and pathological changes. *Mechanisms of Ageing and Development* 13, 1-39.

Povero D, Busletta C, Novo E, Di Bonzo LV, Cannito S, Paternostro C, Parola M (2010). Liver fibrosis: a dynamic and potentially reversible process. *Histology and Histopathology* 25, 1075-1091.

Quinn R (2005) Comparing rat's to human's age: How old is my rat in people years? *Nutrition* 21, 775-777.

Rappaport AM, Borowy ZJ, Lougheed WM, Lotto WN (1954) Subdivision of hexagonal liver lobules into a structural and functional unit; role in hepatic physiology and pathology. *Anatomical Record* 119, 11-33.

Regev A, Schiff ER (2001) Liver disease in the elderly. *Gastroenterology Clinics of North America* 30, 547-563.

Reuber MD, Glover EL (1968) Carbon tetrachloride induced cirrhosis. Effect of age and sex. *Archives of Pathology* 85, 275-279.

Roberts N, Puddephat MJ, Mcnulty V (2000) The benefit of stereology for quantitative radiology. *The British Journal of Radiology* 73, 679-697.

Rocha E, Monteiro RA, Oliveira MH, Silva MW (2001) The hepatocytes of the brown trout (*Salmo trutta f. fario*): a quantitative study using design-based stereology. *Histology and Histopathology* 16, 423-437.

Rohr HP, Lfithy J, Gudat F, Oberholzer M, Gysin C, Bianchi L (1976) Stereology of liver biopsies from healthy volunteers. *Virchows Archives [A]: Pathology, Anatomy and Histology* 371, 251-263.

Rojkind M, Philips GG, Diehl AE (2011) Microarchitecture of the liver: a jigsaw puzzle. *Journal of Hepatology* 54, 187-188.

Roskams T, Desmet VJ, Verslype C (2007) Development, structure and function of the liver. In: *MacSween's Pathology of the liver, 5th edition* (Burt A, Portmann B, Ferrell L eds), pp. 1-74. Churchill Livingstone Elsevier.

Ruijter JM, Gieling RG, Markman MM, Hagoort J, Lamers WH (2004) Stereological measurement of porto-central gradients in gene expression in mouse liver. *Hepatology* 39, 343-352.

Sahin B, Emirzeoglu M, Uzun A, Incesu L, Bek Y, Bilgic S, Kaplan S (2003) Unbiased estimation of the liver volume by the Cavalieri principle using magnetic resonance images. *European Journal of Radiology* 47, 164-170.

Sahin B, Ergur H (2006) Assessment of the optimum section thickness for the estimation of liver volume using magnetic resonance images: a stereological gold standard study. *European Journal of Radiology* 27, 96-101.

Santos M, Marcos R, Santos N, Malhão F, Monteiro RAF, Rocha E (2009) An unbiased stereological study on subpopulations of rat liver macrophages and on their numerical relation with the hepatocytes and stellate cells. *Journal of Anatomy* 214, 744-751.

Sawada M, Carlson J (1987) Changes in the superoxide radical and lipid peroxide formation in the brain, heart and liver during the lifetime of the rat. *Mechanisms of Ageing and Development* 41, 125-137.

Scherle W (1970) A simple method for volumetry of organs in quantitative stereology. *Mikroskopie* 26, 57-60.

Schmitz C, Hof PR (2000) Recommendations for straightforward and rigorous methods of counting neurons based on a computer simulation approach. *Journal of Chemical Neuroanatomy* 20, 93-114.

Schmucker DL, Mooney JS, Jones AL (1978) Stereological analysis of hepatic fine structure in the Fischer 344 rat. Influence of sublobular location and animal age. *Journal of Cell Biology* 78, 319-337.

Schmucker DL, Sanchez H (2011) Liver regeneration and aging: a current perspective. *Current Gerontology and Geriatric Research* 2011, 526379.

Sharp PE, La Regina MC (1998). Important biological features. In: *The laboratory rat*. CRC press.

Scotland RS, Stables MJ, Madalli S, Watson P, Gilroy DW (2011) Sex differences in resident immune cell phenotype underlie more efficient acute inflammatory responses in female mice. *Blood* 118, 5918-5927.

Shimizu I, Yasuda M, Mizobuchi Y, Ma YR, Liu F, Shiba M, Horie T, Ito S (1998). Suppressive effects of estradiol in chemical hepatocarcinogenesis in rats. *Gut* 42, 112-119.

Shimizu I, Mizobuchi Y, Yasuda M, Shiba M, Ma Y-R, Horie T, Liu F, Ito S (1999) Inhibitory effect of estradiol on activation of rat hepatic stellate cells *in vivo* and *in vitro*. *Gut* 44, 127-136.

Shimizu I, Kohno N, Tamaki K, Shono M, Huang HW, He JH, Yao DF (2007) Female hepatology: favorable role of estrogen in chronic liver disease with hepatitis B virus infection. *World Journal of Gastroenterology* 13, 4295-4305.

Sørensen FB (1992) Stereological estimation of the mean and variance of nuclear volume from vertical sections. *Journal of Microscopy* 162, 203-229.

Souza-Mello V, Mandarim-de-Lacerda CA, Aguila MB (2007) Hepatic structural alteration in adult programmed offspring (severe maternal protein restriction) is aggravated by post-weaning high-fat diet. *The British Journal of Nutrition* 98, 1159–1169.

Stark AK, Gundersen HJ, Gardi JE, Pakkenberg B, Hahn U (2011) The saucor, a new stereological tool for analysing the spatial distributions of cells, exemplified by human neocortical neurons and glial cells. *Journal of Microscopy* 242, 132–147.

Sterio DC (1984) The unbiased estimation of number and sizes of arbitrary particles using the disector. *Journal of Microscopy* 134, 127-136.

Tandrup T (2004) Unbiased estimates of number and size of rat dorsal root ganglion cells in studies of structure and cell survival. *Journal of Neurocytology* 33, 173-192.

Teutsch HF, Schuerfeld D, Groezinger E (1999) Three-dimensional reconstruction of parenchymal units in the liver of the rat. *Hepatology* 29, 494-505.

Teutsch HF (2005) The modular microarchitecture of human liver. *Hepatology* 42, 317-325.

Thuluvath PJ, Guidinger MK, Fung JJ, Johnson LB, Rayhill SC, Pelletier SJ (2010) Liver transplantation in the United States, 1999-2008. *American Journal of Transplantation* 10, 1003-1019.

Tsukamoto H, Matsuoka M, French SW (1990) Experimental models of hepatic fibrosis: a review. *Seminars in Liver Disease* 10, 56-65.

Valenca SS, Gouveia L, Pimenta WA, Porto LC (2008) Effects of oral nicotine on rat liver stereology. *International Journal of Morphology* 26, 1013-1022.

Veiga P (2011) Hepatoscopia. *Jornal Português de Gastroenterologia* 18, 143-144.

Vertemati M, Minola E, Goffredi M, Sabatella G, Gambacorta M, Vizzotto L (2004) Computerized morphometry of the cirrhotic liver: comparative analysis in primary biliary cirrhosis, alcoholic cirrhosis, and posthepatitic cirrhosis. *Microscopy Research and Technique* 65, 113-121.

Vertemati M, Sabatella G, Minola E, Gambacorta M, Goffredi M, Vizzotto L (2005) Morphometric analysis of primary graft non-function in liver transplantation. *Histopathology* 46, 451-459.

Vertemati M, Vizzotto L, Moscheni C, Dhillon A, Quaglia A (2008) A morphometric model to minimize subjectivity in the histological assessment of hepatocellular carcinoma and its precursors in cirrhosis. *Microscopy Research and Technique* 71, 606-613.

Vizzotto L, Vertemati M, Gambacorta M, Sabatella G, Spina V, Minola E (2002) Analysis of histological and immunohistochemical patterns of the liver in posthepatitic and alcoholic cirrhosis by computerized morphometry. *Modern Pathology* 15, 798-806.

Vom Saal FS, Finch CE, Nelson JF (1994) Natural history and mechanisms of reproductive aging in humans, laboratory rodents, and other selected vertebrates. In: *Physiology of Reproduction* (Knobil E, Neill JD eds), pp. 1213-1314. Raven Press.

Von Bartheld CS (2002) Counting particles in tissue sections: choices of methods and importance of calibration to minimize biases. *Histology and Histopathology* 17, 639-648.

Vollmar B, Pradarutti S, Richter S, Menger MD (2002) *In vivo* quantification of ageing changes in the rat liver from early juvenile to senescent life. *Liver* 22, 330-341.

Wagenaar GTM, Chamuleau RAFM, Pool JG, De Haan JG, Maas MAW, Korfage JAM, Lamers WH (1993) Distribution and activity of glutamine synthase and carbamoylphosphate synthase upon enlargement of the liver lobule by repeated hepatectomies. *Journal of Hepatology* 17, 397-407.

Wake K (2006) Hepatic stellate cells: three dimensional structure, localization, heterogeneity and development. *Proceedings of the Japanese Academy [B]* 82, 155-164.

Warren A, Cogger VC, Fraser R, DeLeve LD, McCuskey RS, LeCouteur DG (2011) The effects of old age on hepatic stellate cells. *Current Gerontology and Geriatrics Research* 2011, 439835.

Washburn WK, Johnson LB, Lewis WD, Jenkins RL (1996) Graft function and outcome of older (> or = 60 years) donor livers. *Transplantation* 61, 1062-1066.

Wasser S, Tan CE (1999) Experimental models of hepatic fibrosis in the rat. *Annals of the Academy of Medicine Singapore* 28, 109-111.

Weibel ER, Stäubli W, Gnägi HR, Hess FA (1969) Correlated morphometric and biochemical studies on the liver cell. *Journal of Cell Biology* 42, 68-91.

Weibel ER, Paumgartner D (1978) Integrated stereological and biochemical studies on hepatocytic membranes. *Journal of Cell Biology* 77, 584-597.

West MJ, Slomianka L, Gundersen HJ (1991) Unbiased stereological estimation of the total number of neurons in the subdivisions of the rat hippocampus using the optical fractionator. *The Anatomical Record* 231, 482-497.

West MJ (1993) New stereological methods for counting neurons. *Neurobiology of Aging* 14, 275-285.

Wisse E, Braet F, Duimel H, Vreuls C, Koek G, Olde Damink SW, van den Broek MA, De Geest B, Dejong CH, Tateno C, Frederik P (2010) Fixation methods for electron microscopy of human and other liver. *World Journal of Gastroenterology* 16, 2851-2866.

World Health Organization (2008) In: *Atlas of Health in Europe*, *2nd edition*. World Health Organization Regional Office for Europe, Denmark.

Xu JW, Gong J, Chang XM, Luo JY, Dong L, Hao ZM, Jia A, Xu GP (2002) Estrogen reduces CCl_4-induced liver fibrosis in rats. *World Journal of Gastroenterology* 8, 883-887.

Yasuda M, Shimizu I, Shiba M, Ito S (1999) Suppressive effects of estradiol on dimethylnitrosamine-induced fibrosis of the liver in rats. *Hepatology* 29, 719-727

Yörükoglu K, Aktas S, Güler C, Sade M, Kirkali Z (1998) Volume-weighted mean nuclear volume in renal cell carcinoma. *Urology* 52, 44-47.

Zivna H, Zivny P, Palicka V, Nozicka J (2001) The differences in selected biochemical markers and histological findings after bile duct ligation in male and female rats. *Advanced Clinical Pathology* 5, 147-153.

Chapter 2 – Hepatic stellate cells

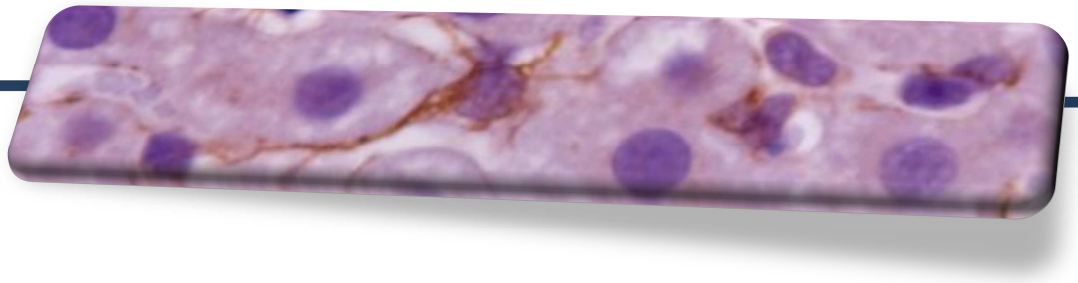

2 - Hepatic stellate cells

2.1- Introduction

2.1.1- Portrait of an intriguing cell

HSC are unique cells for a number of reasons. Firstly, no other cell in the liver was "discovered" so many times. Indeed, these cells were first observed in the 19th century, primarily by a medical student, Franz Boll, who described star-shaped liver cells with granules after an osmium staining, and seven years later by Karl von Kupffer (Boll, 1869; Kupffer, 1876). While searching for nervous elements in the dog's liver, with the Gerlach's gold chloride method, that famous scientist described the existence of stellate cells ("*sternzellen"*) in a letter to his colleague anatomist Waldeyer (Kupffer, 1876). A few years later, a doctor course student of Kupffer, Paul Rothe, used the same gold chloride method and confirmed the existence of *sternzellen* in the liver of different mammals (including the rat) and in the chick liver (Aterman, 1986; Wake, 2004). Then, after studies on the uptake of India-ink in the rabbit's liver, Kupffer "corrected" his original description in the 12th Congress of Anatomists, concluding that the gold-chloride *sternzellen* were a special "endothelial" cell with phagocytic properties (Kupffer, 1899). Indeed, the cells that Kupffer visualized by India-ink (*i.e.*, the now called KC) also have an irregular and stellate shape [it is noteworthy that even some histology textbooks name KC as stellate macrophages (Banks, 1993)]. Twenty-five years later, HSC were again described by Zimmermann, as capillary attached pericytes, and later on they were ultimately rediscovered by Toshio Ito, an eminent histologist at the Gunma University in Japan, who observed cells rich in lipid droplets in the human liver, which were obviously different from KC. He reported this in the 55th Annual Meeting of the Japanese Society of Anatomy in 1950 and named the cells as "*fettspeicherungszellen"* (fat-storing cells) in a paper published two years later (Ito and Nemoto, 1952). Still in that decade, Ito's group carried out studies with electron microscopy, demonstrating that the cells were wrapped in collagen fibres (Aterman, 1986; Suematsu and Aiso, 2001). Also in Japan, Suzuki reported that those cells could be stained by a silver-impregnation method and named the cells as interstitial cells (Aterman, 1986). Finally, Wake used von Kupffer's original gold chloride method, as well as the silver impregnation of Suzuki, vitamin A autofluorescence, and electron microscopy in order to conclude that all those studies actually reported the same cell (Wake, 1971; 1980).

Another reason that makes HSC a unique cell is that no other liver cell has such a plethora of names: in the list of twenty designations, names like Ito cells, interstitial cells, lipocytes, perisinusoidal cels, parasinusoidal cells, fat-storing cells, vitamin A-storing cells and, more recently, arachnocytes can be found (Ekataksin and Kaneda, 1999; Reuben,

2002). Only after a meeting of the International Society of the Cells of the Hepatic Sinusoid held in 1996, a group of researchers agreed that the cells should be named as HSC, since this does not includes personal names, and indicates the morphology and location of the cells (Hepatic stellate cell nomenclature, 1996). By an ironic twist of fate, the consensual name was very close to that given by von Kupffer 120 years earlier. At the end of the 20th century, researchers hoped that this nomenclature clarification could definitively eliminate some confusion in a rapidly growing field. Undoubtedly, the popularity of HSC clearly surpasses all other sinusoidal cells, like KC: the number of studies referring to HSC has increased 5-fold in the last fifteen years, and this number continues to increase year after year (Figure 2.1).

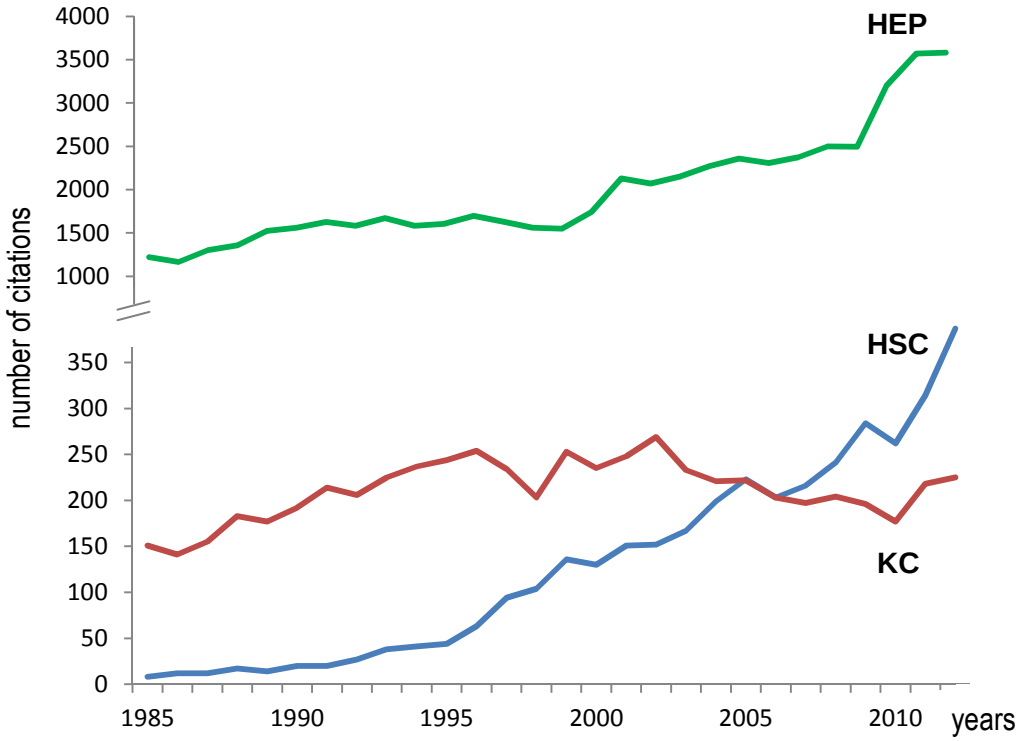

Figure 2.1 - Number of citations in Web of Knowledge[SM] devoted to hepatic stellate cells (HSC), hepatocytes (HEP) and Kupffer cells (KC) between 1985 and 2012. For HSC the search terms also included the designation of “Ito cells”.

Respecting the morphology, HSC fully honour their current name: these cells have a perikaryon that is usually in the perisinusoidal space of Disse, typically in a recess between two adjacent HEP. The cells have multiple cytoplasmic processes that give a true stellate appearance, especially when viewed in 3D (Marcos *et al*, 2003). These processes can be found under LSEC and between HEP and usually wrap one to four sinusoids (Senoo *et al*, 2010); by those processes HSC contact with HEP, LSEC, KC and nerve endings (Geerts, 2001). Additionally, it has been demonstrated that HSC contact with other by *adherens junctions* (Higashi *et al*, 2004). The processes are extended by

thorny microprojections, often called spines, by which the cell “senses” chemotactic signals and further contacts with HEP (Friedman, 2008). In the perikaryon, as well as in large cytoplasmic processes, there are lipid droplets whose numbers and diameters seem to vary under physiological conditions and between species: they are particularly abundant in polar bears, seals and artic foxes, being sparse or absent in calves, guinea-pigs, sheep, goats, pigs, cats, dogs and bats (Beresford and Henninger, 1986; Higashi and Senoo, 2003).

It is now consensual that HSC have, at least, three important functions: 1) storage (and metabolism) of vitamin A; 2) regulation of sinusoidal blood flow; 3) production of ECM. The storage of vitamin A was the first function to be discovered (Wake, 1971). In physiological conditions, most of the vitamin A is found in the liver and in HSC — these cells store 50 to 80% of the total vitamin A (Azaïs-Braesco *et al*, 1997; Senoo *et al*, 2010). Almost 95% of this is present as retinyl esters, packed together in cytoplasmic lipid droplets (Senoo *et al*, 2010). Two types of droplets have been described (Wake, 1974): type I are membrane bound, electron dense, with a diameter smaller than 2 µm, whereas type II are larger (up to 8 µm in diameter), and have no membrane surrounding. Despite this is known for long, the formation of this two droplets and their functional significance is still debated (Friedman, 2008). The vitamin A gives HSC a striking, but rapidly fading, blue-green autofluorescence when excited with the light of ~ 328 nm (Wake, 1971).

The HSC regulation of blood flow in the sinusoids is related with their privileged anatomical location, for acting like pericytes, and with their content of α-smooth muscle actin (ASMA) (Ramadori *et al*, 1990) as well as non-skeletal myosin (Rockey *et al*, 1992). Contractile properties of HSC have been shown *in vitro*, in response to angiotensin II and endothelin I, as well as *in vivo*, using *in vivo* microscopy (Clemens and Zhang, 1999; Oikawa *et al*, 2002). HSC contribute to increase the portal resistance during the early stages of fibrosis (as previously mentioned, in the late stages of cirrhosis the increased portal pressure is mainly due to the distortion of the angioarchitecture) (Forbes and Parola, 2011).

The last function mentioned regards to the production of ECM and has been subjected to intense research over the last decade (Bedossa and Paradis, 2003; Friedman, 2008). As mentioned in Chapter 1, HSC are not only considered the main producers of ECM but they also participate in their degradation (Friedman, 2008). In the space of Disse, the following components of the ECM can be considered: collagens (I, III, IV, V, VI, XIV, and XVIII), structural glycoproteins (*e.g.*, fibronectin, laminin, tenascin), proteoglycans and hyaluronic acid (Roskams *et al*, 2007). In normal conditions, collagen I and III comprise more than 95% of the collagen in the liver (Roskams *et al*, 2007). Different cell types are responsible for their production: HSC express mainly collagen III and laminin, whereas

LSEC and HEP produce collagen IV and fibronectin, respectively (Geerts, 2001). These three cell types express small amounts of collagen I (Geerts, 2001). In pathological conditions this changes dramatically: HSC become devoted to collagen I production [which then represents ≈ 88% of the total collagen, whereas collagen III and IV account for only 10% and 1%, respectively (Senoo *et al*, 2010)]. In such conditions, the total collagen content increases by three to tenfold (Friedman, 2008).

Another uniqueness of HSC regards to the fact that these cells can exist in two different phenotypes: quiescent and activated. In normal organ, the cells are quiescent, have a low proliferative rate and the aforementioned stellate appearance with lipid droplets (Enzan, 1985). However, when there is necrosis, inflammation or cirrhosis, HSC originate myofibroblastic-like cells by the process of activation. This has also been extensively studied over the last decade (Lee and Friedman, 2011) and the sustained activation actually involves many discrete features in HSC: chemotaxis, cytokine release, contractility, fibrogenesis, ECM degradation, retinoid loss and proliferation (Gressner *et al*, 2008; Lee and Friedman, 2011). Regarding the latter, it should be stressed that the average lifespan of the quiescent cells *in vivo* is still unknown (Geerts, 2001; Friedman, 2008), but following partial hepatectomy, in focal hepatic lesions or granulomas (as well as in many other conditions leading to fibrosis), a considerable *in vivo* proliferative activity may be detected (Geerts, 2001; Friedman, 2008). The activation can be summarised in a three-step cascade model (Lee and Friedman, 2011): 1) in the pre-inflammatory phase, it is triggered by ROS and cytokines, like the insulin-growth factor-1 released by damaged HEP [this stimulus parallels the release of lactate dehydrogenase and aspartate aminotransferase (AST)]; 2) in the inflammatory phase, the pre-activated HSC are further stimulated by cytokines released by KC, platelets, LSEC and invading leukocytes, leading to the myofibroblastic-like phenotype; 3) in the post-inflammatory phase or perpetuation of fibrosis, the myofibroblastic-like cells release fibrogenic cytokines, some of which act on HSC autocrinally, while others recruit more HSC by a paracrine fashion (Gressner *et al*, 2008; Lee and Friedman, 2011).

2.1.2- Quantification of HSC

Much more emphasis has been given to functional aspects of HSC than to quantitative structural issues. In different reviews, these cells have been reported to account for 5 to 15% of all liver cells (Ramadori, 1991; Geerts, 2001; Friedman, 2008) and the ratio to HEP — the so-called hepatic stellate cell index (HSCI), has varied from 36 to 130 HSC per 1000 HEP (Geerts, 2001; Moreira, 2007). However, it should be noted that these figures have been based in a few classical studies: the HSCI, for instance, was first defined in the early seventies (Horvath *et al*, 1973), whereas the numerical estimations

were mostly obtained during the eighties (Giamperi *et al*, 1981; Sztark *et al*, 1986). These studies used thin sections and obtained “numbers per area” or relative volumes, and they did not use any specific tagging for HSC. Apart from the vitamin A autofluorescence, HSC are hardly recognised in optical microscopy (Roskams *et al*, 2007). For this reason, different cell markers, either belonging to the membrane or cytoskeleton, have been proposed and evaluated over the years (Geerts, 2001; Friedman, 2008). Regarding the former, the insulin-growth factor (De Bleser *et al*, 1995), platelet derived growth factor (Pinzani *et al*, 1996), synaptophysin (Cassiman *et al*, 1999) and neurotrophin receptors (Roskams *et al*, 2004) have been evaluated. In respect to the cytoskeleton, four cell markers have been proposed: 1) ASMA, which is a marker present in activated HSC and in myofibroblasts (Ramadori *et al*, 1990); 2) vimentin that is common to fibroblasts (Geerts *et al*, 1994); 3) desmin, which also exists in smooth muscle cells (Yokoi *et al*, 1984); 4) glial fibrillary acidic protein (GFAP) (Gard *et al*, 1985). It should be noted that the value of these markers depends on the species under study: antibodies against desmin identify HSC in the rat and mouse, but fail to do so in humans, baboons and rabbits. Inversely, ASMA immunostaining identifies some normal cells in humans, despite being negative in non-activated HSC of the rat (Hautekeete and Geerts, 1997; Geerts, 2001).

Regarding GFAP, it is an intermediate filament widely distributed in mammals, staining neural and non-neural tissues (Dahl *et al*, 1985). For instance, positivity has been observed in Schwann cells of the olfactory system, in cells of the rat’s intestine, as well as in lens epithelium, salivary glands, liver and pancreas (Gard *et al*, 1985; Neubauer *et al*, 1996; Haber *et al*, 1999). This protein is considered a specific marker of HSC both *in vivo* and *in vitro*, being used in normal conditions, because it is lost during activation (Buniatian *et al*, 1996). In those conditions it is unanimous that the vast majority of rat’s HSC are marked after a GFAP immunohistochemistry (Niki *et al*, 1996; Geerts, 2001). However, species related differences also exist for this marker: in humans the protein has been reported to be absent (Geerts, 2001) or limited to a small population of cells located at the edge or around portal tracts (Hautekeete and Geerts, 1997). It is noteworthy that despite all the existing knowledge, the specific function of this filament in HSC is not yet fully clarified (Friedman, 2008).

2.1.3- Lobular heterogeneity and HSC

As we mentioned in Chapter 1, the liver parenchyma exhibits a considerable lobular heterogeneity. Along the porto-central axis, a metabolic zonation of HEP exists, mainly driven by the oxygen gradient (Kmiec, 2001). Regarding HSC, some studies reported a centrilobular predominance in humans (Bronfenmajer *et al*, 1966; Giamperi *et al*, 1981; Kmiec, 2001), whilst others observed more cells periportally in rats and pigs (Geerts *et al*,

1991; Wake and Sato, 1993; Azaïs-Braesco *et al*, 1997; McCuskey, 2006). It has been suggested that HSC display a heterogeneous structure and function based in their zonal distribution (Roskams *et al*, 2007). In the rat, it has been proposed that HSC are shorter (Wake, 1980) and express more desmin periportally (Niki *et al*, 1996), whilst centrilobular HSC contain longer cytoplasmic processes (Wake, 1980) and more GFAP (Niki *et al*, 1996). In the rat, a narrow periportal zone of GFAP-negative HSC was once reported, in a study by Niki *et al* (1996). More recently, studies based in vitamin A autofluorescence, have also shown that a (slightly) smaller area of lipid droplets exists in the centrilobular *versus* periportal zone (Senoo *et al*, 2007). The functional significance of such heterogeneity is still unclear (Friedman, 2008), but it has been speculated that periportal HSC have a stronger contractile apparatus, suited for regulating blood flow through individual sinusoids (Geerts, 2001). The zonal character of HSC has also been related to the streaming liver theory, which sustains that HEP (as well as sinusoidal cells) move from the portal stem cell compartment, to the central regions during their specific lifespan (Zajicek *et al*, 1988). Although this theory has been strongly debated (Roskams *et al*, 2007; Grisham, 2009), it was suggested that periportal HSC are younger and less differentiated cells, opposed to older and more differentiated centrilobular cells (Geerts, 2001).

2.1.4- Ageing, gender dimorphism and HSC

The last decade started to reveal a new picture in the aged liver, and particularly in the hepatic sinusoids. Various studies have now reported that sinusoids have LSEC with less *fenestrae*, surrounded by basal lamina and collagen, leading to the so-called pseudocapillarisation (Le Couteur *et al*, 2001; 2008). However, a clear scenario is still missing for HSC: apart from a study published recently (Warren *et al*, 2011) there have been only a few reports of the effects of ageing in HSC. These have been purely qualitative (Enzan *et al*, 1991) or semi-quantitative, in the sense that “numbers per area” (Imai *et al*, 2000; Vollmar *et al*, 2002; Warren *et al*, 2011) or relative volumes were determined (Martin *et al*, 1992). As mentioned in Chapter 1, the former correspond to biased estimations that may well not correlate with variations in the cell number. Besides, the latter relative volumes may be affected by the reference trap (as discussed in Chapter 1). So far, it is unknown whether HSC contribute to the mild perisinusoidal collagen deposition seen in old age (Le Couteur *et al*, 2008). As already mentioned, it is recognised that HSC have the capacity to divide both *in vivo* and *in vitro* (when activated), but the average lifespan of quiescent HSC is still unknown (Geerts, 2001; Friedman, 2008). Analysis of the specific lifespan of liver cells, other than HEP, is hampered by the fact that their number can be increased, both by local proliferation of resident cells, and by

repletion from the bone marrow. For this purposes (*i.e.*, to follow the kinetics of HSC throughout ageing) the “design-based” stereological methods are valuable, because they are unbiased (estimating values close to reality), precise (and the level of precision can be tuned by the amount of sampling), highly reproducible and can be applied to liver slides.

For over thirty years evidences emerged, and have been mounting, showing that age and sex hormones play modulating roles in the progression from hepatic fibrosis to cirrhosis. This is supported by epidemiological facts, since the male sex and age (over 50) are independent predictors of cirrhosis in HBV and HCV infected patients (Di Martino *et al*, 2004; Zarski *et al*, 2006; Villa *et al*, 2012). The male to female ratio ranges from 3:1 to 5:1 (Shimizu and Ito, 2007; Villa, 2008) and men can have a 10-times faster progression to cirrhosis than women (Poynard *et al*, 2001; Massard *et al*, 2006; Villa, 2008). Although some authors state that such difference is markedly influenced by the shorter lifespan of men compared with women (Kim *et al*, 2004), epidemiology data shows that menopause boosts the fibrosis progression (Shimizu and Ito, 2007; Villa *et al*, 2012). This can be attenuated by hormone replacement therapy, even if oral contraceptives seem not to present significant effects in liver fibrosis (Di Martino *et al*, 2004). Additionally, *in vitro* studies have shown that oestrogens have antioxidant properties, reducing proliferation and collagen synthesis in cultured HSC (Yasuda *et al*, 1999). Apart from the lower prevalence of alcohol, tobacco consumption, lower probability of iron overload and overweight in the female gender, a direct effect of oestrogens and/or oestrogen receptors (ER) have been proposed (Shimizu and Ito, 2007; Villa, 2008). Male and female contain ER in different liver cells, including HSC (Eagon *et al*, 1985; Zhou *et al*, 2001; Barros and Gustafsson, 2011). In the rat, a predominance of fibrosis in males over females appears to exist, although it may depend on the used model (Zivna *et al*, 2001). Despite much is now known about the endogenous antioxidant role of oestrogens (Shimizu *et al*, 2007), the existence of intrinsic differences in the liver (*i.e.*, differences in the cell composition) have never been evaluated in detail.

In this part of the work we aimed to: 1) establish baseline methodology for estimating the N and number per gram (N/g) of HSC in the rat liver, using modern stereology; 2) study the lobular heterogeneity of HSC; 3) determine if ageing involves an hyperplastic or hypertrophic response in HSC — for this we followed the N and mean volume of HSC throughout ageing by stereological methods; 4) evaluate if gender differences in HSC exist throughout ageing; 5) determine the HSCI using stereological methods — this means that we also quantified HEP (as it will be discussed in the next Chapter).

2.2- Materials and Methods

2.2.1- Baseline study: 1) Animals

We used 5 male Wistar rats provided by the "Fundação Calouste Gulbenkian" (Lisboa). The animals were ≈ 3 months old, and weighed 336 g [coefficient of variation (CV) = 0.12]; their liver weighed 14.85 g (CV = 0.10). The animals were kept in standard conditions, receiving food (standard rat chow) and water *ad-libitum*. Animal handling and experiments followed the Guidelines of the European Union Council (86/609/EEC and 2010/63/EU) and national law (Decreto-Lei no. 129/92).

2.2.1- Baseline study: 2) Tissue preparation and sampling protocol

The animals were deeply anaesthetised with chloral hydrate and transcardiacally perfused for 15 minutes, using a peristaltic pump (Gilson, Villiers le Bel, France). The fixative used was 10% buffered formalin (pH = 7.4). The liver was then removed, weighed and a SUR sampling was applied (Figure 2.2). As previously mentioned (Chapter 1) it involves a sampling cascade: firstly, the liver was placed in a plastic plate (with 1 mm spaced grooves) being hand sliced with a microtome blade, into ≈ 4 mm thick slabs (first cut at a random distance between 1 and 4 mm from the edge). Then, every second slab was sampled (also with a random start) and the sampling cascade followed by cutting the slabs into ≈ 4 mm thick chips; half of these were SUR sampled. To increase efficiency, the smooth fractionator was used in the above steps (Nyengaard, 1999; Gundersen, 2002), as discussed in Chapter 1. On average, 10 liver fragments were obtained per animal, which were post-fixed for 16 hours in the same fixative used for perfusion. After washing in running tap water for 2 hours, to aid antigen recovery (Polak and Van Noorden, 1997), the fragments were routinely processed for paraffin embedding (Merck, Histosech, Darmstadt, Germany).

Another smooth fractionator step was performed for the paraffin blocks, as only half of these were SUR sampled (Figure 2.2). These were exhaustively sectioned (30 μm thick) in a rotary microtome (Leica RM2155, Nusloch, Germany) according to fractionator rules (Gundersen, 1986). To avoid chatter, the surface of the paraffin block was warmed (by breathing on) immediately before cutting each section. In every 20 ones, a group of 4 sections were SUR sampled: one for determining the N of HSC, other for estimating the N of HEP and the latter two for obtaining the N of KC. After being picked from the water-bath, the sections were covered with a cotton cloth and gently pressed against the slide with a finger, for ensuring adhesion. For that reason, the sections were all mounted on precleaned slides primed with aminopropyltriethoxy-silane (Marcos *et al*, 2001a). Finally, sections were dried overnight at 37°C.

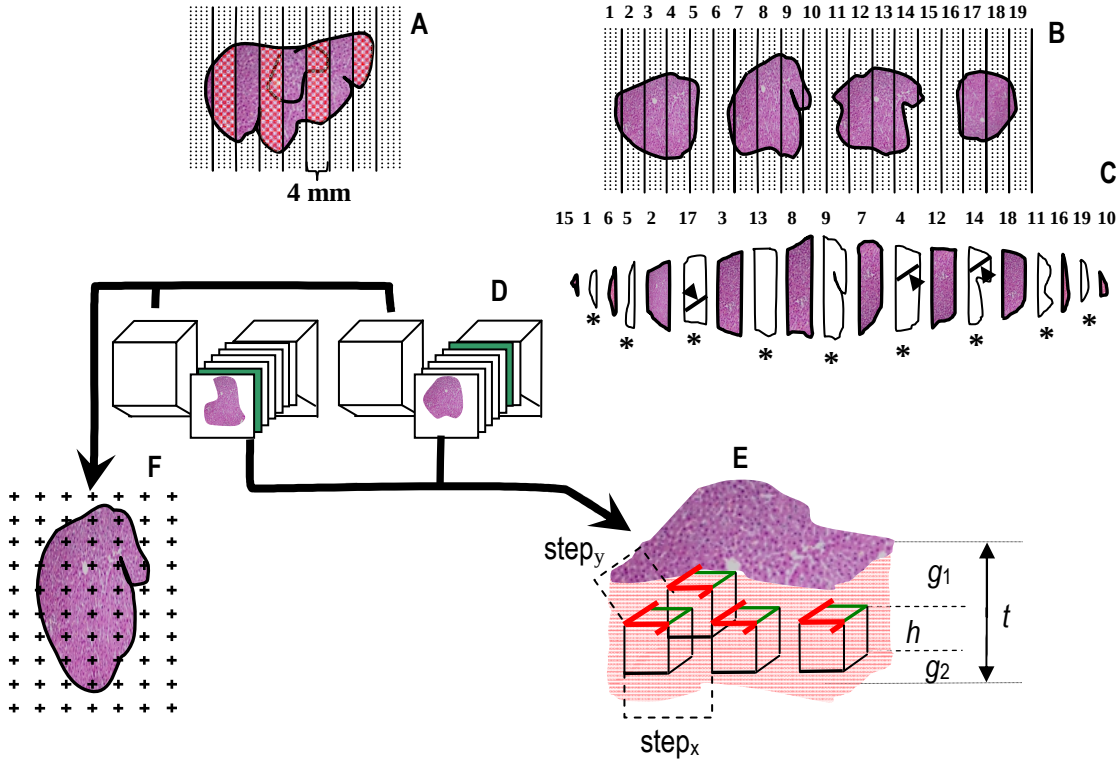

Figure 2.2 - Diagram of the sampling scheme. (A) Liver was sectioned and slabs were systematically randomly sampled (cross-hatched). (B) Slabs were cut into chips and (C) rearranged following a smooth pattern according to their size (note the change in number sequence from B to C). Every two chips were systematically random sampled (coloured). (D) Every second paraffin block was sampled and exhaustively sectioned, and every 20th section (in the baseline study) or every 30th section (in the the age and gender study) was sampled. (E) An unbiased counting frame was placed throughout the live video image of the section; the sampling of fields was carried out by software-controlled stepwise movements of the motorised stage, in the *x*- and *y*- directions ($x = y$ = 1250 µm and 1750 µm in the baseline and age and gender study, respectively). A continuous scan was performed through the disector height (h = 20 µm), which is a fraction of the section thickness ($t \approx$ 30 µm). Thus, guard heights, g_1 and g_2, were left in the upper and lower surfaces (g_1 = 4 µm; $g_2 \approx$ 6 µm). (F) Thin paraffin sections were used for immunohistochemistry against α-smooth muscle actin, and glial fibrillary acidic protein, and for staining with picro-sirius red, for collagen assessment; in these latter two, a grid of points was applied in order to estimate the relative volumes [(F) only applies for the age and gender study]; (*): material frozen in liquid nitrogen for flow cytometry and biochemical studies [only in the age and gender study of hepatocytes (Chapter 3)]; arrowheads: tiny pieces sampled for electron microscopy (only in the age and gender study). (Adapted from *Marcos et al, Journal of Microscopy*, *2004.*)

2.2.1- Baseline study: Immunohistochemistry for GFAP

After deparaffinising, treatment in a microwave oven (Moulinex Y53, Ecully, France) was carried out for antigen retrieval. The microwave was set for 4 plus 4 minutes, at 600 W. To standardise this procedure, the same slide-containing rack was always used, with a constant number of slides (n = 10), dipped in a defined level of buffered citrate (pH = 6.0) (Shi *et al*, 1999). The sections were then rinsed in tap water and dipped in 0.3% H_2O_2

(Merck) for 30 minutes, to block endogenous peroxidase. After rinsing in tap and distilled water and phosphate buffered saline (PBS), each for 10 minutes, a streptavidin–biotin protocol followed (Histostain Plus, Zymed, San Francisco, California) in a moistened chamber. Briefly, a 10% non-immune goat serum was applied over the thick sections for 90 minutes, followed by incubation with 1:3000 rabbit polyclonal antibody against GFAP (Dako, Glostrup, Denmark), for 4 days at 4° C. Then, intermingled with three rinses in PBS for 10 minutes, the secondary antibody and streptavidin–peroxidase complex were applied, each for 60 minutes. Subsequently, after rinsing in PBS and in Tris-buffered saline (TBS), sections were immersed for 10 minutes in 0.05% 3, 3′-diaminobenzidine (Sigma, Saint Louis, Missouri) in TBS with 0.03% H_2O_2. Finally, after rinsing in tap water for 10 minutes, sections were counterstained in Gill's haematoxylin (Merck) for 2 minutes and, after dehydration and clearing, mounted in DPX.

The following controls were performed: (1) positive controls, in which astrocytes were tagged by GFAP in the rat brain (Pilegaard and Ladefoged, 1996); (2) negative controls, in which the first antibody was either omitted or replaced by rabbit non-immune serum (Dako) (Polak and Van Noorden, 1997).

2.2.1- Baseline study: 4) Stereological analysis

The N of HSC was estimated with the optical fractionator, using a workstation comprising a microscope (Olympus BX-50, Tokyo, Japan) equipped with a 100x oil-immersion lens (Olympus Uplan NA = 1.35) and a matching condenser, a high-accuracy length gauge (commonly named as microcator in the stereological field) (Heidenhain MT-12, Traumrent, Germany) to control the movements and position in the *z*-direction (0.5 µm accuracy), a motorised stage (Prior, Fulbourm, United Kingdom) for stepwise displacement in the *x–y* directions (1 µm accuracy), and a CCD video camera (Sony, Tokyo, Japan) connected to a 17″ PC monitor (Sony). The S-video signal was captured by the PC add-on board Screen Machine II (Fast Electronic GmbH, Hamburg, Germany). The whole system was controlled by the software Olympus CAST-Grid (version 1.5). At the monitor, a final magnification of 4750x allowed an easy and accurate recognition of immunostained HSC. The first field of vision was randomly selected by the software, and thereafter fields were sampled systematically by stepwise movements of the stage in the *x*- and *y*-directions ($step_{x,y}$ = 1250 µm). Throughout the disector height (20 µm), a software generated counting frame was superimposed, having a defined area of 1673 μm^2, forbidden lines to avoid edge effects (Gundersen, 1977), and a defined test point (P) to evaluate its position in the reference space. For counting HSC, their nucleus was selected as the counting unit. To guarantee that the N of nuclei equaled the N of HSC, we confirmed that these cells

were indeed mononucleated, as emphasised in the literature (Kawada, 1997; Geerts, 2001; Friedman, 2008).

HSC were counted when two conditions were met: (1) at the plane of focus, the nucleus was within the counting frame or touching the inclusion lines and not touching the forbidden lines or their extensions; (2) the rim of the nucleus was in perfect focus at a plane below 4 µm and above or equal to 24 µm in the *z*-axis. It was always certified that the immunomarking extended beyond this latter, in order to ensure that every HSC could be unambiguously recognised. The potential bias from lost caps was avoided by having upper and lower guard heights. Because their use is still a matter of debate (as discussed in Chapter 1), we reduced these heights to a recommended minimum, about the length of the nuclei longer axis (Dorph-Petersen *et al*, 2001). This resulted in a guard height of 4 µm, at the upper surface, and ≈ 6 µm, at the lower surface (Figure 2.2). It is noteworthy that their use was validated by analysing the distribution of particles in thick paraffin liver sections (Annex 1).

At the same time, collapse in the *z*-direction was evaluated. As we expected a very small variation in section thickness, this was only measured (with the microcator) in every fifth field (Dorph-Petersen *et al*, 2001). The coefficient of error of the section thickness, CE(t), was computed as standard error of the mean/mean. As a result of the SUR sampling, we anticipated that counting frames would, from time to time, hit artificial borders generated during tissue slicing. In practical terms, given the high magnification used and the low sampling density, this rarely occurred. Therefore, this feature was not expected to affect the accuracy (unbiasedness) of the estimates (Gundersen *et al*, 1999). Nevertheless, in those rare occasions we followed the approach detailed by Gundersen (1986); briefly, a counting frame was accepted only if there were no artificial edges of the section within the computer monitor. The aggregate areal fraction actually used for counting (*pa*) was then calculated as (Gundersen, 1986):

$$1/pa = \Sigma Pf/\Sigma Ps \qquad (2.1)$$

where ΣPf is the number of test points hitting the reference space (*i.e.*, the liver), in accepted counting frames, and ΣPs is the number of test points in the reference space from all counting frames (accepted and non-accepted, according to the above rules). The N of HSC in the whole liver was primarily estimated as

$$N = (1/bsf) \times (1/ssf) \times (1/asf) \times (1/hsf) \times pa\Sigma Q^{-} \qquad (2.2)$$

where ΣQ^{-} is the number of HSC counted throughout the liver and *pa* is the aggregate areal fraction. The *bsf* is the block sampling fraction (*bsf* = 1/8); *ssf* refers to the section sampling fraction (*ssf* = 1/20). The *asf* is the area sampling fraction, and was calculated by dividing the area of the frame, *a*, by the area associated with movement in *x-y*, *A* [*asf* =

a(frame)/*A*(step$_{x,y}$) = 1/935]. Finally, *hsf* is the height sampling fraction, and it was obtained by dividing the height of the disector (*h* = 20 µm), *h*, by the mean section thickness, *t* (*hsf* = *h*/*t* = 0.66). Simultaneously, two other parameters were determined: 1) the N of HSC per block [in that case the *bsf* fraction was omitted in Equation (2.2)]; 2) the N/g, as this can aid in comparing values between animals with different liver weights.

The N_V(HSC, liver) was estimated using the formula:

$$N_V(\text{HSC, liver}) = \Sigma Q^- / [h \times a(\text{frame}) \times \Sigma P f] \quad (2.3)$$

where ΣQ^- is the total number of cells counted in the sampled fields, and *a, h and* P*f* are, respectively, the area of the counting frame, height of the disector and number of test points hitting the reference space. The N_V(HSC, liver) was determined for the sections, blocks and for each animal.

The coefficient of error of the number of cells counted, CE(ΣQ^-), was estimated with two approaches, differing in the weight given to the variance between and within the slices, *i.e.* blocks. One assumes that the frequency of distribution of ΣQ^- approximates a Poisson distribution (Schmitz and Hof, 2000), dealing only with the variance within blocks:

$$CE(\Sigma Q^-) = 1/\sqrt{\Sigma Q^-} \quad (2.4)$$

The other approach for estimating the CE(ΣQ^-) used a variant of the ”quadratic approximation formula”, the so-called explicit Nugget formula [Equation (2.12), Table 2.2] considering the liver as a continuous object (Cruz-Orive, 1999). This formula, somewhat similar to a revised version used by Gundersen *et al* (1999), deals with the contribution from both the systematic sampling (variance between blocks) and the Nugget contribution (variance within blocks). As no noticeable tissue inhomogeneity was detected for HSC, the eventual error due to smooth sampling was unimportant (Gundersen, 2002); therefore, the coefficient of error of the HSC number, CE(N), was estimated taking that into account (West, 1993; Gundersen, 2002):

$$CE(N) = \sqrt{[CE^2(\Sigma Q^-) + CE^2(t)]} \quad (2.5)$$

but, as the CE(*t*) was insignificant (as detailed in Results), it was disregarded, and, for practical purposes, the CE(N) was considered to equal the so-called counting noise, CE(ΣQ^-). The CE(N) estimations were then compared with the observed relative variance among animals, OCV^2(N), according to the formula (West, 1993; Howard and Reed, 2005):

$$OCV^2(N) = BCV^2(N) + CE^2(N) \quad (2.6)$$

where BCV^2(N) is the inherent biological relative variance of individuals and CE^2(N) is the observed mean square of the individual estimates of the CE(N).

2.2.1- Baseline study: 5) Assessment of the optimum sampling

For evaluating a possible reduction in the sampling effort, two strategies corresponding to different sampling intensities were evaluated by computer simulations. In strategy 1, the sampling was reduced at the field level – the $step_{x,y}$ was 1768 μm, and only half of the fields were considered. In strategy 2, the sampling was reduced at the section level – the $step_{x,y}$ was maintained (at 1250 μm), but only half of the sections were analysed. To better assess the variability of the estimates of the CE(N) per sampling strategy, and to increase the precision of the respective CE(N), six replicas were performed per rat (for both strategies). In each of these replicas, the ΣQ^{-} was determined and the CE(N) estimated, as above described.

2.2.1- Baseline study: 5) Statistical analysis

After checking the normal distribution of data with the Shapiro–Wilk's test, a parametric correlation analysis was applied for detecting linear associations. The non-parametrical Spearman's correlation test was performed to access a possible correlation between the N of HSC and the liver weight (which did not show a normal distribution). The tissue homogeneity was checked by evaluating the distribution pattern of the N_V(HSC, liver), within blocks (*i.e.* within and between sections) and between blocks. Results were considered statistically significant for $p \leq 0.05$.

2.2.2- Age and gender study

2.2.2- Age and gender study: 1) Animals

In this part of the study, we included eight groups (n = 5 per group) of young (2 months old), adults (6 months old), middle-aged or mature (12 months old), and old (18 months old) Wistar rats, initially bought from Charles-River Laboratories (Barcelona, Spain). Considering that the mean lifespan of this strain fed *ad-libitum* is ≈ 19 to 24 months (Porta *et al*, 1980; Sawada and Carlson, 1987, Manikonda and Jagota, 2012), rats aged 2, 6, 12 and 18 months have lived ≈ 8%, ≈ 25%, ≈ 50% and ≈ 75% of their lifespan.

All the animals had been weaned at 20 days and then were kept in standard conditions, receiving water and food (Mucedola® 4RF21, Settimo Milanese, Italy) *ad-libitum*. This standard rat chow has 19% protein (5:1 ratio of vegetable and animal protein) and 3% fat (1:4 saturated and unsaturated fat), being routinely supplemented with vitamin A (14400 UI/kg) and vitamin E (64 mg/kg), among other vitamins and minerals. The rats were housed in pairs or individually (old males) in solid-bottom polycarbonate cages. They were in a controlled environment [temperature (25ºC) and 12 hours alternated light-dark cycle, with light period starting at 7.00 AM].

2.2.2- Age and gender study: 2) Tissue preparation and sampling protocol

The process was like that described in the baseline study, with minor modifications. In this case the animals were deeply anaesthetised with ketamine plus xylazine (because it causes less respiratory dysfunction than chloral hydrate), blood was collected from the heart and a transcardiac perfusion was performed for 15 minutes, but only with an isosmotic solution. Blood was centrifuged to obtain serum which was used to determine the alanine transaminase (ALT), AST and oestradiol levels (in female rats). The latter was measured using a competitive immunoassay oestradiol kit (Immulite, Siemens Healthcare, Gwynedd, United Kingdom) according to manufacturer instructions. It is opportune to mention that in the case of females, vaginal cytology was performed daily, in order to avoid collecting samples in proestrous/oestrous days. Additionally, the sampling collection was always performed during the morning period (from 10 to 12 AM), to circumvent oscillations in liver functions due to circadian rhythmicity (Davidson *et al*, 2004).

After being removed, the liver was weighed and its volume determined by the Scherle's method, by immersing the liver in isotonic saline, 0.90% w/v of NaCl (as described in Chapter 1). Then a smooth fractionator sampling scheme was applied under ice-cold buffer solution (to minimize oxidative reactions in the organ). Three sets of liver samples were collected: 1) Liver fragments were fixed in buffered formalin (pH = 7.4) for 20 hours; these were used for stereological procedures in optical microscopy. 2) liver pieces frozen in liquid nitrogen and kept at -80ºC; this was used for flow cytometry and biochemical studies (to be detailed in Chapter 3). 3) Tiny pieces that were fixed in glutaraldehyde for 2 hours and processed for electron microscopy (Figure 2.2).

Regarding the material for optical microscopy, the fragments (10 in average) were routinely processed for paraffin embedding. Another smooth fractionator step was applied for the paraffin blocks (Figure 2.2D): one half was used for obtaining thin sections (3 µm thick) needed for immunohistochemical procedures and picro-sirius red staining, while the other was exhaustively sectioned (30 µm thick) in a motorised microtome. In every 30 sections, 3 consecutive ones were SUR sampled and used for immunohistochemistry against: 1) GFAP; 2) E-cadherin, to differentiate mononucleated hepatocytes (MnHEP) from BnHEP; 3) ED2, for estimating the N of KC. The procedures related with the latter will be detailed in Chapters 3 and 4, respectively. Additionally 10 extra slides were obtained per animal for the double immunohistochemistry against GFAP and GS, to study the lobular heterogeneity (detailed below), and for GFAP and ED2 (which will be considered in Chapter 4). As mentioned above, thin paraffin sections were mounted on precleaned slides primed with aminopropyl-triethoxy-silane (Marcos *et al*, 2001a). Three techniques were applied to these thinner sections: 1) GFAP immunohistochemistry; 2) ASMA immunohistochemistry; 3) picro-sirius red staining (for collagen assessment).

2.2.2- Age and gender study: 3) Immunohistochemistry for GFAP

The protocol used for thick sections was similar to that described in the baseline study, keeping in mind that maximum standardisation should be pursued, especially during antigen recovery procedures. Regarding the thin sections, a streptavidin–biotin protocol was also used (Histostain Plus), but with shorter incubation times: the non-immune goat serum was applied for 20 minutes, the polyclonal antibody against GFAP (Dako) was diluted to 1:1200 and incubated overnight, whilst secondary antibody and streptavidin–peroxidase complex were both applied for 20 minutes. Positive and negative controls were included, as detailed in the baseline study.

2.2.2- Age and gender study: 4) Double immunohistochemistry for GFAP and GS

After deparaffinising, slides were placed in the microwave (three cycles of 4 minutes) immersed in citrate buffer. After rinsing in PBS, the endogenous biotin was blocked, by immersing the slides in avidin and biotin (Zymed) for 12 and 10 minutes, respectively. Then, the endogenous peroxidise was blocked and the first streptavidin–biotin protocol followed (Histostain Plus). After rinsing in PBS, 10% non-immune goat serum was applied for 40 minutes, followed by a long incubation with 1:1500 rabbit polyclonal antibody against GFAP (Dako) (4 days at 4ºC). Another rinse in PBS followed and the secondary antibody and the streptavidin–peroxidase complex were applied, each for 40 minutes. Then, after rinsing in PBS and TBS the slides were developed for 2 minutes in 0.05% 3, 3′-diaminobenzidine (Sigma) in TBS with 0.03% H_2O_2. Following a rinse in tap water, the sections were dipped in 50 mM glycine buffer (pH = 2.2) for 5 minutes to strip the antibodies of the first immunoreaction. The second streptavidin–biotin protocol then followed. This was similar to that above described, except that sections were incubated with 1:4000 rabbit polyclonal antibody against GS (kindly gifted by Professor Rolf Gebhardt, University of Leipzig, Germany), for another 4 days at 4ºC. For this reaction, slides were developed aminoethylcarbazole (Dako) for 10 to 20 minutes (the final red colour was controlled by microscopic observation). Finally, the slides were mounted in Aquatex (Dako).

2.2.2- Age and gender study: Immunohistochemistry for ASMA

After deparaffinising, slides were placed in a pressure cooker for 3 minutes in citrate buffer. After rinsing in PBS, a polymer based immunohistochemical protocol was followed, [Novocastra Novolink Polymer (Leica Biosystems, Newcastle, United Kingdom)]. The protein blocking solution was applied for 5 minutes, whereas the ASMA antibody (clone HM45, Dako) diluted at 1:500 immersed the slides overnight. Then the post-primary

solution and polymer were applied both for 30 minutes. Finally, slides were developed for 2 minutes in 0.05% 3, 3′-diaminobenzidine (Sigma) in TBS with 0.03% H_2O_2.

2.2.2- Age and gender study: 6) Picro-sirius red staining

Five thin sections were randomly selected per animal, de-waxed and hydrated. The counterstaining was achieved with celestial blue and haematoxylin, each for 5 minutes. After washing in tap water, the picro-sirius red (Sigma, coloration index 35782) dissolved in picric acid (1 mg/ml) was applied for 1 hour at room temperature (Junqueira *et al*, 1978, Kumar, 2005). After washing in acidified water (1% acetic acid), the sections were dehydrated in ethanol, cleared in xylene and mounted in DPX.

2.2.2- Age and gender study: 7) Electron microscopy

After liver perfusion, tiny fragments (< 0.5 mm^3) were removed and fixed in 2.5% glutaraldehyde in 0.1M phosphate buffer (pH = 7.4) for 2 hours and subsequently post-fixed in phosphate buffered 1% OsO_4 for another 2 hours. After dehydration in ethanol and propylene oxide, the pieces were embedded in an epoxy resin (dissection needles rolled the pieces inside the resin, so that no particular orientation was given). Semithin sections were obtained with glass knifes and stained with methylene blue-azur II; these were used to quantify volume densities of HSC. Additionally, ultrathin sections were obtained with a diamond knife (Diatome, Hatfield, USA) and contrasted with uranyl acetate and lead citrate; afterwards, they were observed in a transmission electron microscope, JEOL 100CXII, at 60 kV.

2.2.2- Age and gender study: 8) Stereological analysis

The procedure for the N estimation of HSC in the thick sections was similar to that described in the baseline study (the only difference was that the $step_{x,y}$ was 1750 μm, instead of 1250 μm). In addition, the distribution of particles in the z-axis was checked — so that guard heights could be safely used (Annex 1) — and the HSCI was determined. This latter refers to the number of HSC per 1000 HEP, being obtained by:

$$HSCI = N_{(HSC)} \times 1000 / N_{(HEP)} \quad (2.7)$$

in which $N_{(HSC)}$ is the total number of HSC and $N_{(HEP)}$ is the total number of HEP (which will be detailed in Chapter 3).

In the slides used for the double immunohistochemistry, a SUR sampling was also used (similar to the above described), but in this case cells were counted only if fields were in the vicinity of the portal tracts or central venules (by convention, these areas comprised five to six hepatocytes neighbouring those landmarks). Considering that the average diameter of HEP is 20 μm, independently of gender and age (see Chapter 3 for details), it

means that the border of periportal and centrilobular areas was settled at 100-120 μm around portal tracts or central venules.

Regarding the thin paraffin sections, 5 were randomly selected per animal and an average 150 oil-immersion fields were quantified per animal (the fields were "selected" after SUR sampling performed by the CAST-Grid software). A test-system of points was superimposed by the software in order to determine the relative volume of HSC in the liver [V_V(HSC, liver)]. As discussed in Chapter 1, the test-system of points included 12 sparser points, used to quantify the reference space (whole liver) and 108 denser ones used for HSC, according to the formula:

$$V_V(\text{HSC, liver}) = P(\text{HSC}) / [P(\text{liver}) \times \kappa] \quad (2.8)$$

in which P(HSC) refers to the points falling in HSC (perikaryon and cytoplasmic processes immunomarked by GFAP), P(liver) refers to the points falling in liver and κ was a constant; (in this case κ = 9, so that each sparser point "controlled" 9 denser ones). The screen covered an area of 2433 μm^2, and the area per point was 23.5 μm^2.

This procedure was also applied to the semithin sections, but in a lower number of fields (50 in average). However, it should be noted that in semithin sections only the perikaryon (with nucleus and lipid droplets) of HSC was evaluated, thus estimating the V_V(HSC*per*, liver). It is opportune to mention that all these slides (thin and semithin sections) were blindly evaluated (*i.e.*, the observer was unaware of the age or gender of the animal), in order to avoid eventual observer-related bias.

The CE(V_V) was also approximately estimated by the formula (Howard and Reed, 2005):

$$CE(V_V) = \sqrt{\frac{k}{k-1}.[\frac{\Sigma u^2}{\Sigma u.\Sigma u} + \frac{\Sigma v^2}{\Sigma v.\Sigma v} - 2\frac{\Sigma u.v}{\Sigma u.\Sigma v}]} \quad (2.9)$$

where *k* refers to the number of fields examined, *u* and *v* stands for the number of points in the reference space (liver) and in the analysed structure (HSC marked by GFAP in the immunohistochemical stained slides, or perikaryon in the semithin sections), respectively.

In order to estimate the number-weighted cell volume ($\bar{v}_N$) of HSC, we used the formula:

$$\bar{v}_N = V_{(\text{HSC})} / N_{(\text{HSC})} \quad (2.10)$$

in which $N_{(HSC)}$ refers to the total number of HSC and $V_{(HSC)}$ refers to the total volume occupied by these cells in the liver. Assuming no differential shrinkage, the latter was computed by the product of the volume density and the liver volume determined by Scherle's method (Scherle, 1970), according to the formula:

$$V_{(\text{HSC})} = V_V(\text{HSC, liver}) \times V(\text{liver}) \quad (2.11)$$

The amount of collagen was also assessed by a similar strategy (5 random slides per animal were also blindly screened). In this case, a test-system of 36 points was applied to

estimate the V_V(collagen, liver). The 40x magnification lens rendered a final magnification of 1608x at the screen, which allowed an easy discrimination of fibres. The screen covered an area of 16070 μm^2, meaning that each point controlled an area of 446 μm^2. The collagen fibres were sorted in three categories according to their position: 1) those associated with the capsule; 2) around venules (in portal tracts and around central venules); 3) surrounding sinusoids (intralobular location). Since HSC are related with collagen production within the lobule, we also estimated the total amount of intralobular collagen (using Equation 2.11).

2.2.2- Age and gender study: 9) Statistical analysis

As the variables have a low number of cases, it was tested if they follow a normal distribution by the Shapiro-Wilk's test. In most cases the assumption of normal distribution was met by a logarithmic transformation of the original variable, namely in the body and liver weight, N_V(HSC, liver), V_V(HSC*per*, liver), $\overline{v}_N$ of HSC and $V_{(HSC)}$. A parametric correlation analysis was applied for detecting linear associations between parameters. After checking the homogeneity of variances (Levene's test) a two-way ANOVA was performed taking in consideration the effects of gender and ageing. When significant differences existed ($p \leq 0.05$), multiple comparisons were done using the *post-hoc* Tukey's test. Only in two cases we performed a different analysis, namely when evaluating the serum oestradiol in females (one-way ANOVA) and in the evaluation of lobular heterogeneity (two-way ANOVA, considering the effects of ageing and location in the lobule). The software SPSS18 (IBM, Armonk, USA) was used in the analysis.

2.3- Results

2.3.1- Qualitative findings

All the livers displayed a normal histology. A consistent and reliable marking of HSC was achieved with GFAP: the cells exhibited their typical stellate morphology (Figure 2.3), and were clearly visualized in both periportal and centrilobular areas. In all the thick sections, HSC marking was observed beyond the 24 µm of the section thickness. Most HSC had clear cytoplasmic spots intermingled with the GFAP staining ('reticular' pattern). Staining was not detected in other sinusoidal and parenchymal cells, nor in the negative controls.

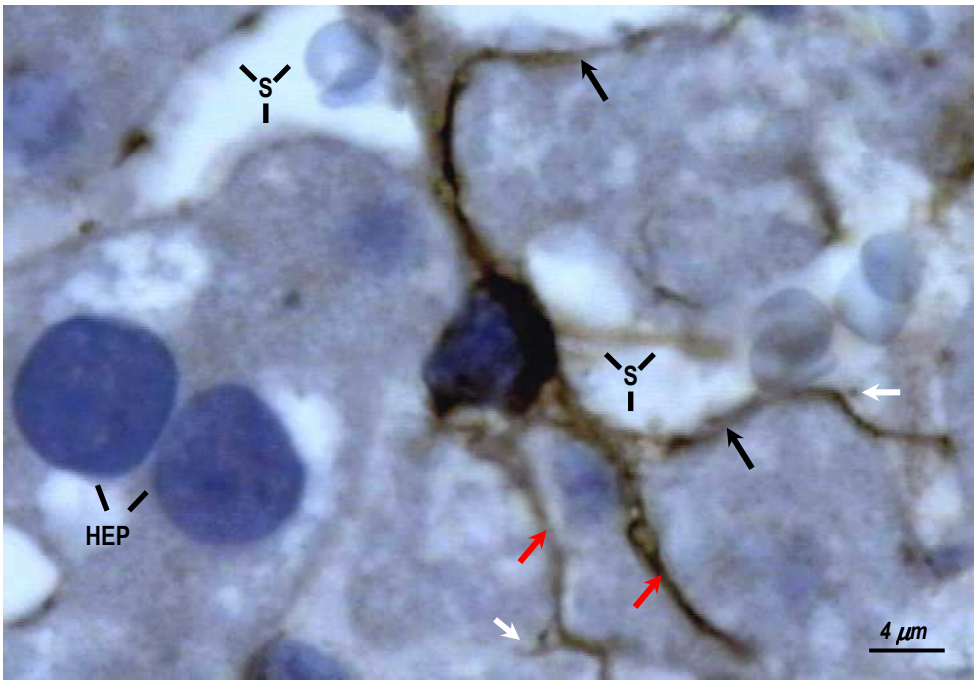

Figure 2.3 – Hepatic stellate cell immunomarked against glial fibrillary acidic protein. The cell has an irregular nucleus, smaller than those of hepatocytes (HEP) and a reticular cytoplasm. Three types of cytoplasmic processes can be seen: primary subendothelial (black arrows), that extend over two sinusoids (S), primary interhepatocytic (red arrows) and secondary processes or spines (white arrows).

Comparing the liver of young and aged rats, the HSC had larger and more numerous lipid droplets. This was already visible in 6 months old rats, being clearly perceptible in semithin sections (Figure 2.4). No differences seemed to exist between HSC of males and females at optical or electron microscopy (Figures 2.5 and 2.6). It is noteworthy that mitotic figures were rare in HEP but were never noticed in HSC. In this cell type, we seldom observed apoptotic features.

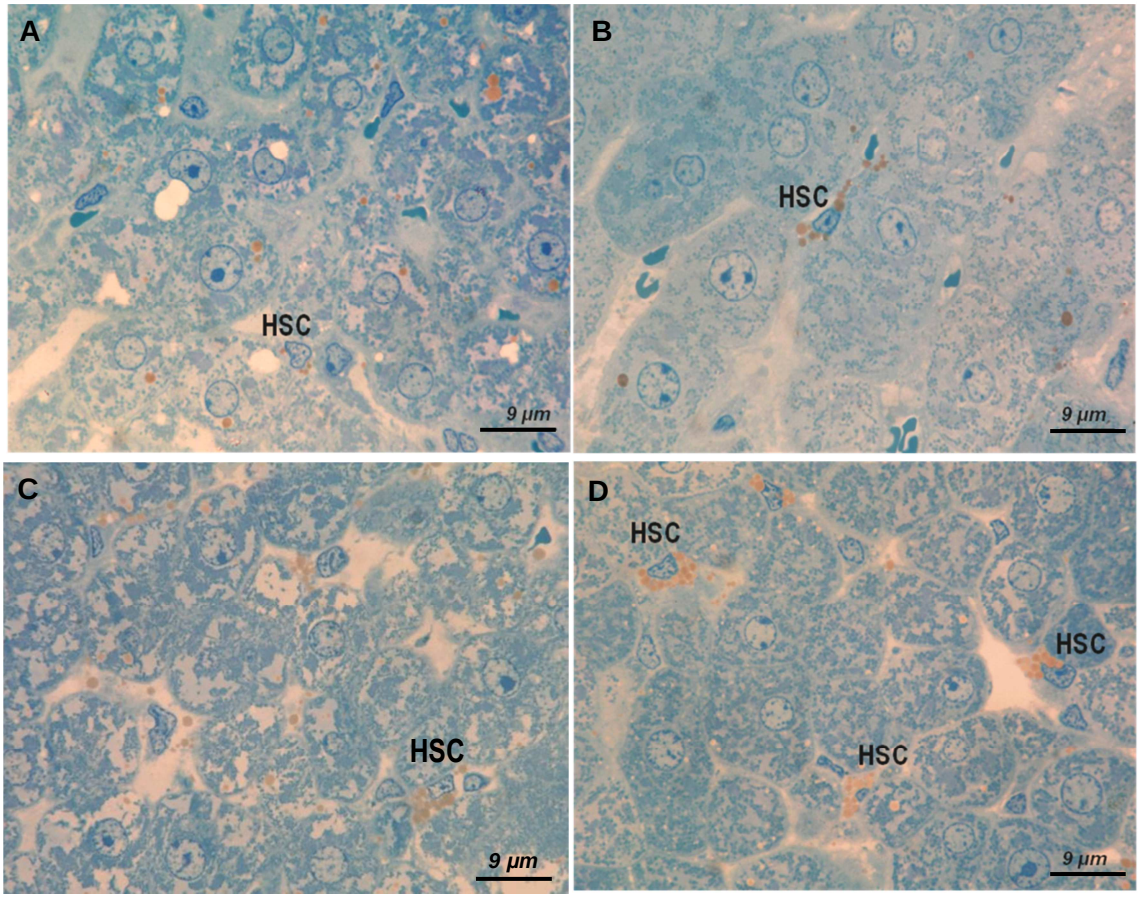

Figure 2.4 – Hepatic stellate cells (HSC) in semithin sections of the liver of young female (A), adult male (B), middle-aged male (C), and old female (D). The perikaryon of the cell increases markedly due to their lipid content.

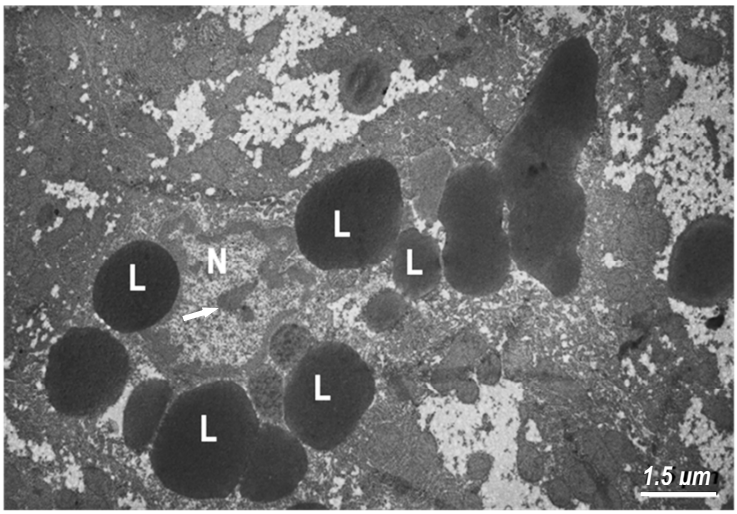

Figure 2.5 – Hepatic stellate cell of a middle-aged female at electron microscopy. The irregular nucleus (N) has a visible nucleolus (arrow) and peripheral chromatin. The cytoplasm is filled with lipid vacuoles (L).

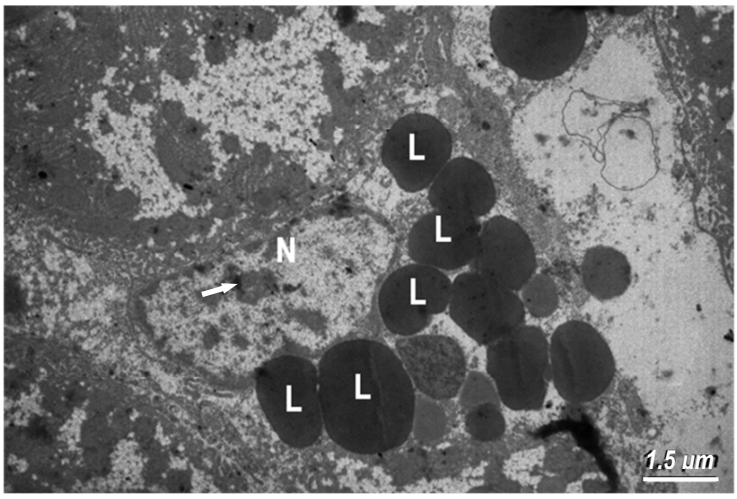

Figure 2.6 – Hepatic stellate cell in a middle-aged male at electron microscopy. Similar to the previous Figure 2.5, the nucleus (N) has also a visible nucleolus (arrow), with peripheral chromatin, and the cytoplasm is filled with lipid vacuoles (L).

Regarding the double immunohistochemistry against GFAP and GS, the latter marked HEP around efferent vessels, not only circling central venules, but also sublobular veins, or even the larger efferent veins in the hilar region. Females tended to present a wider GS positive area (2-3 HEP in females in contrast with 1-2 HEP in males) (Figure 2.7).

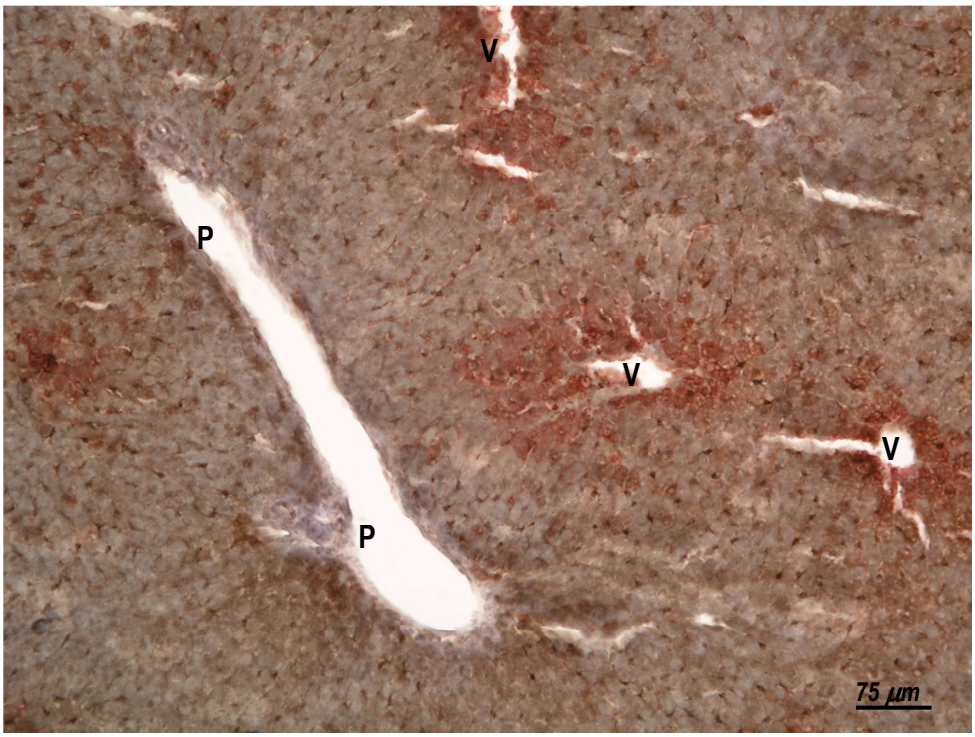

Figure 2.7 – Thick section of an adult male liver immunostained against GFAP (brown colour) and GS (red). Hepatic stellate cells can be seen along the hepatic lobules; qualitatively no centrilobular (V) or periportal (P) predominance can be foresighted here.

We observed HSC across the lobule, from periportal to centrilobular areas (Figure 2.7). In the former, elongated and smaller cells tended to be slightly more abundant, and no

GFAP-negative zone was seen (Figure 2.8). Lipid enriched HSC were more abundant in centrilobular areas of older animals (Figure 2.9).

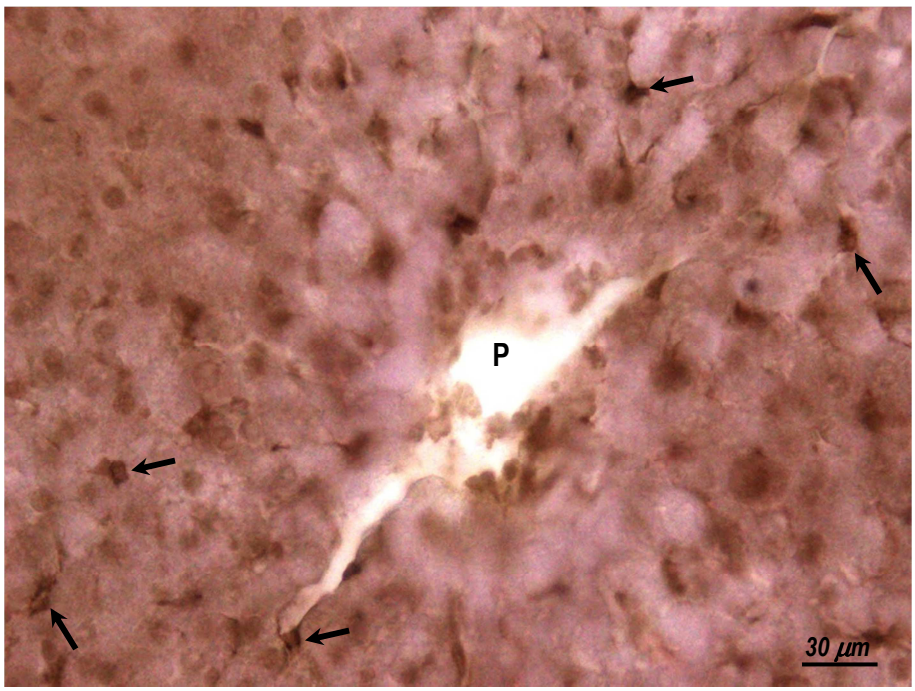

Figure 2.8 – Thick section of an adult male liver, immunostained against GFAP (brown colour) and GS. Hepatic stellate cells (arrows) can be seen around the portal tract (P).

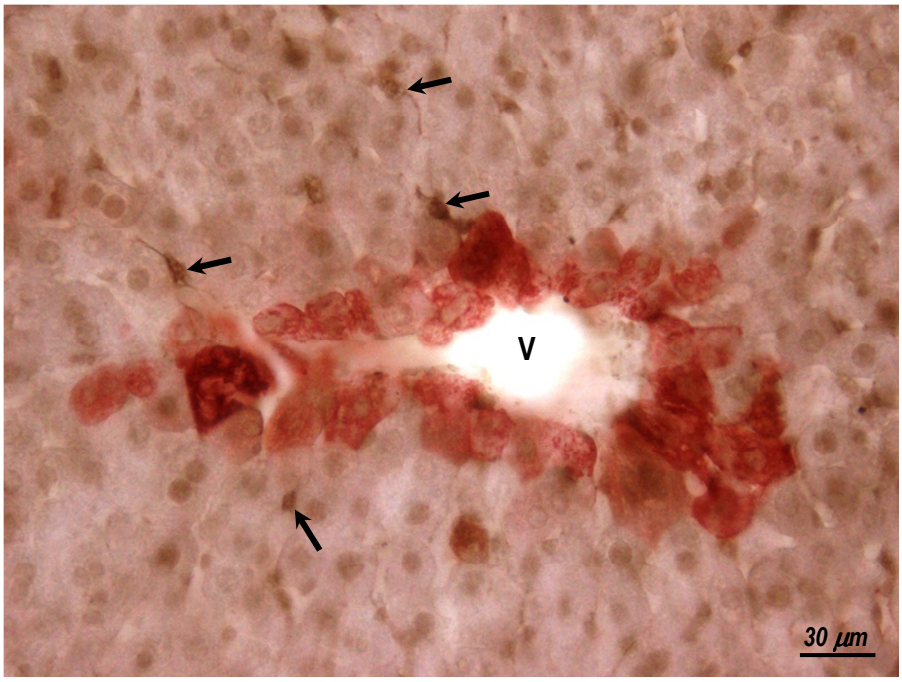

Figure 2.9 – Thick section of a middle-aged male liver, immunostained against GFAP (brown colour) and GS (red). Hepatic stellate cells (arrows) can be seen in a centrilobular location; the central venule (V) is clearly outlined by GS marking.

Within the lobules, GS also marked many KC, and in some occasions these cells appeared in close vicinity with HSC (Figure 2.10) (this will be further detailed in Chapter 4).

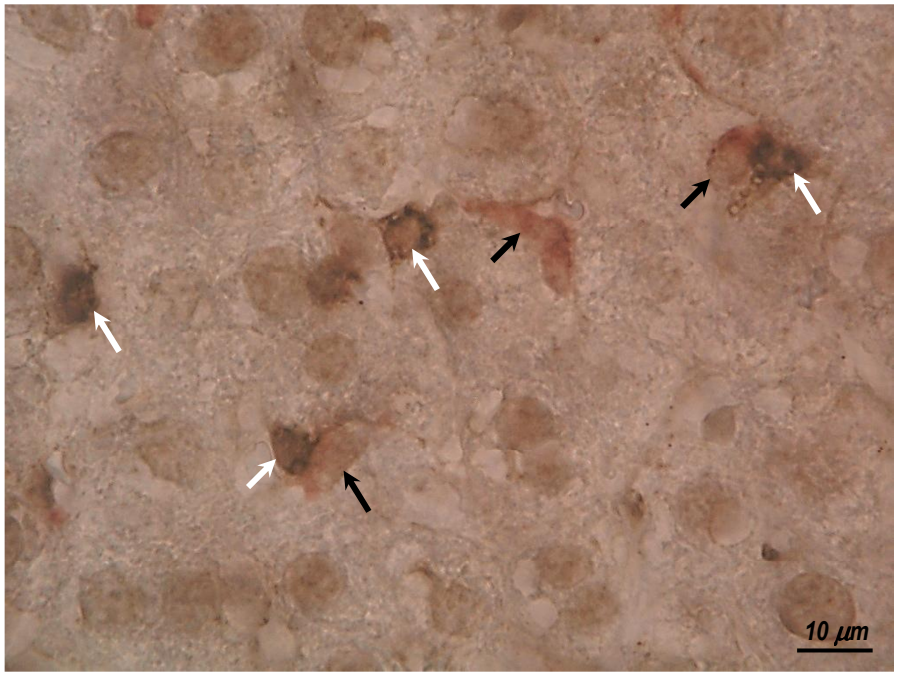

Figure 2.10 – Thick section of a middle-aged male liver, immunostained against GFAP and GS. Kupffer cells (black arrows) are neighbouring hepatic stellate cells (white arrows).

Regarding ASMA, immunomarking was restricted to the walls of blood vessels; no reactive cells were seen within the lobules across the ages studied (data not shown).

The picro-sirius red marked collagen fibres in the capsule, portal tracts and around the central venules, as well as within the lobules. The specificity of the staining was confirmed with polarization microscopy (Figure 2.11), in which we observed thicker fibres, with typical yellow and red birefringence (collagen I), mixed with thinner and green ones (collagen III). The intralobular collagen fibres appeared to be more abundant in old livers, especially in males (Figure 2.12).

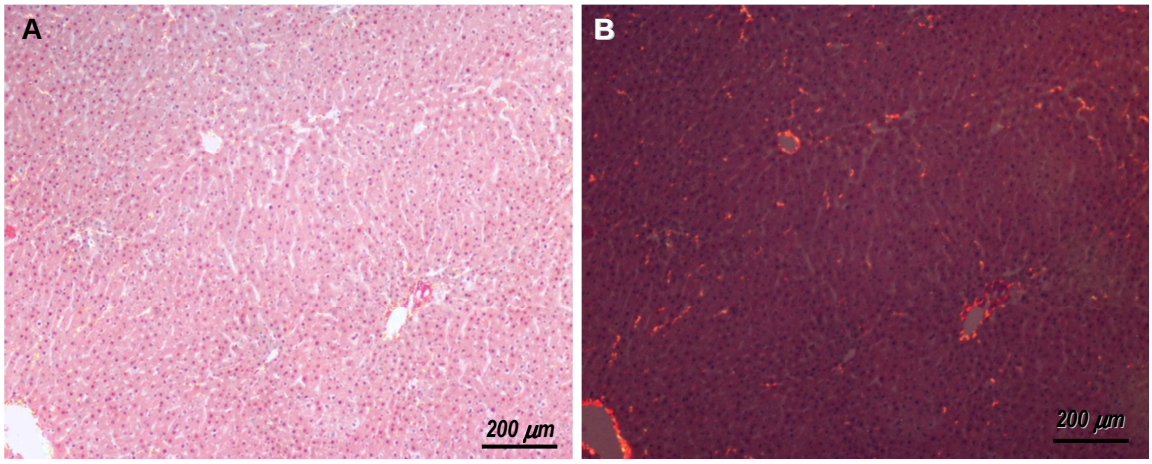

Figure 2.11 – Picro-sirius red staining at light (A) and polarization microscopy (B).

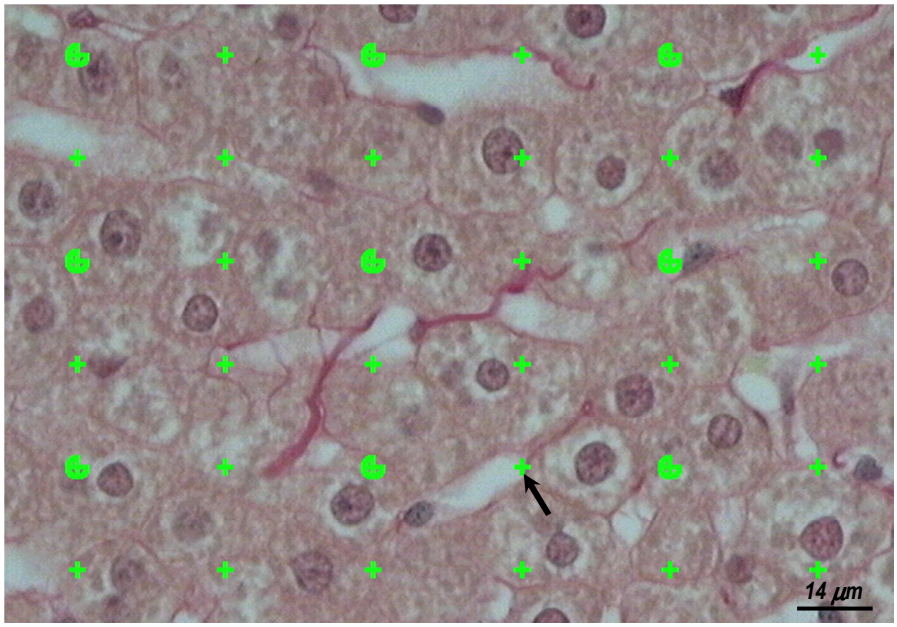

Figure 2.12 – Sinusoidal picro-sirius red staining in an old male liver. For illustrative purposes the counting grid (composed of 36 points) is shown; in this case only one point would be counted (arrow).

2.3.2- Quantitative findings

2.3.2.1- Baseline study: *1) Total number, number per gram and numerical density*

Using the baseline sampling scheme, a mean of 1340 disectors per rat were analysed, in which a mean of 907 HSC were counted; the number of cells counted per animal, ΣQ^{-}, ranged from 642 to 1058.

Table 2.1 – Numerical density, N_V(HSC, liver) of hepatic stellate cells (HSC), expressed as number/mm^3, number per gram of liver, N/g, and total number, N, of HSC in the whole liver. CE(N) is the coefficient of error of N, estimated according to Schmitz and Hof (2000), $CE(N)_1$, and according to Cruz-Orive, 1999, $CE(N)_2$. (Table published in *Marcos et al, Journal of Microscopy, 2004.*)

Rat	N_V	N/g	N	$CE(N)_1$	$CE(N)_2$
1	19.8 E^{03}	14.4 E^{06}	238 E^{06}	0.04	0.04
2	19.3 E^{03}	15.7 E^{06}	218 E^{06}	0.05	0.04
3	22.6 E^{03}	15.1 E^{06}	207 E^{06}	0.03*	0.04*
4	21.6 E^{03}	10.8 E^{06}	147 E^{06}	0.04	0.04
5	18.9 E^{03}	13.5 E^{06}	223 E^{06}	0.03	0.04
Average	20.4 E^{03}	13.9 E^{06}	207 E^{06}	0.04	0.04
CV	0.09	0.14	0.17	0.16	0.09

The N_V(HSC, liver) in 3 month old males was 20.4x10^3 HSC per mm^3 (CV = 0.09), whereas the N was 207x10^6 (CV = 0.17), estimated with a CE(N) of 0.04, independently of the formula used (Table 2.1). In fact, the CE(N) estimated with Equation (2.12) rendered

similar figures to those obtained with Equation (2.4), implying that the variation due to systematic sampling was small. In order to illustrate this, computation details of the CE(N) for one animal in the baseline study are presented in Table 2.2. The aggregate areal fraction (*pa*) was estimated as 1.005. Thus, ΣPf ≈ ΣPs meaning that the influence from artificial borders was negligible for practical purposes. The mean section thickness was 30.2 µm (CV = 0.02) and the CE(t) was 0.005. Within a section, no significant differential deformation (collapse) was observed in the z-direction.

Table 2.2 - Estimation of the coefficient of error (CE) of the HSC counted for rat 3 (Table 2.1), as proposed by Cruz-Orive (1999), $CE(N)_2$, and by Schmitz and Hof (2000), $CE(N)_1$, considering that in our study $CE(N) \cong CE(\Sigma Q^-)$. (Table adapted from *Marcos et al, Journal of Microscopy, 2004.*)

Blocks, i	Sections	Q_i^-	$Q_i^- \cdot Q_i^-$	$Q_i^- \cdot Q_{i+1}^-$	$Q_i^- \cdot Q_{i+2}^-$
1	5	75	5625	15375	18075
2	11	205	42025	49405	47355
3	17	241	58081	55671	36873
4	14	231	53361	35343	
5	6	153	23409		
Σ	53	905 ($\sum Q^-$)	182 501 (A)	155 794 (B)	102 303 (C)

$$CE(\hat{N})_1 = 1\Big/\sqrt{\sum Q^-} = 0.033 \qquad (2.4)$$

$$CE(\hat{N})_2 = \sqrt{\alpha \cdot [3(A - \sum Q^-) + C - 4B]/(\sum Q^-)^2 + 1/\sum Q^-} = 0.035 \qquad (2.12)$$

$$\alpha = \frac{1}{6} \cdot \frac{[1 + 2(t/T) - 2(t/T)^2] \cdot [1 - (t/T)]^2}{40 - 10(t/T)^2 + 3(t/T)^3} \qquad (2.13)$$

As detailed in the text, Equation (2.4) is based in a Poisson distribution, and simply inputs ΣQ^-. In contrast, the estimate of the $CE(N)_2$ considers the number of HSC counted in each of the *i* paraffin blocks and Equation (2.12) is based in the quadratic approximation formula. To use it, the α was calculated using Equation (2.13), defined for continuous objects; in this, *t*/T is the sampling period, expressing the ratio between used and total material (*t*/T = 1/2 x 1/2 x 1/2 = 1/8). In Equation (2.12) the α was 1/256, the ΣQ^- is the sum of counted HSC in each block and [A] is the sum of the squares of cells counted in every block; [B] is the sum of the products of Q^- from each block and Q^- from the next in the series (*i* + 1); and [C] is the sum of the products of Q^- from each block and the second next in the series (*i* + 2).

For rats in the baseline study, the N_V(HSC, liver) and N of HSC per block were also calculated and are shown in Figure 2.13. The former presented no trend (the graph lines range from plateaus to mildly undulating). By contrast, in the N of HSC for the smoothly arranged blocks, a dome-shape distribution was constantly observed; the smaller pieces

(more peripheral in the smooth arrangement), contained fewer HSC than the larger, more central ones.

In estimating the N of HSC, and according to Equation (2.6), the sampling procedure was responsible for about 5% of the total observed variance, irrespective of the formula used to calculate CE(N). As expected, the variance in section thickness was responsible for only 0.07% of the total variance. This means that the inherent (biological) relative variance (among rats) contributed to 95% of the total variance, being far more important than the mean variance of the individual estimates of the CE(N).

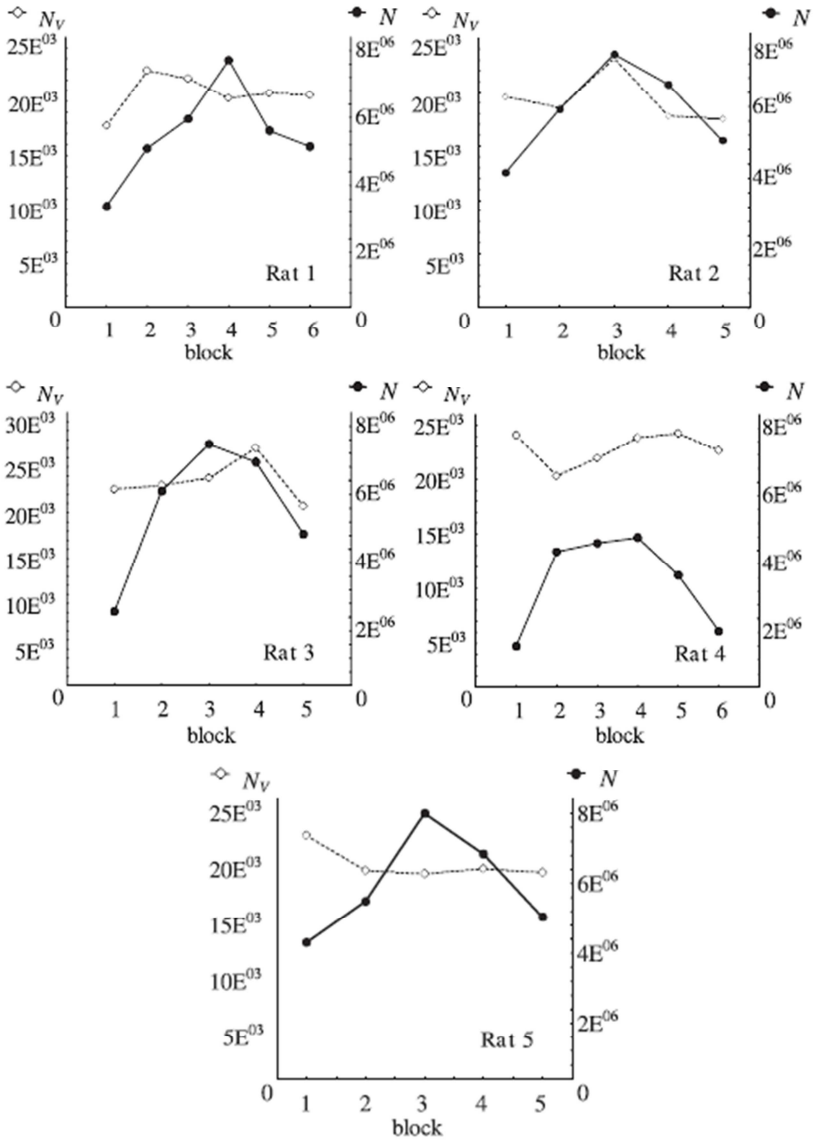

Figure 2.13 – Estimations of HSC number per block (N) and numerical density [N_V(HSC, liver)]. The constant dome-shaped pattern for N and the lack of a trend for N_V(HSC, liver) are evident. (Image published in *Marcos et al, Journal of Microscopy, 2004.*)

A statistically significant correlation was found between the *N* of HSC and the liver weight (Spearman R = 1.0; $p < 0.01$).

2.3.2.1- Baseline study: 2) Assessment of the optimum sampling

Considering the two 'half-sampling' strategies, the number of cells actually counted was similar in both groups. When half of the fields were considered (strategy 1), an average of 456 HSC were counted ($\Sigma Q^- \approx 274–578$), whereas with half of the sections (strategy 2), we counted an average of 460 ($\Sigma Q^- \approx 286–562$). As shown in Figure 2.14, the CE(N) was just slightly lower in strategy 1 [CE(N) = 0.052] than in strategy 2 [CE(N) = 0.054]. According to Equation (2.6), and considering half of the fields or sections, the contribution of the sampling procedure to the total variance was still small, about 9% in both cases.

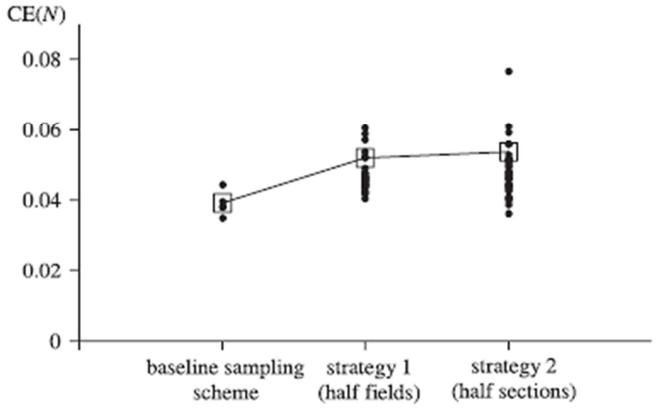

Figure 2.14 – Estimated coefficient of error of number estimates, CE(N), for the baseline sampling scheme and for the six replicas performed per rat in strategy 1 (half of the fields) and strategy 2 (half of the sections). (□) Squared mean of CE(N). (Image published in *Marcos et al, Journal of Microscopy, 2004.*)

2.3.2.2- Age and gender study

2.3.2.2- Age and gender study: 1) Body, liver weight, liver-to-body ratio and liver volume

The animals increased their weight with ageing, peaking at 12 months [677.4 g (CV = 0.11) and 408.5 g (CV = 0.14) in males and females, respectively] (Figure 2.15). Middle-aged males were twice as heavy as youngsters, whereas middle-aged females increased their weight by 75%. In all age groups, males were heavier than females. Significant correlations existed between body weight: 1) liver weight ($r = 0.77$, $p < 0.001$); 2) N of HSC ($r = 0.68$, $p < 0.001$); 3) $V_{(HSC)}$ ($r = 0.50$, $p < 0.05$).

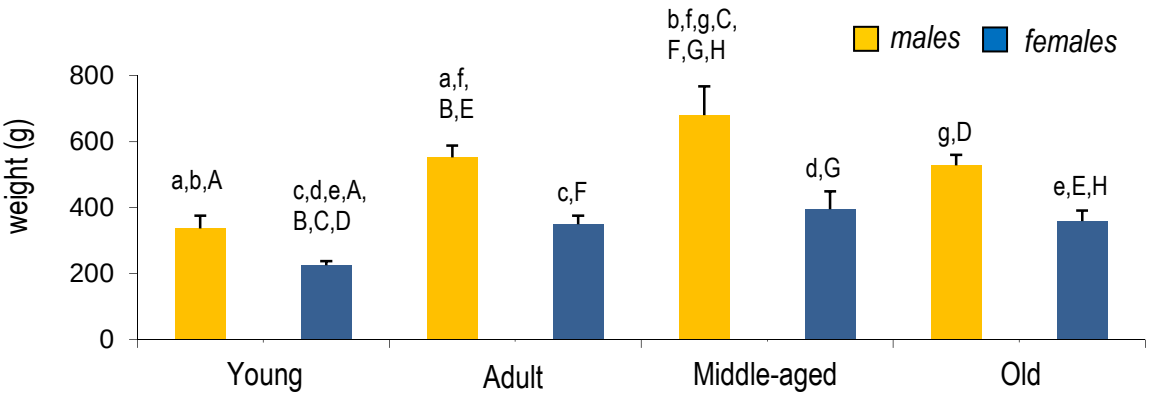

Figure 2.15 – Body weights of male and female in young (2 months), adult (6 months), middle-aged (12 months) and old (18 months) rats. Paired letters indicate significant differences (lowercase: same gender; uppercase: across genders); data expressed as mean + SD.

Respecting liver weight (Figure 2.16) it also peaked at 12 months [17.2 g (CV = 0.20) in males and 12.0 g (CV = 0.14) in females], but the middle-aged liver was only 22% heavier than a young one. Comparing with youngsters, older animals presented no significant differences [13.2 g (CV = 0.08) and 9.6 g (CV = 0.12) in males and females, respectively]. In all age groups, males also had heavier livers than females and this difference was statistically significant ($p < 0.001$). Despite the ANOVA rendered ageing differences, these did not occur within the same gender. As mentioned, a strong correlation existed between the liver weight and body weight. Moreover, the liver weight was correlated with the N of HSC ($r = 0.77$, $p < 0.001$), as well as with the $V_{(HSC)}$ ($r = 0.64$, $p < 0.001$).

The liver-to-body weight ratio was highest at the age of two months with 4.4% (CV = 0.05) in males and 4.3% (CV = 0.06) in females, while it ranged between 2.6% to 2.9% in males and 2.7% to 3.1% in females, in the other age groups (Figure 2.17); such difference was statistically significant.

As to the liver volume, it followed the same trend of weight. It was maintained throughout ageing [12.9 cm^3 (CV = 0.21) in young and 12.3 cm^3 (CV = 0.07) in old males, whereas in females the liver had 9.2 cm^3 (CV = 0.07) and 8.9 cm^3 (CV = 0.12) in young and old females, respectively]. It is opportune to mention that the liver density varied from 1.07 to 1.09 g/cm^3 in males, and from 1.06 to 1.08 g/cm^3 in females.

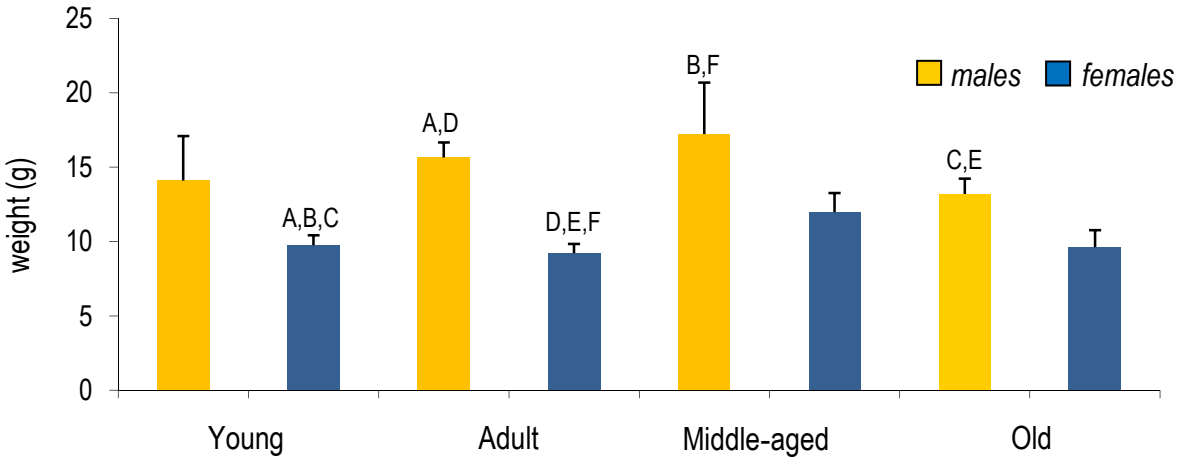

Figure 2.16 – Liver weights of male and female young (2 months), adult (6 months), middle-aged (12 months) and old (18 months) rats. Paired letters indicate significant differences (uppercase: across genders); data expressed as mean + SD.

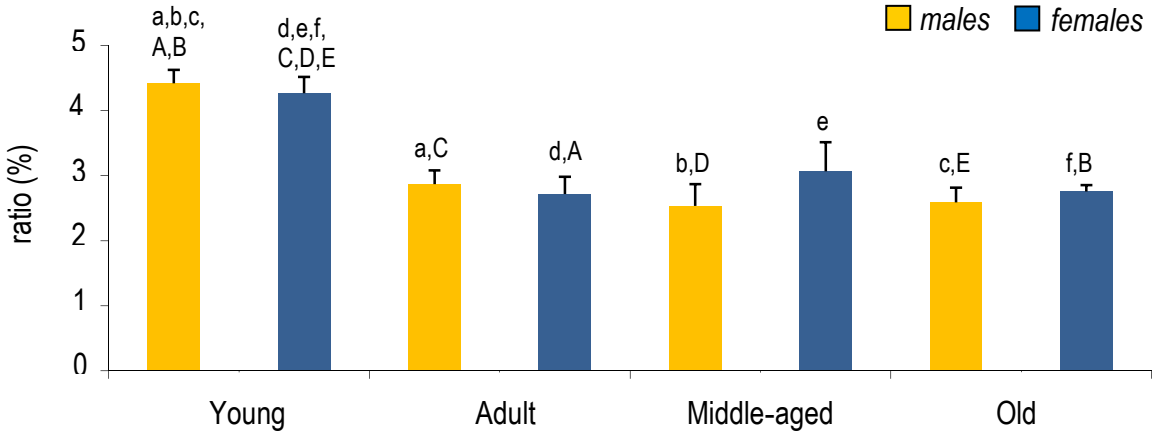

Figure 2.17 – Liver-to-body weight ratio of male and female young (2 months), adult (6 months), middle-aged (12 months) and old (18 months) rats. Paired letters indicate significant differences (uppercase: across genders; lower case: same gender); data expressed as mean + SD.

2.3.2.2- Age and gender study: 2) Hepatic transaminases and serum oestradiol levels

Hepatic transaminases values were within the reference values throughout the groups [14-80 IU/L for alanine aminotransferase (ALT) and 40-383 IU/L for AST]. The ALT and AST values did not vary with ageing or gender (Figure 2.18). In contrast, serum oestradiol levels (Figure 2.19) were consistent with reported reference values for rodents (*e.g.*, Scotland *et al*, 2011), even if they tended to increase with ageing ($p < 0.01$).

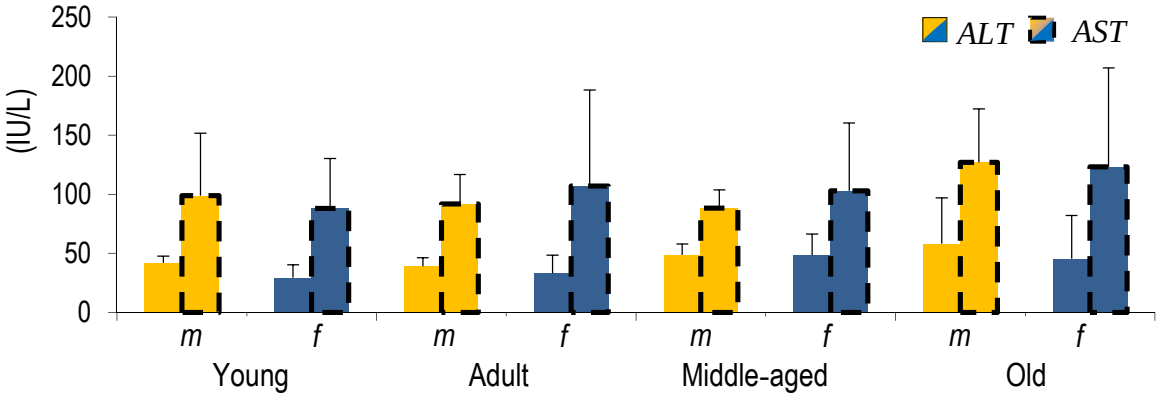

Figure 2.18 – Alanine transaminase (ALT) and aspartate transaminase (AST) (IU/L) in male (*m*) and female (*f*) young (2 months), adult (6 months), middle-aged (12 months) and old (18 months) rats; data expressed as mean + SD. (Columns without contour: ALT; columns with dashed contour: AST.)

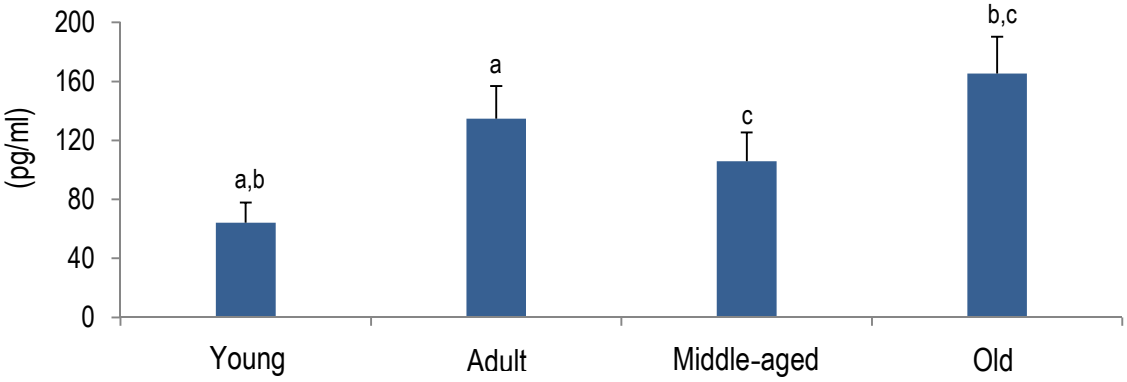

Figure 2.19 – Serum oestradiol (pg/ml) in female young (2 months), adult (6 months), middle-aged (12 months) and old (18 months) female rats. Paired letters indicate significant differences. Data expressed as mean + SD.

2.3.2.2- Age and gender study: 3) Section thickness and distribution of particles in the z-axis

The mean section thickness was 36.3 µm (CV = 0.03) varying from 34.7 µm in male adults to 37.4 µm in old females; the corresponding CE(t) was low (varying from 0.005 to 0.013). As mentioned in Chapter 1, we evaluated the distribution of particles in the z-axis, in order to know if guard heights should be used in the optical disector (Annex 1).

2.3.2.2- Age and gender study: 4) Total number, number per gram and numerical density of HSC

An average of 780 and 459 optical disectors were analysed per male and female rat, counting 439 and 350 HSC, respectively [the ΣQ^- varied from 271 (in young females) to 569 HSC (in adult males)].

The N of HSC (computed after Equation 2.2) did not vary significantly with ageing (Figure 2.20) in males (that were particularly stable) and females. Anyway, the young males had

the lowest average estimate [190x10^6 HSC (CV = 0.20)] and the highest value was seen in old males [206x10^6 HSC (CV = 0.11)]. The same stability occurred in females, with the young having 131x10^6 HSC (CV = 0.14), and the old 148x10^6 HSC (CV = 0.21). Contrarily to ageing, significant statistical differences existed for gender (p < 0.001), with males having an overall (grouped) greater N of HSC. Besides the correlation with the liver weight, the N of HSC was also moderate, but nevertheless significantly correlated with the HSCI (r = 0.56, p < 0.01) and $V_{(HSC)}$ (r = 0.68, p < 0.001).

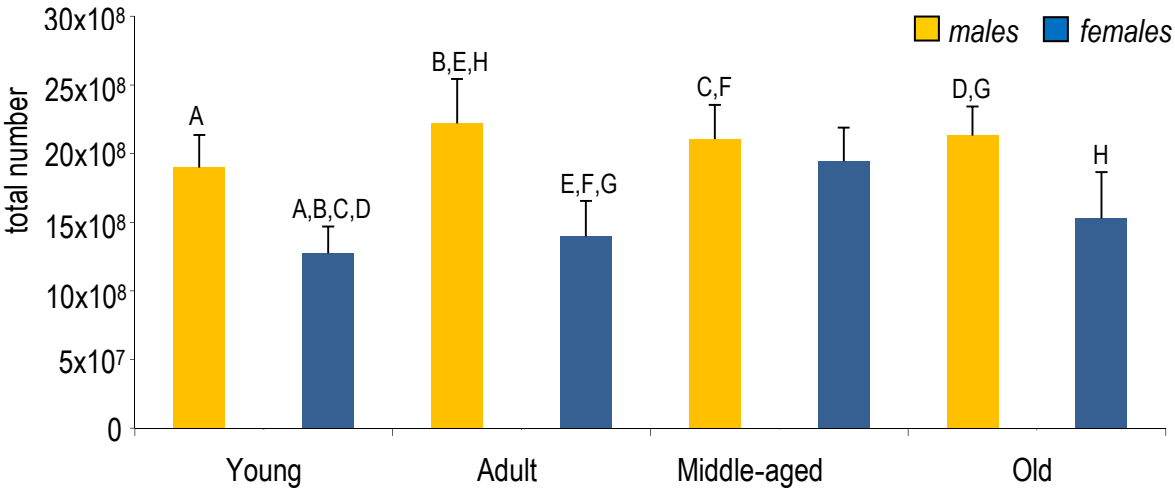

Figure 2.20 – Total number (N) of hepatic stellate cells in male and female rats young (2 months), adult (6 months), middle-aged (12 months) and old (18 months) rats. Paired letters indicate significant differences (uppercase: across genders); data expressed as mean + SD.

When estimating the N of HSC, and according to Equation (2.6), the sampling procedure was responsible for less than 20% of the total observed variance for all the animals (Figure 2.21). In detail, the sampling was responsible for 13% and 18% in young, and 17% and 7% in old animals (values for males and females, respectively). Variance due to section thickness was small, being responsible for a maximum of 2% of the observed variability. Therefore, the biological variability was by far the most important component of the observed variability for the estimation of the N of HSC.

The number of HSC per gram of liver (N/g) was also estimated. It was very constant throughout ageing (Figure 2.22): with mean values ranging from 12.5x10^6 (CV = 0.21) to 15.6x10^6 HSC (CV = 0.08) in males and from 13.5x10^6 (CV = 0.19) to 16.4x10^6 HSC (CV = 0.18) in females. Besides the negative correlation with the liver weight, the N/g was moderately correlated with the N_V(HSC, liver) (r = 0.66, p < 0.001). No matter the graphical fluctuations of mean values, there were no statistically significant differences between genders, at any age.

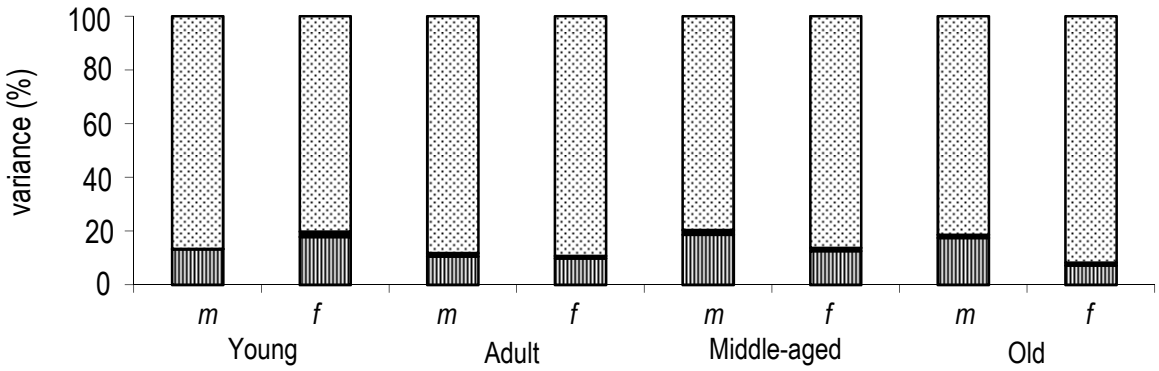

Figure 2.21 – Decomposition of the observed variance of the N estimations (according to Equation 2.6) in male (m) and female (f) of young (2 months), adult (6 months), middle-aged (12 months) and old (18 months) rats; ⁞ = biological variance; ▮ = section thickness variance; ▩ = average sampling variance.

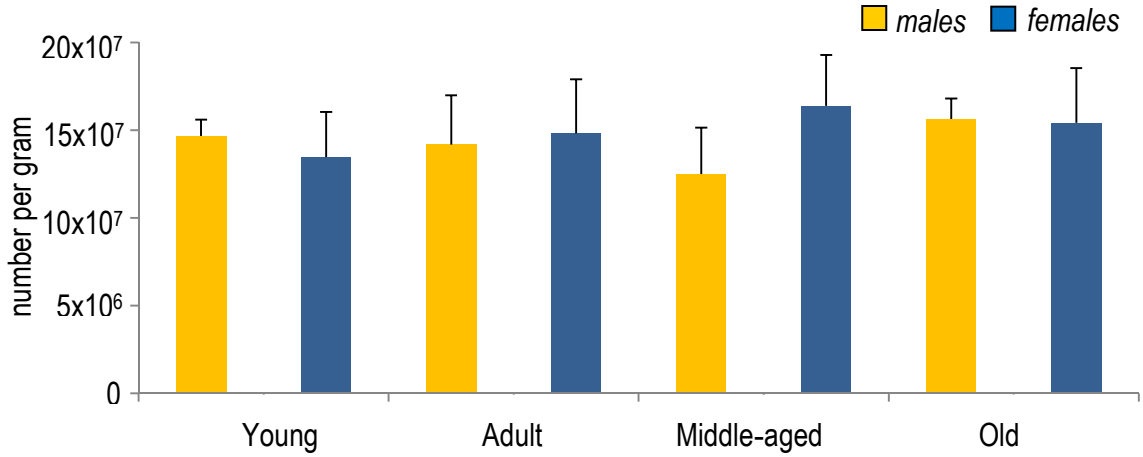

Figure 2.22 – Number per gram (N/g) of hepatic stellate cells in male and female in young (2 months), adult (6 months), middle-aged (12 months) and old (18 months) rats. Data expressed as mean + SD. There were no statistically significant differences.

The numerical density (N_V) estimated from paraffin sections is markedly overestimated. In this study, shrinkage seemed more pronounced in youngsters, but no statistical differences existed (neither throughout ageing, nor between genders). Shrinkage varied from 24% (in old females) to 36% (in young females). In Figure 2.23 we present the N_V(HSC, liver) already corrected for shrinkage; it varied from 13.3×10^3 (CV = 0.12) HSC per mm^3 in middle-aged females to 17.5×10^3 (CV = 0.23) HSC per mm^3 in middle-aged males. No statistically significant differences existed for ageing or gender. As mentioned above, the N_V(HSC, liver) was moderately correlated with the N/g, as well as with the V_V(HSC, liver) ($r = 0.57$, $p < 0.01$).

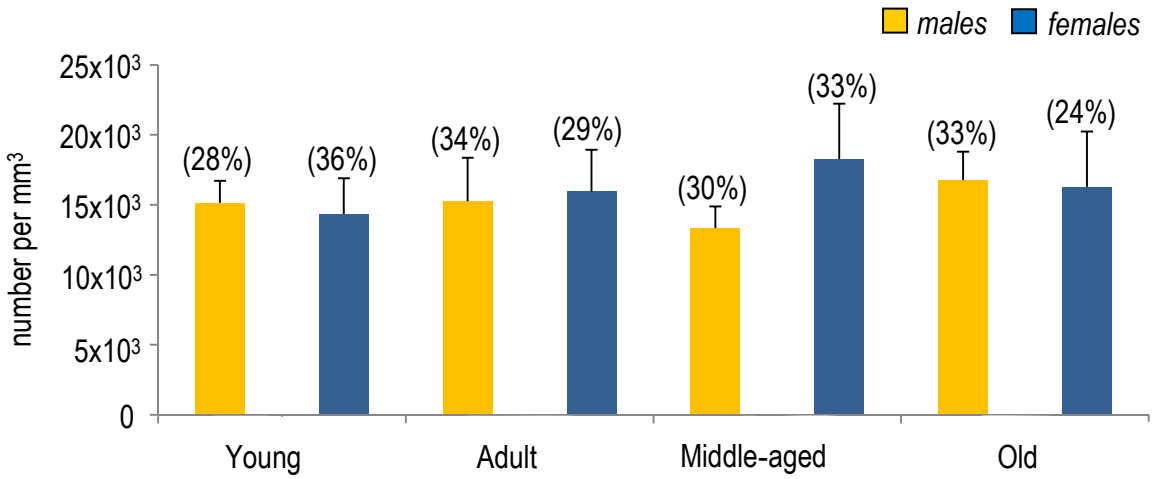

Figure 2.23 – Numerical density N_V(HSC, liver) of hepatic stellate cells (presented as number/mm^3) in male and female in young (2 months), adult (6 months), middle-aged (12 months) and old (18 months) rats. Data corrected for shrinkage (in brackets) and expressed as mean + SD. There were no statistically significant differences.

2.3.2.2- Age and gender study: 5) Hepatic stellate cell index

The HSCI seemed to have a decreasing trend in males, from 109 (CV = 0.10) in young to 86 (CV = 0.11) in old rats (Figure 2.24). In females a different graphical pattern appeared: it suggested a slight increase from young [HSCI of 74 (CV = 0.12)] to middle-aged females [HSCI of 101 (CV = 0.03)] and then it decreased [HSCI of 83 (CV = 0.16) in old females]. Yet, no statistically significant differences existed, either for males or females. Despite this fact, the HSCI of males and females were (in the young) significantly different ($p < 0.05$). As already mentioned, the HSCI was correlated with the liver weight and with the N of HSC.

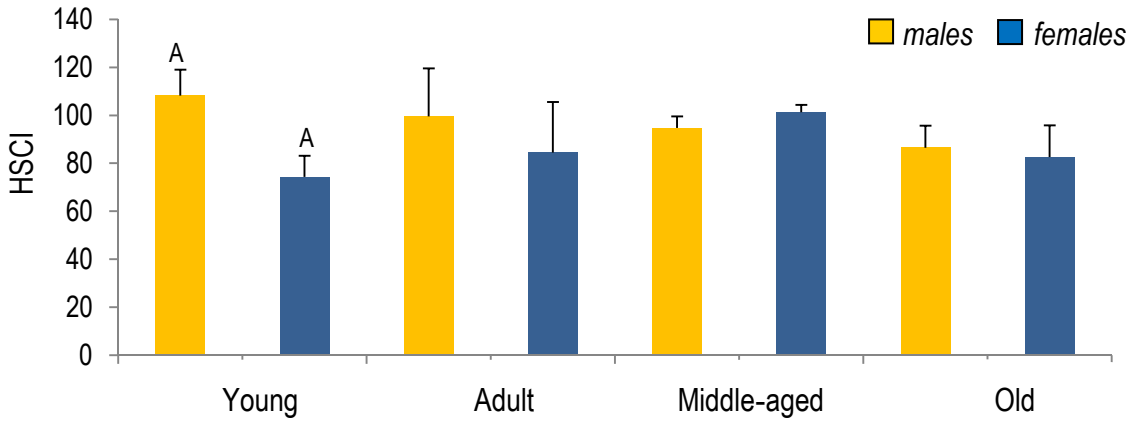

Figure 2.24 – Hepatic stellate cell index (HSCI; *i.e.*, number of HSC per 1000 hepatocytes) in male and female in young (2 months), adult (6 months), middle-aged (12 months) and old (18 months) rats. Paired letters indicates a significant difference (uppercase: across genders); data expressed as mean + SD.

2.3.2.2- Age and gender study: 6) Volume density and number-weighted mean volume

Two kinds of volume densities were estimated: in epoxy sections we assessed the perikaryon [expressed as V_V(HSC*per*, liver)], whereas in thin paraffin sections immunostained against GFAP we evaluated the "whole" cell, *i.e.*, perikaryon and the cytoplasmic processes that contained this intermediate filament [this was designated by V_V(HSC, liver)]. As expected, the latter was always greater than that of the perikaryon [V_V(HSC*per*, liver)], but in old animals the difference was attenuated (Figure 2.25). Despite females seemed to have a larger V_V(HSC, liver) than males (except in old animals), this suspected difference was not statistically significant (p = 0.065). Regarding the V_V(HSC*per*, liver), ageing differences existed for all the groups (p < 0.05 for differences between adult *versus* middle-aged, and p < 0.01 for all the others). As mentioned, the V_V(HSC, liver) was correlated with the N/g of HSC and N_V(HSC, liver). Since V_V(HSC, liver) was used to estimate the $V_{(HSC)}$ and number-weighted cell volume ($\overline{v}_N$), a moderate correlation also existed for these parameters (r = 0.55, p < 0.01 and r = 0.66, p < 0.01, respectively).

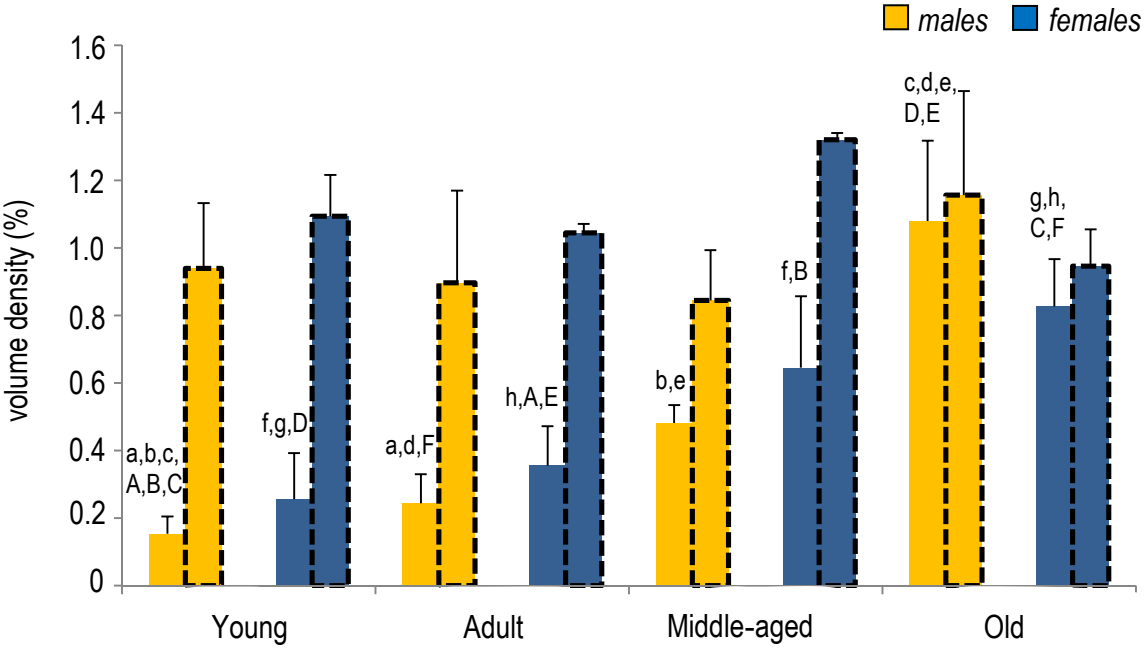

Figure 2.25 – Volume density of hepatic stellate cells (expressed in percentage) in young (2 months), adult (6 months), middle-aged (12 months) and old (18 months) rats. Columns without contour correspond to the perikaryon [V_V(HSC*per*, liver)], and those with dashed contour to the "whole" cell [V_V(HSC, liver)]. Paired letters indicate significant differences (lowercase: same gender; uppercase: across genders); data expressed as mean + SD.

The scenario described for the V_V(HSC, liver) changed when considering the total volume occupied by HSC, *i.e.*, the $V_{(HSC)}$ (estimated by Equation 2.11). In that case, the $V_{(HSC)}$ showed a mean of 0.127 cm^3 (CV = 0.18) in young and of 0.147 cm^3 (CV = 0.28) in old rats (despite no significant differences existed), whereas in females the $V_{(HSC)}$ was

relatively more constant throughout age [≈ 0.09 cm^3 (CV ≈ 0.15) in young and old females]. No significant gender differences existed for the $V_{(HSC)}$. As already mentioned, the $V_{(HSC)}$ was correlated with the N of HSC, as well as with the V_V(HSC, liver) and liver weight.

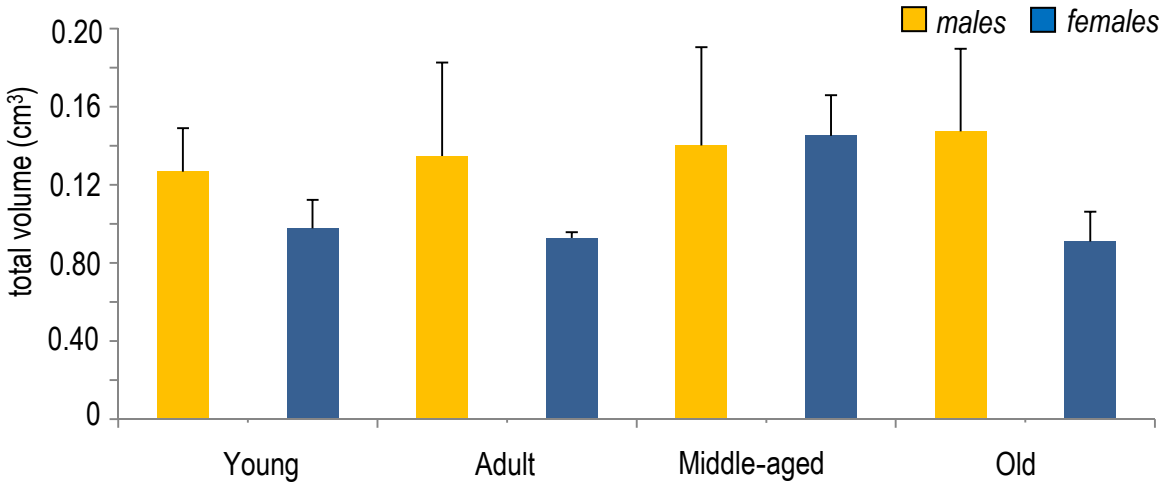

Figure 2.26 – Total volume occupied by hepatic stellate cells in young (2 months), adult (6 months), middle-aged (12 months) and old (18 months) animals. Data expressed as mean + SD. There were no statistically significant differences.

Regarding the mean number-weighted cell volume ($\overline{v}_N$) of HSC, the pattern was somewhat similar to the V_V(HSC, liver): in females there was a 30% non-statistically significant difference throughout ageing, from 785 μm^3 (CV = 0.24) to 603 μm^3 (CV = 0.12), whereas in males the opposite trend occurred, since the $\overline{v}_N$ varied from 619 μm^3 (CV = 0.20) in young to 689 μm^3 (CV = 0.27) in old rats (Figure 2.27). For this parameter, no differences existed for ageing or gender.

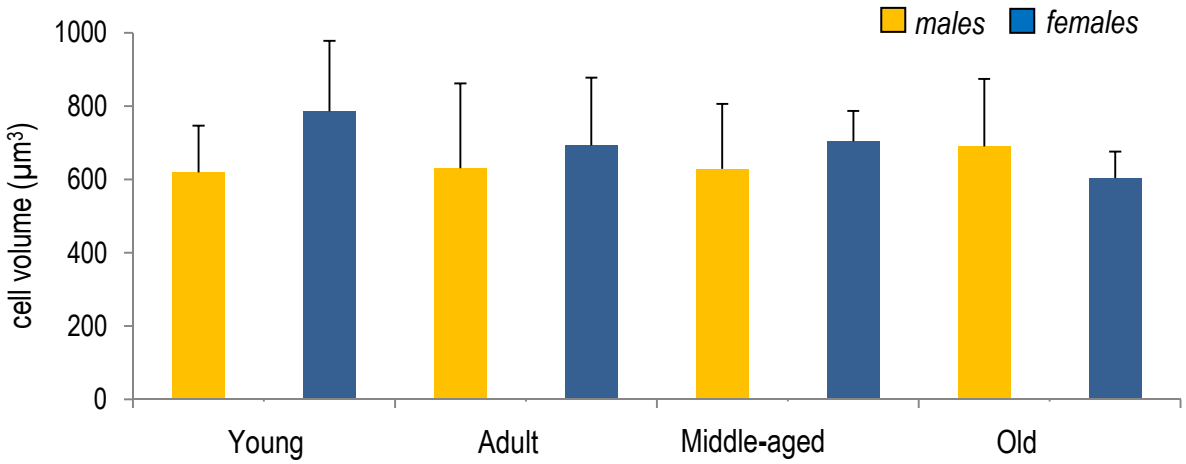

Figure 2.27 – Mean number-weighted cell volume (in μm^3) of hepatic stellate cells in male and female young (2 months), adult (6 months), middle-aged (12 months) and old (18 months) rats. Data expressed as mean + SD. There were no statistically significant differences.

2.3.2.2- Age and gender study: 7) Lobular heterogeneity

In order to assess lobular heterogeneity, an average of 303 HSC was evaluated per rat. The distribution of these cells was not influenced by gender; however, a pattern appeared to exist with ageing, since cells shifted from slight centrilobular predominance, seen in younger animals, to periportal abundance in older rats (Figure 2.28). This difference was statistically significant for ageing ($p < 0.001$), with a two-way ANOVA for ageing and gender effects. Additionally, similar results whre obtained with a two-way ANOVA considering the effects of ageing and localisation.

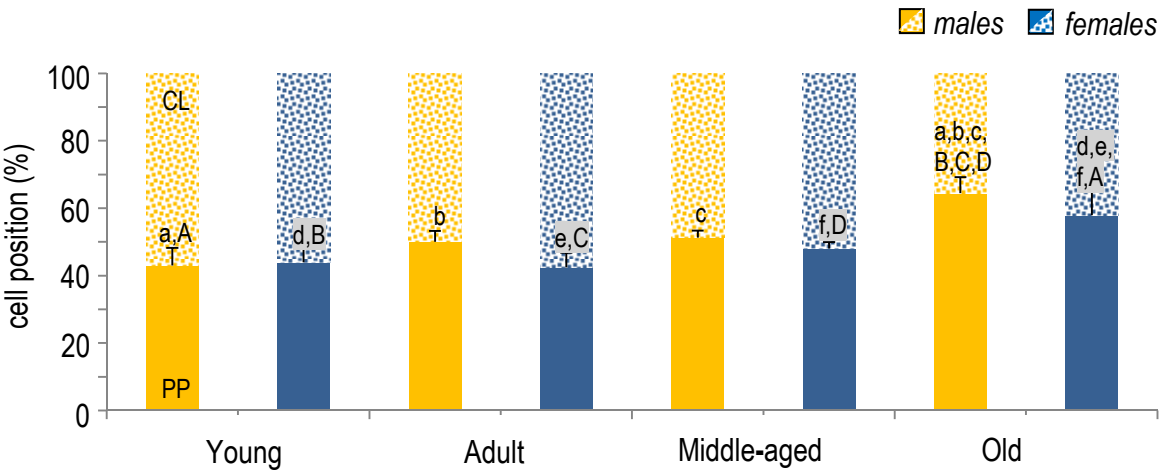

Figure 2.28 – Percentage of hepatic stellate cells located in a periportal (PP, full colored) or centrilobular (CL, dashed coloured) position in male and female young (2 months), adult (6 months), middle-aged (12 months) and old (18 months) rats. Paired letters indicate significant differences (lowercase: same gender; uppercase: across genders); data expressed as mean + SD.

2.3.2.2- Age and gender study: 8) Picro-sirius red staining

An average of 216 fields was screened per animal. By using a 40x objective, a good discrimination of collagen fibres was achieved. Since HSC are involved in collagen deposition within the lobule, we were particularly interested in intralobular collagen. In males, it corresponded to 56% of the total collagen, whereas 20% and 14% were located in portal tracts and around central venules, respectively; only 10% was found in the Glisson's capsule. A similar scenario was seen in females: 46 % was intralobular, 42% around vessels (respectively, 28% and 14% in a portal and central location) and 12% in the capsule. No significant differences existed in these proportions throughout ageing and gender. We determined the volume content of intralobular collagen in the liver (Table 2.3), and the relative volume of collagen (Figure 2.29). The picro-sirius red within the lobule was moderately correlated with the N of HSC ($r = 0.50$; $p < 0.01$). These parameters were influenced by gender ($p < 0.001$) and by ageing ($p < 0.01$), namely in males. The collagen

was significantly more abundant in males, namely in adults and in old rats; in females, no significant differences existed.

Table 2.3 – Total intralobular collagen content (in mm^3) present in male and female young (2 months), adult (6 months), middle-aged (12 months) and old (18 months) rats. Paired letters indicate significant differences (lowercase: same gender; uppercase: across genders). (For the sake of simplicity, only gender comparisons of animals with the same age are presented.) Data expressed as mean ± SD.

Collagen (mm^3)	Young	Adult	Middle-aged	Old
Male	$127 \pm 27^{a,b,A}$	$305 \pm 135^{a,B}$	179 ± 39	$222 \pm 34^{b,C}$
Female	77 ± 18^{A}	88 ± 18^{B}	117 ± 15	93 ± 20^{C}

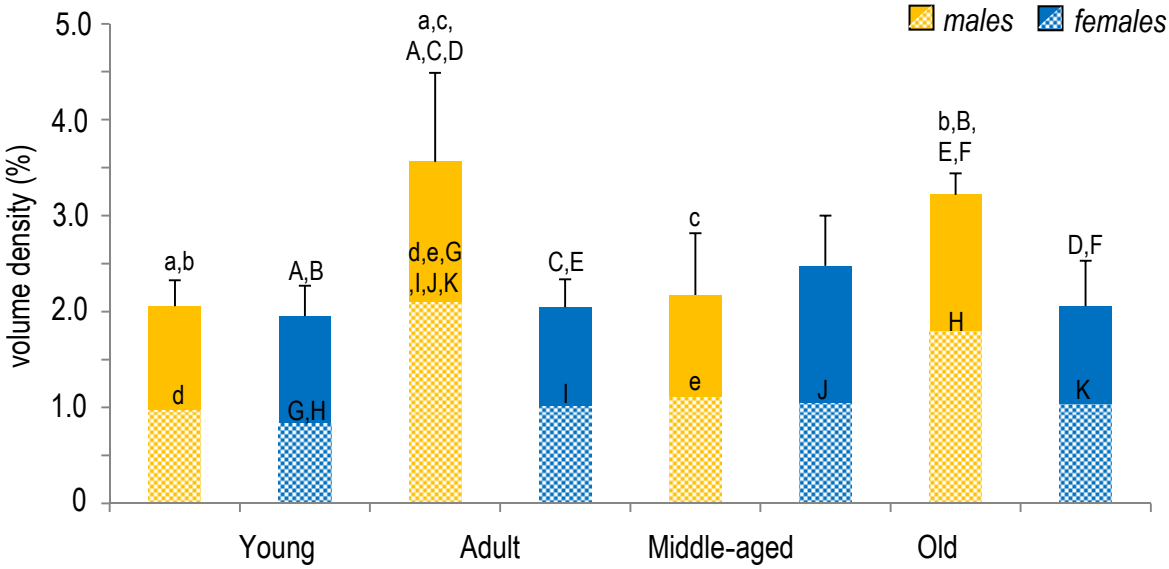

Figure 2.29 – Volume density of lobular collagen (dashed colour) and total collagen (dashed and solid colour) in male and female young (2 months), adult (6 months), middle-aged (12 months) and old (18 months) rats. Paired letters indicate significant differences (lowercase: same gender; uppercase: across genders). Data expressed as mean + SD.

2.4- Discussion

2.4.1- Baseline study

2.4.1- Baseline study: 1) About HSC quantification

This was the first in depth estimation of HSC number in the rat liver using stereological tools. So far, the few quantitative studies on HSC in human (Bronfenmajer *et al*, 1966; Giamperi *et al*, 1981) and rat (Geerts *et al*, 1991; Niki *et al*, 1996; Azaïs-Braesco *et al*, 1997, Warren *et al*, 2011) counted particle profiles in 2D sections (3-10 μm), obtaining "numbers per area". As previously mentioned in Chapter 1, these are undermined by uncontrolled bias due to the lost caps and the most often unrealistic assumptions on size, shape and orientation of particles (Gundersen *et al*, 1988).

In the continuous scans of the optical disector, recognition of the irregular HSC profiles was made easy, and, as the optical sections were naturally aligned, the counting was much faster than when using the physical disector — found best suited for HSC counting in liver biopsies (Marcos *et al*, 2012). By combining the disector with the fractionator in paraffin sections (which presented no differential deformation and practically no collapse in the z-axis), the estimation of N of HSC also became unaffected by shrinkage (Dorph-Petersen *et al*, 2001). Additionally, an increased efficiency was granted by the smooth fractionator design (Gundersen, 2002).

From disector readings, the N_V(HSC, liver) could be estimated, despite corresponding to an overestimation due to the paraffin shrinkage. We observed a total of 38% of volume shrinkage from fresh to mounted sections (data not shown), which is in accordance with previous reports (Salisbury, 1994) and with the age and gender study. Although the N_V(HSC, liver) may be useful, it should be used cautiously regarding its inferences, as it tells us nothing about the N of HSC. (In this regard, we should stress that no statistic correlation was found between the two parameters, neither in the baseline study nor in the age and gender study.)

2.4.1- Baseline study: 2) The tagging of HSC

The immunohistochemistry approach here used was mandatory as HSC cannot be adequately recognised in routine sections (Roskams *et al*, 2007). Gard *et al* (1985) first demonstrated GFAP in HSC, and nowadays it is recognised as a specific marker for these cells (Neubauer *et al*, 1996; Geerts, 2001; Friedman, 2008). It allows a more precise identification and quantification than desmin (Ballardini *et al*, 1994; Niki *et al*, 1996), often used to tag HSC. GFAP is also preferable to other markers, like lipid staining (Bronfenmajer *et al*, 1966; Giamperi *et al*, 1981) and vitamin A autofluorescence (Ballardini *et al*, 1983), as these are influenced by the age and diet of the animals

(Buniatian *et al*, 1996) and by the fact that some HSC have no lipid droplets — the so-called empty HSC (Ito and Nemoto, 1952; Sztark *et al*, 1986). (We presumably observed these empty cells, because in some HSC the cytoplasmic “reticular” pattern — due to the usual washout of the lipid droplets — was absent.) HSC have been immunomarked in paraffin (Marcos and Rocha, 2001b), but here this was achieved in thick sections. To mark HSC throughout the full section depth, we used quite long incubation times with the antibodies, following the approach used for marking astrocytes with GFAP in thick brain sections (Ontoniente *et al*, 1983).

2.4.1- Baseline study: 3) The sampling procedure

When analysing the eventual variation of the N_V(HSC, liver) among blocks, we concluded that the graphic pattern in the five rats (Figure 2.13) was in agreement with a globally homogeneous organ, and therefore cells were equally distributed in density within the final sampled liver pieces. In true, there was not a single noteworthy difference in the N_V(HSC, liver). Accordingly, the graphic pattern of the N of HSC per block was dome-shaped, as expected from carrying the smooth fractionator in a specimen with homogeneous particle distribution (Gundersen, 2002).

Our sampling design was planned to obtain a precise estimation of N, with a CE(N) lower than 10% (West *et al*, 1996; Boyce *et al*, 2010). Facing the no-pattern of the N_V(HSC, liver) among liver chips, and because the computation of the CE(N) is still being debated among stereologists, we used two different approaches recommended for particles without a noticeable heterogeneous distribution, following the *formulae* appraisal and conclusions by Schmitz and Hof (2000). Formula (2.4) was used as it was proved that when more than 10 sections are sampled, the variation due to systematic sampling is small (Gundersen *et al*, 1999) and the CE(N) can be estimated as in random independent sampling designs. By the contrary, formula (2.12) was used as it was conceived, and recommended, for systematic sampling designs (Cruz-Orive, 1999), thus computing both the sum of blocks and the within blocks contribution to the CE(N). Despite it was less practical, presenting a priori more time-consuming calculations, in our case, it was worth programming the formula, as it allowed us to conclude that the slice contribution to the CE(N) was negligible. Indeed, with both the approaches, the CE(N)s were similar, lower than the pretended threshold, and contributed to much less than 50% to the total variance. Taking all this into account, we can regard our baseline sampling procedure as adequate and quite precise.

The optimum sampling (*i.e.*, minimal effort for having a sufficiently good estimate precision) is still debated today (Boyce *et al*, 2010), and the general rule of about "200

cells per individual" (Gundersen *et al*, 1988) has been questioned (Schmitz and Hof, 2000). The number of HSC we initially counted per liver was within the range that has been advised (700-1000) for estimating total neuronal numbers with a CE(N) similar to ours (Schmitz and Hof, 2000). Despite this, we decided to further evaluate the sampling effort and whether it could be reduced, by simulating a half sampling reduction at the level of either fields or sections. The CE(N)s were similar and both acceptable [$CE(N) \leq 0.1$ and $CE^2(N)/CV^2(N) < 0.5$]; nevertheless, the practical implications differ substantially — by sampling only half of the sections, *i.e.,* strategy 2, costing reagents would be saved and the more time-consuming steps of the immunohistochemistry would be much reduced than in strategy 1. So, the optimum sampling scheme in HSC quantification depends on the kind of study in mind. Our baseline sampling would be appropriate for assessing the N of HSC and at the same time evaluate in detail a subset of HSC (*e.g.*, estimate the N of centrilobular HSC). However, if the N of HSC is the only parameter to be estimated, around half of our baseline sampling (counting 250-600 cells per rat) would generate sufficiently precise estimates, being more efficient to reduce the number of sections than to reduce the sampled fields. This approach was followed in the age and gender study.

2.4.2- Age and gender study

2.4.2- Age and gender study: 1) About the obtained data

In recent years, the role of HSC in liver pathology has emerged. It is now clear that the activation of these cells is a key process — for instance, the number of activated HSC (expressed as a score) has been shown to have a prognostic role, determining the need for a new liver transplant (Gawrich *et al*, 2005). In fact, after the advent of HSC isolation, several studies focused their attention on the activation and substances affecting fibrogenesis and proliferation of HSC *in vitro*. Although it has been assumed that activation may be recapitulated by *in vitro* methodologies, the use of proteomics has demonstrated that several proteins regulated in those conditions were unchanged during *in vivo* activation (Kristensen *et al*, 2000). Puzzlingly, considerable less attention has been devoted to the normal liver and to the best of our knowledge a quantitative study focusing gender differences of HSC has never been performed and only one detailed ageing effects on HSC (Warren *et al*, 2011).

At a first glance at a microscope, the liver seems to be formed by endless tortuous labyrinths, but the organisation of liver cells is far from random. In fact, the N of liver cells is highly correlated: apart from the strong linear correlation between the liver weight and the N of HSC, this latter is also strongly correlated with the N of HEP ($r = 0.73$, $p < 0.001$) as it will be detailed in Chapter 3. Moreover, correlations with BnHEP and KC also exist

(these will be discussed in Chapters 3 and 4, respectively) and this emphasises the complexity of the liver. Since this Thesis was the first studying ageing and gender effects in the rat liver, with unbiased stereological techniques, we opted to present a wide exploratory range of numerical parameters and to mention the various correlations that existed between cells and the studied parameters. To the best of our knowledge, such correlations between liver cells have never been reported in the liver *in vivo*; nevertheless, they could be somehow inferred since *in vitro* data has shown a reciprocal important interplay between HSC and HEP (and with other liver cells) (Senoo *et al*, 2010).

2.4.2- Age and gender study: 2) Ageing and liver

Three criteria have been of particular importance for selecting Wistar rats for this study: firstly, in the baseline study we have developed a stereological quantification strategy for this strain; secondly, this is one of the most common stock of animals used in liver research (as illustrated in Figure 1.4 in Chapter 1); thirdly, this strain has few age-related liver lesions. The only lesion consistently reported are altered cell foci, but these tend to occur at a later age (around 2.5 years) (Van Bezooijen, 1984). In this regard, Wistar rats differ from other strains used in gerontology research: Fischer rats, for instance, also present altered cell foci, but at an earlier age and may bare focal chronic hepatitis and bile duct hyperplasia (Van Bezooijen, 1984). Moreover, these rats have the propensity to lymphoreticular neoplasia as they become senescent (Sakai *et al*, 1997). On the other hand, various lesions (periportal inflammation, sinusoidal enlargement, fatty change and eosinophilic foci) have been described in aged Sprague-Dawley rats (Van Bezooijen, 1984; Sakai *et al*, 1997). However, a major drawback exists when considering Wistar rats for ageing studies: the number of aged animals available from suppliers is small and restricted to males — females over 6 months cannot be bought from the existing companies (*e.g.*, Harlan, Charles River, National Institute of Aging). Therefore, animals have to be aged in-house, which increases the costs and, most importantly, delays the studies.

Regarding the global parameters, the body weight was in accordance to published data for this strain. The maximum weight is usually attained between 6 to 12 months (Porta *et al*, 1980; Sawada and Carlson, 1987), depending on the diet, and then the weight tends to decrease or to be (more or less) maintained. This contrasts with Sprague-Dawley rats, which continue to gain weight throughout their lifespan (Schoeffner *et al*, 1999). Regarding Fischer rats, some authors also report that they lose weight during senescence (Schmucker, 2005). Our older animals were slightly lighter than middle-aged, a feature also observed by Porta *et al* (1980) and Sawada and Carlson (1987); in our set of rats, older animals were 22% and 9% lighter than middle-aged males and females, respectively

(this difference was only significant for males). This decrease was probably due to a lower deposition of fat in older rats (Porta *et al*, 1981) and it is known for long that aged rats often present a period of weight loss at the end of their lifespan (Yiengst *et al*, 1959). The greater longevity reported for females probably accounts for the absence of such a body weight reduction in this gender.

The liver weight was also in accordance with the existing literature (Porta *et al*, 1981; Sawada and Carlson, 1987). This parameter is a frequent target of toxicological studies, as it reflects physiologic and metabolic changes, being sensible enough to predict toxicity and presenting small animal-to-animal variability (Michael *et al*, 2007) — we also observed this latter feature in our set of rats. Regarding the liver weight and volume, our data differs from published values for Fischer and Sprague-Dawley rat strains, since in those strains the liver of aged animals (24 months) has been reported to increase by 70% and 50% respectively, comparing with young rats (Schoeffner *et al*, 1999; Vollmar *et al*, 2002). This has been reported as a major drawback for extrapolating conclusions based in rat studies to the human field, in which the total hepatic volume declines across their lifespan (Vollmar *et al*, 2002; Schmucker, 2005). For instance, Le Couteur and McLean (1998) estimated a 25% reduction of liver volume from 25 to 80 years old humans and Marchesini *et al* (1988) also reported a 12% reduction of liver volume from less than 50 years old to sexagenarians. In our data, the liver of 18 months rats (equivalent to $\approx$ 55 years old human) remained virtually unchanged comparing with young animals (equivalent to an adolescent). In this vein, and as usual with most animal models and circumstances, extrapolation of our data to humans should be done with great care, even if aged Wistar rats present some features typical of old humans [*e.g.*, increased levels of circulating cholesterol and increased secretion of high density lipopoprotein cholesterol (Bravo *et al*, 1996)].

The liver-to-body weight ratio was also in accordance to previously published data for rats (Porta *et al*, 1981; Van Bezooijen, 1984; Bravo *et al*, 1996; Schoeffner *et al*, 1999; Vollmar *et al*, 2002; Furukawa *et al*, 2003). This parameter is most relevant, since the dosage of drugs mostly depends on body weight. It has been reported to range from 2.2% to 4.4% depending on the strain, age and gender of the rats (Van Bezooijen, 1984). In our case it did not vary with gender, being significantly higher in younger animals, and fairly constant in adult to old ones. This pattern is not restricted to rats; for instance in humans, the liver-to-body weight ratio declines 50% from adolescent to maturity and remains stable thereafter (Munro and Young, 1978; Roskams *et al*, 2007). The importance of this ratio has been illustrated experimentally in dogs receiving liver transplants (Kam *et al*, 1987): when a small liver is transplanted to a larger dog recipient, it grows until the species liver-to-body weight ratio is attained. The opposite is also true, because if a larger liver is

transplanted to a smaller recipient, the excessive amount of liver tissue disappears, presumably by apoptosis (Roskams *et al*, 2007). A similar decrease in liver mass occurs in man — large livers (that do not fit well in the abdomen) decrease in size, permitting the perfect closure of the abdominal cavity in about one week (Fausto and Campbell, 2009).

2.4.2- Age and gender study: 3) Ageing and HSC

Age is considered an important independent factor for progression of liver fibrosis in humans (the number of deaths attributed to chronic liver diseases markedly increases with age, especially over 50 years old). In rats a similar pattern exists, at least for some models of hepatic fibrosis. For instance, Reuber and Glover (1968) compared fibrosis induced by CCl_4 in young (2/3 months), adults (6 months) and middle-aged rats (12 months) of the Buffalo strain. In that classical study, the authors noticed that fibrosis was more severe and precocious in middle-aged animals, especially in males (in females, the severity was actually more pronounced in 3 months old rats). Despite it is nowadays consensual that HSC are implicated in the aetiology of hepatic fibrosis, there have been few studies on the effects of ageing in this cell population (Schmucker, 2005).

As already mentioned, the N of HSC has never been assessed throughout ageing. So far, only “numbers per area” have been determined and these resulted in controversial conclusions. According to Cogger and Le Couteur (2009) ageing is associated with increased numbers of non-activated HSC, and this occurs in mice, rats, baboons and humans. More recently, Warren *et al* (2011) studied Fischer rats in two time points (3-6 months and 24-27 months) and, after doing an immunohistochemistry against desmin, reported that doubling “numbers per area” existed in old animals. In contrast, ten years ago, Vollmar *et al* (2002) studied male Sprague-Dawley rats in four time points (from 1 to 24 months) and, based in the number of vitamin A fluorescent spots, suggested that the number of HSC could be decreased (up to 30%) with ageing (Vollmar *et al*, 2002; Schmucker, 2005). Previously, Enzan *et al* (1991) studied young (2 months) and old (24 months of age) male Wistar rats by electron microscopy and reported that HSC were equally frequent in young and old animals. Apart from eventual differences between rat strains or markers, our data is more in accordance with the observations of Enzan *et al* (1991), since the N of HSC is fairly maintained with ageing (no statistical differences existed and the N only varied 12-20% between young and old animals). We already stressed that two dimensional counts (number per area) are unquestionably biased and do not traduce the three dimensional reality of biological tissues. In the case of Warren *et al* (2011), an overestimation probably existed: since HSC in older animals have a larger perikaryon than young cells (as evidenced by our study), they would have a greater

probability of being cut and counted, thus producing a false increase in their number per area.

Based in our data of the N and N/g of HSC, it appears that HSC represent a stable population throughout ageing. Accordingly, Guyot *et al* (2006) has suggested that pure populations of HSC do not proliferate. The half-life of HSC has never been determined *in vivo* (Friedman, 2008), but our constant figures of the N and N/g of HSC, suggest that HSC are long-lived cells. It is unlikely that a significant turnover exists for this population in normal conditions, since we observed more than ten thousand cells marked by GFAP and never saw a single mitotic figure; moreover, the apoptotic events were extremely rare.

Regarding the volume of HSC, the classical studies have reported that cells in old rats are larger, with more lipid droplets (Enzan *et al*, 1991), but more recent studies either confirmed this (Vollmar *et al*, 2002; Warren *et al*, 2011) or failed to demonstrate significant differences (Martin *et al*, 1992; Grizzi *et al*, 2003). In our case, we estimated both the relative volume [V_V(HSC, liver)] and the mean volume ($\overline{v}_N$) of these cells.

The relative volume (or volume density) of sinusoidal cells has already been studied throughout ageing: Martin *et al* (1992) estimated the V_V(HSC, liver) in female Sprague-Dawley rats in two time-points (2 and 24 months). Using point counting in a total of 12 micrographs per animal, this author obtained figures similar to ours — the V_V(HSC, liver) was 0.4% ± 0.1% in youngsters, which is comparable to our estimation (0.3% ± 0.1%). However, probably due to the small number of sampled micrographs, Martin *et al* (1992) failed to obtain statistical significances between young and old animals. In our case, we obtained those differences, but this only means that old HSC have a larger perikaryon, with more lipids than youngsters [because the $\overline{v}_N$ was constant, according to our data]. Fat-engorged HSC have been reported in old animals of different species (mice, rats, baboons and humans) (Cogger and Le Couteur, 2009). In the rat it has been shown that HSC store an increased content of vitamin A with age, especially during their first year (Vollmar *et al*, 2002). Classical and more recent studies have reported that HSC in aged animals appear swollen, having significantly more and larger lipid droplets (Enzan *et al*, 1991; Warren *et al*, 2011). Likewise, we also observed a significant growth of the perikaryon (it almost tripled during the first year). Based in such differences, some authors have stated that older HSC are larger (Vollmar *et al*, 2002; Schmucker, 2005), but this seems to be only partially true, considering our estimation of the $\overline{v}_N$. According to our data, it can be hypothesised that cell shape changes occur throughout ageing: from a small perikaryon with longer and thinner extensions in youngsters, to a large perikaryon with thicker but shorter extensions in older animals. Yet, another possible explanation to our data is that the GFAP content of HSC actually decreases throughout ageing. The content of desmin, the other intermediate filament protein of the cytoplasmic processes of

HSC, has been shown to remain unchanged with ageing (Ballardini *et al*, 1994) but the GFAP content has never been evaluated. Thus we cannot exclude this possibility and further studies are needed to address this issue.

Classical studies have determined the maximum cell diameter of HSC using morphometric methods in semithin sections (Enzan *et al*, 1991), and more recently, in thick ones, immunostained against GFAP (Oikawa *et al*, 2002). Nevertheless, the mean cellular volume of HSC has never been reported. In our case, we opted for an indirect approach to estimate the $\overline{v}_N$ of HSC, because a direct one (for instance using the nucleator) would be extremely difficult to implement. HSC are highly irregular cells with cellular extensions that extend in five different directions (Oikawa *et al*, 2002) in and out of focus (particularly in thick sections). In such case, the most used local estimators (nucleator or rotator) would lead to underestimations, by only measuring the perikaryon and some large processes protruding from it (in a focal plane). Instead, by determining the volume density in semithin and paraffin sections immunostained against GFAP, a double objective was accomplished. In the former, the volume of the perikaryon (and of larger cellular extensions with lipid droplets) was estimated, whereas in the latter, the volume of the whole cell was considered [even the small extensions (without lipid droplets) in the limit of resolution of the microscope were considered, as far as they were positively stained]. It should be noted, that GFAP constitutes the cytoskeleton of the processes and even the smallest ones are fulfilled by tightly packed bundles of the protein (Buniatian *et al*, 1996, Oikawa *et al*, 2002). In this vein, a disadvantage of our approach was that it still underestimated the cell volume (because we were not highlighting the cell borders, *i.e.*, the cytoplasmic membrane and likely also peripherally associated cytoplasm). However, the introduced error introduced should be small and it seems reasonable to assume that it was equally distributed across age and gender. This is a small price to pay, since our approach was much less cumbersome than estimating the volume density in electron micrographs (in which a large sample of micrographs would be needed in order to include the smaller processes). Interestingly, the $\overline{v}_N$ did not vary with ageing or gender despite the changes in the cell shape.

It is unknown whether differences in the N or N/g of HSC or in the V_V(HSC, liver) exist between rat strains. Data from different studies are often incomparable, either because markers with variable specificity were used, or because data is difficult to extrapolate (for instance when reported as “number per area”). However, the existing studies seem to point for small differences: as mentioned, the estimations of V_V(HSC, liver) in Sprague-Dawley rats (Martin *et al*, 1992) were similar to our data. Accordingly, Imai *et al* (2000) found no differences in the area of lipid droplets or in the proportion of lipid droplets to cytoplasm between Wistar and Long Evans Agouti rats. Additionally, a classical study by

Blaner *et al* (1985) estimated (by a different approach than ours) a N/g of $16x10^6$ HSC in 12 months females of the BN/BiRij strain, which is a figure quite similar to our estimation ($17x10^6$) in female Wistar rats of the same age.

In recent years, some authors have questioned if the functionality of HSC used by *in vitro* studies, isolated from 6 months rats (or older), may reflect those of the *in vivo* studies (usually performed in 2 months old animals) (Tacke and Weiskirchen, 2012). In fact, a comprehensive comparison between activation *in vivo* and *in vitro* in rat, as well as in murine HSC, has underlined that different genes are regulated (Kristensen *et al*, 2000; De Minicis *et al*, 2007). Based in our study, HSC seem to be comparable in terms of morphological features (volume and number), but we would expect some functional differences, at least in the secretion of collagen and/or metalloproteinases (as we will detail below). Still, it should be kept in mind that an *in vitro* approach only deals with a part of the *in vivo* population of HSC (Tacke and Weiskirchen, 2012). According to our data, the average yield reported in an adult male rat, $25x10^6$ (Kawada, 1997; Ramadori and Saile, 2002), only corresponds to 12% of the whole population of HSC. Even in an optimised protocol (in experienced hands and with good enzyme batches) an adult male will yield no more than $40\text{-}50x10^6$ HSC (Tacke and Weiskirchen, 2012), *i.e.*, ≈ 20% of the N we estimated. This may be even more relevant because, at least in the murine model, different isolation methods have yielded subpopulations functionally different in their lipid storage and collagen production (D'Ambrosio *et al*, 2011).

2.4.2- Age and gender study: 4) Ageing and liver collagen

Regarding the collagen assessment, we used the picro-sirius red (Junqueira *et al*, 1978; Kumar, 2005) because the visualisation of fibrillar ECM (*i.e*., collagen type I and III) is difficult with haematoxylin-eosin, and even with Masson's trichrome an underestimation of collagen deposition can occur (Pinzani *et al*, 2005). The picro-sirius red provided an excellent definition of collagen. This staining, sometimes coupled with reticulin, has been considered, by many pathologists, as an essential tool for diagnosing fibrosis (Kumar, 2005; Lee *et al*, 2005; Pinzani *et al*, 2005); algorithms for assessing fibrotic liver sections stained by picro-sirius red have even been developed (Wu *et al*, 2008). It can be argued that it would be faster to analyse the collagen content by image analysis than to use point-counting. However, we opted for the latter because we wanted to discriminate the collagen in three different locations (capsule, around portal or central vessels and intralobular), since HSC are only related with intralobular collagen deposition. Point-counting is a simple, reproducible and accurate procedure, as long as the grid is appropriately applied (Howard and Reed, 2005). Although in theory image analysis could be faster, it would introduce additional variables, like light source, threshold definition and

setting of exclusion areas (Kumar, 2005). The time needed to allocate pictures in the three locations of interest would probably be equally (or even more) time-consuming. Still, another possibility for collagen assessment would be to analyse the hydroxyproline content in liver homogenates (Bergman and Loxley, 1963). We opted not to perform this because: 1) in general the estimates are similar to those obtained with picro-sirius red staining (James *et al*, 1990; Gagliano *et al*, 2002); 2) it only determines total collagen content; 3) it tends to present some variability, depending on the size and location of the used fragment (Lee *et al*, 2005).

The liver is a unique organ, not only because the collagen secretion is tightly regulated by different cell types, but also because it has less content than most organs — collagen stands for ≈ 30% of total protein in general connective tissue, but in the liver it only represents ≈ 5% (Roskams *et al*, 2007; Friedman 2008). Our data is in accordance with this threshold, being noteworthy that Porta *et al* (1981) and Gagliano *et al* (2002) also followed the collagen content throughout the lifespan of rats, noting that it increased with ageing and peaked in 6 months animals. Those authors only studied males and observed that adults had the same (Gagliano *et al*, 2002) or even higher content of collagen than older animals (Porta *et al*, 1981). The reason for such an increased collagen in male adults is unknown, but it may traduce a remodelling activity with formation of new lobules, which is believed to occur during liver growth (Roskams *et al*, 2007).

It should be emphasised that intralobular collagen cannot be solely related to HSC, since the expression of collagen I has been attributed to HSC, LSEC and HEP (Roskams *et al*, 2007). In this vein, we observed a moderate, but still significant, correlation between the intralobular picro-sirius red and the N of HEP ($r = 0.47$; $p < 0.01$). Collagen deposition results from a complex balance between synthesis and degradation by metalloproteinases (MMP); these are regulated at many levels, but the most important is their inactivation by tissue inhibitors of metalloproteinases (TIMP) (Lee and Friedman, 2011). These have not been studied in the context of ageing: only Gagliano *et al* (2002) studied the MMP-1, MMP-2 and TIMP-1 expression in male Sprague-Dawley rats in age-groups similar to ours. These authors noted that MMP activity was significantly reduced in adult and old rats (the two age groups in which we also observed significant collagen deposition). Additionally, Gagliano *et al* (2002) reported that TIMP-1, a protein produced by HSC and KC, was increased in old rats comparing with young. Those authors did not include in-between age groups in this comparison and they did not study females, but this would be interesting because we observed gender differences throughout ageing in the collagen deposition, with lower levels in females. Interestingly, it was recently reported that significant gender differences in the gene expression of TIMP-1, but not of TIMP-4, exist in the rat (Kwekel *et al*, 2010).

At a first glance, the fact that HSC of old males have an increased content of lipids, in which vitamin A is stored (Vollmar *et al*, 2002), seems contradictory with a stronger collagen deposition reported for older animals, in pathological conditions as well as in the normal setting (Gagliano *et al*, 2002). Indeed, it is known for long that retinol and especially retinoic acid suppress HSC proliferation and production of collagen *in vitro* (Davis *et al*, 1990) and that the loss of retinoid is a prominent feature accompanying HSC activation *in vivo* and *in vitro* (Minato *et al*, 1983; Friedman, 2008). However, the overall effects of vitamin A on HSC functions still remain unclear, since contradictory effects of retinoids and fibrogenesis have been reported (Friedman, 2008; Senoo *et al*, 2010; Tacke and Weiskirchen, 2012). For instance, exposure of HSC to supra-physiological concentrations of retinoic acid, as well as exposure to their metabolites, leads to fibrosis, via activation of transforming growth factor-β (Okuno *et al*, 1997). Moreover, a recent study with a knockout mice model lacking retinoid-containing lipid droplets in HSC, established that these cells did not present enhanced activation and fibrogenesis, thus suggesting that vitamin A storage and fibrogenesis are not functionally linked (Kluwe *et al*, 2011).

2.4.2- Age and gender study: 5) Ageing and the hepatic stellate cell index

The correlation between N of HSC (as well as the N/g and N_V) and the N HEP justifies the use of the HSCI (such correlations will be further detailed in Chapter 3). Unlike other pericytes, HSC have processes and spines, making intimate contacts with the sinusoidal facet of HEP (Wake, 1971). Although their functions are still unknown, it has been proposed that these membrane contacts inhibit activation and proliferation of HSC in normal conditions and that under conditions of HEP damage, a “de-inactivation” would occur (Gressner *et al*, 1995). The relation of HSC and HEP is mutually dynamic, since HEP may regulate the number of activated HSC, via induction of apoptosis, whilst these regulate the proliferation of HEP, via hepatocyte growth factor production (Senoo *et al*, 2010); moreover, HSC are essential to maintain HEP functions (Krause *et al*, 2009).

The qualitative relation between HSC and HEP can be traduced by the HSCI. It has been used in human hepatology (Bronfenmajer *et al*, 1966; Giamperi *et al*, 1981; Sztark *et al*, 1986), as well as in rodents (Ballardini *et al*, 1983; Azaïs-Braesco *et al*, 1997, Imai *et al*, 2000). This HSCI changes in all situations that involve the proliferation of HSC (Geerts, 2001), including hepatic fibrosis (Ballardini *et al*, 1983). In the former, an increased HSCI is due to the proliferation of HSC and to an overall reduction of viable HEP. According to our data, the HSCI seems to be less valuable in a normal scenario. In the absence of activation with ageing (which was confirmed by the absence of ASMA staining) and of proliferative activity in HSC, this index seems no to correlate with the intralobular

deposition of collagen. Adult and old males did not present an increased HSCI; instead the highest mean value (despite not significantly different from the others) was observed in young males, a feature already reported by Imai *et al* (2000) in Long-Evans Agouti rats. In accordance with this author, we observed no statistical differences throughout ageing. In our case, the decreasing trend observed in the HSCI of males was probably only due to the fact that the N of HSC remained fairly constant, whilst the N of HEP tended to (slightly) increase with ageing. This also accounts for the gender differences in the HSCI (young animals have differences in the HSCI that did not exist in the other ages). Young females have a lower HSCI mainly because their liver has an increased N of HEP (as it will be detailed in Chapter 3).

2.4.2- Age and gender study: 6) Ageing and the lobulation of HSC

Regarding the study of the lobulation of HSC, we opted to consider only periportal and centrilobular areas. In this way, using the boundaries of 5-6 HEP, we covered ≈ 70% of the porto-central axis and it was always possible to identify zones by their respective landmarks. Indeed, since pericentral areas are consistently marked by GS (Gebhardt and Mecke, 1983) we were able to easily differentiate them from periportal areas. Theoretically, we may have missed portal areas cut tangentially, without visible portal elements within the limits of the thick section (or central areas without the 2-3 HEP positive to GS). Probably, this occurred rarely and, *a priori*, it seems reasonable to assume that those fields would present a similar scenario to the ones included herein. Therefore, for practical purposes, the concomitant use of a periportal marker (for instance in the following section), like connexin 26 (Kuraoka *et al*, 1993) or phosphoenolpyruvate carboxykinase (Wagenaar *et al*, 1993), can be considered redundant. In this study, we choose not to include a midzonal area because it is very difficult to establish their boundaries — according to our data, it can comprise 3 to 9 HEP. Moreover, the end-zones of the porto-central axis, by their differential supply of oxygen, hormones and different ECM composition (Roskams *et al*, 2007) are more likely to mirror any existing lobular heterogeneity.

The distribution of HSC has been controversial and technical reasons probably underlie most of the dispute. For instance Geerts *et al* (1991) using immunohistochemistry against desmin and observing a single liver lobe reported that HSC predominated in periportal areas in the rat, and that this difference was not due to the lack of this maker in a central location. Nevertheless, this conclusion was refuted a couple of years later (Ballardini *et al*, 1994; Grinko *et al*, 1995). Likewise, based in autofluorescence against vitamin A, Wake (1980) also reported that HSC predominate periportally, whereas using the same methods, Higashi and Senoo (2003) and Senoo *et al* (2007) reported that HSC tend to be

slightly more abundant in centrilobular areas (but no significant differences existed). Additionally, Niki *et al* (1996) reported that GFAP tagging was absent in a periportal rim — which is in contrast with the observations of Oikawa *et al* (2002) and with ours (as depicted in Figure 2.8). The fact that we used antigen retrieval methods and long incubation times, instead of cryostat sections, probably accounts for the differences to Niki *et al* (1996). It should be noted that when an entire lobule is observed in order to evaluate heterogeneity (*i.e.*, assessing heterogeneity with a low magnification), a natural bias towards periportal cells is introduced, since it has been estimated that there are 5 times more HEP periportally than in a pericentral location (Teutsch *et al*, 1999).

In our set of rats, males and females had a similar a pattern and both pointed to a shift from a central to portal predominance with ageing. This higher proportion of HSC in a periportal location in old rats has never been reported, but it may contribute to a reduced blood flow of the sinusoids encountered in those animals (Vollmar *et al*, 2002; Warren *et al*, 2011). This is relevant because HSC of older animals have a larger perikaryon and it has been shown that these cells tend to protrude into sinusoids (Warren *et al*, 2011) — a feature that we also observed in some HSC (data not shown). It is still possible that a lower expression of GFAP takes place in centrilobular areas in aged animals. It is known that HSC loose GFAP when activated (Geerts, 2001; Friedman, 2008), but we have excluded this possibility in our rats. In this vein, it is opportune to mention that most previous studies showed that HSC of old animals are not-activated (Grizzi *et al*, 2003; Cogger and Le Couteur, 2009; Warren *et al*, 2011). Still, we need to conduct further studies to exclude the possibility of a lower expression of GFAP, for example by performing *in situ* hybridisation in our material or by isolating HSC from younger and older animals and doing quantitative reverse transcription polymerase chain reaction plus western blot. Assuming that no differences in GFAP expression occur with ageing, it is tempting to relate this finding with the liver “streaming theory” (Zajicek *et al*, 1988). This theory has been extensively disputed (McCuskey, 2006; Roskams *et al*, 2007) and we hardly if ever saw evidences of apoptosis in HSC (this event was too rare to establish any lobular predominance), but it is still conceivable that HSC are being renewed in these older animals through a periportal influx of HSC. Another hypothesis is that these cells are being originated by epithelial-mesenchymal transition, which has been shown to occur in the normal rat liver (Lim and Lee, 2002; Gressner *et al*, 2008; Friedman, 2008). Further studies using caspase immunostaining and terminal deoxynucleotidyl transferase nick end labelling methods would be needed to address this issue. Alternatively, the shift from a central to portal predominance, which we observed with ageing, could be simply explained by cell migration. In fact, it has been described that HSC are able to slowly move through the space of Disse and accumulate around hepatic focal lesions (Senoo *et al*, 2007;

Friedman, 2008). The cellular processes of HSC have been shown to extend and retract according to the ECM composition (Sato *et al*, 2003) and it has been suggested that these cells are dynamic in the changeable 3D structure of the sinusoids (Sato *et al*, 2003; Senoo *et al*, 2007). It is known for long that ECM differs along the porto-central axis (Reid *et al*, 1992; Roskams *et al*, 2007; Senoo *et al*, 2010) and it may be hypothesised that the periportal ECM composition could also change with ageing, driving HSC to that location.

2.4.2- Age and gender study: 7) Gender and HSC

We already mentioned that for a similar prevalence, chronic infection with HBV and HCV tends to be more severe in men, with increased progression to cirrhosis and hepatocellular carcinoma (Di Martino *et al*, 2004; Zarski *et al*, 2006; Villa *et al*, 2012). In the rat model, some contradictory data has been gathered: for instance, two classical studies by Reuber and Glover (1968) and Bengmark and Olsson (1962) reported contradictory results for CCl_4 induced fibrosis in females. More recently, Kang *et al* (2005) reported an increased severity in thioacetamide induced cirrhosis in female rats treated with oestradiol-3-benzoate (an oestrogen metabolite), whereas in dimethylnitrosamine and pig-serum induced fibrosis, oestradiol produced opposite effects: it reduced fibrosis in males (Shimizu *et al*, 1999) and ovarioectomy in females had a fibrogenic effect (Yasuda *et al*, 1999). These authors also showed that in cultured HSC, oestradiol in concentrations similar to those observed during the late follicular phase of the normal cycle and gestation, inhibited collagen type I production, ASMA expression and cell proliferation (Shimizu *et al*, 1999). In this vein, it was tempting to hypothesise that the female liver had a reduced number of HSC, as a result of cumulative effect of oestradiol in the normal liver, during the lifespan of rats. This has never been evaluated, but, from our data, this hypothesis was now denied, since no differences existed between genders in the N, N/g and N_V(HSC, liver). We also determined the average volume of HSC, because differences in this parameter could traduce, for instance, an increased content of rough endoplasmic reticulum needed for collagen synthesis. However, it also does not differ between male *versus* female, meaning that gender differences *per se* seem not to exist in HSC. Even so, we discovered for the first time that significant differences existed for the collagen content in the normal liver, namely in adults and older animals. For young rats, males and females did not differ significantly as to the amount of lobular collagen — which is in accordance with previous studies (Shimizu *et al*, 1999). Maybe the differences are too subtle at young ages to be revealed by the power of our study or the exact onset of the gender differences varies with age, strain or species. Curiously, a recent study in healthy humans revealed differences in the liver stiffness (measured by transient elastography), suggesting that the normal organ of men has an increased density of ECM (Corpechot *et al*, 2006). This

gender dimorphism in the matrix can either be due to influences of oestrogen, either in collagen production or in the remodelling process. In this regard, Shimizu *et al* (1999) noted that the levels of RNA-messenger of TIMP-1 were higher in young males and, as we mentioned above, Gagliano *et al* (2002) found that old males have increased levels of this protein. We hypothesise that females should have lower levels of TIMP-1 that are maintained throughout ageing. Interestingly, Woodrum *et al* (2005) studied rat aortic smooth cells of males and females, in order to elucidate the predilection of men for developing abdominal aortic aneurysms, and found that those cells of males had a 4-fold higher activity of TIMP-1.

The differences in the lobular collagen that we reported probably underlie the practical observation that the isolation protocols render more HSC in females than in males (Ramadori and Saile, 2002). According to this author, a maximum of $100x10^6$ HSC can be isolated from a female (retired breeder) rat, which is 2-times more than that obtained with males. According to our data, this would correspond to ≈ 75% of the N we estimated here, meaning that an isolation protocol in females seems to be more representative of the whole population of HSC. [As above mentioned, an adult male will yield no more than $40\text{-}50x10^6$ HSC (Tacke and Weiskirchen, 2012), *i.e.*, ≈ 20% of the N of HSC we estimated herein].

In conclusion, we have shown that HSC appear to represent a quite stable population in the liver, without significant numerical differences throughout ageing and between gender. Nevertheless, ageing does not entirely spare HSC of the rat. Like many of us humans, these cells appear to get fatter, to work more and even to migrate (or being replaced) with ageing. Further studies are needed to disclose whether or not migration is occurring and if differences in the composition of ECM (and in MMP and TIMP) occur with gender.

2.5- References

Aterman K (1986) The parasinusoidal cells of the liver: a historical account. *Histochemical Journal* 18, 279-305.

Auvigne I, Pichard V, Aubert D, Robillard N, Ferry N (2002) *In vivo* cell lineage analysis in cyproterone acetate-treated rat liver using genetic labelling of hepatocytes. *Hepatology* 35, 281-288.

Azaïs-Braesco V, Hautekeete ML, Dodeman I, Geerts A (1997) Morphology of liver stellate cells and liver vitamin A content in 3,4,3',4'-tetrachlorobiphenyl-treated rats. *Journal of Hepatology* 27, 545-553.

Ballardini G, Degli ES, Bianchi FB, de Georgi LB, Faccani A, Biolchini L, Busachi CA, Pisi E (1983) Correlation between Ito cells and fibrogenesis in an experimental model of hepatic fibrosis. A sequential stereological study. *Liver* 3, 58-63.

Ballardini G, Groff P, De Georgi LB, Schuppan D, Bianchi FB (1994) Ito cell heterogeneity: desmin-negative Ito cells in normal rat liver. *Hepatology* 19, 440-446.

Banks WJ (1993) Digestive system II – extramural organs. In: *Applied Veterinary Histology, 3rd edition,* pp. 360-73. Mosby

Barros RP, Gustafsson JÅ (2011) Estrogen receptors and the metabolic network. *Cell Metabolism* 14, 289-299.

Bengmark S, Olsson R (1962) The effect of sex and testosterone on toxic liver damage. *Journal of Endocrinology* 25, 293-297.

Bedossa P, Paradis V (2003) Liver extracellular matrix in health and disease. *Journal of Pathology* 200, 504-515.

Beresford WA, Henninger JM (1986) A tabular comparative histology of the liver. *Archivum Histologicum Japonicum* 49, 267-281.

Bergman I, Loxley R (1963) Two improved and simplified methods for the spectrophotometric determination of hydroxyproline. *Analytical Chemistry* 35, 1961-1965.

Blaner WS, Hendriks HF, Brouwer A, De Leeuw A, Knook DL, Goodman DS (1985) Retinoids, retinoid-binding proteins, and retinyl palmitate hydrolase distributions in different types of rat liver cells. *Journal of Lipid Research* 26, 1241-1251.

Boll F (1869) Die bindesubstanz der drüsen. *Archiv für Mikroskopische Anatomie* 5, 334-355.

Boyce RW, Dorph-Petersen KA, Lyck L, Gundersen HJ (2010) Design-based stereology: introduction to basic concepts and practical approaches for estimating cell number. *Toxicologic Pathology* 38, 1011-1025.

Bravo E, Rivabene R, Bruscalpi G, Calcabrini A, Arancia G, Cantafora A (1996) Age-related changes in lipid secretion of perfused livers from male Wistar rats donors. *Journal of Biochemistry* 119, 240-245.

Bronfenmajer S, Schaffner F, Popper H (1966) Fat-storing cells (lipocytes) in human liver. *Archives of Pathology* 82, 447-453.

Buniatian G, Hamprecht B, Gebhardt R (1996) Glial fibrillary acidic protein as a marker of perisinusoidal stellate cells that can distinguish between the normal and myofibroblast-like phenotypes. *Biology of the Cell* 87, 65-73.

Cassiman D, Van Pelt J, De Vos R, Van Lommel F, Desmet V, Yap SH, Roskams T (1999) Synaptophysin: A novel marker for human and rat hepatic stellate cells. *American Journal of Pathology* 155, 1831-1839.

Clemens MG, Zhang JX (1999) Regulation of sinusoidal perfusion: *in vivo* methodology and control by endothelins. *Seminars in Liver Disease* 19, 383-396.

Collier TJ, Coleman PD (1991) Divergence of biological and chronological aging: evidence from in rodent models. *Neurobiology of Aging* 12, 685-693.

Cogger VC, Le Couteur DG (2009) Fenestrations in the liver sinusoidal endothelial cell. In: *The liver: biology and pathobiology, 5th edition* (Arias IM, Alter HJ, Boyer JL, Cohen DE, Fausto N, Shafritz DA, Wolkoff AW eds), pp 389-406. John Wiley & Sons Ltd.

Corpechot C, Nagar A, Poupon R (2006) Gender and the liver: is the liver stiffness weaker in the weaker sex? *Hepatology* 44, 513-514.

Cruz-Orive LM (1999) Precision of Cavalieri sections and slices with local errors. *Journal of Microscopy* 193, 182-198.

D'Ambrosio DN, Walewski JL, Clugston RD, Berk PD, Rippe RA, Blaner WS (2011) Distinct populations of hepatic stellate cells in the mouse liver have different capacities for retinoid and lipid storage. *PLoS One* 6, e24993.

Dahl D, Crosby CJ, Sethi JS, Bignami A (1985) Glial fibrillary acidic (GFA) protein in vertebrates: immunofluorescence and immunoblotting study with monoclonal and polyclonal antibodies. *Journal of Comparative Neurology* 239, 75-88.

Davis BH, Kramer RT, Davidson NO (1990) Retinoic acid modulates rat Ito cell proliferation, collagen, transforming growth factor beta production. *Journal of Clinical Investigation* 86, 2062-2070.

Davidson AJ, Castañón-Cervantes O, Stephan FK (2004) Daily oscillations in liver function: diurnal *vs* circadian rhythmicity. *Liver International* 24, 179-86.

De Bleser PJ, Jannes P, Van Buul-Offers SC, Hoogerbrugge CM, van Schravendijk CF, Niki T, Rogiers V, van den Brande JL, Wisse E, Geerts A (1995) Insulin-like growth factor-II/mannose 6-phosphate receptor is expressed on CCl_4-exposed rat fat-storing cells and facilitates activation of latent transforming growth factor-beta in cocultures with sinusoidal endothelial cells. *Hepatology* 21, 1429-1437.

De Minicis S, Seki E, Uchinami H, Kluwe J, Zhang Y, Brenner DA, Schwabe RF (2007) Gene expression profiles during hepatic stellate cell activation in culture and *in vivo*. *Gastroenterology* 132, 1937-1946.

Di Martino V, Lebray P, Myers RP, Pannier E, Paradis V, Charlotte F, Moussalli J, Thabut D, Buffet C, Poynard T (2004) Progression of liver fibrosis in women infected with hepatitis C: long-term benefit of estrogen exposure. *Hepatology* 40, 1426–1433.

Dorph-Petersen KA, Nyengaard JR, Gundersen HJG (2001) Tissue shrinkage and unbiased stereological estimation of particle number and size. *Journal of Microscopy* 204, 232-246.

Eagon PK, Porter LE, Francavilla A, DiLeo A, Van Thiel DH (1985) Estrogen and androgen receptors in liver: their role in liver disease and regeneration. *Seminars in Liver Disease* 5, 59-69.

Ekataksin W, Kaneda K (1999) Liver microvascular architecture: an insight into the pathophysiology of portal hypertension. *Seminars in Liver Disease* 19, 359-382

Enzan H (1985) Proliferation of Ito cells (fat-storing cells) in acute carbon tetrachloride liver injury. *Acta Pathologica of Japan* 35, 1301-1308.

Enzan H, Saibara T, Ueda H, Onishi S, Yamamoto Y, Okada T, Hara H (1991) Ultrastructural observation of Ito cells in the aged rats. In: *Cells of the Hepatic Sinusoid* (Wisse E, Knook DL, McCuskey RS eds), pp. 226–229. Kupffer Cell Foundation.

Fausto N, Campbell JS (2009) Liver regeneration. In: *The liver: biology and pathobiology, 5th edition* (Arias IM, Alter HJ, Boyer JL, Cohen DE, Fausto N, Shafritz DA, Wolkoff AW eds), pp. 549-65. John Wiley & Sons Ltd.

Forbes SJ, Parola M (2011) Liver fibrogenic cells. *Best Practice & Research. Clinical Gastroenterology* 25, 207-217.

Friedman SL (2008) Hepatic stellate cells: protean, multifunctional, and enigmatic cells of the liver. *Physiological Reviews* 88, 125-172.

Furukawa F, Matsuzaki K, Mori S, Tahashi Y, Yoshida K, Sugano Y, Yamagata H, Matsushita M, Seki T, Inagaki Y, Nishizawa M, Fujisawa J, Inoue K (2003) p38 MAPK mediates fibrogenic signal through Smad3 phosphorylation in rat myofibroblasts. *Hepatology* 38, 879-889.

Gagliano N, Arosio B, Grizzi F, Masson S, Tagliabue J, Dioguardi N, Vergani C, Annoni G (2002) Reduced collagenolytic activity of matrix metalloproteinases and development of liver fibrosis in the aging rat. *Mechanisms of Ageing and Development* 123, 413-425.

Gard AL, White FP, Dutton GR (1985) Extra-neural glial fibrillary acidic protein (GFAP) immunoreactivity in perisinusoidal stellate cells of rat liver. *Journal of Neuroimmunology* 8, 359-375.

Gawrich S, Papouchado B, Burgart L, Kobayashi S, Charlton M, Gores G (2005) Early hepatic stellate cell activation predicts severe hepatitis C recurrence after liver transplantation. *Liver Transplantation* 11, 1207-1213.

Gebhardt R, Mecke D (1983) Heterogeneous distribution of glutamine synthetase among rat liver parenchymal cells *in situ* and in primary culture. *The EMBO Journal* 2, 567-570.

Geerts A, Lazou JM, De Bleser P, Wisse E (1991) Tissue distribution, quantitation and proliferation kinetics of fat-storing cells in carbon tetrachloride-injured rat liver. *Hepatology* 13, 1193-1202.

Geerts A, De Bleser P, Hautekeete ML, Niki T, Wisse E (1994) Fat-Storing (Ito) Cell Biology. In: *The liver: biology and pathobiology, 3rd edition* (Arias IM, Boyer JL, Fausto N, Jakoby WB, Schachter DA, Shafritz DA eds), pp. 819-838. Raven Press Ltd.

Geerts A (2001) History, heterogeneity, developmental biology, and functions of quiescent Hepatic stellate cells. *Seminars in Liver Disease* 21, 311-335.

Giamperi MP, Jezequel AM, Orlandi F (1981) The lipocytes in normal human liver. A quantitative study. *Digestion* 22, 165-169.

Gressner AM, Lahme B, Brenzel A (1995) Molecular dissection of the mitogenic effect of hepatocytes on cultured hepatic stellate cells. *Hepatology* 22, 1507-1518.

Gressner OA, Rizk MS, Kovalenko E, Weiskirchen R, Gressner AM (2008) Changing the pathogenetic roadmap of liver fibrosis? Where did it start; where will it go? *Journal of Gastroenterolology and Hepatology* 23, 1024-1035.

Grinko I, Geerts A, Wisse E (1995) Experimental biliary fibrosis correlates with increased numbers of fat-storing and Kupffer cells, and portal endotoxemia. *Journal of Hepatology* 23, 449-458.

Grisham JW (2009) Organizational principles of the liver. In: *The liver: biology and pathobiology, 5th edition* (Arias IM, Alter HJ, Boyer JL, Cohen DE, Fausto N, Shafritz DA, Wolkoff AW eds), pp. 3-15. John Wiley & Sons Ltd.

Grizzi F, Franceschini B, Gagliano N, Moscheni C, Annoni G, Vergani C, Hermonat PL, Chiriva-Internati M, Dioguardi N (2003) Mast cell density, hepatic stellate cell activation and TGF-beta1 transcripts in the aging Sprague-Dawley rat during early acute liver injury. *Toxicologic Pathology* 31, 173-178.

Gundersen HJ (1977) Notes on the estimation of numerical density of arbitrary particles: the edge effect. *Journal of Microscopy* 111, 219-223.

Gundersen HJ (1986) Stereology of arbitrary particles: a review of unbiased number and size estimators and the presentation of some new ones, in memory of William R. Thompson. *Journal of Microscopy* 143, 3-45.

Gundersen HJ, Bagger P, Bendtsen TF, Evans SM, Korbo L, Marcussen N, Møller A, Nielsen K, Nyengaard JR, Pakkernberg B, Sørensen FB, Vesterby A, West MJ (1988)

The new stereological tools: disector, fractionator, nucleator and point sampling intercepts and their use in pathological research and diagnosis. *APMIS* 96, 857-881.

Gundersen HJ, Jensen EB, Kieu K, Nielsen J (1999) The efficiency of systematic sampling in stereology — reconsidered. *Journal of Microscopy* 193, 199-211.

Gundersen HJ (2002) The smooth fractionator. *Journal of Microscopy* 207, 191-210.

Guyot C, Lepreux S, Combe C, Doudnikoff E, Bioulac-Sage P, Balabaud C, Desmoulière A (2006) Hepatic fibrosis and cirrhosis: the (myo)fibroblastic cell subpopulations involved. *The International Journal of Biochemistry and Cell Biology* 38, 135-151.

Haber PS, Keogh GW, Apte MV, Moran CS, Stewart NL, Crawford DHG, Pirola RC, McGaughan GW, Ramm GA, Wilson JS (1999) Activation of pancreatic stellate cells in human and experimental pancreatic fibrosis. *American Journal of Pathology* 155, 1087-1095.

Hautekeete ML, Geerts A (1997) The hepatic stellate (Ito) cell: its role in human liver disease. *Virchows Archives* 430, 195-207.

Hepatic stellate cell nomenclature (1996) *Hepatology* 23, 193.

Higashi N, Kojima N, Miura M, Imai K, Sato M, Senoo H (2004) Cell-cell junctions between mammalian (human and rat) hepatic stellate cells. *Cell and Tissue Research* 317, 35-43.

Higashi N, Senoo H (2003) Distribution of vitamin A-storing lipid droplets in hepatic stellate cells in liver lobules - a comparative study. *Anatomical Record. Part A, Discoveries in Molecular Cellular and Evolutionary Biology* 271, 240-248.

Horvath E, Kovacs K, Ross RC (1973) Liver ultrastructure in methotrexate treatment of psoriasis. *Archives of Dermatology* 108, 427-428.

Howard CV, Reed MG (2005) *Unbiased stereology. Three-dimensional measurements in microscopy*, *2nd edition*. Bios Scientific Publishers.

Imai K, Sato M, Kojima N, Miura M, Sato T, Sugiyama T, Enomoto K, Senoo H (2000) Storage of lipid droplets in and production of extracellular matrix by hepatic stellate cells (vitamin A-storing cells) in Long-Evans cinnamon-like colored (LEC) rats. *Anatomical Record* 258, 338-348.

Ito T, Nemoto M (1952) Über die Kupfferschen Sternzellen und die fettspeicherungszellen (fat-storing cells) in der blutilapillarenwand der menschlichen leber. *Okajimas Folia Anatomica Japan* 24, 243-258.

James J, Bosch KS, Aronson DC, Houtkooper JM (1990) Sirius red histophotometry and spectrophotometry of sections in the assessment of the collagen content of liver tissue and its application in growing rat liver. *Liver* 10, 1-5.

Junqueira LC, Cossermelli W, Brentani R (1978) Differential staining of collagens type I, II and III by Sirius Red and polarization microscopy. *Archivum Histologicum Japonicum* 41, 267-274.

Kam I, Lynch S, Svanas G, Todo S, Polimeno L, Francavilla A Penkrot RJ, Takaya S, Ericzon BG, Starzl TE, Van Thiel DH (1987) Evidence that host size determines liver size: studies in dogs receiving orthotopic liver transplants. *Hepatology* 7, 362-366.

Kang JS, Wanibuchi H, Morimura K, Puatanachokchai R, Salim EI, Hagihara A, Seki S, Fukushima S (2005) Enhancement by estradiol 3-benzoate in thioacetamide-induced liver cirrhosis of rats. *Toxicological Sciences* 85, 720-726.

Kawada N (1997) The hepatic perisinusoidal stellate cell. *Histology and Histopathology* 12, 1069-1080.

Kim WR, Poterucha JJ, Benson JT, Therneau TM (2004) The impact of competing risks on the observed rate of chronic hepatitis C progression. *Gastroenterology* 127, 749-755.

Kluwe J, Wongsiriroj N, Troeger JS, Gwak GY, Dapito DH, Pradere JP, Jiang H, Siddiqi M, Piantedosi R, O'Byrne SM, Blaner WS, Schwabe RF (2011) Absence of hepatic stellate cell retinoid lipid droplets does not enhance hepatic fibrosis but decreases hepatic carcinogenesis. *Gut* 60, 1260-1268.

Kmiec Z (2001) Cooperation of liver cells in health and disease. *Advances in Anatomy, Embryology and Cell Biology* 161, 1-151.

Kristensen DB, Kawada N, Imamura K, Miyamoto Y, Tateno C, Seki S, Kuroki T, Yoshizato K (2000) Proteome analysis of rat hepatic stellate cells. *Hepatology 3*2, 268-277.

Krause P, Saghatolislam F, Koenig S, Unthan-Fechner K, Probst I (2009) Maintaining hepatocyte differentiation *in vitro* through co-culture with hepatic stellate cells. *In Vitro Cellular & Developmental Biology* 45, 205-212.

Kumar RK (2005) Morphological methods for assessment of fibrosis. In: *Fibrosis Research, Methods and Protocols* (Varga J, Brenner DA, Phan SH eds), pp. 179-207. Humana Press.

Kupffer K (1876) Über Sternezellen der leber. Briefliche mitteilung au Professor Waldeyer. *Archiv für Mikroskopische Anatomie* 12, 353-358.

Kupffer K (1899) Üeber die sogennanten Sternezellen der Säugethierleber. *Archiv für Mikroskopische Anatomie* 54, 254-288.

Kuraoka A, Iida H, Hatae T, Shibata Y, Itoh M, Kurita T (1993) Localization of gap junction proteins, connexins 32 and 26, in rat and guinea pig liver as revealed by quick-freeze, deep-etch immunoelectron microscopy. *Journal of Histochemistry & Cytochemistry* 41, 971-980.

Le Couteur DG, McLean AJ (1998) The aging liver. Drug clearance and an oxygen diffusion barrier hypothesis. *Clinical Pharmacokinetics* 34, 359-373.

Le Couteur DG, Cogger VC, Markus AM, Harvey PJ, Yin ZL, Ansselin AD, McLean AJ (2001) Pseudocapillarization and associated energy limitation in the aged rat liver. *Hepatology* 33, 537-543.

Le Couteur DG, Warren A, Cogger VC, Smedsrød B, Sørensen KK, De Cabo R, Fraser R, McCuskey RS (2008) Old age and the hepatic sinusoid. *The Anatomical Record* 291, 672-683.

Lee HS, Shun CT, Chiou LL, Chen CH, Huang GT, Sheu JC (2005) Hydroxyproline content of needle biopsies as an objective measure of liver fibrosis: Emphasis on sampling variability. *Journal of Gastroenterology and Hepatology* 20, 1109-1114.

Lee UE, Friedman SL (2011) Mechanisms of hepatic fibrogenesis. *Best Practice & Research. Clinical Gastroenterology* 25, 195-206.

Lim YS, Lee HS (2002) The expression of E-cadherin in human and rat hepatic stellate cells: evidence of epithelial-mesenchymal transition. *The Korean Journal of Hepatology* 8, 90-99.

Manikonda PK, Jagota A (2012) Melatonin administration differentially affects age-induced alterations in daily rhythms of lipid peroxidation and oxidant enzymes in male rat liver. *Biogerontology* 13, 511-524.

Marchesini G, Bua V, Brunori A, Bianchi G, Pisi P, Fabbri A, Zoli M, Pisi E (1988) Galactose elimination capacity and liver volume in aging man. *Hepatology* 8, 1079-83.

Marcos R, Rocha E, Monteiro RAF (2001a) Strategies to maximise adhesion of thick paraffin sections of the brown trout liver for stereological purposes. *Journal of Histotechnology* 24, 37-42.

Marcos R, Rocha E (2001b) Counting GFAP-marked Ito cells using the unbiased *disector* principle. In: *Cells of the hepatic sinusoid, Volume 8* (Wisse E, Knook DL, Zanger R, Arthur MJP eds), pp. 203-204. Kupffer Cell Foundation.

Marcos R, Rocha E, Henrique RMF, Monteiro RAF (2003) A new approach to an unbiased estimate of the hepatic stellate cell index in the rat liver — an example in healthy conditions. *Journal of Histochemistry & Cytochemistry* 51, 1101-1104.

Marcos R, Monteiro RA, Rocha E (2004) Estimation of the number of stellate cells in a liver with the smooth fractionator. *Journal of Microscopy* 215, 174-182.

Marcos R, Monteiro RAF, Rocha E (2012) The use of design based stereology to evaluate volumes and numbers in the liver: a review with practical guidelines. *Journal of Anatomy* 220, 303-317.

Martin G, Sewell RB, Yeomans ND, Smallwood RA (1992) Ageing has no effect on the volume density of hepatocytes, reticulo-endothelial cells or the extracellular space in livers of female Sprague-Dawley rats. *Clinical and Experimental Pharmacology & Physiology* 19, 537-539.

Massard J, Ratziu V, Thabut D, Moussalli J, Lebray P, Benhamou Y, Poynard T (2006) Natural history and predictors of disease severity in chronic hepatitis C. *Journal of Hepatology* 44, S19-24.

McCuskey RS (2006) Anatomy of the liver. In: *Zakim and Boyer's Hepatology. A textbook of liver disease, 5th edition* (Boyer TD, Wright TL, Manns MP eds), pp. 3-21. Saunders.

Michael B, Yano B, Sellers RS, Perry R, Morton D, Roome N, Johnson JK, Schafer K, Pitsch S (2007) Evaluation of organ weights for rodent and non-rodent toxicity studies: a review of regulatory guidelines and a survey of current practices. *Toxicologic Pathology* 35, 742-750.

Minato Y, Hasumura Y, Takeuchi J (1983) The role of fat-storing cells in Disse space fibrogenesis in alcoholic liver disease. *Hepatology* 3, 559-566.

Moreira RK (2007) Hepatic stellate cells and liver fibrosis. *Archives of Pathology and Laboratory Medicine* 131, 1728-1734.

Munro HN, Young VR (1978) Protein metabolism in the elderly: observations relating to dietary needs. *Postgraduate Medicine* 63, 143-148.

Neubauer K, Knittel T, Aurish S, Fellmer P, Ramadori G (1996) Glial fibrillary acidic protein – a cell type specific marker for Ito cells *in vivo* and *in vitro*. *Journal of Hepatology* 24, 719-730.

Niki T, De Bleser PJ, Xu G, Van Den Berg K, Wisse E, Geerts A (1996) Comparison of glial fibrillary acidic protein and desmin staining in normal and CCl_4-induced fibrotic rat livers. *Hepatology* 23, 1538-1545.

Nyengaard JR (1999) Stereologic methods and their application in kidney research. *Journal of the American Society of Nephrology* 10, 1100-1123.

Oikawa H, Masuda T, Kamaguchi J, Sato S (2002) Three-dimensional examination of hepatic stellate cells in rat liver and response to endothelin-1 using confocal laser scanning microscopy. *Journal of Gastroenterology and Hepatology* 17, 861-872.

Okuno M, Moriwaki H, Imai S, Muto YY, Kawada N, Suzuki Y, Kojima S (1997) Retinoids exacerbate rat liver fibrosis by inducing TGF-beta in liver stellate cells. *Hepatology* 26, 913-921.

Ontoniente B, Kimura H, Maeda T (1983) Comparative study of the glial fibrillary acidic protein in vertebrates by PAP immunocytochemistry. *The Journal of Comparative Neurology* 215, 427-436.

Pilegaard K, Ladefoged O (1996) Total number of astrocytes in the molecular layer of the dentate gyrus of rats at different ages. *Analytical and Quantitative Cytology and Histology* 18, 279-285.

Pinzani M, Milani S, Herbst H, De Franco R, Grappone C, Gentilini A, Caligiuri A, Pellegrini G, Ngo DV, Romanelli RG, Gentilini P (1996) Expression of platelet-derived growth factor and its receptors in normal human liver and during active hepatic fibrogenesis. *American Journal of Pathology* 148, 785-800.

Pinzani M, Rombouts K, Colagrande S (2005) Fibrosis in chronic liver diseases: diagnosis and management. *Journal of Hepatology* 42, S22-36.

Polak JM, Van Noorden S (1997) Requirements for Immunocytochemistry. In: *Introduction to Immunocytochemistry, 2nd edition,* pp. 11-35. Bios Scientific Publishers.

Porta E, Joun N, Nitta R (1980) Effects of the type on dietary fat at two levels of vitamin E in Wistar male rats during development and aging. I. Life span, serum biochemical parameters and pathological changes. *Mechanisms of Ageing and Development* 13, 1-39.

Porta E, Keopuhiwa L, Joun N, Nitta R (1981) Effects of the type on dietary fat at two levels of vitamin E in Wistar male rats during development and aging. III. Biochemical and morphometric parameters of the liver. *Mechanisms of Ageing and Development* 15, 297-335.

Poynard T, Ratziu V, Charlotte F, Goodman Z, McHutchison J, Albrecht J (2001) Rates and risk factors of liver fibrosis progression in patients with chronic hepatitis C. *Journal of Hepatology* 34, 730-739.

Ramadori G, Veit T, Schwögler S, Dienes HP, Knittel T, Rieder H, Zum Büschenfelde KHM (1990) Expression of the gene of the α-smooth muscle-actin isoform in rat liver and in fat-storing (Ito) cells. *Virchow's Archives [B] Cell Pathology* 59, 349-357.

Ramadori G (1991) The stellate cell (Ito-cell, fat storing cell, lipocyte, perisinusoidal cell) of the liver. New insights into the pathophysiology of an intriguing cell. *Virchows Archives [B] Cell Pathology* 61, 147-158.

Ramadori G, Saile B (2002) Mesenchymal cells in the liver — one cell or two? *Liver* 22, 283-294.

Reid LM, Fiorino AS, Sigal SH, Brill S, Holst PA (1992) Extracellular matrix gradients in the space of Disse: relevance to liver biology. *Hepatology* 15, 1198-1203

Reuben A (2002) Ito becomes a star. *Hepatology* 35, 503-504.

Reuber MD, Glover EL (1968) Carbon tetrachloride induced cirrhosis. Effect of age and sex. *Archives of Pathology* 85, 275-279.

Rockey DC, Boyles JK, Gabbiani G, Friedman SL (1992) Rat hepatic lipocytes express smooth muscle actin upon activation *in vivo* and in culture. *Journal of Submicroscopic Cytology and Pathology* 24, 193-203.

Roskams T, Cassiman D, De Vos R, Libbrecht L (2004) Neuroregulation of the neuroendocrine compartment of the liver. *The Anatomical Record* 280, 910-923.

Roskams T, Desmet VJ, Verslype C (2007) Development, structure and function of the liver. In: *MacSween's pathology of the liver, 5th edition* (Burt A, Portmann B, Ferrell L eds), pp. 1-73. Churchill Livingstone.

Sakai Y, Zhong RR, Garcia B, Zhu L, Wall WJ (1997) Assessment of the longevity of the liver using a rat transplant model. *Hepatology* 25, 421-425.

Salisbury JR (1994) Three-dimensional reconstruction in microscopical morphology. *Histology and Histopathology* 9, 773-780.

Sato M, Suzuki S, Senoo H (2003) Hepatic stellate cells: unique characteristics in cell biology and phenotype. *Cell Structure and Function* 28, 105-112.

Sawada M, Carlson JC (1987) Changes in superoxide radical and lipid peroxide formation in the brain, heart and liver during the lifetime of the rat. *Mechanisms of Ageing and Development* 41, 125-137.

Scherle W (1970) A simple method for volumetry of organs in quantitative stereology. *Mikroskopie* 26, 57-60.

Schmitz C, Hof PR (2000) Recommendations for straightforward and rigorous methods of counting neurons based on a computer simulation approach. *Journal of Chemical Neuroanatomy* 20, 93-114.

Schmucker DL (2005) Age-related changes in liver structure and function: Implications for disease? *Experimental Gerontology* 40, 650-659.

Schoeffner DJ, Warren DA, Muralidara S, Bruckner JV, Simmons JE (1999) Organ weights and fat volume in rats as a function of strain and age. *Journal of Toxicology and Environmental Health [A]* 56, 449-462.

Scotland RS, Stables MJ, Madalli S, Watson P, Gilroy DW (2011) Sex differences in resident immune cell phenotype underlie more efficient acute inflammatory responses in female mice. *Blood* 118, 5918-5927.

Senoo H, Kojima N, Sato M (2007) Vitamin A-storing cells (stellate cells). *Vitamins and Hormones* 75, 131-159.

Senoo H, Yoshikawa K, Morii M, Miura M, Imai K, Mezaki Y (2010) Hepatic stellate cell (vitamin A-storing cell) and its relative — past, present and future. *Cell Biology International* 34, 1247-1272.

Shi SR, Cote RJ, Taylor CR (1999) Standardization and further development of antigen retrieval immunocytochemistry: strategies and future goals. *Journal of Histotechnology* 22, 163-167.

Shimizu I, Mizobuchi Y, Yasuda M, Shiba M, Ma YR, Horie T, Liu F, Ito S (1999) Inhibitory effect of oestradiol on activation of rat hepatic stellate cells *in vivo* and *in vitro*. *Gut* 44, 127-136.

Shimizu I, Ito S (2007) Protection of estrogens against the progression of chronic liver disease. *Hepatology Research* 37, 239-247.

Shimizu I, Kohno N, Tamaki K, Shono M, Huang H-W, He J-H, Yao D-F (2007) Female Hepatology: favorable role of estrogen in chronic liver disease with hepatitis B virus infection. *World Journal of Gastroenterology* 13, 4295-4305.

Suematsu M, Aiso S (2001) Professor Toshio Ito: a clairvoyant in pericyte biology. *Keio Journal of Medicine* 50, 66-71.

Sztark F, Dubroca J, Latry P, Quinton A, Balabaud C, Bioulac-Sage P (1986) Perisinusoidal cells in patients with normal liver histology. A morphometric study. *Journal of Hepatology* 2, 358-369.

Tacke F, Weiskirchen R (2012) Update on hepatic stellate cells: pathogenic role in liver fibrosis and novel isolation techniques. *Expert Review of Gastroenterology & Hepatology* 6, 67-80.

Teutsch HF, Schuerfeld D, Groezinger E (1999) Three-dimensional reconstruction of parenchymal units in the liver of the rat. *Hepatology* 29, 494-505.

Van Bezooijen CFA (1984) Influence of age-related changes in rodent liver morphology and physiology on drug metabolism — a review. *Mechanisms of Ageing and Development* 25, 1-22.

Villa E (2008) Role of estrogen in liver cancer. *Womens Health* 4, 41-50.

Villa E, Vukotic R, Cammà C, Petta S, Di Leo A, Gitto S, Turola E, Karampatou A, Losi L, Bernabucci V, Cenci A, Tagliavini S, Baraldi E, De Maria N, Gelmini R, Bertolini E, Rendina M, Francavilla A (2012) Reproductive status is associated with the severity of fibrosis in women with hepatitis C. *PLoS One* 7, e44624.

Vollmar B, Pradarutti S, Richter S, Menger MD (2002) *In vivo* quantification of ageing changes in the rat liver from early juvenile to senescent life. *Liver* 22, 330-341.

Wagenaar G, Chamuleau R, Haan JG, Maas M, Boer P, Marx F, Moorman A, Frederiks W, Lamers W (1993) Experimental evidence that the physiological position of the liver within the circulation is not a major determinant of zonation of gene expression. *Hepatology* 18, 1144-1153.

Wake K (1971) *Sternezellen* in the liver: perisinusoidal cells with special reference to storage of vitamin A. *American Journal of Anatomy* 132, 429-462.

Wake K (1974) Development of vitamin A-rich lipid droplets in multivesicular bodies of rat liver stellate cells. *Journal of Cell Biology* 63, 683-691.

Wake K (1980) Perisinusoidal stellate cells (fat-storing cells, interstitial cells, lipocytes), their related structure in and around the liver sinusoids, and vitamin A-storing cells in extrahepatic organs. *International Review of Cytology* 66, 303-353.

Wake K, Sato T (1993) Intralobular heterogeneity of perisinusoidal stellate cells in porcine liver. *Cell and Tissue Research* 273, 227-237.

Wake K (2004) Karl Wilhelm Kupffer and his contributions to modern Hepatology. *Comparative Hepatology* 3: S2.

Warren A, Cogger VC, Fraser R, Deleve LD, McCuskey RS, Le Couteur DG (2011) The effects of old age on hepatic stellate cells. *Current Gerontology and Geriatric Research* 2011, 439835.

West MJ (1993) New stereological methods for counting neurons. *Neurobiology of Aging* 14, 275-285.

West MJ, Ostergaard K, Andreassen OA, Finsen B (1996) Estimation of the number of somatostatin neurons in the striatum: an *in situ* hibridization study using the optical fractionator. *The Journal of Comparative Neurology* 370, 11-22.

Woodrum DT, Ford JW, Ailawadi G, Pearce CG, Sinha I, Eagleton MJ, Henke PK, Stanley JC, Upchurch GR Jr (2005) Gender differences in rat aortic smooth muscle cell matrix metalloproteinase-9. *Journal of the American College of Surgeons* 201, 398-404.

Wu H-S, Fiel MI, Schiano TD, Gil J (2008) Image segmentation of liver fibrosis. *Journal of Microscopy* 231, 70-80.

Yasuda M, Shimizu I, Shiba M, Ito S (1999) Suppressive effects of estradiol on Dimethylnitrosamine-induced fibrosis of the liver in rats. *Hepatology* 29, 719-727.

Yiengst MJ, Barrows CH, Shock NW (1959) Age changes in the chemical composition of muscle and liver in the rat. *Journal of Gerontology* 14, 400-404.

Yokoi Y, Namihisa T, Kuroda H, Komatsu I, Miyazaki A, Watanabe S, Usui K (1984) Immunocytochemical detection of desmin in fat-storing cells (Ito cells). *Hepatology* 4, 709-714.

Zajicek G, Ariel I, Arber N (1988) The streaming liver. III. Littoral cells accompany the streaming hepatocyte. *Liver* 8, 213-218.

Zarski JP, Marcellin P, Leroy V, Trepo C, Samuel D, Ganne-Carrie N, Barange K, Canva V, Doffoel M, Cales P (2006) Characteristics of patients with chronic hepatitis B in France: predominant frequency of HBe antigen negative cases. *Journal of Hepatology* 45, 355-360.

Zivna H, Zivny P, Palicka V, Nozicka J (2001) The differences in selected biochemical markers and histological findings after bile duct ligation in male and female rats. *Advances in Clinical Pathology* 5, 147-153.

Zhou Y, Shimizu I, Lu G, Itonaga M, Okamura Y, Shono M, Honda H, Inoue S, Muramatsu M, Ito S (2001). Hepatic stellate cells contain the functional estrogen receptor beta but not the estrogen receptor alpha in male and female rats. *Biochemical and Biophysical Research Communications* 286, 1059-1065.

Chapter 3 – Hepatocytes

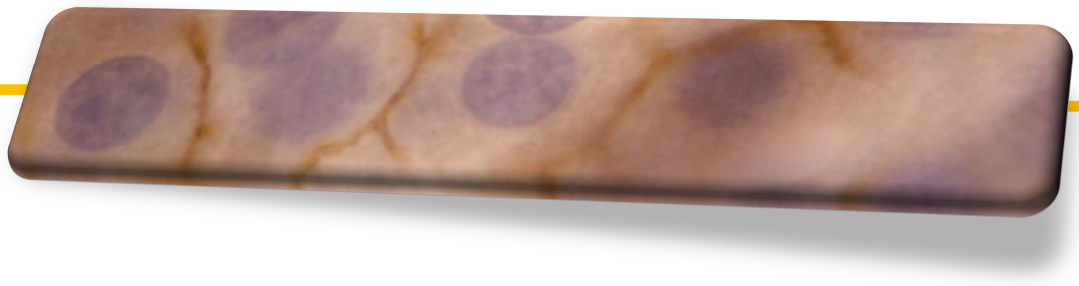

3 – Hepatocytes

3.1- Introduction

3.1.1- Quantification of HEP

The vast number of functions performed by the liver [more than 5000 according to some authors (Biondo-Simões *et al*, 2006)] always placed HEP at the centre of liver research. Indeed, these polyhedral epithelial cells are probably the most versatile somatic cells in the entire body. HEP are arranged in plates of cords with one (occasionally two) cell thickness, that branch and anastomose in a continuous labyrinth. In this way, each of these cells can be in contact with several sinusoids (as well as other HEP) (Roskams *et al*, 2007). Consequently, they lack a true apical and basal surfaces of the typical epithelium (Fawcett, 1994); instead, HEP have the so-called domains (sinusoidal, lateral and canalicular), which are specialised areas of the plasma membrane. Classical stereological studies in the rat showed that these domains comprise, respectively, ≈ 70%, ≈ 15% and ≈ 15% of the total cell surface area (Hubbard *et al*, 1983). In fact, some attention has been given to HEP quantitative morphology, especially in the rat (*e.g.*, Loud, 1968; Weibel *et al*, 1969; Greengard *et al*, 1972; Blouin *et al*, 1977; Jack *et al*, 1990; Carthew *et al*, 1996; 1998a; 1998b), with a few studies devoted to the human liver (Rohr *et al*, 1976; Bioulac-Sage *et al*, 1984). Over the last decade, stereological methods were applied to HEP, characterising their response to different diets and chemical substances (Table 3.1). However, it should be stressed that most of these studies assessed cell or organelle volumes — only a few estimated the N or N_V(HEP, liver). Nevertheless, these data are important because: 1) hyperplasia of HEP has been correlated for long with hepatocarcinogenesis in the rat (Bannasch, 1976) and humans (Kondo *et al*, 1988); 2) hyperplasia has been reported to occur not only in cirrhosis but also in non-cirrhotic conditions, like in non-alcoholic fatty liver disease (Yang *et al*, 2001); 3) a mechanistic interpretation of hepatomegaly can only be made when the N of HEP is known (thus discriminating whether hyperplasia or hypertrophy occurred) (Carthew *et al*, 1998a).

More than thirty years ago, classical studies by Weibel *et al* (1969) and Blouin *et al* (1977) established that HEP occupy 80 to 85% of the liver volume, comprising about 65% of all liver cells. However, at least theoretically, these estimations may be undermined by some bias, not only because they were obtained using the "model-based" stereological methods available at that time, but also because they did not consider the existence of BnHEP. These cells are common in the liver of all mammals, varying from as little as 2%, in cows and goats, to as much as 85% in the common shrew. As a rule of thumb, smaller species (with a body mass below 250 g) tend to have a large number of polyploidal cells (Vinogradov *et al*, 2001).

The proportion of BnHEP is said to be characteristic of a given species, being reported either not to change (Falzone *et al*, 1959; Schmucker, 1998) or to increase throughout life, existing an intense period of production of these cells during weaning (Wheatley, 1972; Styles, 1993; Hayashi *et al*, 2008; Holt and Smith, 2008). However, it should be noted that this proportion varies extensively between authors: figures between 13% (Vinogradov *et al*, 2001) to 43% (Fujii *et al*, 2004) of BnHEP have been reported for rats of the same age (≈ 2 months). These cells have an important role in hyperplastic liver reactions, acting as a cell reservoir for rapid liver regeneration (Styles, 1990; Gandillet *et al*, 2003), producing MnHEP by an amitotic cytokinesis (Styles *et al*, 1987; Guidotti *et al*, 2003). Thus, an increase in the proportion of MnHEP follows a decrease in the percentage of BnHEP — this has been reported in response to: partial hepatectomy (Fausto and Campbell, 2009); hyperthermia (Molodykh *et al*, 2000); treatment with peroxisome proliferators (Carthew *et al*, 1996; Styles *et al*, 1987; 1991); thioacetamide induced cirrhosis (Torres-Lopez *et al*, 1996); and iron overload (Madra *et al*, 1995). Also, in dimethylaminobenzene (Styles, 1990) and diethylnitrosamine/phenobarbitone (Jack *et al*, 1990) induced hepatocarcinogenesis, the percentage of BnHEP was reduced — this has been reported as a consistent change in the carcinogenic process (Jack *et al*, 1990). The ratio of MnHEP to BnHEP is known to shift when regeneration or proliferation occurs in the rat liver. In humans, the percentage of BnHEP, coupled to a ploidy distribution analysis, has been shown to provide valuable information for diagnoses and survival predictions of hepatocellular carcinoma (Melchiorri *et al*, 1994).

Table 3.1- Compilation of some stereological data (mean values) of hepatocytes using "model-" and "design-based" stereology. (Table published in *Marcos et al*, *Journal of Anatomy*, *2012*.)

Reference	Species	Embedding medium	Methods	V_V (HEP, liver)	$\bar{v}_N$ (μm^3)	N ($\times 10^8$)	N_V (HEP/mm^3) ($\times 10^3$)
Karbalay-Doust & Noorafshan (2009)	Mouse (balb-c), females, 31.8 g BW	Paraffin	Sc, O, PC, OD, RT, N′	70.9	5300	5.30	
Odaci et al. (2009)	Rat (Wistar), males, 200–210 g BW	Paraffin	OD, F			1.58	266
Altunkaynak & Özbek (2009)	Rat (Sprague–Dawley), females, 150–200 g BW	Paraffin	FD, Cv, PC, PD, RT	67.2		18.1 (MnHEP) 2.3 (BnHEP)	181 (MnHEP) 24 (BnHEP)
Souza-Mello et al. (2007)	Rat (Wistar), females/males, 230/359 g BW	Paraffin	Sc, PD			7.28 (males) 5.16 (females)	
Marcos et al. (2006)	Rat (Wistar), males, 336 g BW	Paraffin	OD, F			14.1 (MnHEP) 5.2 (BnHEP)	141 (MnHEP) 49 (BnHEP)
Burity et al. (2004)	Primates species *Leontopithecus* (ϕ)	Paraffin	PC, OD	90.1-94.9			489-521
Carthew et al. (1998)	Rat (F344), males, 150–160 g BW	Paraffin	PC, OD			24.3	370
Jack et al. (1990)	Rat (Tif:RAlf), females	Epon	PD, N′		4740 (MnHEP) 6930 (BnHEP)		
Weibel et al. (1969)	Rat (Wistar), males, 174 g BW	Epon	PC, MBM	83.7	4940	9.88	169
Rohr et al. (1976)	Humans (biopsies), males/females	Epon	PC, MBM	79.3	11305		102

BW, body weight; Cv, Cavalieri; FD, fluid displacement; F, fractionator; HEP, hepatocytes (MnHEP, mononucleated; BnHEP, binucleated); MBM, model-based methods; $\bar{v}_N$, number-weighted nuclear volume; N_V, numerical density; N′, nucleator; O, orientator; OD, optical disector; PD, physical disector; PC, point-counting; RT, ratio-technique; Sc, Scherle's method; N, total number; V_V, volume density; (Φ) *L. rosalia*, *L. chrysomelas* and *L. chrysopygus*.

The functional diversity of HEP implies a large number of organelles, and the cytology of these cells is now very well characterised. The nuclei are round, with peripheral clumps of heterochromatin and one (or two) prominent nucleoli can be easily recognised in light microscopy — this is considered typical of HEP (McCuskey, 2006). The nucleus varies somewhat in size, occupying up to 10% of the cell volume (Loud, 1968). It is said to be proportional to their DNA content, and polyploid cells are common in the liver of all mammals (Roskams *et al*, 2007). Ultrastructural aspects of HEP have also been characterised: apart from the above mentioned domains, it is known that these cells contain large numbers of mitochondria (≈ 1700 per cell), and endoplasmic reticulum, accounting for 22% and 15% of the cell volume, respectively (Loud, 1968). The proportion and location of the two types of reticulum varies among animal species. The rough type is predominantly located along the sinusoidal domain, emphasising the role of protein exportation of HEP (over 90% of the protein produced in the liver is synthesised by these cells) (Holt and Smith, 2008). Aggregations of rough endoplasmic reticulum are readily visible in light microscopy as conspicuous basophilic bodies, traditionally named ergatoplasm (Fawcett, 1994). In contrast, the smooth endoplasmic reticulum is dispersed in the cytoplasm. Besides their role in the synthesis of very low density serum lipoprotein, this organelle is fundamental for metabolising drugs and steroids, since it contains enzymes of the CYP family. Apart from Golgi complexes, peroxisomes and lysosomes, the cytoplasm of HEP contains varying amounts of glycogen granules and electron-dense lipid droplets, not enclosed by membrane (Fawcett, 1994).

The liver is a peculiar organ in that, no matter the angle of sectioning, it basically has the same histological appearance — *i.e.*, presence of hepatic lobules. The organisation of these units has been discussed for more than three centuries, but it is generally accepted that human lobules have 1-2 mm in diameter (these are approximately twice the size of the rat), being composed of interconnected cords of HEP separated by sinusoids (Wagenaar *et al*, 1994; Malarkey *et al*, 2005; Guyot *et al*, 2006). In general, the cords have 15-25 HEP in length (Ishibashi *et al*, 2009). This complex architecture ensures maximal exchange area between HEP and sinusoids: a recent and elegant study used 3D reconstruction in the regenerating liver and showed that cell contact between HEP does not determine the alignment of cell cords; instead, these tend to align in order to meet the maximum contact with sinusoids (Hoheme *et al*, 2010). Although it has been established that the liver grows by division and expansion of their lobules (Roskams *et al*, 2007), it is relatively unknown whether their size and number are maintained throughout ageing.

3.1.2- Ageing, gender and HEP

It is known for long that the liver of aged man presents a reduction in blood flow (Popper, 1985). The same occurs in mice and rats: the blood flow is reduced after 9 months of age (Kitani, 1992; Vollmar *et al*, 2002; Warren *et al*, 2008). Apart from this, aged sinusoids of man and rodents are wrapped in basal membrane material — the so-called pseudocapillarisation (Le Couteur *et al*, 2002; Cogger and Le Couteur, 2009). In consequence, the function of HEP is altered: *e.g.*, there is a reduction in the transhepatocellular transport of dyes and IgA (Popper, 1985), diffusion of small lipoproteins (Hilmer *et al*, 2005) and bile salt formation (Le Couteur and McLean, 1998; Vollmar *et al*, 2002). Additionally, differences in the microsomes have been reported, with a decrease in CYP concentration and in the NADPH-cytochrome C reductase activity with ageing (Van Bezooijen, 1984). This occurs mainly in male rats, because levels in females remain fairly unchanged (Kitani, 1992). Truly, a sort of feminization of the male rat liver has been reported for various enzyme activities, meaning that those more active in younger males (than in females), usually decline throughout ageing, approaching the respective levels of the female rat liver (and the opposite is also true, *i.e.*, less active enzymes tend to increase with ageing) (Kitani, 1992; 2007). However, the ageing effects in HEP structure are less clear. In fact, the present state of knowledge in the field is characterised by few consistent and reproducible observations and by a lack of correlation between structural and functional data (Zeeh, 2001). Histology textbooks often obviate this subject: while the early ontogenesis of the liver has been widely studied (and is taught in all medical courses), the other end-point received much less attention (Popper, 1985; Kitani, 2007). Even if it is accepted that the liver appears to age fairly well (Popper, 1985; Zeeh, 2001; Kitani, 2007), there have been few comprehensive studies on liver morphology during ageing and most of the analyses were purely qualitative (Schmucker, 2001; Schmucker and Sanchez, 2011). The aged liver has been viewed has having fewer and larger HEP, with increased levels of nuclear ploidy and BnHEP, but conflictive data has been reported in humans, as well as in rodents (Popper, 1986; Schmucker, 2001; Malarkey *et al*, 2005; Roskams *et al*, 2007). For instance, the volume of HEP has been reported to increase (around 25%) beyond 60 years of age or to remain relatively unchanged throughout the entire lifespan of man (Watanabe and Tanaka, 1982; Schmucker, 1990). In order to reveal morphological age differences, the approach should be as quantitative as possible, namely using stereology or (painstaking) 3D reconstruction, since the qualitative morphology alone may overlook important structural changes. Moreover, it has been stressed that the true aspects of ageing are difficult to obtain from a simple comparison between young *versus* old animals (since changes can occur in between), from a single gender of a particular strain (Kitani, 1992; Schmucker,

2001). As discussed in Chapter 1, the currently available (scarce) data has been restricted to a single gender and to either Sprague-Dawley or Fischer rats (with a clear over-representation of males of the latter strain).

Despite the controversy, a consensus exists regarding some findings in the aged liver. For instance, the volume of the dense body compartment (including secondary lysosomes, residual bodies and lipofuscin) increases (Schmucker and Sanchez, 2011) and this latter is responsible for the brown atrophy of the human liver (that is less visible in rodents) (Wynne and James, 1990). Additionally, there is a (more or less) pronounced age related change towards a polyploid organ. In the rat, this occurs mostly within the first year of life (afterwards only small changes occur) (Van Bezooijen, 1984), whilst in mice the ploidy increases up to 28 months, when 80-90% of HEP are polyploid and 16N and 32N cells are quite common (Van Bezooijen, 1984; Vinogradov *et al*, 2001; Celton-Morizur and Desdouets, 2010). It has been reported that the extent of polyploidy is strain dependent, in the sense that the time of beginning and end varies between strains (Van Bezooijen, 1984), being largely unknown if gender differences also occur throughout ageing.

Another consensual finding is that the regenerative potential is also altered with ageing. After 70% hepatectomy, the organ is fully regenerated in young as in elders, but the process is much slower in the latter (Schmucker and Sanchez, 2011). This fact is known from the early studies in hepatic regeneration: in young rats, virtually all HEP enter the cell cycle, whereas only one third do so in the aged liver (Bucher *et al*, 1964; Stocker and Heine, 1971). HEP are long-lived cells, with little turnover in the absence of cell loss. According to some researchers, the liver tissue renews entirely approximately once a year (Ramadori and Ramadori, 2010), but the actual lifespan in normal conditions is still debated: for some, it should be in excess of 150 days (Fawcett, 1994) whereas for others it is around 400 days (Grisham, 2009), or it may even be measured in years, namely in laboratory rodents (Roskams *et al*, 2007). One reason that may underlie such disagreement is the gender of the animals used (Popper, 1985). In fact, male and female rats have been used interchangeably in some liver studies, and there is no doubt that the liver morphology is alike in males and females. However, some functional differences have been reported: apart from the differences in CYP, diverse contents of glucose-6-phosphatase (Teutsch, 1984) and of GS (Sirma *et al*, 1996) have been reported. Oestrogens influence the levels of sex steroid-binding globulin, as well as the production of circulating substances, like angiotensinogen, ceruloplasmin and transport proteins (Francavilla *et al*, 1986). It was observed that oestrogens increased high-density lipoprotein and triglycerides and decreased low-density lipoprotein, total cholesterol, fasting insulin and glucose levels (Espeland *et al*, 1998). More recently, a micro-array analysis revealed that more than half of the genes were differentially expressed between

male and female mice (Yang *et al*, 2006), and this observation was confirmed in rats (of the Fischer strain) (Kwekel *et al*, 2010). This biological inequality is related with the so-called gender dimorphism, in which females have an increased resistance to premature ageing, nutrient deprivation, vascular and heart diseases, brain disorders, as well as hepatic neoplasms (Li *et al*, 2012).

The liver gender dimorphism is not a mere academic issue: in the clinical scenario, most liver surgeons feel better when performing a major intervention in a female liver than in a male one (Yokoyama *et al*, 2007). A number of studies have showed a dimorphic pattern in the response of this organ under various types of stress, like ischemia and reperfusion injury (Yokoyama *et al*, 2005). However, the exact mechanism underlying gender dimorphism is still unknown (Yokoyama *et al*, 2007): differences in the levels of circulating steroid sex hormones, and of their receptors in the liver, as well as the pattern of growth hormone secretion have been postulated to account for the dimorphic pathophysiology (Yokoyama *et al*, 2005), and the more efficient generation of 3, 3', 5'-triido-L-thyronine in the liver of female rats, comparing with males, may also play a role (Da Costa *et al*, 2001). Despite the most updated techniques have been applied for studying this subject (Li *et al*, 2012), some morphological quantitative baseline data is still missing in literature. To the best of our knowledge, gender dimorphism (at microscopy level) has not been fully addressed using stereological techniques, able to disclose such differences — namely assessing the volume and number of HEP — that could help explaining the different responses to disease. Only two recent studies compared the N_V(HEP, liver) between normal (sham-operated) and ovariectomised females, reaching to opposite conclusions (Dursun *et al*, 2010; Trujillo *et al*, 2011).

The historical background of the "liver and oestrogen relationship" dates back to mid seventies, when hepatic neoplasms were correlated with the use of oral contraceptives (Vana *et al*, 1977). Since then, it has become increasingly evident that the mammalian liver, in both genders, is responsive to steroid sex hormones, which can modulate morphological and functional features of the organ (as above mentioned). Their action can be mediated through steroid receptors, which have been extensively studied over the past decades — first discovering the α variant of the ER and later the β isoform (Kuiper *et al*, 1997) — as well as through androgen receptors in the liver (Pelletier, 2000). Although some controversy still exists, it is generally accepted that rat HEP express mainly the ERα (Pelletier, 2000; Kalra *et al*, 2008; Villa, 2008), whereas cholangiocytes express both types of receptors, and in HSC the ERβ isoform predominates (Zhou *et al*, 2001). ERα is the main mediator of hepatic oestrogenic effects, involving inhibition of the local glucose production and lipogenesis (Barros and Gustafsson, 2011).

In accordance to this, epidemiological studies indicate that the incidence of steatosis is higher in men (Kolovou *et al*, 2009), and more importantly, the incidence of hepatocellular carcinoma is two to four times higher in men than in women, regardless the aetiologies (El-Serag and Rudolph, 2007). Regarding the latter, androgens have been suggested to promote this neoplasia, in men as in rodents, since male mice lacking the androgen receptor were protected (Ma *et al*, 2008). Even so, the role of oestrogen has been controversial, with evidence suggesting both carcinogenic and protective effects in the liver (Kalra *et al*, 2008). Even if chemically induced carcinogenesis in rodents definitely points to more liver tumours in ovariectomised females (comparing with normal animals) and to decreased incidences in male mice and rats treated with oestrogens (Yamamoto *et al*, 1991; Shimizu *et al*, 1998; Naugler *et al*, 2007), it is recognised that limited information is still available, regarding the mechanisms of oestrogen and androgen actions in normal organ, as well as in hepatocellular carcinoma (Kalra *et al*, 2008).

To put simply, we may say that for a plethora of harmful events that mitigate the liver throughout life, the organ has only a handful of responses: 1) necrosis and apoptosis; 2) inflammation; 3) regeneration; 4) degeneration and intracellular accumulation; 5) ECM deposition and fibrosis. In Chapter 2 we already evaluated the ECM deposition throughout ageing, and in this Chapter we intend to study the former: namely the intracellular accumulation of ROS in the liver. As previously mentioned, inflammatory responses often begin in ROS produced by HEP, which trigger HSC activation and ultimately may lead to liver fibrosis. In detail, there are four main sites of ROS generation in the liver: 1) mitochondrial electron transport; 2) peroxisomal fatty acid metabolism; 3) CYP in microsomes; 4) respiratory burst in phagocytic cells, namely in KC (Beckman and Ames, 1998). Classic experiments during the seventies estimated that 1-2% of all oxygen used in mitochondrial electron transport chain is converted in superoxide radicals and its reactive metabolites, in and around mitochondria (Boveris and Chance, 1973). The reactivity of the superoxide anion ($O_2^{-}\bullet$) is quite low, but it is able to initiate a free-radical chain of reactions in which the anion is converted, either spontaneously or by enzymes (superoxide dismutases), into H_2O_2 (alternatively, superoxide can also react with nitric oxide to form peroxynitrite). Hydrogen peroxide is much more stable: if not scavenged locally by catalase (CAT) or glutathione peroxidase (GPX), it can diffuse through the plasma membrane and promote oxidative stress far from its origin. In the presence of free transition metals, like iron and copper, H_2O_2 solely or coupled with $O_2^{-}\bullet$ (respectively, through the Fenton and Haber-Weiss reactions) can generate the extremely reactive hydroxyl radical (·OH). Ultimately, this is the main responsible for the destruction of biomolecules. Collectively, ROS can damage different biomolecules randomly: 1) lipids, in the so-called lipid peroxidation (LPO), that generates hydroperoxyl radicals and leads to

decreased membrane fluidity; 2) DNA, producing strand breaks, mutations and oxidation of purine and pyrimidine bases; 3) proteins, in which the oxidation of sulfhydryl groups and the modification of amino acids can either activate or inactivate them (Beckman and Ames, 1998). One of the most prominent theories for ageing, the “free radical theory” of Harman (1956), postulates that the generation of ROS supplants the counterbalance by antioxidant systems, resulting in oxidative damage of cells and tissues. In principle, this theory could substantiate the epidemiological evidence that liver diseases tend to progress faster with ageing (Roskams *et al*, 2007). Moreover, the long proposed ROS-scavenging activity of oestrogen (Sugioka *et al*, 1987) could account for less severe liver disease in females. In this vein, the increased longevity of females has been correlated with the antioxidant protection of oestrogen (Viña *et al*, 2005). However, studies investigating LPO in aged rats have also generated contradictory results (Van Bezooijen, 1984; Dogru-Abbasoglu *et al*, 1997) and the antioxidant protection of females was recently disputed (Aydin *et al*, 2010).

In conclusion, in this part of the work (in the baseline and in the age and gender study) we aimed to: 1) establish the methodology for obtaining an accurate and precise estimate of the N of HEP, as well as the fraction of BnHEP (since these cells constitute an important pool for regenerative responses of the liver); 2) determine the porto-central distance, in order to assess if the lobular structure is altered throughout ageing (and eventually with gender); 3) evaluate if ageing involves an hyperplastic or hypertrophic progression in HEP — for this we followed the N and mean volume of HEP throughout ageing using “design-based” stereological methods; 4) assess if gender differences can offer new fundamental knowledge to better explain the higher regenerative response of young rats, particularly in females — to achieve this we conducted a flow cytometry evaluation; 6) evaluate if differences in antioxidant defences, throughout ageing and gender, could help explaining the higher collagen deposition trend of male rats.

3.2- Materials and Methods

3.2.1- Baseline study: 1) Animals, tissue preparation and sampling protocol

For establishing the immunohistochemical and stereological protocol, we used the same biological material described in Chapter 2 (*i.e*., 5 male Wistar rats with ≈ 3 months, from "Fundação Calouste Gulbenkian"). The sampling followed the rules of the smooth optical fractionator, which were detailed in Chapter 2. As mentioned, in every 20 sections, a group of four sections were SUR sampled and the second one of that series was used for estimating the N of HEP.

3.2.1- Baseline study: 2) Immunohistochemistry for CEA

After deparaffinisation, treatment in a microwave oven (Moulinex, Y53) was carried out for antigen retrieval. The microwave was set for 3 cycles of 4 minutes, at 600W, and the following steps were similar to the protocol described in Chapter 2, except for the antibody. Here we used 1:1600 dilution of rabbit polyclonal antibody against CEA (Dako), incubated during 4 days at 4ºC. Immunohistochemistry using anti-CEA polyclonal antibodies delineated the biliary canaliculi, circumscribing the cell limits, and thus allowed a clear distinction between MnHEP and BnHEP. Negative controls were included, in which the first antibody was either omitted or replaced by rabbit non-immune serum (Dako).

3.2.1- Baseline study: 3) Stereological analysis

The N of HEP and of non-hepatocytic cells (NHC) were estimated with the optical fractionator, using the workstation described in Chapter 2. The NHC includes sinusoidal (LSEC, HSC, KC and pit cells) as well as stromal cells, from the portal tracts and central venules. The first field of vision was selected randomly, and thereafter fields were sampled by stepwise movements of the stage in *x*- and *y*-directions ($step_{x,y}$ = 1250 µm). Through the disector height (20 µm), a software generated counting frame was superimposed — in this case, the frame had an area of 418 μm^2, with forbidden lines and a defined point to evaluate its position on the reference space (Howard and Reed, 2005).

The HEP and NHC were counted when two conditions were met: 1) the rim of nucleus was in perfect focus at a plane below 4 µm and above or equal to 24 µm in the *z*-axis — in the case of BnHEP, the first nucleus coming to focus was considered for the counting; 2) at the plane of focus, the nucleus was within the counting frame, or touching the inclusion lines, without touching the forbidden lines or their extensions. Rarely, a BnHEP presented both nuclei in focus at the same plane — in such cases, a predefined nucleus (left and/or uppermost) was used for the counting. To assure that no bias in the distinction between MnHEP and BnHEP would be introduced by failure of the immunomarking, it was always verified that the CEA marking extended beyond 24 µm from the top of the section. The

potential bias from lost caps was avoided by having upper and lower guard heights, of 4 µm and ≈ 6 µm in thickness, respectively. Their use was validated by analysing the distribution of particles in thick paraffin liver sections (Annex 1). The section thickness was measured (with the microcator) in every 5th field, as a very small variation in section thickness was expected (see Results) (Dorph-Petersen *et al*, 2001). The coefficient of error (CE = standard error of the mean/mean) of these measurements was calculated.

From the systematic sampling of the fractionator we expected that the counting frame could hit the artificial borders generated during slicing, and potentially introduce a small bias in the estimates. Like in Chapter 2, this happened rarely, and was irrelevant in practical terms. Nevertheless, in the rare occasions in which artificial borders were faced, we followed the approach detailed in Chapter 2 (Gundersen, 1986; Marcos *et al*, 2004): *i.e.*, the counting frame was accepted only if there were no artificial edges within the counting frame or its guard area.

The N of HEP in the whole liver was estimated as:

$$N = (1/bsf) \times (1/ssf) \times (1/asf) \times (1/hsf) \times \Sigma Q^- \quad (3.1)$$

where ΣQ^- is the number MnHEP and BnHEP counted throughout the liver. The *bsf* is the block sampling fraction (*bsf* = 1/8); *ssf* refers to the section sampling fraction (*ssf* = 1/20). The *asf* is the area sampling fraction, calculated by dividing the area of the frame, *a*, by the area associated with each *x*-, *y*-movement, *A* (*asf* = 1/3736). Finally, *hsf* is the height sampling fraction, being obtained by dividing the height of the disector, *h*, by the mean section thickness, *t* (*hsf* = 0.66). The number of HEP/g of liver (N/g) was also estimated, as it could help comparing values between animals with different liver weights. Formula 3.1 was also applied to determine the N of BnHEP and of NHC in the whole liver (in this case ΣQ^- was the number of BnHEP or NHC counted).

The N_V was estimated as well, by the formula:

$$N_V(\text{HEP, liver}) = \Sigma Q^- / [h \times a(\text{frame}) \times \Sigma P] \quad (3.2)$$

where ΣQ^- is the number of cells counted in the sampled fields (either HEP, MnHEP, BnHEP or NHC), *h* is the disector height, *a* is the area of the frame, and ΣP is the number of the accepted counting frames. This formula was also used to estimate the N_V(BnHEP, liver) and the N_V(NHC, liver).

The coefficient of error of the number of cells counted [$CE(\Sigma Q^-)$], either HEP, BnHEP or NHC was estimated by the formula proposed by Schmitz and Hof (2000):

$$CE(\Sigma Q^-) \cong 1/\sqrt{\Sigma Q^-} \quad (3.3)$$

Theoretically, the mean coefficient of error of the N estimations [CE(N)] is equal to the square root of the sum of $CE^2(\Sigma Q^-)$ and the coefficient of error related to section thickness $CE^2(t)$; but, as the CE(t) was minimal (see Results), and for the sake of simplification, it

was disregarded here. Thus, the CE(N) was considered to be equal to the so-called counting noise, *i.e.*, the CE(ΣQ^-).

The CE(N) of the estimates were compared with the observed relative variance between animals, $OCV^2(N)$, according to the formula:

$$OCV^2(N) = BCV^2(N) + CE^2(N) \quad (3.4)$$

where BCV^2 is the biological relative variance of individuals and $CE^2(N)$ is the observed mean square CE of the individual estimates of the CE(N). This formula was applied for all the above mentioned estimations [CE(N) of HEP, BnHEP and NHC].

3.2.1- Baseline study: 4) Computer simulations to determine the optimum sampling

In order to determine the optimum sampling effort, the ΣQ^- of HEP, BnHEP and NHC and their respective CE(N) were computed under different simulations based on the final data. With these, the sampling was reduced to a half, a third, a quarter and a sixth of the sections considered for the final estimates. The simulations were also performed at the level of the sampled fields, meaning that the $step_{x-y}$ was increased to 1768 µm, 2165 µm, 2500 µm and 3062 µm, respectively for the half, third, quarter and sixth reduction of sampling.

3.2.1- Baseline study: 5) Statistical analysis

The software Statistica 5.0 for Windows was used. After checking the normal distribution of data with the Shapiro-Wilk's test, a parametric correlation analysis was applied for detecting linear associations. The Student's t-test for unpaired samples, and its non-parametric equivalent, the Mann-Whitney's U-test, were used for comparing the N of MnHEP and BnHEP for the whole liver. Significance level was set at $p \leq 0.05$.

3.2.2- Age and gender study

3.2.2- Age and gender study: 1) Animals, tissue preparation and sampling protocol

For this part of the study, we used the same material described in Chapter 2 [*i.e.*, 8 groups of young (2 months), adults (6 months), middle-aged or mature (12 months), and old (18 months) rats]. Regarding the tissue preparation, the procedures have been mostly detailed in Chapter 2 and were illustrated in Figure 2.2 of Chpater 2. Only the differences will be detailed here. A major one refers to the fact that we took small liver samples, which were kept at -80ºC (asterisks in Figure 2.2), for studying the antioxidant defences and for the ploidy analysis (as detailed below).

Like in the baseline study, MnHEP, BnHEP and NHC were counted but here we used an immunohistochemistry against E-cadherin (Ogou *et al*, 1983) for differentiating MnHEP from BnHEP. This marker renders estimations of BnHEP similar to that obtained with CEA

(data not shown), but here we opted for E-cadherin because it delineates all the cell membrane (contrasting with the belt-like marking of the CEA), and this was a pre-requisite for applying the nucleator to estimate the cell volume.

Additionally, two sections per block were stained by haematoxylin-eosin, for evaluating the general liver morphology, and by immunohistochemistry against GS (diluted at 1:4000, as detailed in Chapter 2). The latter GS immunostained sections were used to measure the porto-central distance, in order to assess if lobular enlargement occurred with ageing. For this purpose we followed a simple morphometrical approach: the linear distance between a central venule and the closest portal tract was measured (using the CAST-Grid). Measurements were made across the liver sections (recording if it referred to peripheral or to inner lobules).

3.2.2- Age and gender study: 2) Immunohistochemistry for E-cadherin and stereological analysis

The protocol used for thick sections was similar to that described in the baseline study, except for the primary antibody: in this case we used E-cadherin monoclonal mouse antibody (clone NCH 38, Dako) diluted at 1:250. Regarding the procedure for the N estimation in the thick sections, it was also similar to that described in the baseline study, except for the $step_{x,y}$ which was 2000 μm (instead of 1250 μm).

Additionally, the number-weighted mean cell and nuclear volume ($\overline{v}_N$) of MnHEP and BnHEP was estimated by the nucleator method (described in Chapter 1 and illustrated in Figure 1.7). This method is a two-step procedure: firstly, HEP were sampled by the optical disector (using the above described counting frame and guard heights) and the nucleolus was selected; secondly, the CAST-Grid software generated two isotropic lines from the nucleolus and the intersections between these lines and nuclear and cell borders were marked. The average distance from the intersections to the nucleolus (*l*) was used (automatically by the software) to estimate the cell $\overline{v}_N$ by the formula:

$$\overline{v}_N = (4\pi / 3) \times \overline{l}_n^3 \qquad (3.5)$$

In BnHEP, the first nucleus with the first nucleolus (that appeared in focus) was considered for the measurements (Jack *et al,* 1990). In the case of HEP with two nucleoli (or more), the measurements were performed for the two (or more) particles (Howard and Reed, 2005). Additionally, the $\overline{v}_V$ was calculated, by an already introduced formula (Chapter 1):

$$\overline{v}_V = \overline{v}_N \times (1 + CV_n^2(v)) \qquad (3.6)$$

Finally, we further characterised HEP, by assessing the nuclear-cytoplasmic (N:C) ratio (*i.e.*, the nuclear volume divided by the cell volume).

3.2.2- Age and gender study: 3) Ploidy analysis by flow cytometry

Since we would only expect differences between old and young animals (see Results), only 2 and 18 months rats were included in this analysis. A liver piece (≈ 0.7 g) frozen at -80ºC was gently thawed in PBS (pH = 7.4), and mechanically disaggregated with tweezers. The resulting homogenate was centrifuged at 750 G for 5 minutes and the supernatant decanted. The pellet was then resuspended in PBS, and the cell yield calculated in a haematology analyser (LH 780, Beckman Coulter, Brea, USA). The suspension was split into two parts: one for cytological examination used to perform cytospin smears and the other for flow cytometry analysis. For this latter, 100 µl aliquot of each sample (with an average of $3x10^6$ cells/µl) was stained using the DNA-Prep Reagent Kit (Beckman Coulter), which sequentially dispenses and mixes 100 µl of the lysing and permeabilising reagent and 1 ml of the staining solution (containing 50 µg/ml propidium iodide and 4 KU/ml bovine pancreas type III RNAase). Finally, the samples were incubated at room temperature for 20 minutes in darkness. The flow cytometry analysis was performed with a Coulter EPICS-XL-MCL (Beckman Coulter) and a 488 nm argon ion laser. The analysis was performed for 30 minutes, using blood rat lymphocytes as a diploid control. A minimum of twenty thousand events per sample were acquired and analysed with the MultiCycle software (Phoenix Flow Systems, San Diego, USA). A modified exponential debris function was used to subtract the debris in the DNA histograms. The following parameters were calculated: percentage of diploid, tetraploid and aneuploid particles. The S-phase fraction was established, being defined as the proportion of particles in the DNA histogram with intermediate DNA content, between that of G0/G1 and G2/M.

3.2.2- Age and gender study: 4) Biochemical analysis of oxidative stress

Liver pieces (≈ 0.3 g) were homogenised in ice-cold potassium phosphate buffer (KPB) 0.1 M (pH = 7.4), in a 1:10 proportion (w/v). Part of the fine homogenate (200 µl) was used to evaluate the LPO, by measuring the thiobarbituric acid reactive species (TBARS), according to the procedure of Ohkawa (1979) and Bird and Draper (1984). We added 4 µl of butylhydroxytoluene (0.2 mM) to this part of the homogenate, in order to prevent artifactual lipid oxidation, and the mixture was also frozen (at -80ºC) until use (Almeida *et al*, 2010). The remnant part of the fine homogenate was centrifuged at 10000 G for 20 minutes, at 4ºC, in order to obtain the post-mitochondrial supernatant. Afterwards, the supernatant was split into tubes which were frozen (at -80ºC) until use for determining the protein content, as well as the activity of the following enzymes: 1) glutathione S-transferase (GST); 2) glutathione disulfide reductase (GR); 3) GPX; and 4) CAT. The procedures involved in these assessments will be briefly detailed below.

The protein was quantified according to Bradford's method (1976), using bovine γ-globulins (Sigma) as a standard. The samples were diluted at 1:40 with KPB 0.1 M (pH = 7.4) and 4 replicas per sample were plated in a 96 well microplate (10 µl per well). Then 250 µl of Bradford's reagent (diluted five times in ultra-pure water) were added. After 15 minutes of incubation, at 25ºC, the absorbance was read at 600 nm in a microplate reader (Bio Tek Power Wave 340, Winooski, USA), at 25ºC. Unless stated otherwise, all enzymatic activities are expressed as the amount of substrate hydrolysed per minute per mg of protein.

The GST activity was determined following the method described by Habig *et al* (1974). Firstly, the reaction solution was prepared: 75 ml of KPB 0.2 M (pH = 6.5), 2.34 ml of 1-chloro-2,4-dinitrobenzene (Merck) 60 mM, in ethanol, and 13.5 ml of reduced glutathione (GSH) (Sigma) 10 mM, in ultra-pure water. Then, 200 µl of this was added to 100 µl of the samples (four replicas, diluted in KPB, so that protein concentrations were ≈ 0.5 mg/ml). The optical density was measured at 340 nm, in the above cited microplate reader, every 20 seconds during 5 minutes, at 25ºC.

For assessing the GR activity, the method of Carlberg and Mannervik (1985) was followed. It monitors the decrease of reduced nicotinamide adenine dinucleotide phosphate (NADPH), at 340 nm, as a result of the reduction of oxidized glutathione (GSSG) to its reduced form, GSH. Firstly, a reaction buffer was made that included 2.5 mM NADPH (Sigma), 20 mM GSSG (Sigma) and 6 mM diethylene triamine penta-acetic acid (DTPA) (Merck), in 110 ml of KPB 0.05 M (pH = 7.0). Then, 950 µl of the reaction buffer were added to 50 µl of the samples, and the absorbance was read at 340 nm, in a Jasco V-630 (Tokyo, Japan) spectrophotometer, during 1 minute, at 25ºC.

Regarding the GPX activity, the method of Flohé and Günzler (1984) was used. In this method, the decrease of NADPH at 340 nm, after 1 minute, is also measured, but using H_2O_2 as a substrate. In this case, 840 µl of KPB 0.05 M (pH = 7.0), with 1 mM of sodium azide (Merck), 1 U/ml of GR (Roche Applied Science, Indianapolis, USA), and 1 mM of ethylenediamine tetra-acetic acid (Merck), was added to 50 µl of 4 mM GSH and to 50 µl of 0.8 mM of NADPH. Finally, 10 µl of 0.5 mM H_2O_2 and 40 µl of the liver samples were mixed.

The CAT activity was determined by measuring the consumption of H_2O_2 at 240 nm (Claiborne, 1985). In this case, samples were diluted at 1:40 in KPB 0.05 M (pH = 7.0), and then 5 µl were mixed with 950 µl of KPB 0.05 M (pH = 7.0), and 500 µl H_2O_2 30 mM. The enzymatic activity was measured in the Jasco V-630 spectrophotometer, during 30 seconds, at 25ºC.

Finally, to complete the assessment of LPO, we followed the method of Ohkawa (1979) and Bird and Draper (1984). Briefly, 1 ml of 12% trichloroacetic acid, 0.8 ml of 60 mM Tris-

HCl buffer with DTPA, and 1 ml of 0.73% thiobarbituric acid, were added to 200 µl of the liver homogenate. This mixture was then incubated during 60 minutes, at 100ºC. Afterwards, this was centrifuged at 12000 G, during 5 minutes, and TBARS levels were determined at 535 nm in the Jasco V-630 spectrophotometer; in this case, results were expressed in nmol TBARS per g of liver (wet weight).

3.2.2- Age and gender study: 5) Statistical analysis

As the variables have a low number of cases, it was first tested if they followed a normal distribution, by using the Shapiro-Wilk's test. In most cases the assumption of normal distribution was met by a logarithmic transformation of the original variable, namely in the N of HEP, N_V(HEP, liver), N of BnHEP, N of all liver cells, as well as in $\overline{v}_N$ of MnHEP and BnHEP. A parametric correlation analysis was applied for detecting linear associations between parameters. After checking the homogeneity of variances (Levene's test), a two-way ANOVA was performed taking in consideration the effects of gender and age. When significant differences existed ($p \leq 0.05$), multiple comparisons were done by the *post-hoc* Tukey's test. The software SPSS18 (IBM) was used in the analysis.

3.3- Results

3.3.1- Qualitative findings

The lobular morphology was similar for all the groups studied. The liver tissue clearly exhibited a polygonal network of sinusoids draining into central venules (Figure 3.1). These were mostly perpendicular or showed acute angles in relation to the liver capsule (but in rare occasions they were parallel). In liver borders, the portal tracts were much more frequent than central venules.

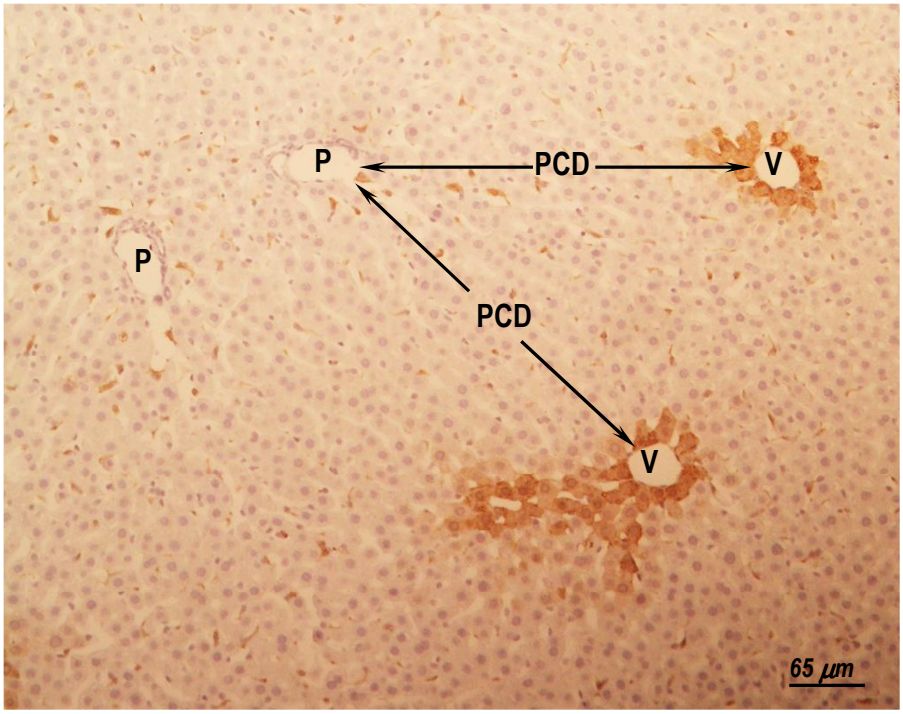

Figure 3.1 – Thin (5 µm) section of a young male liver immunostained against glutamine synthetase (GS). The portal tracts (P) are clearly distinguished from central venules (V) outlined by hepatocytes positive to GS. The linear porto-central distance (PCD) was measured in these sections. Immunomarked cells within the lobules are GS-positive Kupffer cells.

Regarding the distinction of MnHEP and BnHEP, it was either achievable with antibodies against CEA and E-cadherin; since the latter were monoclonal, they produced much less background (and this was relevant for the thick sections). With CEA polyclonal antibodies, a sharp marking of biliary canaliculi revealed the exuberant biliary network, whereas with E-cadherin the whole cell membrane of HEP was outlined throughout the liver lobules (even if it tended to be more intense in periportal areas). The epithelium of biliary ducts was unstained by CEA, but was positive for E-cadherin, whereas the connective tissue presented no staining with both antibodies. Immunomarking extended beyond the 24 µm depth in all the thick sections. The nuclei of BnHEP were generally smaller and closer to each other than the nuclei from two adjacent MnHEP. The nuclei of NHC, either for their smaller size or irregular contour, were easily distinguished from that of HEP (Figure 3.2).

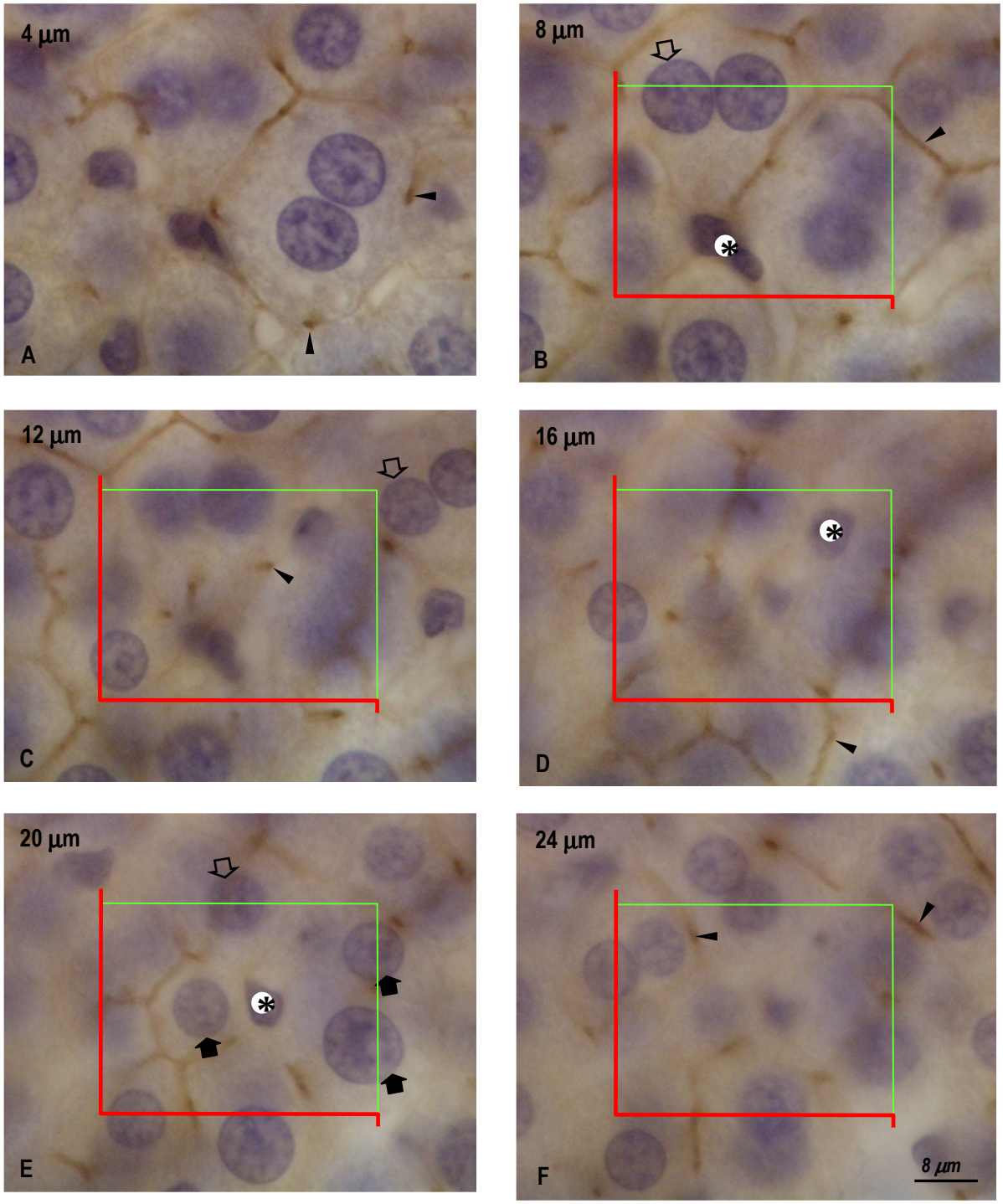

Figure 3.2 – Series of light micrographs from a thick liver section (30 µm) immunostained against carcinoembryonic antigen (CEA) that form an optical disector (the depth of each optical plane is indicated in the upper left corner). Counts are not made in the starting plane (A); from that point on, particles are counted if their nuclei are within the counting frame or touching the inclusion (green) lines, but not touching the exclusion (red) lines. In this illustrative field, 3 mononucleated hepatocytes (black arrows), 3 binucleated hepatocytes (open arrows) and 3 non-hepatocytic cells (asterisks) are counted; arrowheads: biliary canaliculi. Note that the belt-like immunomarking of CEA is sometimes restricted to single spots, namely when the canaliculus is cut perpendicularly (A and C). (Adapted from *Marcos et al, Liver International, 2006.*)

3.2.2- Quantitative findings

3.2.2.1- Baseline study: *total number, number per gram and numerical density of HEP*

Using the baseline sampling scheme, a mean of 1340 disectors per rat was analysed and 3565 liver cells were counted, in average. These corresponded to 1441 NHC and to 2124 HEP (1577 MnHEP and 547 BnHEP). The N and N_V of HEP, BnHEP and NHC from each rat of the baseline study are presented in Table 3.2, which also includes the estimates of the CE(N) per animal. The percentage of BnHEP (in relation to HEP) and of NHC are also presented.

The N/g of HEP was estimated as $129x10^6$ HEP/g of liver (CV = 0.13). A significant difference existed between the N of MnHEP and the N of BnHEP ($p < 0.05$). Significant and strong correlations were observed between: 1) liver weight and body weight (r = 0.91, $p < 0.05$); 2) N BnHEP and body weight (r = 0.99, $p < 0.05$); 3) N HEP and liver weight (r = 0.93, $p < 0.05$); 4) N HEP and N/g HEP (r = 0.94, $p < 0.05$); 5) N HEP and N MnHEP (r = 0.93, $p < 0.05$).

For the estimation of the N of HEP, and according to the Equation 3.4, the sampling procedure was responsible for 1% of the total observed variance. The variance in section thickness was credited for much less (only 0.07% of total variance). Thus, the so-called "biological variance" was, by far, the most important variance component (99% of the total observed variance). This was also true for the estimation of the N of BnHEP and NHC, for which biological variance contributed to 98% and 99%, respectively, of the total variance.

As expected, by reducing the sampling effort, the ΣQ^- decreased up to 7 times and the CE(N) increased just slightly. No statistical difference was observed between the output of the two sampling reduction approaches (*i.e.*, to reduce the sections or the sampled fields). For estimating the N of HEP and the N of NHC in the whole liver, with both approaches, a sixth of the sampling load still allowed precise estimations, being counted around 297-342 HEP and 198-228 NHC, with a CE(N) of 0.06-0.07. In contrast, for BnHEP the sampling could be only reduced to a quarter, counting 122-150 cells, with a CE(N) of 0.09.

Table 3.2 - Estimations of hepatocyte (HEP) and non-hepatocytic cell (NHC) number per mm^3 (N_V) and of total number (N) in the whole liver. CE is the coefficient of error of N, estimated according to Schmitz and Hof (2000). %BnHEP refers to the numerical percentage of binucleated hepatocytes (BnHEP) in relation to the HEP. %NHC refers to the numerical percentage of NHC (in relation to all liver cells). Values of N_V were not corrected for the shrinkage (38%); BW (body weight); LW (liver weight). (Table published in *Marcos et al, Liver International, 2006*.)

Parameter	BW	LW	N_V HEP	N HEP	CE (N_{HEP})	N_V BnHEP	N BnHEP	CE (N_{BnHEP})	%BnHEP	N_V NHC	N NHC	CE (N_{NHC})	%NHC
Rat 1	396	16.6	193×10^3	2.32×10^9	0.02	64.2×10^3	771×10^6	0.03	33.2	109×10^3	1.31×10^9	0.03	36.1
Rat 2	301	13.9	169×10^3	1.91×10^9	0.02	31.2×10^3	353×10^6	0.05	18.4	117×10^3	1.32×10^9	0.03	40.1
Rat 3	317	13.7	179×10^3	1.64×10^9	0.02	46.7×10^3	428×10^6	0.05	26.0	115×10^3	1.06×10^9	0.03	39.0
Rat 4	315	13.6	206×10^3	1.41×10^9	0.03	59.7×10^3	408×10^6	0.05	29.0	149×10^3	1.02×10^9	0.03	41.9
Rat 5	354	16.4	203×10^3	2.38×10^9	0.02	44.9×10^3	528×10^6	0.04	22.1	158×10^3	1.86×10^9	0.02	43.8
Mean	337	14.8	190×10^3	1.93×10^9	0.02	49.3×10^3	520×10^6	0.05	25.8	129×10^3	1.31×10^9	0.03	40.3
CV	0.12	0.10	0.08	0.22	0.12	0.26	0.31	0.15	0.22	0.17	0.26	0.12	0.07

3.2.2.2- Age and gender study

Data for the body weight, liver weight and liver-to-body weight ratio have been presented in Chapter 2, and some of the correlations refer to that data.

3.2.2.2- Age and gender study: 1) Porto-central distance

An average of 62 lobules was analysed by morphometry, per animal. The average porto-central distance was 449 μm (CV = 0.04) in males, and 412 μm in females (CV = 0.05) (data corrected for shrinkage). Data for the individual age groups are presented in Table 3.3. No significant differences existed regarding the size of lobules (throughout ageing and gender). Considering the volume estimation of MnHEP and BnHEP, as well as their relative abundance (see below), this makes a porto-central cell cord composed of 17 ± 1 HEP in males and 16 ± 1 HEP in females (Table 3.3). It should be noted that the porto-central distance is a theoretical value, valid only for comparative purposes; it assumes a linear orientation of all HEP from portal to central areas (*i.e.*, without the deviations or ramifications of the cell cords that exist in the normal liver).

Table 3.3 - Porto-central distance in young (2 months), adult (6 months), middle-aged (12 months) and old (18 months) male and female rats. Values are presented in μm, corresponding to linear measurements (corrected for shrinkage), as well as in the average number of hepatocytes (HEP) that compose the porto-central cell cord. Data expressed as mean ± SD.

Porto-central	Linear distance	Young	Adult	Middle-aged	Old
Males	in μm	463 ± 27	452 ± 14	427 ± 21	454 ± 28
	in HEP	≈ 17 ± 1	≈ 17 ± 1	≈ 17 ± 1	≈ 17 ± 1
Females	in μm	442 ± 12	398 ± 15	414 ± 25	394 ± 18
	in HEP	≈ 17 ± 1	≈ 16 ± 1	≈ 16 ± 1	≈ 16 ± 1

3.2.2.2- Age and gender study: 2) Total number, number per gram and numerical density of HEP

An average of 302 and 200 disectors were evaluated in males and females, respectively. In these, an average of 640 HEP were counted in males and 514 HEP in females. The estimated N of HEP presented moderate significant correlations with the body and liver weights (r = 0.60; $p < 0.0001$), as well as with the N of all liver cells (r = 0.68; $p < 0.0001$), and the N of HSC (r = 0.73; $p < 0.0001$). Even if males tended to have a slightly higher N of HEP than females, no statistically significant differences existed for gender (Figure 3.3). The same occurred with ageing, where the N of males seemed to present a slight

increasing trend [1.8x10^9 HEP (CV = 0.21) in young and 2.49x10^9 HEP (CV = 0.15) in old] that was not present in females.

The CE was comprised between 0.04 and 0.05 for all the estimations of the N of HEP. In the partition of the variance, the biological variance was, by far, the most relevant component, being responsible for 79% to 94% of the total observed variance (Figure 3.4).

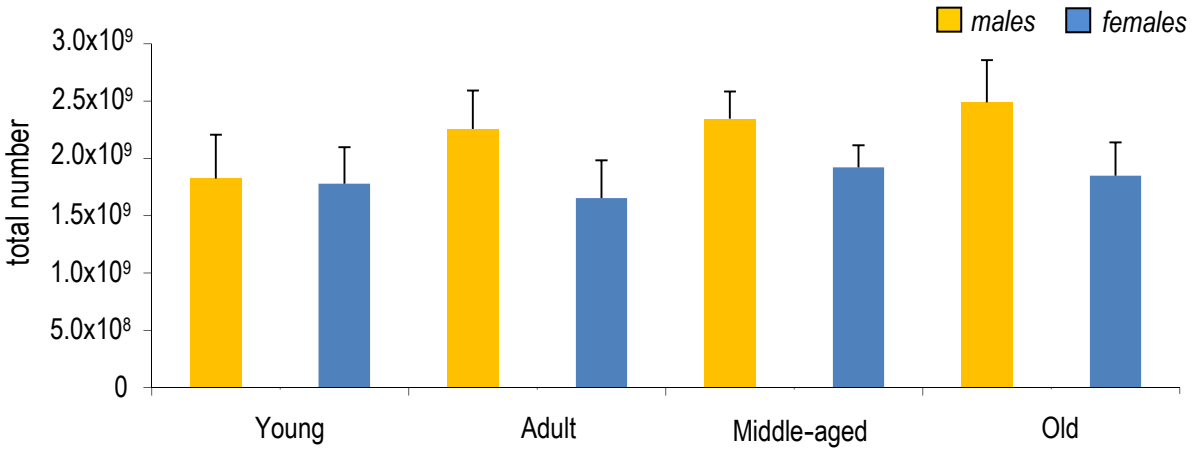

Figure 3.3 – Total number (N) of hepatocytes in male and female young (2 months), adult (6 months), middle-aged (12 months) and old (18 months) rats; data expressed as mean + SD. There were no statistically significant differences.

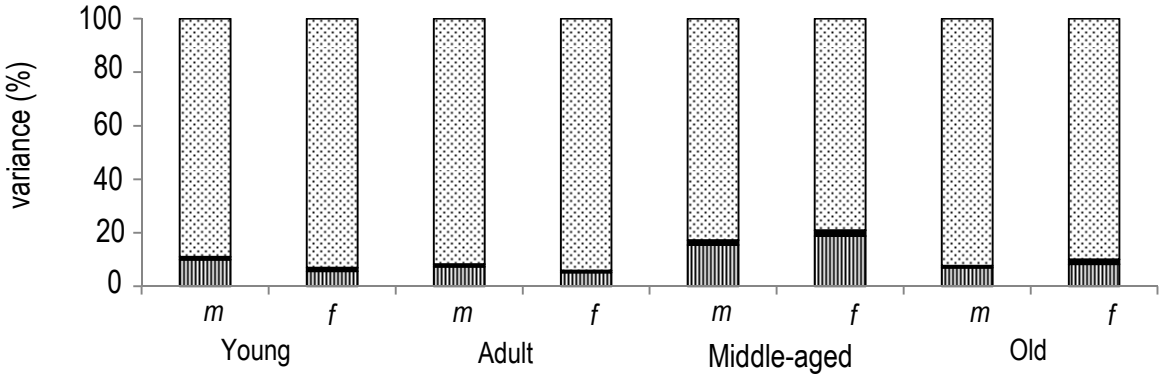

Figure 3.4 – Decomposition of the observed variance of the estimations of N of hepatocytes (according to Equation 3.4) in male (m) and female (f) young (2 months), adult (6 months), middle-aged (12 months) and old (18 months) rats; ⁞ = biological variance; ▮ = section thickness variance; ▒ = average sampling variance.

As to the N/g of HEP, it was also moderately but significantly correlated with the N/g of HSC (r = 0.50, $p < 0.01$). The N/g of HEP presented statistically significant differences for gender ($p < 0.001$) and ageing ($p < 0.05$) (Figure 3.5). Overall gender differences were attenuated with ageing: at young age females had more HEP per gram [the adjusted p value was 0.07, but when only young animals were considered, the p value became

significant (p = 0.03)]. On the contrary, old males had virtually the same N/g [182x10^6 (CV = 0.13) in males and 186x10^6 HEP per gram of liver (CV = 0.16) in females].

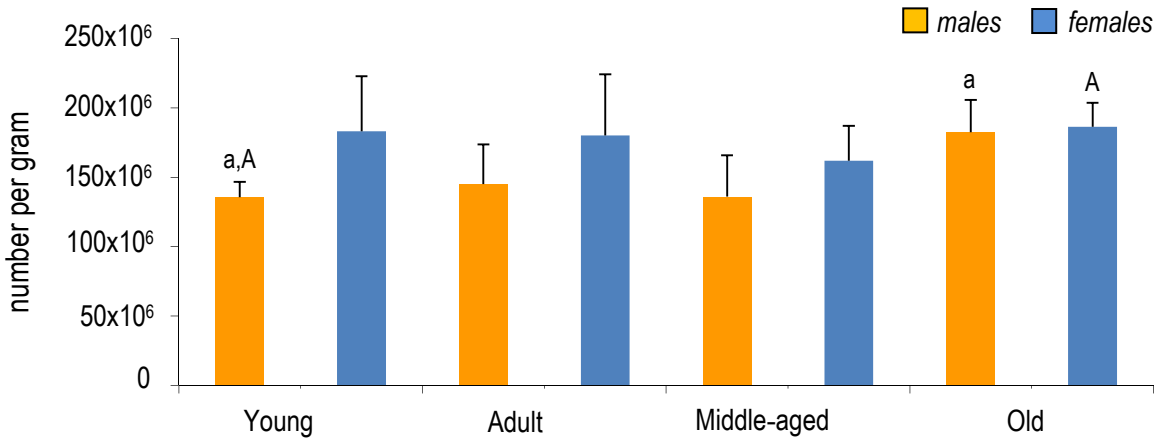

Figure 3.5 – Number per gram (N/g) of hepatocytes in male and female young (2 months), adult (6 months), middle-aged (12 months) and old (18 months) rats. Paired letters indicate significant differences (lowercase: same gender; uppercase: across genders); data expressed as mean + SD.

As mentioned in Chapter 2, no statistical differences existed for the paraffin shrinkage (that always tends to overestimate the N_V). The N_V(HEP, liver) was moderately correlated with the N/g HEP (r = 0.69, p < 0.01), and with the proportion of BnHEP (r = 0.51, p < 0.01). In this parameter, there were significant differences for gender (p < 0.001), but not for ageing (p = 0.09). In males the N_V(HEP, liver) varied from 137x10^3 HEP/mm^3 (CV = 0.11) in young to 215x10^3 HEP/mm^3 (CV = 0.16) in old, whereas in females it tended to be more stable, ranging from 190x10^3 HEP/mm^3 (CV = 0.14) in old and 232x10^3 HEP/mm^3 (CV = 0.13) in adult female rats (Figure 3.6).

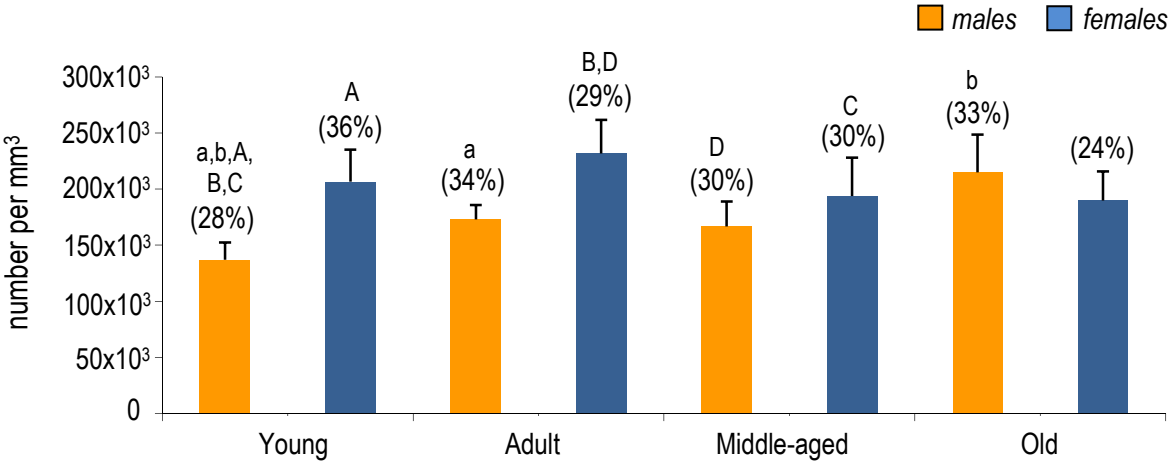

Figure 3.6 – Numerical density N_V(HEP, liver) of hepatocytes (HEP), expressed as number/mm^3, in male and female young (2 months), adult (6 months), middle-aged (12 months) and old (18 months) rats; numbers in brackets correspond to the shrinkage. Paired letters indicate significant differences (lowercase: same gender; uppercase: across genders); data corrected for paraffin shrinkage and expressed as mean + SD.

3.2.2.2- Ageing and gender study: 3) Number of BnHEP, their number per gram and percentage

The N of BnHEP was moderately correlated with the N of HEP (r = 0.50, $p < 0.01$) and with the N/g HEP (r = 0.57, $p < 0.01$), being negatively correlated with the cell volume $\overline{v}_N$ of BnHEP (r = -0.61, $p < 0.01$). As to the ratio of BnHEP it was negatively correlated with body weight (r = -0.59, $p < 0.001$), liver weight (r = -0.70, $p < 0.001$) and to a lesser extent with the N of HEP and N of all liver cells (r = -0.50, $p < 0.01$). The N of BnHEP remained unchanged with ageing and gender (Figure 3.7); differences regarding this cell type were only highlighted when the N/g BnHEP (Figure 3.8) or their proportion (Figure 3.9) were considered [in these cases there were differences for gender, but not for ageing (p = 0.06)]. As a general trend, the number per gram, as well as the percentage, was higher in females, but these differences tended to be reduced with ageing. In this vein, the N/g of BnHEP in young rats was $33x10^6$ (CV = 0.24) in males and $60x10^6$ (CV = 0.13) BnHEP/g in females, whereas in old animals it was $50x10^6$ (CV = 0.27) in males and $58x10^6$ (CV = 0.18) BnHEP/g in females. As to the proportion of BnHEP (in relation to HEP) it varied from 24.8% (CV = 0.17) and 33.8% (CV = 0.14) in young males and females, respectively, to 27.2% (CV = 0.17) and 31.0% (CV = 0.12) in old males and females, respectively.

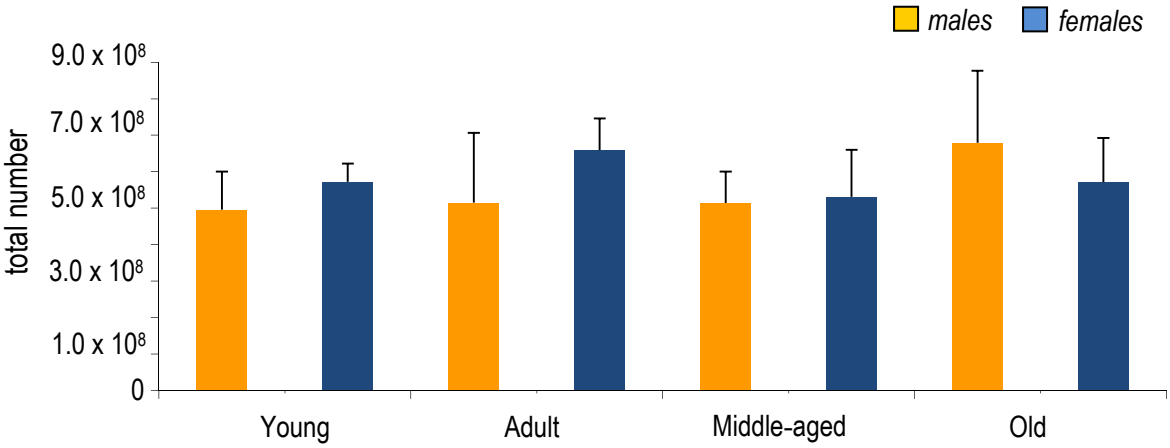

Figure 3.7 – Total number of binucleated hepatocytes, in male and female young (2 months), adult (6 months), middle-aged (12 months) and old (18 months) rats. Data expressed as mean + SD. There were no statistically significant differences.

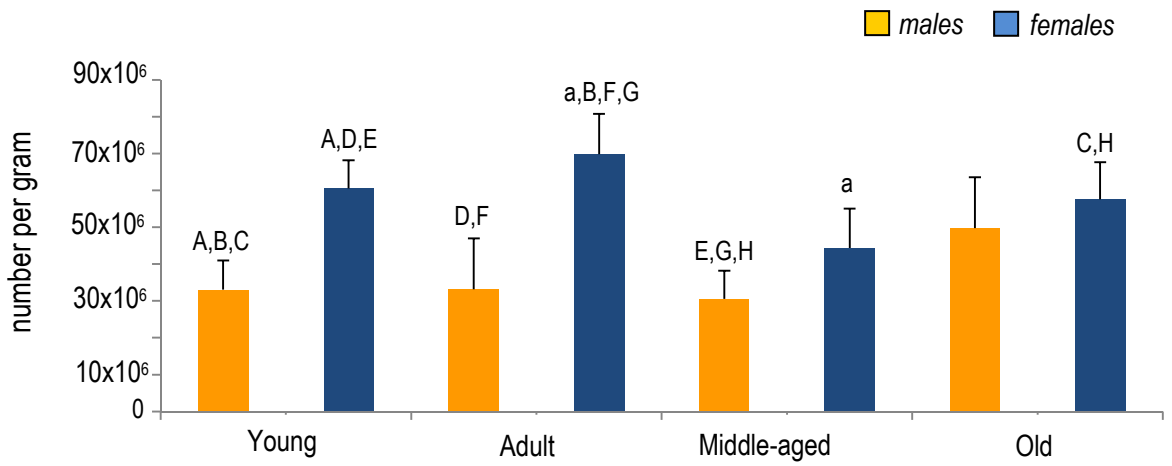

Figure 3.8 – Number per gram of binucleated hepatocytes in male and female young (2 months), adult (6 months), middle-aged (12 months) and old (18 months) rats. Paired letters indicate significant differences (lowercase: same gender; uppercase: across genders); data expressed as mean + SD.

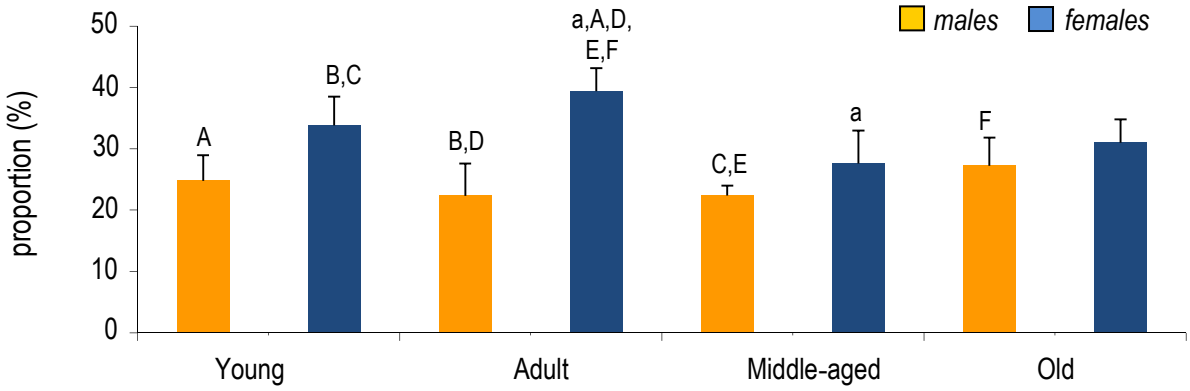

Figure 3.9 – Percentage of binucleated hepatocytes (in relation to all hepatocytes) in male and female young (2 months), adult (6 months), middle-aged (12 months) and old (18 months) rats. Paired letters indicate significant differences (lowercase: same gender; uppercase: across genders); data expressed as mean + SD.

3.2.2.2- Age and gender study: 4) Mean volume of HEP

An average of 107 HEP were analysed per animal (96 in males and 118 in females). The number-weighted mean cell volume ($\overline{v}_N$) of MnHEP (Figure 3.10) was moderately correlated with the N_V(HEP, liver) (r = 0.58, $p < 0.01$), whereas that of BnHEP was negatively correlated (moderately) with the N of BnHEP (r = -0.61, $p < 0.01$) and (strongly) with the percentage of BnHEP (r = -0.74, $p < 0.001$). As to gender differences, regarding the MnHEP, they were close to the level of significance ($p = 0.055$): indeed, only the cells from young rats differed ($p < 0.01$). As to BnHEP, no gender or ageing differences existed. Overall, the the $\overline{v}_N$ of BnHEP was 31 to 59% larger than that of MnHEP ($p < 0.001$).

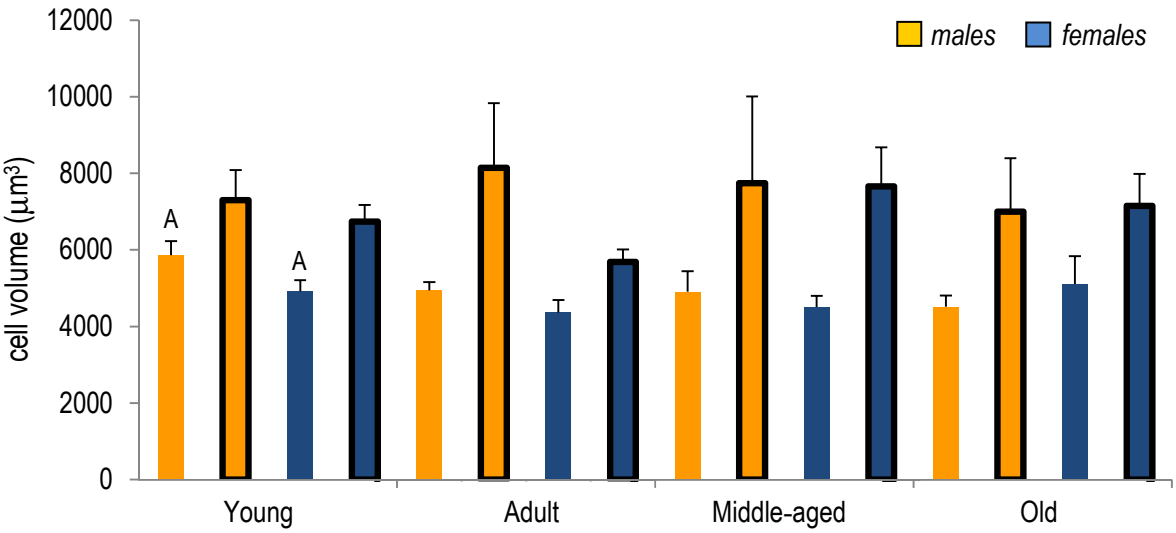

Figure 3.10 – Number-weighted mean cell volume ($\overline{v}_N$) of mononucleated hepatocytes (column without contour) and binucleated hepatocytes (outlined columns), in male and female young (2 months), adult (6 months), middle-aged (12 months) and old (18 months) rats. Paired letters indicate significant differences (uppercase: across genders). Data corrected for paraffin shrinkage and expressed as mean + SD.

As expected, the $\overline{v}_V$ (Table 3.4) was greater than the $\overline{v}_N$. In contrast with the latter parameter, the $\overline{v}_V$ presented significant ageing differences (p < 0.001), especially in males. In this parameter no significant gender differences could be proved (p = 0.067). The $\overline{v}_v$ of BnHEP did not vary significantly with ageing or gender.

Table 3.4 – Volume-weighted mean cell volume ($\overline{v}_v$) of mononucleated (MnHEP) and binucleated hepatocytes (BnHEP) in male and female young (2 months), adult (6 months), middle-aged (12 months) and old (18 months) rats. Paired letters indicate significant differences (uppercase: across genders; lowercase: same gender). Data expressed as mean ± SD.

$\overline{v}_v$ (µm³)		Young	Adult	Middle-aged	Old
Male	MnHEP	7130 ± 545 ^{A,B,a,b,c}	5549 ± 60 ^{a}	5387 ± 689 ^{b}	5357 ± 299 ^{c}
	BnHEP	8665 ± 983	9770 ± 2570	8587 ± 2310	8646 ±2258
Female	MnHEP	6040 ± 537	4899 ± 406 ^{A}	4968 ± 293 ^{B}	5912 ± 900
	BnHEP	8124 ± 156	7050 ± 538	8395 ± 767	9535 ± 1372

3.2.2.2- Age and gender study: 5) Stereological analysis of young and old HEP nuclei

An average of 104 nuclei of MnHEP and 82 nuclei of BnHEP were evaluated per animal. The $\overline{v}_N$ of nuclei increased with ageing, except for MnHEP of males (Table 3.5). The CV of nuclei was high in both MnHEP and BnHEP, varying from 0.3 to 0.4, being noteworthy

that it varied more within than between animals. The $\overline{v}_N$ of MnHEP and BnHEP nuclei were not significantly correlated with their respective cell volumes (p = 0.085 and 0.072, respectively). In BnHEP, the two nuclei presented volumes of the same order of magnitude, but the CV between nuclei varied up to 14%. The N:C of both MnHEP and BnHEP increased with ageing in males (Table 3.5).

Table 3.5 - Number-weighted mean nuclear volume ($\overline{v}_N$) and nucleo-cytoplasmic ratio (N:C), in mononucleated (MnHEP) and binucleated hepatocytes (BnHEP) of young (2 months) and old (18 months) male and female rats. Paired letters indicate significant differences (lowercase: same gender; uppercase: across genders); data expressed as mean) ± SD.

		Young		Old	
		$\overline{v}_N$ (μm³)	N:C (%)	$\overline{v}_N$ (μm³)	N:C (%)
Male	MnHEP	418 ± 19^{A}	$9.6 \pm 0.7^{B,d}$	399 ± 20	11.5 ± 0.4^{d}
	BnHEP	249 ± 40^{b}	$8.9 \pm 1.6^{C,e}$	312 ± 13^{b}	11.5 ± 0.9^{e}
Female	MnHEP	$384 \pm 14^{A,a}$	11.5 ± 0.9^{B}	449 ± 39^{a}	12.0 ± 0.7
	BnHEP	280 ± 20^{c}	12.0 ± 0.9^{C}	347 ± 42^{c}	13.2 ± 1.8

The histogram of the $\overline{v}_N$ of nuclei revealed small differences: young females exhibited a slightly skewed pattern (Pearson's skewness = 1.0; kurtosis = 3.38) comparing to males (Pearson's skewness = 0.34; kurtosis = 0.51) (Figure 3.11). In old animals, the distribution of nuclei was skewed to larger volumes. Considering the volume histograms, we estimated that the $\overline{v}_N$ of the diploid nuclei was 225 μm³ ± 36 μm³, whereas the tetraploid nuclei had a volume of 447 μm³ ± 52 μm³.

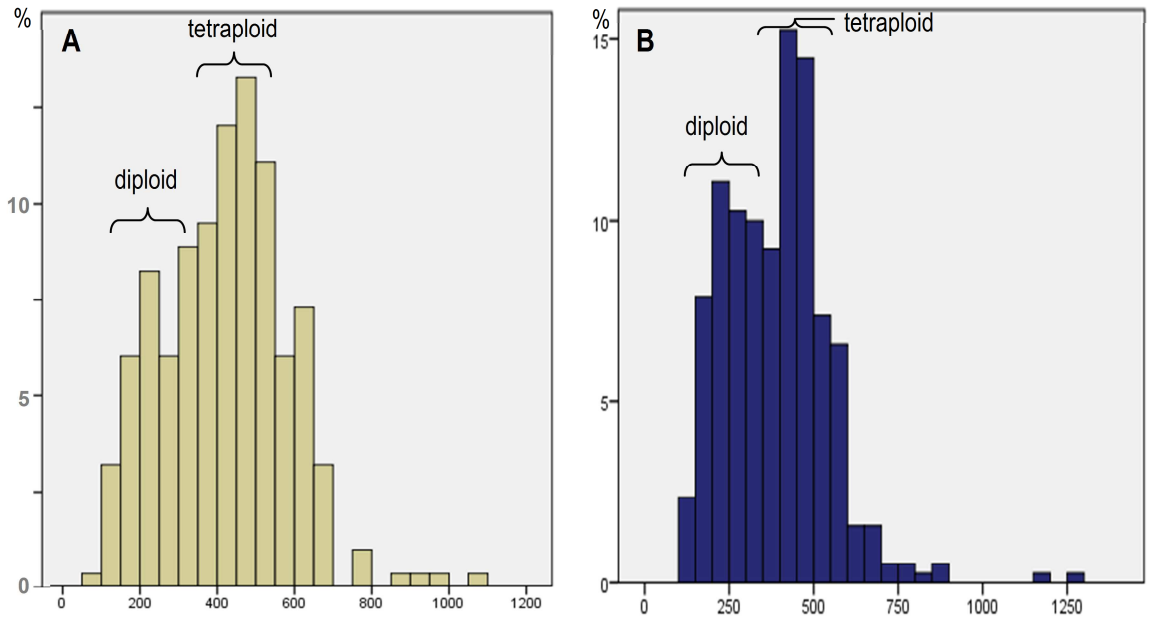

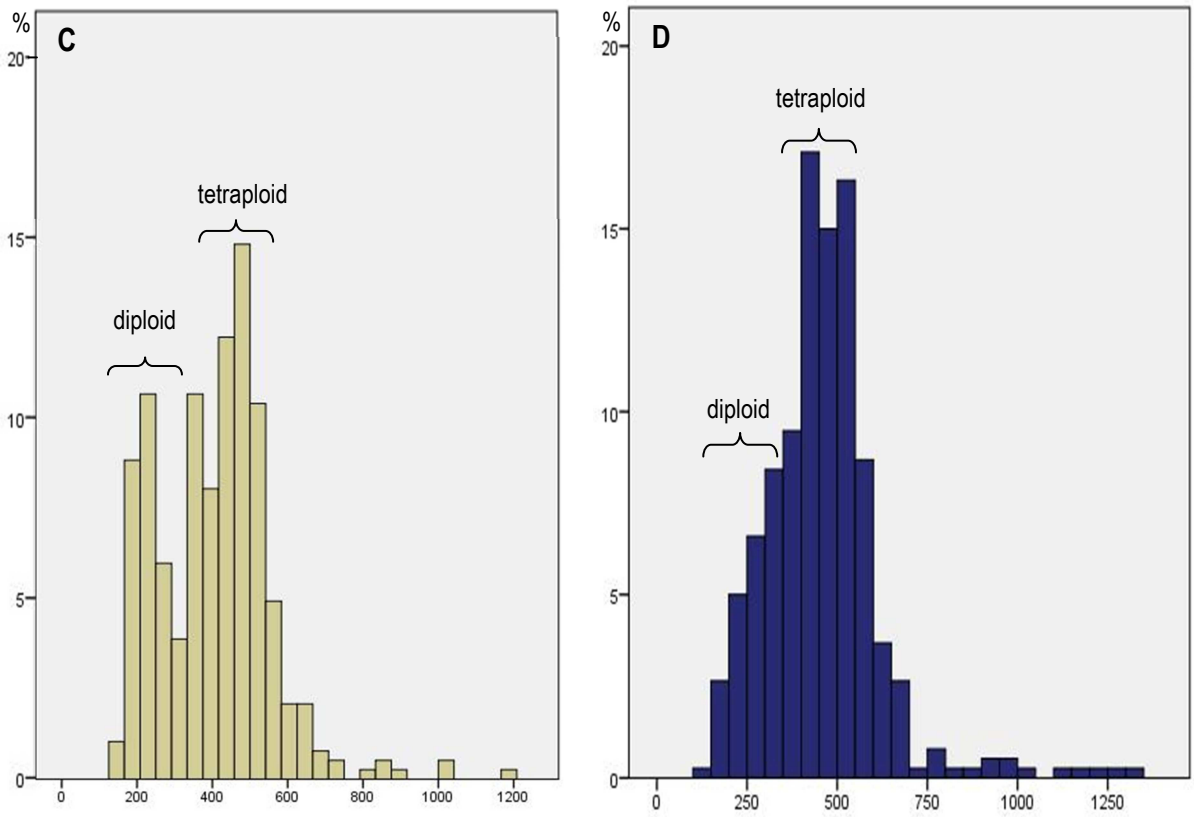

Figure 3.11 – Histogram of the mean nuclear volume of mononucleated hepatocytes in young (2 months) males (A) and females (B) and in old (18 months) males (C) and females (D) rats; the mean volume of diploid and tetraploid nuclei is indicated.

3.2.2.2- Age and gender study: 6) Ploidy analysis of young and old livers by flow cytometry

The mechanical dissociation of the liver rendered a mixture of particles, mostly formed by HEP nuclei (easily identified by their large size and presence of nucleoli) and well preserved HEP (both MnHEP and BnHEP), in variable proportions. In all the samples, we noted a contamination by NHC. Owing to the mechanical dispersion of the liver cells and to the washing procedure, with slow speed centrifugation, these were present in low numbers: in average, less than 5% of the nuclei (as verified by light microscopy, in the cytospin smears).

The flow cytometry analysis showed that the percentage of diploid particles (*i.e.*, naked nuclei with 2N mixed with cells with 2N) decreased in old animals (Table 3.6). These tended to be more abundant in females, but no significant differences were noted [even so, a significant difference existed (p = 0.02) when nearly diploid/pure diploid particles were compared between genders]. In old animals, tetraploid particles were more abundant and, only in that group, octaploid particles could be detected. Quite surprisingly, we detected abnormal DNA content (corresponding to S-phase and aneuploidy) in all groups, regardless of age and sex; most of these particles were tetraploid (or nearly). These particles tended to appear more in young males than in females (21% ± 9.5%

versus 11.4% ± 9.4% respectively), but such a difference was attenuated in older rats. In this vein, almost half of the rats studied could be classified as having HEP with aneuploidy (in 2.3% to 23.8% of particles); the DNA histograms of four rats are presented in Figure 3.12. The percentage of particles in the S-phase varied from 0.2% to 4.4% for diploid and 1% to 12% for tetraploid particles. No differences existed between males *versus* females and young *versus* old animals.

Table 3.6 - Percentage of diploid and tetraploid particles in male and female young (2 months) and old (18 months) rat livers. Note that the sum of diploid and tetraploid particles does not account for 100% (the remaining part corresponds to octaploid and aneuploid particles); data expressed as mean ± SD. No statistically significant differences existed.

	Young		Old	
	Diploid	Tetraploid	Diploid	Tetraploid
Males	79.0 ± 9.5	15.0 ± 5.1	72.7 ± 17.4	23.1 ± 14.7
Females	88.6 ± 9.4	7.1 ± 2.0	72.1 ± 9.0	25.1 ± 7.6

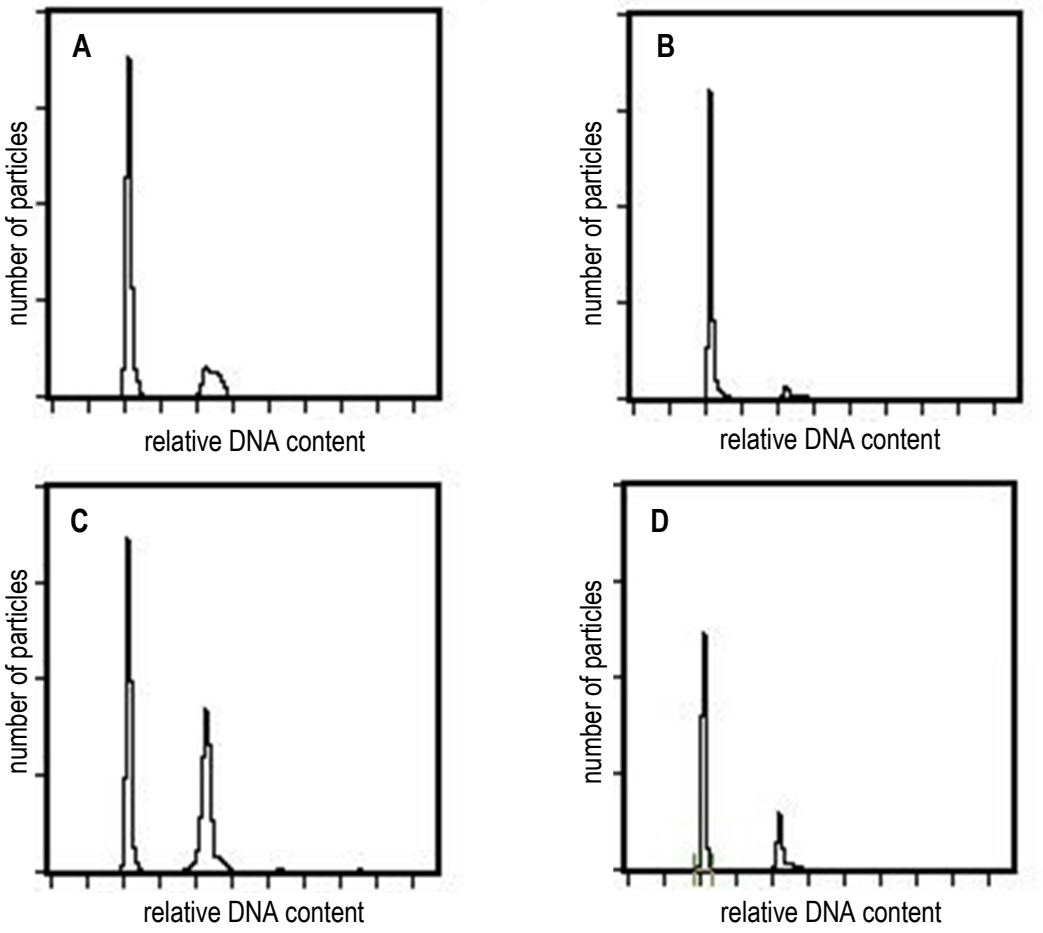

Figure 3.12 – DNA histogram of a young male (A), young female (B), old male (C) and old female (D) rat, evaluated by flow cytometry. Rat blood lymphocytes were used as internal controls. First and second peaks correspond to diploid and tetraploid particles, respectively.

3.2.2.2- Age and gender study: 7) Study of biomarkers throughout ageing and gender

The total amount of protein in the post-mitochondrial supernatant varied from 9.5 to 38.4 mg/ml. This content was relevant because, except for LPO products, all enzymatic activities were expressed as the amount of substrate hydrolysed per minute and per mg of protein. No significant differences for ageing or gender were noted for this parameter.

Overall, the GST activity varied with ageing ($p < 0.001$) and gender ($p < 0.001$) (Figure 3.13). It remained fairly constant in females, whereas it peaked in male adults.

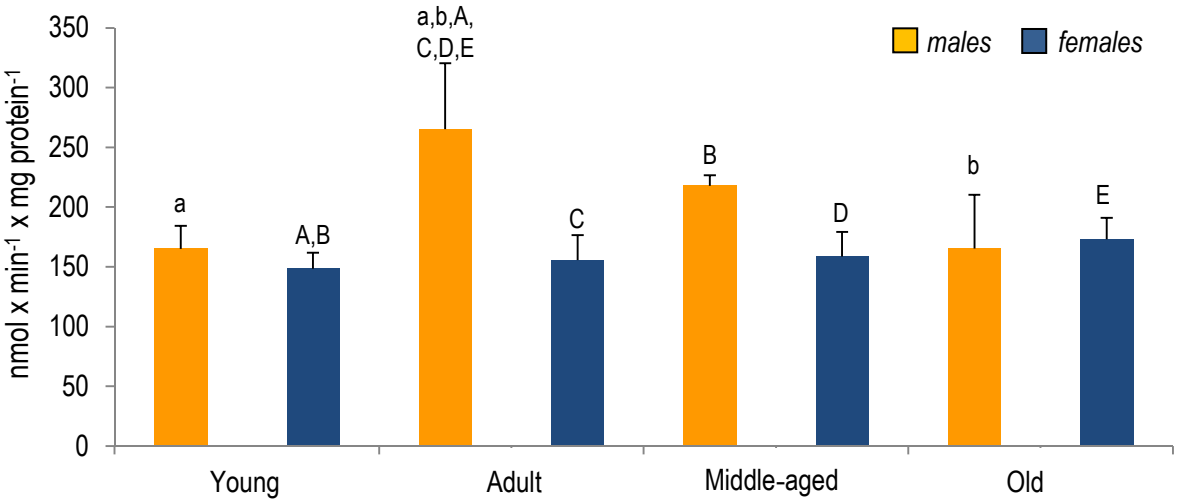

Figure 3.13 – Time course of glutathione S-transferase activity in the liver of male and female young (2 months), adult (6 months), middle-aged (12 months) and old (18 months) rats. Paired letters indicate significant differences (lowercase: same gender; uppercase: across genders). Enzyme activity expressed in nmol x min^{-1} x mg of total liver $protein^{-1}$ and presented as mean + SD.

The GR activity fluctuated over time, without significant differences (Figure 3.14). It also remained fairly constant with gender: in fact, the mean activity in males and females was similar [14 nmol x min^{-1} x mg of liver $protein^{-1}$ (CV ≈ 0.10)].

The GPX activity also did not vary significantly with ageing (Figure 3.15). Regarding gender effects, minor differences existed ($p < 0.05$). A significant negative correlation with CAT was noted, namely in young animals ($r = -0.71$; $p < 0.05$).

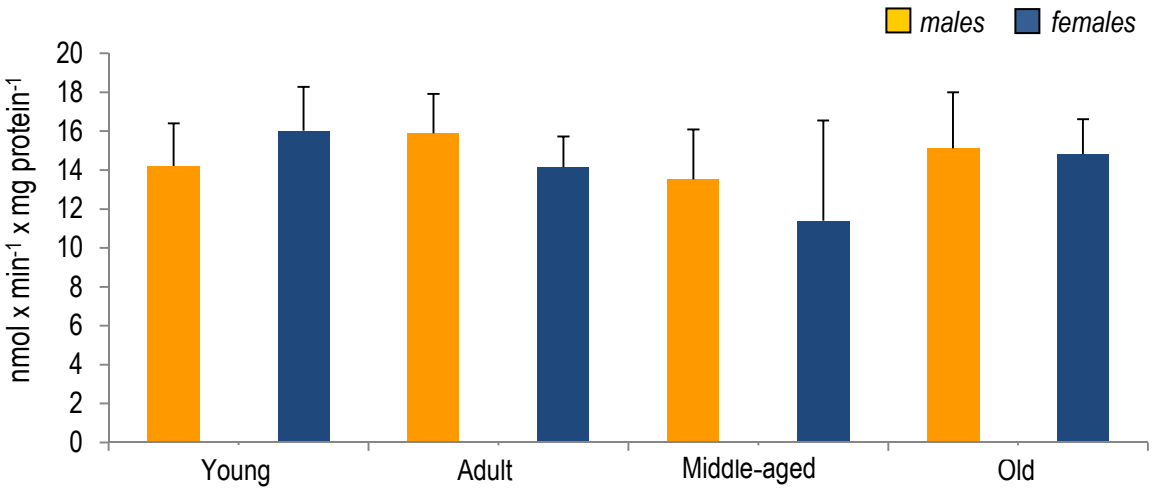

Figure 3.14 – Time course of glutathione disulfide reductase activity in the liver of male and female young (2 months), adult (6 months), middle-aged (12 months) and old (18 months) rats. Enzyme activity expressed in nmol x min^{-1} x mg of total liver $protein^{-1}$ and presented as mean + SD. There were no statistically significant differences.

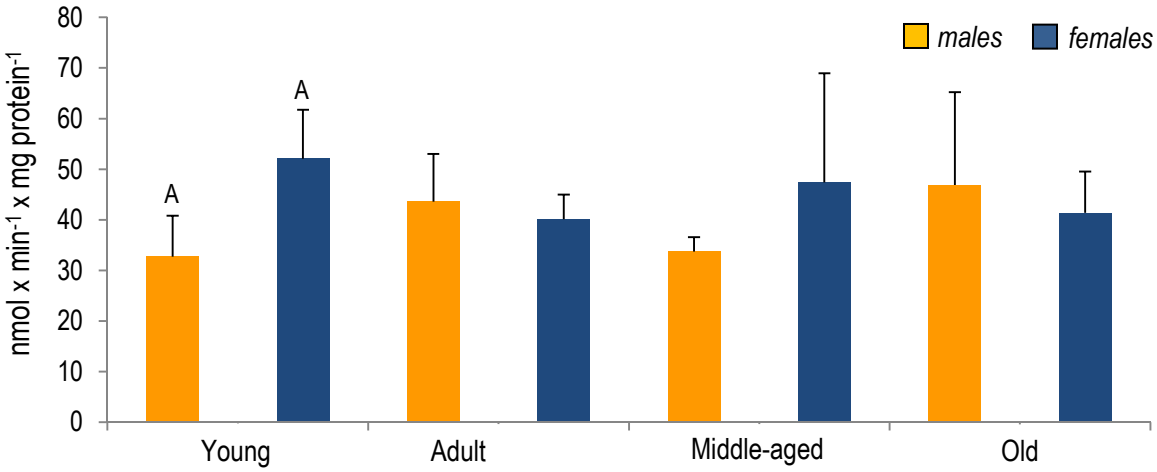

Figure 3.15 – Time course of glutathione peroxidase activity in the liver of male and female young (2 months), adult (6 months), middle-aged (12 months) and old (18 months) rats. Paired letters indicate significant differences (uppercase: across genders). Enzyme activity expressed in nmol x min^{-1} x mg of total liver $protein^{-1}$ and presented as mean + SD.

Globally, CAT varied significantly with ageing ($p < 0.05$) and gender ($p < 0.01$) (Figure 3.16). However, systematic significant differences among group pairs were not disclosed, neither regarding gender (just young animals differed) nor ageing (only one significant pair difference was found). Anyway, the statistical output for the analysis of the factor gender does support that, in general, this scavenger enzyme tended to be more active in males than females.

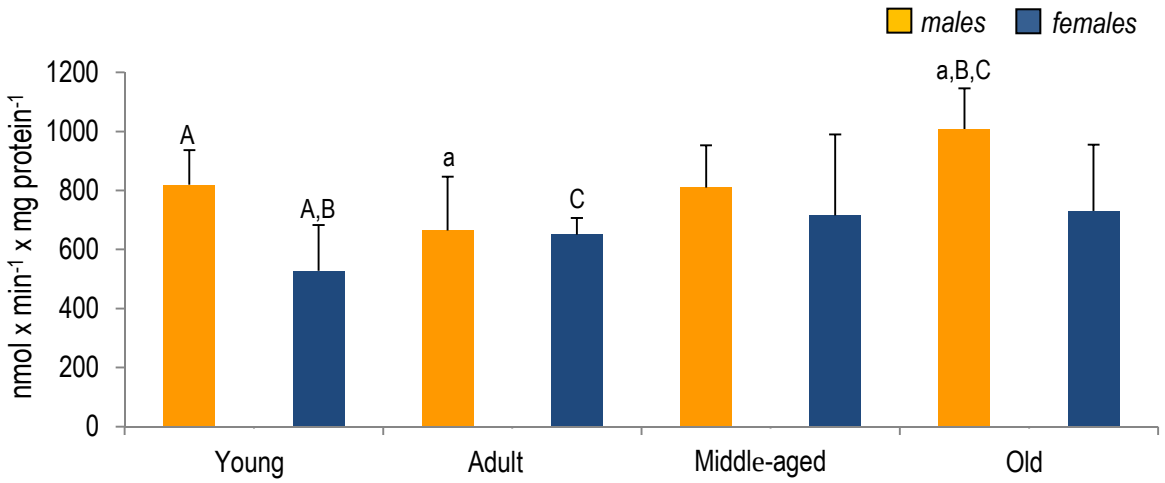

Figure 3.16 – Time course of catalase activity in the liver of male and female young (2 months), adult (6 months), middle-aged (12 months) and old (18 months) rats. Paired letters indicate significant differences (lowercase: same gender; uppercase: across genders). Enzyme activity expressed in mmol x min^{-1} x mg of total liver $protein^{-1}$ and presented as mean + SD.

The endogenous LPO was assessed by the TBARS levels (Figure 3.17); in general, these by-products increased in older ages ($p < 0.05$), and females tended to have more ($p < 0.001$). In adults, a significant strong and negative correlation existed with GST ($r = -0.76$; $p < 0.01$).

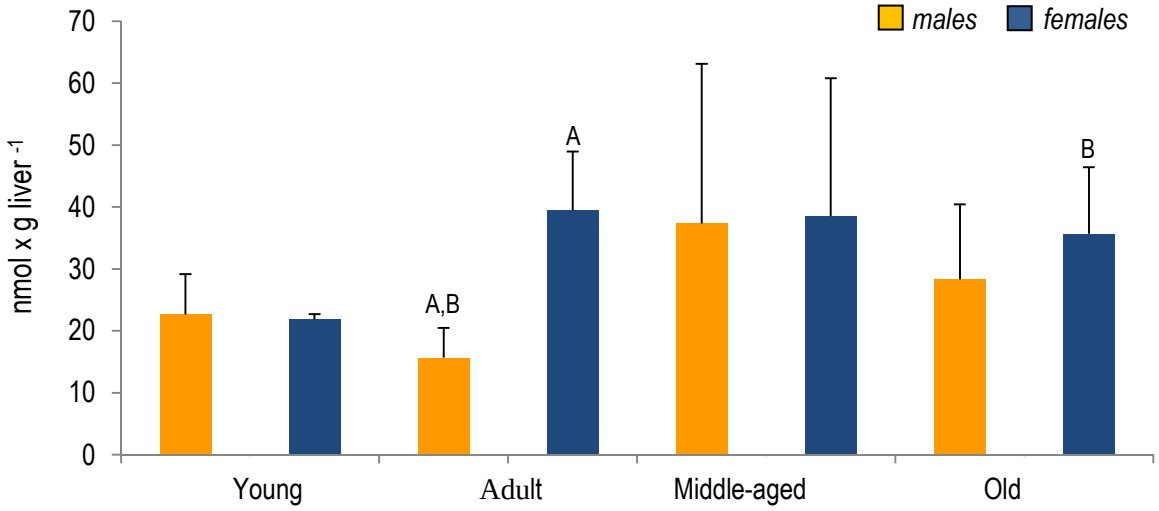

Figure 3.17 – Time course of lipid peroxidation products in the liver of male and female young (2 months), adult (6 months), middle-aged (12 months) and old (18 months) rats. Paired letters indicate significant differences (uppercase: across genders). Data are expressed in nmol of thiobarbituric acid reactive species x g liver $weight^{-1}$ and presented as mean + SD.

3.2.2.2- Age and gender study: 8) Number of all liver cells

The N of all liver cells had the following moderate significant correlations: 1) body weight (r = 0.50, $p < 0.01$); 2) liver weight (r = 0.65, $p < 0.001$); 3) N of HSC (r = 0.65, $p < 0.001$); 4) N of HEP (r = 0.68, $p < 0.001$); and 5) percentage of BnHEP (r = -0.50, $p < 0.01$). Regarding the N of all liver cells, significant differences existed for ageing ($p < 0.01$) and gender ($p < 0.001$). In males, adult and middle-aged animals had the highest mean values [$\approx 4.1 \times 10^9$ liver cells (CV = 0.17) in adults and (CV = 0.08) in middle-aged)] (Figure 3.18), whereas in females, the highest value existed in middle-aged animals [3.6×10^9 liver cells (CV = 0.06)]. It is opportune to mention once again that this parameter includes both HEP and sinusoidal cells, plus cells of portal tracts and those surrounding central venules.

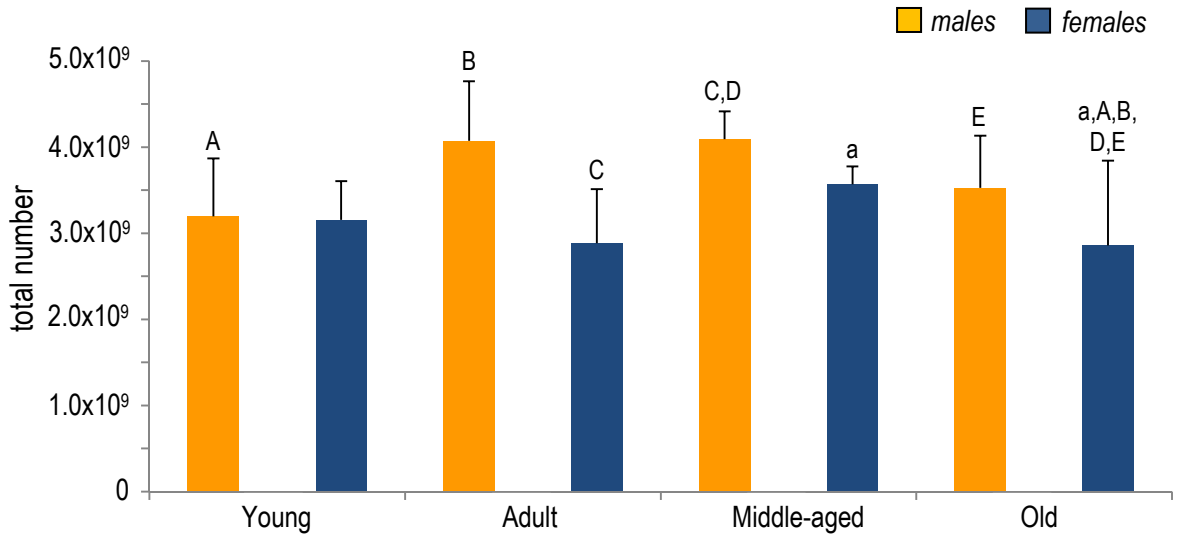

Figure 3.18 – Total number of cells existing in the liver in male and female young (2 months), adult (6 months), middle-aged (12 months) and old (18 months) rats. Paired letters indicate significant differences (lower case: same gender; uppercase: across genders); data expressed as mean + SD.

3.4- Discussion

3.4.1- Baseline study

3.4.1- Baseline study: 1) The tagging of BnHEP and the stereological methods

In this study we present an in depth estimation of HEP and NHC number in the rat liver, using design-based stereological tools. In mammals, HEP comprise populations of mononucleated and binucleated cells and because their accurate (and permanent) distinction (as single cell units) is not possible in routine sections, we combined stereology with immunohistochemistry for obtaining an accurate counting. Biliary glycoprotein I, a CEA subfamily member, is present in biliary canaliculi ─ therefore these structures can be identified using polyclonal antibodies against this glycoprotein (as we did in this part of the study). This has been described for long (Svenberg *et al*, 1979), but herein the immunomarking was performed in thick (30 μm) paraffin sections, required for the optical fractionator. In this technique, staining must be seen throughout the full section depth; this was attained via a long incubation time (4 days) with the antibodies, following an approach already used for HSC (as detailed in Chapter 2).

The optical fractionator here applied proved to be highly effective in practical terms. The distinction between MnHEP, BnHEP and NHC was unequivocal, cells were counted straightaway, and the estimations of N were unaffected by the shrinkage (Howard and Reed, 2005), as detailed in Chapter 1. Additionally, like we verified for HSC, HEP also present a homogeneous distribution in the liver, in the sense that these cells are virtually everywhere, meaning that the smooth variant of the optical fractionator could be easily applied. *A priori* this granted an increased efficiency at virtually no extra-cost (Gundersen, 2002).

3.4.1- Baseline study: 2) About the quantification of HEP

It has been stated that HEP occupy in average 80% - 87% of rat liver volume (Weibel *et al*, 1969; Greengard *et al*, 1972; Blouin *et al*, 1977; Ramadori and Ramadori, 2010), but the N of different liver cells has been rarely reported. A classical study by Weibel *et al* (1969) estimated that HEP comprise 65% of all liver cells in the rat — a figure similar to our estimation in the baseline study — and reported 568×10^6 "hepatocytes" and 309×10^6 NHC per 100 g of body weight. In a first analysis, these values are 1% and 20% lower than ours, respectively. Differences likely reside in the younger age of the animals used by Weibel *et al* (1969), and in the so-called "model-based" techniques then applied. One additional assumption was that, as the authors counted cell nuclei, they openly conceived all HEP as "theoretically mononucleated". Truly, this makes our data quite different, because if we had followed that assumption (thus disregarding BnHEP), we would have

estimated that HEP comprise 75% (and not 60%) of all liver cells, corresponding to 723×10^6 HEP nuclei/100 g of body weight (and not to 574×10^6 HEP/100 g).

Like us, Carthew *et al* (1996; 1998a) took into consideration BnHEP (≈ 20%), and estimated an average N of HEP ranging from 1.52×10^9 to 4.77×10^9 in 3 months Fischer rats. The differences to the N we estimated could be attributed to the distinct rat strain, the technical approach and the sampling scheme. As to the rat strain, Fischer rats tend to have smaller and lighter livers than the Wistar rats here used — thus, they should have a lower N of HEP. As to the technical approach, in the older report, Carthew *et al* (1996) employed "model-based" methodologies that involved simple 2D countings and additional corrections for lost caps, size and shape distributions. This inherently causes a systematic and uncontrolled bias, which only emerges when estimations by the former "model-based" and modern "design-based" techniques are compared (West, 1993; Von Bartheld, 2002). In the more recent report, Carthew *et al* (1998a) applied the physical disector, composed of a pair of low magnification (330x) images. From our experience, and without the recently available solutions (*e.g.*, AutoDisector™ from newCast, Visiopharm), this renders some problems, because the section pairs are difficult to perfectly align in x-y axis, resulting in a tedious and lengthily counting procedure, prone to induce error in a large series, as a high number of particles have to be identified and counted per disector. Finally, respecting the sampling, Carthew *et al* (1998a) examined merely 18 low magnification fields per animal; such small sampling effort can lead to (erratic) estimations of N of HEP with a high CE, and clearly contrasts with the 1340 high magnification fields we analysed in the baseline procedure.

In our study, the N_V of HEP, BnHEP and NHC were directly derived from counts with the optical disector probe. As such, it must be noticed that owing to the shrinkage inherent to paraffin embedding, the reported values are overestimations, serving only for comparative purposes. Some estimations of the N_V can be found in literature, namely those by Carthew *et al* (1996) who reported a much higher N_V (225×10^3 HEP/mm^3) for paraffin sections, but using "model-based" methods. The shrinkage problem can be overcome by using epoxy sections, and this was performed by Loud (1968), Weibel *et al* (1969) and Greengard *et al* (1972), who reported a N_V slightly lower than our estimation (186×10^3, 169×10^3 and 120×10^3 hepatocyte nuclei per mm^3, respectively). Nevertheless, those authors applied the "model-based" techniques available at that time, with the additional premise of all HEP being "mononucleated" (Loud, 1968; Weibel *et al*, 1969). Considering our shrinkage value, the corrected N_V is 118×10^3 HEP/mm^3 (with 31×10^3 BnHEP/mm^3). It is noteworthy that we found no statistic correlation between the N_V, corrected or not for the shrinkage, and the N of HEP (either in the baseline study or in the age and gender

one), meaning that the N_V has to be used cautiously regarding its inferences, as it really tell us nothing about the true N of HEP.

3.4.1- Baseline study: 3) The quantification of BnHEP

In mammals, binuclear cells are frequently encountered in the adrenal gland (cortex and medulla), urinary bladder, endometrium, salivary glands and in the liver, but their functional significance is still unknown (Grizzi and Chiriva-Internati, 2007). In the latter, the percentage of BnHEP is reported to be characteristic of a given species (Wheatley, 1972). It does not change due to dietary or endocrine status of the animal, but is drastically altered during normal rat growth, partial hepatectomy, or after the administration of certain mitogenic and/or hepatocarcinogenic compounds (Fujii *et al*, 2004). Classical studies have established that the liver of suckling rats is almost exclusively made up of diploid MnHEP, and that the appearance of BnHEP is affected by the time of weaning (Wheatley, 1972). Recently, this issue has been revisited: in Wistar rats weaned at 17 days, BnHEP appeared after 5 days and their proportion rose rapidly between the 25^{th} and 30^{th} day of life (Guidotti *et al*, 2003; Celton-Morizur and Desdouets, 2010). Indeed, the transition to solid food and the increased levels of circulating insulin seem to be determinant for the appearance of BnHEP (Celton-Morizur and Desdouets, 2010). The downstream of the insulin signal has been determined to be the PI3K-Akt pathway that results in failure of cytokinesis, and thus generates BnHEP (Celton-Morizur and Desdouets, 2010).

The BnHEP have been implicated in regenerative responses, which can only be accurately evaluated after defining the percentage of those cells in the normal liver. In different reports (St Aubin and Bucher, 1952; Wheatley, 1972; Belyaeva and Ivleva, 1979; Styles *et al*, 1987; 1991; Jack *et al*, 1990; Styles, 1990; Madra *et al*, 1995; Carthew *et al*, 1996, 1998a, b; Molodykh *et al*, 2000; Auvigne *et al*, 2002; Gandillet *et al*, 2003; Guidotti *et al*, 2003; Fujii *et al*, 2004; Fausto and Campbell, 2009) the average percentage varied from 20% (Styles *et al*, 1991) to 58% (St Aubin and Bucher, 1952). This wide range can be hypothetically and partially justified, on the one hand, by reported differences between strains (Wheatley, 1972), and on the other hand, by the used methodologies. Most of the referred studies estimated the percentage of BnHEP using isolation techniques (or mechanical separation of liver cells) followed by morphometry or a direct cell counting in 2D (thin) sections. Different results between the two methodologies have been classically reported (St Aubin and Bucher, 1952; Wheatley, 1972), and both may present significant drawbacks. Respecting the studies based in isolation, it should be stressed that: 1) with current procedures the highest yields, around 50.5×10^6 HEP/g liver (Puviani *et al*, 1998), represent only 39% of the N/g estimated in the baseline study (this percentage would be even lower for female rats); 2) there is no guarantee, *a priori*, that MnHEP and BnHEP are

being isolated in proportion to their real number *in situ* (Burns *et al*, 1996) or that they have the same degree of fragility — some cells may be destroyed, especially when mechanical dissociation or proteolytic enzymes are used (St Aubin and Bucher, 1952). Concerning the simple 2D counting studies, these are also mined by the fact that, as BnHEP are larger, they have a greater probability of being sectioned, thus introducing an undetermined amount of bias in the estimations of their number in relation to all the HEP (Jack *et al*, 1990). If ordinary histological sections are used (ranging from 5 to 8 μm), many BnHEP are cut so that only one nucleus falls within the section, and the cell may erroneously be considered as MnHEP (as illustrated further ahead, in Figure 3.20). This error has been reported to vary according to several factors (section thickness, nuclei diameter, distance between them and the angle formed between the nuclei and the plane of section) (St Aubin and Bucher, 1952). Complex mathematical *formulae* were once proposed to correct for these errors. A classical one was developed by Pfuhl (1930), who studied the oviduct of one earthworm (where all cells are binucleated) and the liver of rabbits, thus establishing a correction factor of three for counts in 5 to 6 μm sections (for thicker sections that factor would be lower) (Pfuhl, 1930).

To overcome these corrections, stereological methods or (tedious) 3D reconstructions can be used. Using "design-based" techniques, Jack *et al* (1990) estimated a proportion of BnHEP of 30% in the Tif:RAIf strain. These authors tracked and differentiated HEP without any special stain for highlighting the membranes, in series of semithin sections (that constituted physical disectors). From our experience with the rat liver (unpublished observations), dubious distinctions of the cell boundaries can emerge with that approach, even when epoxy semithin sections are observed. Besides, for differentiating/counting numerous particles in sections, like HEP, the physical disector becomes much more laborious and time consuming than the optical variant used here (Marcos *et al*, 2012).

3.4.1- Baseline study: 4) The sampling procedure

All the sampling was planned here to obtain a precise estimation of N with a CE lower than 10% (Schmitz and Hof, 2000). For estimating the CE(N), we used a formula proposed for particles with a fairly homogeneous distribution (like it was the case of HEP and NHC in the liver) and when more than 10 sections are sampled (Gundersen, 2002, Marcos *et al*, 2004). For all the estimations, the CE(N) was lower than the pretended threshold, contributing to much less than 50% to the total variance (*i.e.*, the so-called biological variance was far greater than the variance due to the sampling procedure). Considering this, we can regard our baseline sampling as quite precise and adequate for a general study, in which different types of cells are being estimated. Although for the whole liver we counted an exceeding number of cells, for BnHEP the number of cells

counted was close to what has been recommended for estimating the number of neurons with a CE similar to the ones here obtained (Schmitz and Hof, 2000). Actually, the optimum sampling effort (*i.e.*, the minimal workload to provide a sufficiently good precision estimate) can vary with the final target. If only the N of HEP or NHC are to be estimated, we recommend a sixth reduction of our sampling effort, whereas for a simple estimation of the N of BnHEP, we suggest a quarter decrease of our standard sampling. For the estimation of subpopulations of HEP or NHC, namely in the evaluation of lobular heterogeneity, the sampling can be less reduced, probably between a quarter to a half. Taking that no statistical differences were observed between the approaches of sampling reduction (*i.e.*, decreasing the number of sections or reducing the sampled fields), we would advise the former, as the costly reagents and the time consuming steps of the immunohistochemistry would be much saved.

In conclusion, the use of immunostaining in combination with the optical fractionator, allowed an accurate and precise estimate of the N of HEP, BnHEP and NHC in the rat liver. Facing the technical procedures used, the estimates were not biased by shape, orientation, shrinkage, projection effects or by any dubious identification of cell boundaries. This study provides reference morphological data in healthy conditions, along with practical guidelines for the most efficient sampling and counting procedures for assessing the N of HEP, namely for evaluating hyperplasic *versus* hypertrophic growth of the liver in ageing or in rat models of liver regeneration and hepatocarcinogenesis.

3.4.2- Age and gender study

3.4.2- Age and gender study: 1) About ageing and liver

As previously mentioned, conflictive data has been reported regarding the effects of ageing in the liver of humans and rodents. In our opinion, a handful of reasons may explain the discrepancy. Firstly, most stereological analyses of the ultrastructure of HEP employed young rats (usually with three months or less) and very old, senescent rats (Figure 3.19) — by analysing only these two time points, relevant variations in between may be missed (Kitani, 1992). Secondly, different strains have been employed, including Wistar (Pieri *et al*, 1975), Fischer (Schmucker *et al*, 1978) and WAG/Rij rats (Meihuizen and Blansjaar, 1980), being unknown if strain differences exist. Thirdly, male and female rats have been used interchangeably, being also unknown if gender dimorphism is present in the liver. As previously mentioned, the interpretation of data using a single gender of a particular strain needs to be carefully limited, in order to avoid overgeneralisation (Kitani, 1992). Fourthly, technical reasons may underlie some discrepant results: for instance, different methods of fixation, like perfusion (*e.g.*, Schmucker *et al*, 1978) and immersion (*e.g.*, Pieri *et al*, 1975), as well as various

embedding media have been used (*e.g.*, Pieri *et al*, 1975; Blouin *et al*, 1977). Finally, an explanation for divergent results, regarding volumetric changes of HEP, may also reside in the heterogeneity of these cells, since it is well known that centrilobular HEP are larger than periportal cells (Roskams *et al*, 2007). Some authors addressed this by restricting the analysis to centrilobular areas (Papp *et al*, 2009), whereas others sampled an equal number of cells in these two locations (Schmucker *et al*, 1978). In our case, by using SUR sampling design and the disector we gave no preference for any location (the probability of sampling cells was proportional to their number) and since we sampled at least 100 cells for each animal, we can consider our estimations as representative of the rat liver.

Another issue that may have jeopardised ageing studies was that many stereological works (*e.g.*, Loud, 1968; Weibel *et al,* 1969, Pieri *et al*, 1975; Schmucker *et al*, 1978) assumed that BnHEP were approximately twice the size of MnHEP (thus validating the concept of HEP as "theoretically mononucleated" cells). Curiously, this assumption still prevails in both recent textbooks and specialised reviews (Roskams *et al*, 2007; Celton-Morizur and Desdouets, 2010). Truly, this was based in classical studies which mechanically dissociated HEP of mice, rats and humans and showed a two-fold increase in volume for a similar increase in ploidy (Epstein, 1967). However, it should be noted that isolated HEP tend to enlarge, not only because they do not have compressive forces of adjacent cells but also because they appear flattened by the coverslip pressure (St Aubin and Bucher, 1952). Our data strongly contradicts such proportionality: not only because the volume histogram of MnHEP and BnHEP have overlapping areas [some BnHEP (2x2N) cells have exactly the same volume as a MnHEP 2N], but also the $\overline{v}_N$ of BnHEP is significantly different from that of MnHEP, but only 30% to 60% larger. These features are in accordance with Jack *et al* (1990), who also reported a difference of $\approx$ 46% between those cell types, and with Gandillet *et al* (2003). By mechanically separating HEP using different size meshes, the latter authors elegantly showed that cell size is not correlated with binuclearity or ploidy. They observed that BnHEP were more abundant in larger cell fractions, but that the smaller ones (that passed through a 10 μm mesh) still contained a mixture of BnHEP and MnHEP.

3.4.2- Age and gender study: 2) The lobular size

The estimated porto-central distance is in accordance with previous reports for rats (Wagenaar *et al*, 1994; Warren *et al*, 2008), being larger than mice, which is 211 $\pm$ 57 μm (Ruijter *et al*, 2004), and smaller than that reported for humans, around 350 to 420 μm (Takahashi, 1970; Wagenaar *et al*, 1994; Roskams *et al*, 2007). This distance includes 15-18 HEP, which is also in line with the 16 HEP estimated by Wagenaar *et al* (1994), or

13-15 HEP estimated by Ruijter *et al* (2004), being much smaller than 24 HEP proposed by Schmucker and Jones (1975). We measured the porto-central distance superficially and in deeper locations because it is still debated whether traditional histological sections may provide reliable information regarding the size of lobules (Teutsch *et al*, 1999; Papp *et al*, 2009). According to Teutsch *et al* (1999), the liver is composed of primary hepatic units (which correspond to the classical liver lobules) arranged in cone-shaped secondary units. The size of primary units is relatively constant (until 1.1 mm below the surface), being more variable deeper inside the liver (Teutsch *et al*, 1999) — a feature that we also observed. However, we detected no differences in the average porto-central distance in these two locations, in accordance with Ruijter *et al* (2004).

We found no ageing differences in the porto-central axis, a fact that contrasts with Warren *et al* (2008) and Vollmar *et al* (2002). These authors reported a 10% and 50% increase in the size of lobules of Fischer and Sprague-Dawley rats, respectively. According to Warren *et al* (2008), the lobular size increases in parallel to the growth of the organ — which is twofold for those strains. However, in our case, we found no differences in this distance even in age groups that had the heaviest livers (*i.e.,* middle-aged male rats). According to our data, the lobules did not increase their diameter throughout ageing and we find it hard to interpret a 50% growth of the venulo-venular distance, as reported by Vollmar *et al* (2002), since no significant differences exist in the N of HEP and cells did not increase their size (see below). On the one hand, such opposite conclusions may be justified by the sampling scheme [only the left lobe and 10 lobules were considered by Vollmar *et al* (2002)], but, on the other hand, those authors measured venulo-venular distances (*i.e.*, between central venules) using intra-vital fluorescence microscopy. Those authors injected contrast by the jugular vein and it is possible that not all central venules became visible beneath the capsule. More recently, Papp *et al* (2009) stressed that only filling the liver by retrograde flow (*i.e.*, through the hepatic vein) allowed a precise determination of the size of surface lobules.

Studies in the pig's liver have shown that the average diameter increases during normal growth of the liver until puberty is reached (Wagenaar *et al*, 1994; Ekataksin and Kaneda, 1999), but afterwards the diameter is relatively constant (it actually tends to be reduced by 10% in 2 years old pigs). It has been proposed that new lobules may arise by branching of the hepatic venules (Roskams *et al*, 2007), but this is a controversial topic: indeed, it is still debated whether the liver grows by generation of new lobules or by hypertrophy of the existing ones (Fausto and Campbell, 2009; Kandilis *et al*, 2010). After partial hepatectomy it is generally accepted that new lobules are formed, but in the ageing process it is thought that only enlargement of previously existing ones takes place. Considering that the N/g of

HEP increases ≈ 35% between young and old males and the porto-central axis is constant, two hypotheses exist: lobules either grow in height and/or new lobules are formed throughout ageing. Papp *et al* reported a 35% increase in the N of superficial lobules in the rat liver (right lateral lobe), whereas Wagenaar *et al* (1994) observed that such number was fairly maintained in pigs. In our case, it is possible that secondary lobules increased their height bearing an increased number of primary (classical) lobules at their base (*i.e.*, at the liver surface). However, since the relative volume of collagen associated with portal tracts and central venules was maintained throughout ageing, an increase in height (*i.e.*, taller lobules) would be probably more important than an increase in the N of lobules. (If the number of lobules would increase by ≈ 35%, we would expect an increase in interlobular collagen, due to the ramification of portal tracts and central venules.)

3.4.2- Age and gender study: 3) Total number and number per gram of HEP

Regarding the N of HEP throughout ageing, it has been rarely reported and, to the best of our knowledge, it has never been studied in detail with stereological methods. In many organs, like the brain and liver, an early growth phase is characterised by cell proliferation (hyperplasia), whereas the late growth is dominated by cell enlargement (hypertrophy) (Atchley *et al*, 2000). In this later period (*i.e.*, after puberty), the N of HEP is believed to decrease (Malarkey *et al*, 2005). However, we observed the opposite, since the N/g of young *versus* old was increased, in males, or identical, in females. Since HEP have a long lifespan, and small mitotic activity (Roskams *et al*, 2007), it seems logical that their N would not tend to change or to just slightly increase throughout ageing.

The cellular N/g is an important parameter, because it allows a straightforward comparison between studies. Moreover, this parameter is used as a scaling factor, when *in vivo* hepatic clearance needs to be predicted, namely in toxicological studies and in the process of drug discovery and development (Barter *et al*, 2007). “How to scale up results from studies in mice, rats and other animal models to human beings?” is an ever repeating question in medical and pharmaceutical research. The *in vitro versus in vivo* extrapolation is usually based in three parameters: 1) milligram of microsomal protein per gram of liver; 2) milligram of homogenate protein per gram of liver; 3) number of HEP per gram liver (the so-called hepatocellularity, herein referred as the N/g of HEP). Although the pharmaceutical industry devotes enormous resources to address this extrapolation, the hepatocellularity figure, which is still used nowadays for humans (*i.e.*, $120x10^6$ cells per gram), was originally derived directly from rat studies and it was taken for granted that no differences existed between species (Sohlenius-Sternbeck, 2006; Barter *et al*, 2007). However, data for the rat has been reported to range from $85x10^6$ HEP (Carlile *et al*,

1997) to almost the double, $163x10^6$ (Smith *et al*, 2008). Apart from (theoretical) differences between strains [Carlile *et al* (1997) and Smith *et al* (2008) used Sprague-Dawley and Wistar rats, respectively], this wide range also reflects differences in the methodology and the high inter-individual variability reported to exist in this parameter (Barter *et al*, 2007) — a feature that we also observed in our study (the CV for the N/g was invariably larger than that of other number or volume estimations). Regarding the methodology, the N/g can be determined by microscopy methods (image analysis and stereology) or by biochemical techniques, by comparing the protein, DNA content and CYP activity in homogenates with that of HEP suspensions with known cellularity (Sohlenius-Sternbeck, 2006). In contrast with the more time-consuming microscopy methods, biochemical assays allow a much faster analysis of a large number of samples, despite having some major drawbacks: 1) it is usually assumed that BnHEP have the same amount of protein as MnHEP (Marcos *et al*, 2007), which is probably not true, as these cells are 30 to 60% larger, according to our data, and it has been reported that BnHEP secrete more proteins (*e.g.*, retinol-binding protein) than MnHEP (Grizzi and Chiriva-Internati, 2007); 2) measuring the DNA does not account for polyploid cells (either MnHEP or BnHEP), which are frequent in the liver and tend to increase with ageing (Roskams *et al*, 2007); 3) the specific concentration of CYP is difficult to measure in liver homogenates (Carlile *et al*, 1997; Sohlenius-Sternbeck, 2006). Taken all together, this may justify that, for the same sample, a twofold variation was reported between the DNA based (under)estimations and the CYP content (over)estimations (Carlile *et al*, 1997). It is opportune to mention that a recent consensus guideline settled a N/g of man lower than for the rat, and established that a healthy human male of thirty years old has an higher N/g than a sixty years old person (Barter *et al*, 2007). Likewise, we also found differences between young and old animals, but in an opposite direction (thus emphasising the existence of species differences).

3.4.2- Age and gender study: 4) BnHEP throughout ageing

There has been a controversy on the increase of BnHEP with ageing (Wheatley, 1972, Schmucker, 1998). It is generally accepted that polyploidy increases in the aged liver, and some authors reported that the binuclearity also increases (Popper, 1985; Schmucker, 1998; Malarkey *et al*, 2005). Even so, in our set of animals, we did not found significant differences in the N of BnHEP or in the percentage of these cells. This is in agreement with previous reports, based on different methodologies in mouse and rat (Epstein, 1967; Wheatley, 1972; Faggioli *et al*, 2011). We found a negative correlation between the percentage of BnHEP and the body and liver weights, which had already been reported in the rat (Vinogradov *et al*, 2001), with very similar figures ($r \approx -0.57$). Besides the rat, fifty

other mammalian species were evaluated and it was concluded that a negative correlation between binuclearity, nuclear ploidy and body weight (as well as growth rate) was a generalised feature of mammals (Vinogradov *et al*, 2001).

Interestingly, we obtained negative correlations between the percentage of BnHEP and the N of HEP, HSC and KC. It may be a simple result of the inverse correlation with the liver and body weight (all the other variables follow the body and liver weight in parallel), but it is tempting to hypothesise that this may have some functional relevance. As previously mentioned, the percentage of BnHEP decreases whilst the N of HEP increases during normal rat growth and partial hepatectomy and this is known for more than sixty years (St Aubin and Bucher, 1952). Additionally, it has been shown that such a decrease also takes place in pre-neoplastic nodules in the rat and in human hepatocellular carcinoma (Fujii *et al*, 2004, Grizzi and Chiriva-Internati, 2007). This negative correlation may well traduce the generation of MnHEP by BnHEP, but this is one of many possibilities, since the progeny of BnHEP is still a matter of strong debate. For some researchers BnHEP only generate two daughter polyploid MnHEP (Guidotti *et al*, 2003), whereas for others, BnHEP can generate MnHEP with half of the chromosome content (Duncan *et al*, 2010), or even another BnHEP with increased ploidy level (Celton-Morizur and Desdouets, 2010).

3.4.2- Age and gender study: 5) Volume of HEP throughout ageing

As previously mentioned, no general agreement exists regarding volume changes of HEP throughout ageing: some reported increases up to 70% (Pieri *et al*, 1975; Meihuizen and Blansjaar, 1980; De Priester *et al*, 1984; David, 1985), whilst others reported that differences were attenuated in old ages and cell volume in young animals was equal to that of old ones (Scmucker *et al*, 1978) (Figure 3.19). Our data only partially agrees with this, since we did not observe significant differences throughout ageing. At the end-point of our study, and irrespective the non-significant differences, males tended to have (30%) more HEP, which were smaller, while females tended to have (just 7%) more HEP that were slightly larger. It is very possible that our low number of animals per group did not give us the statistical power to prove more significant differences, namely those relative to trends. Anyway, these could contribute to the marginal increase of the V_V(HEP, parenchyma) in the old age group, a feature already reported by Martin *et al* (1992) in female Sprague-Dawley rats. Despite some controversy (Vollmar *et al*, 2002), it is believed that liver growth involves an increase in HEP (mainly through hyperplasia according to our data) that is counter-balanced in part by a reduction in the diameter in sinusoids (Roskams *et al*, 2007).

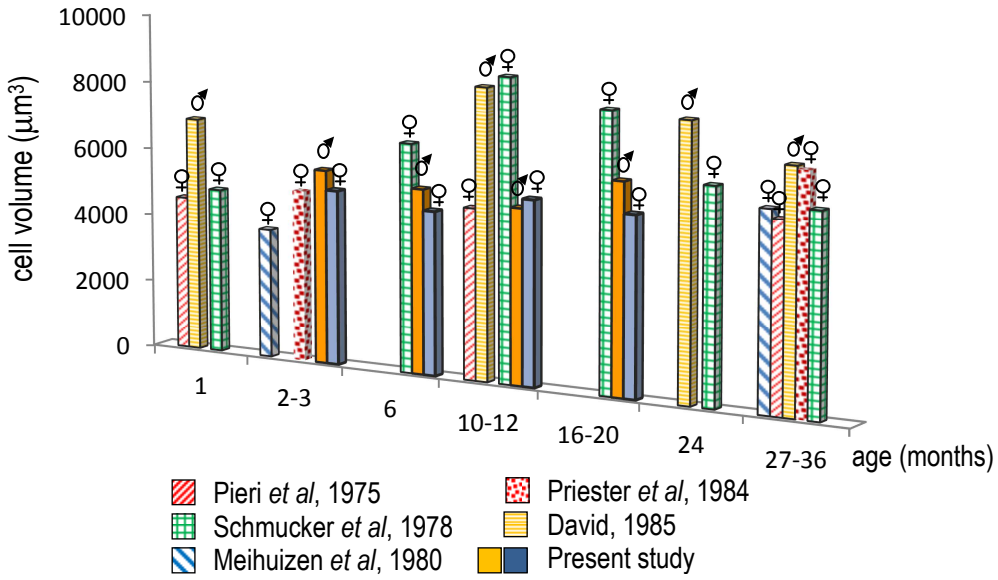

Figure 3.19 – Estimations of the mean cell volume (in μm^3) of mononucleated hepatocytes throughout ageing. The gender of the animals used in each study is indicated (note that only the present one considered both genders).

It should be stressed once more that fundamental differences exist between our approach and the classical studies that determined cell diameters, and then used this to estimate volumes (*e.g.*, Loud, 1968; Pieri *et al*, 1975; Blouin *et al*, 1977), assuming either a pure spherical or a cubical shape. With such an approach, larger cells have an increased probability of being measured and the (larger) BnHEP can be misjudged as MnHEP (Figure 3.20); it is very likely that this may lead to an overestimation. In contrast, the thick sections of this study fully encompassed the largest HEP, and the optical disector granted that all cells were sampled (and measured) in proportion to their number, thus avoiding the assumption of a constant proportion of BnHEP throughout ageing (Schmucker *et al*, 1978). Additionally, the cell volume was better characterised, not only because a geometric cell shape is not assumed, but also because an unbiased estimator of local volumes (the nucleator) was used, and based on 4 intersections per cell. It is not the first time that this method was used in the rat liver: Jack *et al* (1990) and more recently, Karbalay-Doust and Noorafshan (2009) also used it (Table 3.1 at the beginning of this Chapter). Despite the latter study applied the nucleator in paraffin sections, it can be argued that the method is theoretically unsuited for such sections, known to be affected by marked shrinkage. Although this may be a potential source of bias, we should emphasise that technical procedures were similar in all age groups and no differences for shrinkage were noted throughout ageing or gender. Thus, we can consider our group comparisons as valid and not mined by such bias. Additionally, after correcting for shrinkage, our data is coincidental with the general figures reported for the volume of HEP [5000 to 6000 μm^3

(McCuskey, 2006; Grisham, 2009)] and closely resembles those of Jack *et al* (1990), who also used the nucleator (in epoxy sections) estimating local volumes of HEP in young female Sprague-Dawley rats (Table 3.1).

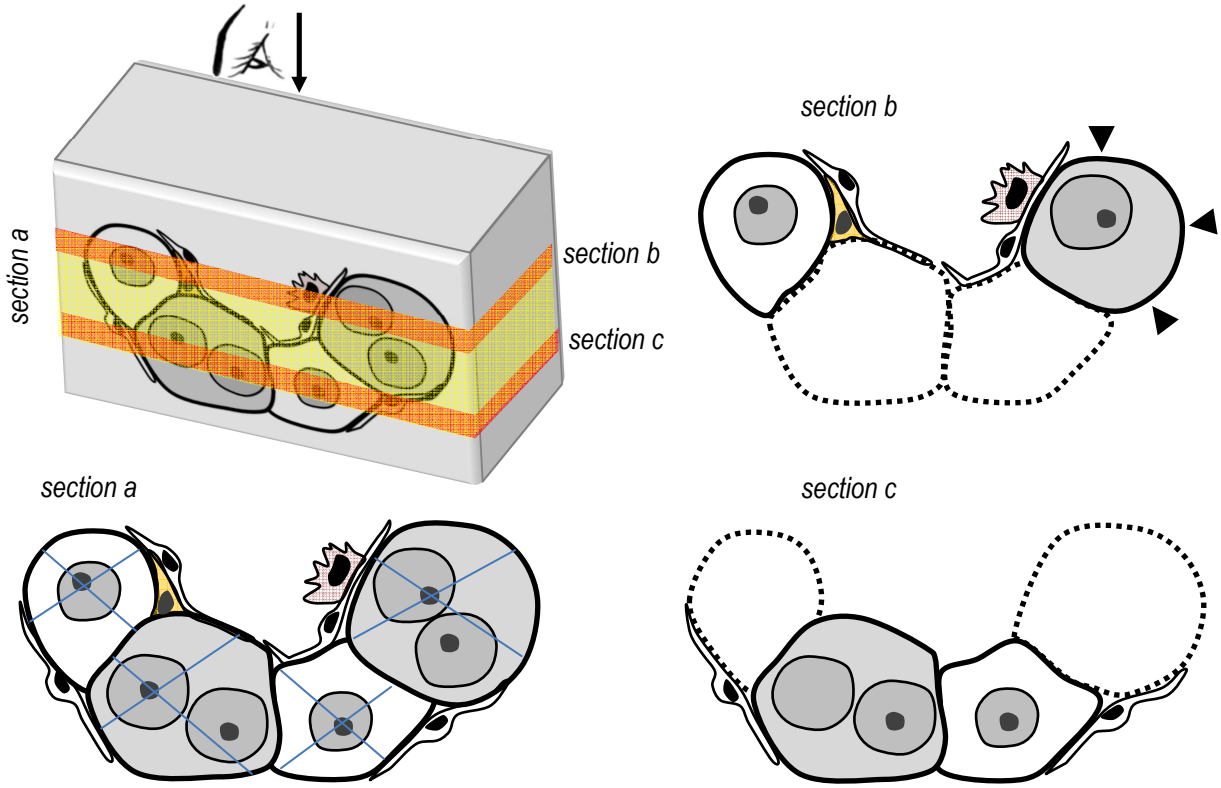

Figure 3.20 – Differences between thick (a) and thin (b, c) sections. For illustrative purposes a hepatic cord is shown (upper left). When it is viewed at the microscope (from above, as indicated by the arrow), all mono- and binucleated hepatocytes are accurately discriminated and measured (by the nucleator) in section (a). In contrast, when using sections made at different planes (b) or (c), the binucleated hepatocytes can be misjudged as large mononucleated cells (arrowheads).

3.4.2- Age and gender study: 6) Ploidy analysis in ageing

Techniques for ploidy discrimination in the liver have been described for more than fifty years. Nuclear staining with propidium iodide, followed by flow cytometry, is viewed as a general tool (Gupta, 2000), but other techniques for studying ploidy include karyometry (Nadal and Zajdela, 1966), cytophotometry using Feulgen staining (An *et al*, 1997), and fluorescence-activated cell sorting (White *et al*, 1987). All these are unable to fully distinguish (2x2N) BnHEP from 4N MnHEP (Celton-Morizur and Desdouets, 2010) and our technique also failed in this regard. This drawback has been recently surpassed by the use of fluorescence imaging with the advent of Hoechst 33342 to stain DNA (Lamas *et al*, 2003; Celton-Morizur and Desdouets, 2010). With the latter approach, the kinetics of polyploidisation can be evaluated and it is possible to differentiate MnHEP from BnHEP,

by using a membrane marker, like β-catenin (Celton-Morizur and Desdouets, 2010). When compared with flow cytometry, the fluorescence technique evaluates a lower number of cells and lacks the sensitivity to detect small differences in the DNA content, resulting from unbalanced chromosomal segregation (Faggioli *et al*, 2011). Additionally, when applied to thin sections (Figure 3.20), it may also lead to erroneous evaluation of binuclearity or of staining intensity — and thus of DNA content — namely when a partial amputation of nuclear material occurs.

Overall, we can consider our approach as satisfactory for evaluating ploidy but we could attempt, in future studies, to refine the methodology in order to avoid studying indistinct "particles" (*i.e.*, a mixture of cells and nuclei). This could be achieved by: 1) sonicating the suspension, so that only nuclei would be present; 2) filtering the suspension through a 10 µm mesh, so that only cells would be studied; and 3) using a membrane marker of HEP in the flow cytometry analysis [for instance an Alexa fluor conjugated antibody against E-cadherin (Bioss, USA)].

In general, our data of the ploidy analysis is in accordance with previous reports for Wistar rats (Sanz *et al*, 1999; Torres *et al*, 1999). However, we found more diploid particles than those two studies. Possible explanations include the inter-individual variability: ploidy has been reported to vary within and between strains of rodents (Severin *et al*, 1984), and also technical reasons. It is possible that the mechanical dissociation of the liver may have released many naked nuclei of HEP [which were considered as diploid particles, even when originated from polyploid BnHEP cell (2x2N)]. Another possibility for having more diploid cells is the contamination by NHC — which seems less likely according to our observations of the cytospin smears. However, and despite the caveats, the flow cytometry data pointed in the same direction as the stereology study, at least in females. The $\overline{v}_N$ was larger in aged rats and the volume histograms were skewed to the right, indicating that polyploidy increased.

Currently, it is unknown why aged animals have an increased polyploidy, but several hypotheses have been raised. Medvedev (1986) proposed that polyploid cells could accumulate somatic mutations, creating aberrant cells with redundant sets of genes. In an organ so strongly engaged in drug detoxification, like the liver, a polyploid genome could then provide protection against the dominant expression of mutated oncogenes (Medvedev, 1986; Guidotti *et al*, 2003). In according to this, it was recently showed that aneuploidy and unbalanced DNA content are common in normal mouse and human liver (Faggioli *et al*, 2011; Duncan *et al*, 2012). The former study analysed BnHEP by fluorescence *in situ* hybridization, using probes for sex chromosomes and for autosomes, and determined that aneuploidy affected more than 21% of cells (Faggioli *et al*, 2011).

This in accordance with our data, since we detected aneuploidy in almost half of the animals studied and it affected up to 24% of the particles. Since we had nuclei mixed with cells, it is difficult to prove by our flow cytometry data that BnHEP were to blame for aneuploidy. However, the stereology data suggests that BnHEP were involved, because we found a relatively high CV (over 10%) among the nuclei of each BnHEP, in aneuploid animals.

Another explanation for the augmented polyploidy in old animals is that it may arise to facilitate an increased gene expression, via increased levels of transcriptional factors (Funk-Keenan *et al*, 2008). With a higher number of genomes, the protein secretion will tend to increase per cell, and this would potentially accelerate growth. In this vein, it has been reported that BnHEP secrete more proteins than MnHEP (Grizzi and Chiriva-Internati, 2007) and that the growth rate (at a fixed body mass) correlates with polyploidy (Vinogradov *et al*, 2001). This can be viewed as a general strategy of cell growth that enables to boost the metabolic output, cell mass and size, being alternative to cell division (Guidotti *et al*, 2003). Finally, it has been observed that polyploidization promotes defence against DNA damage and favours the response to hypoxia, both important features for an aged liver, subjected to diminished blood supply (Anatskaya and Vinogradov, 2007).

3.4.2- Age and gender study: 7) Oxidative stress analysis throughout ageing

Strong evidence supports that one of the first triggers of liver fibrosis are ROS, either released by HEP or KC (Parola and Robino, 2001; Bataller and Brenner, 2009). In this vein, and as we observed increased collagen deposition in the liver of older male rats (Chapter 3), we decided to investigate the generation of ROS throughout ageing. It has been stressed that a combination of different antioxidant enzymes should be considered when evaluating oxidative stress (Beckman and Ames, 1998). Assessing the activity of any particular enzyme is of little interest because these either act in parallel (in the sense two enzymes can play similar roles, *e.g.*, CAT and GPX) and in series (operating in tandem to decompose radicals into harmless products, *e.g.*, SOD and CAT). Additionally, it has been emphasised that the true aspects of ageing are hardly highlighted by a simple comparison of parameters between young and old livers (Kitani, 1992; 2007). Therefore, we studied the liver of all age groups focusing in enzymes related with the glutathione redox cycle (GR and GPX), phase II biotransformation of xenobiotics (GST) and non-glutathione associated enzymes (CAT). Moreover, we evaluated the extent of LPO by measuring TBARS, which traduces the balance between ROS production and the antioxidant defences/repairing systems.

There are more than 300 theories to explain ageing, and new ones continue to be added (Viña *et al* 2007). One that is still highly popular is that proposed by Harman (1956), which

postulates that free radicals derived from oxygen are responsible for the ageing phenomenon. Accordingly, with advanced age the antioxidant systems are unable to counterbalance all the free radicals generated throughout the cell life, resulting in oxidative damage of cells and tissues. This is particularly relevant in liver, because HEP are very rich in mitochondria and have a high respiratory rate. Moreover, these cells are devoted to detoxification of xenobiotics, chronically generating low amounts of O_2^{-}•.

Regarding ageing effects, we should stress that a lack of consensus ruled the research in liver antioxidants, ever since the beginning (Van Bezooijen, 1984) and this scenario still prevails (Table 3.7). Apart from differences between strains and gender, several other variables may contribute to that inconsistency. Put it simply, these can occur in three moments: before, during and after the biochemical analysis. The first variable refers to the selection of animals: comparing old animals with extremely young ones, will focus only on changes occurring during the developmental stage (Kitani, 1992). Rats younger than 5 weeks must be considered as immature (Kwekel *et al*, 2010), whereas those up to 5 or 6 months (depending on the strain) should be regarded as young adults, in the development period (Kitani, 1992; Kwekel *et al*, 2010). Also the sample collection can influence results, if taken at different zeitgebers. Circadian rhythmicity of ROS generation and antioxidant defences has been shown to exist throughout the lifespan of rat (Manikonda and Jagota, 2012). Even prior to the analysis, the storing of samples can yield increased and more erratic values of TBARS, when compared to fresh samples (Rikans *et al*, 1997). Still, in the second moment (*i.e*., during the biochemical analysis), the use of different cell components may generate conflictive results [*e.g.*, the level of TBARS in homogenates increases with ageing, whereas that of the mitochondrial fraction is maintained (Sawada and Carlson, 1987)]. So far, enzymatic activity has been measured in liver homogenates, homogenates of isolated HEP, as well as in mitochondrial (liver and hepatocytic), post-mitochondrial, microsomal and cytosolic fractions (Table 3.7). In the third moment (*i.e.*, after the analysis) results can still be influenced, because authors either express enzymatic activity per mg of protein or per gram of wet weight, which may lead to different conclusions (Tian *et al*, 1998; Langley-Evans and Sculley, 2005; Kireev *et al*, 2007). Moreover, protein content may increase during ageing, namely in liver homogenates (Langley-Evans and Sculley, 2005) — this may lead to an apparent decrease of activity of enzymes in older animals.

Table 3.7 – Compilation of data regarding the effects of ageing and gender in oxidative stress parameters in the rat liver.

Reference	Strain	Ages (months)	Fraction	Catalase	Glutathione peroxidase	Superoxide Dismutase	Glutathione	Glutathione disulfide reductase	Glutathione -S- transferase	Oxidative stress PC	Oxidative stress MDA
Sawada and Carlson, 1987	Wistar M	1, 3, 6, 9, 12, 15, 18, 21, 23	H Mt								↑ ↔
Rikans *et al*, 1991; 1992	Fischer M / F	4, 14, 24, 29	H Mt PMt	 ↓ / ↑	 ↑ / ↓ ↔ / ↔	 ↑ / ↑ ↔ / ↔	↔ / ↔	 ↓ / ↔ ↔ / ↑			↑ / ↓
Sanz *et al*, 1999	Wistar	1, 6, 12, 18, 30	H (HEP) Mt	↑	↑	↑ ↔	↓	↑	↔		↑
Dogru-Abbasoglu *et al*, 1997	Wistar M	6, 22	PMt		↔	↔	↓				↑
Tian *et al*, 1998	Fischer M	1, 6, 12, 18, 24	H Mt	↓	↔	↔ ↔				↑	↔
Sanz *et al*, 2002	Wistar M	2, 6, 12, 18, 30	H (HEP) Mt	↑	↑	↑ ↑	↓		↔		
Kim *et al*, 2003	SD, M	1.5, 9	Ct	↔		↑	↑	↔	↔		
Navarro and Boveris, 2004	Wistar M	6, 14, 21	Mt				↓			↑	↑
Langley-Evans and Sculley, 2005	Wistar M / F	1, 4, 7, 10	H	↓ / ↓	↑ / ↑	↑ / ↑		↓ / ↓		↓ / ↑	
Hamden *et al*, 2009	Wistar M / M+E2	4, 12, 18	H	↓ / ↑	↓ / ↑	↓ / ↑					↑ / ↓
Aydin *et al* 2010	SD, M / F	5, 24	H				↓ / ↓			↑ / ↑	↑ / ↑
Manikonda and Jagota, 2012	Wistar, M	3, 12, 24	Ct	↓	↑	↓	↓				↑
Present study	Wistar, M / F	2, 6, 12, 18	H PMt	 ↑ / ↔	 ↔ / ↔			 ↔ / ↔	 ↓ / ↔		↑ / ↑

SD (Sprague-Dawley); M (males); M+E2 (males treated with oestrogen); F (females); Ct (citosolic); H (homogenate); H (HEP) (homogenate of isolated hepatocytes); Mt (mitochondrial); PMt (post-mitochondrial); PC (protein carbonyl); MDA (malondialdehyde).

Back in the eighties, ageing was generally viewed as a decline in organ functions, and the liver antioxidant systems were no exception (Van Bezooijen, 1984; Kitani, 2007). Still today, many researchers believe in such a decline, but some studies found no change or even an increase in antioxidant enzymes throughout ageing (Table 3.7). In our case, we only observed ageing effects for CAT, GST and TBARS. As to the latter, it is in accordance to the majority of studies (Table 3.7), and traduces the increase in ROS postulated in the free radical theory (Harman, 1956). TBARS are routinely used as LPO markers, but it should be kept in mind that it mostly provides a qualitative approach, since the assay is intrinsically non-specific for MDA: many other substances (including ketones, sucrose, proteins, nucleic acids and urea) may react with TBA (Devasagayam *et al*, 2003). Additionally, MDA is neither the sole end product of LPO nor it is generated exclusively through this process (Janero, 1990). Regarding the effects of ageing in CAT and GST, it is noteworthy that a recent study evaluated gene expression in the rat liver and observed ageing differences in CAT and all genes related with GST (Kwekel *et al*, 2010). Curiously, the GST activity we obtained (in both genders) closely resembles the gene expression profile of Mu-GST reported by that study (Kwekel *et al*, 2010). In the rat, GST has exogenous and endogenous substrates, including products of LPO, like cholesterol epoxides and 4-hydroxyalkenals (Staffas *et al*, 1992). In this vein, it is possible that the higher activity of the enzyme in male adults may explain the lower level of TBARS of this group. Regarding CAT, our findings are similar to Sanz *et al* (1999; 2002); those authors used homogenates of isolated HEP and observed a biphasic pattern for this enzyme, both in the activity and RNA-messenger.

In conclusion, our overall data points to an enzymatic stability throughout ageing. Thus, in the light of the free radical theory, it appears that the liver of aged rats generates more ROS that may not be counterbalanced by the antioxidant defences. In our set of normal rats, we found no clear link between the oxidative stress and collagen deposition (adult and old males had more collagen but did not have significantly more ROS or lower activities of the analysed antioxidant enzymes).

3.4.2- Age and gender study: 8) HEP and gender

Regarding the N of HEP, we did not observe significant gender differences — even if they could be somehow expected, due to the geometric scaling phenomenon (related to a larger liver and body size of males). In fact, according to our data, female rats have more HEP than males, per gram and per mm^3. As far as we know, it is the first time that gender dimorphism is substantiated by stereological methods. As we already mentioned, only two stereological estimations partially addressed this issue, by comparing the N_V(HEP, liver) between ovariectomised and normal females (Dursun *et al*, 2010; Trujillo *et al*, 2011).

Whilst the former estimated a ≈ 30% reduction in the nuclear density in the absence of oestradiol, the latter (probably mined by technical errors) reported an increase. Despite it is generally accepted that the rat, mice and man have, respectively, a high, intermediate and low level of liver gender dimorphism (Mugford and Kedderis, 1998), the issue of hepatocellularity has been controversial. Recent estimations based in biochemical methods also generated different results: for instance, Smith *et al* (2008) evaluated the CYP content in Wistar rats, and reported no gender differences. Likewise, Justo *et al* (2005) and Valle *et al* (2007) reached the same conclusion, by measuring the DNA content per gram of liver, whilst Atchley *et al* (2000) observed the opposite in mice, using that same technique. According to this author, gender differences existed at 70 days of age in mice, and females had significantly more liver cells (that were smaller) than males; overall, this is in accordance with our data. Concerning HEP, 2 months females have ≈ 30% more cells per gram, but ≈ 8% less tetraploid particles and this would probably explain the results of Justo *et al* (2005) and Valle *et al* (2007). In addition to this, Atchley *et al* (2000) reported that the liver dimorphism of the N/g was only attained after puberty. In fact, it has been shown that oestrogens are mitogenic for HEP and, for instance, the liver grows during pregnancy (Roskams *et al*, 2007). It is known that endogenous oestrogens regulate liver size, because ovariectomy produces a reduction in liver size and in liver-to-body weight ratio [and in the numerical density of HEP according to Dursun *et al* (2010)]; these are re-established with oestrogen supplementation (Vickers and Lucier, 1996). It is known for long that ethinylestradiol is a liver cancer promoter (Mayol *et al*, 1992). *In vitro* studies have shown that ethinylestradiol produces a 7-fold increase in the proliferation of HEP, with increased DNA synthesis, but without cytotoxicity or induction of CYP (Vickers and Lucier, 1996). Accordingly, a pioneer study by Fischer *et al* (1984) showed that the livers of female (Fischer) rats receiving multiple injections of oestradiol were 27% heavier, and had an increase of total DNA. These authors also demonstrated that half an hour after a single injection of oestradiol, there was evidence of translocation of the ER from cytoplasm to nuclei, with an increase in the DNA content after one day (Fischer *et al*, 1984).

Regarding the BnHEP, our data contrasts with those from a previous classical report by Wheatley (1972). Despite this author observed a higher ratio of BnHEP in females, no significant differences were reported for three different rat strains (Sprague-Dawley, Lister and Ash). Likewise, the ratio of BnHEP in young females has been reported to vary from 30% (Wheatley, 1972; Jack *et al*, 1990) to 40% (Belyaeva and Ivleva, 1979) in literature. In our case, we observed significant differences in the ratio and in the N/g of BnHEP. It may be hypothesised that this higher level of BnHEP could be related to insulin gender dimorphism. *In vitro* studies have demonstrated that epidermal growth factor and insulin

induced a high rate of binucleation, similar to that normally observed in the liver of growing rats (Mossin *et al*, 1994). In such conditions, a ratio of 50% BnHEP could be observed (Mossin *et al*, 1994). More recently, it was reported that rats with low levels of circulating insulin had less formation of BnHEP comparing with rats injected with the hormone (Celton-Morizur and Desdouets, 2010). Interestingly, differences in insulin appear to exist in normal rats (namely in the Wistar strain): glucose induced insulin secretion of isolated pancreatic islets is twofold higher in females (Da Costa *et al*, 2004), and age-matched females have higher insulin levels and larger pancreatic islets (Vital *et al*, 2006). In fact, it has been shown that such levels are influenced by oestrogens, since ovariectomised rats have significantly lower insulin levels, with are restored with oestradiol administration (but not by progesterone injections) (Ahmadi and Oryan, 2008). Curiously, the insulin secretion in humans is also dimorphic: the proportion of diabetes is higher in women, and adolescent girls have higher insulin resistance than boys (Hoffman *et al*, 2000). In this vein, we hypothesise that gender differences in the BnHEP may also stand for the human field. The functional significance of gender dimorphism in the N/g HEP and BnHEP is still unknown, but it may well traduce a higher regenerative potential.

3.4.2- Age and gender study: 9) Ploidy, oxidative stress analysis and gender

There is some clinical evidence for an advantage in women, comparing to men, in terms of liver regeneration and this also applies to rats (Yokoyama *et al*, 2005; 2007; Tillmann *et al*, 2009). Besides the potential benefits of a higher N/g of HEP and of BnHEP, according to our findings female rats also tend to have more diploid HEP. These cells are known to divide more rapidly than polyploid cells in a hepatectomised liver (Gupta, 2000) and this difference may contribute to the higher regenerative capacity observed in females. It is noteworthy that studies in the rat (Swartz *et al*, 1960; Epstein, 1967; Torres *et al*, 1999) and mice (Ohtsubo and Nomaguchi, 1986; Atchley *et al*, 2000) have also reported more diploid cells in females, and such differences also stand for humans — the liver of men contains significantly more tetraploid nuclei than that of women (Torres *et al*, 1999). Still, another possible explanation for the higher regenerative potential resides in telomeres: they are longer in females than in males, in both species, and oestrogen has been shown to reduce shortening of telomeres during ageing and in chronic liver diseases, both in human (*in vitro* data) and in rat (*in vivo* data) (Tillmann *et al*, 2009). More studies (with different rat strains and techniques) are still needed to elucidate if these differences are universal in rodents. Despite the ethical concerns and the difficulty in obtaining normal material, it would be extremely interesting to know if this dimorphism also applies to humans.

Regarding the oxidative stress analysis, we observed gender differences (more or less in extent) for all the enzymes tested, except for GR. As above mentioned, only a handful of studies evaluated antioxidant enzymes in both genders and contradictory results have been obtained (Table 3.7). Overall, our results contrast with a more recent study that only noted gender differences for SOD in liver homogenates (Langley-Evans and Sculley, 2005), but are mostly concordant with those of Rikans *et al* (1991). In post-mitochondrial fractions, those authors also obtained differences for CAT and GPX; nevertheless, they noticed differences for Cu-ZnSOD (which we did not evaluate) and GR (contrary to us). Another feature that is coincidental with both studies is that, except for SOD, differences disappeared in older ages. This is also in accordance with the observations of Kitani (2007) and the recent studies of gene expression with micro-arrays (Kwekel *et al*, 2010). The latter pointed to maximal dimorphism at ≈ 3 months, which is progressively reduced after ≈ 12 months, being absent in old Fischer rats (Kwekel *et al*, 2010).

As to the gender dimorphism of GST, it was first established in the eighties (Igarashi *et al*, 1985) and, since then, confirmed by several authors (Rikans *et al*, 1991; Kitani 1992; Staffas *et al*, 1992). It has been shown that this gender dimorphism closely resembles that of CYP in rat and it has been associated with the different secretion of growth hormone in males and females (Staffas *et al*, 1992). Twenty years ago, those authors showed that the Mu-GST (one of the cytosolic classes of GST) is the most dimorphic (Staffas *et al*, 1992). More recently, it was demonstrated that genes codifying Mu-GST were indeed gender-dimorphic, in contrast with those related with the Pi and Theta classes or with microsomal-GST (Kwekel *et al*, 2010).

The two enzymes that deal with H_2O_2 (*i.e.*, GPX and CAT) displayed an opposite gender dimorphism. Males tended to have higher CAT activity, whereas females presented more GPX. This was most perceptible in younger animals, in which we observed a negative correlation between the enzyme activities. That pattern disappeared with ageing, as has been reported by others (Rikans *et al* 1991; 1992; Manikonda and Jagota, 2012). Our data is also concordant with gene expression profiles, since CAT has been shown to be much more expressed in males, whereas GPX had a mixed pattern: some genes were female predominant (GPX1 and GPX7), others male predominant (GPX6), while others presented no gender predilection (GPX8) (Kwekel *et al*, 2010). Having high activity of CAT or GPX does not assure equal protection to H_2O_2, because (in rat) CAT exists in peroxisomes of HEP and has a higher Michaelis-Menten constant (Km), being suggested that it only scavenges H_2O_2 at high concentrations. For this reason, the knock-out model for CAT displays normal features (Beckman and Ames, 1998), which contrasts with knock-out animals deficient to GPX, that are much more sensitive to neutrophil induced liver injury (Järveläinen *et al*, 2001). GPX is dispersed in the cell (cytosol, mitochondria

and nuclei), and scavenges both H_2O_2 and lipid peroxides. Therefore, it is pivotal to deal with ROS, and GPX has higher concentrations in periportal HEP (Järveläinen *et al*, 2001).

Finally, we obtained increased levels of TBARS in adult females. This was a surprising and eventually controversial finding, because females are generally viewed as less susceptible to oxidative injury than males. Rat females have been viewed has having a lower oxidant production in mitochondria (50 to 30% less H_2O_2 in the brain and liver, respectively) and this has been related with the increased lifespan of females compared to males (Borrás *et al*, 2003; Viña *et al*, 2005). Nevertheless, this subject is highly disputed, since more recent studies have shown that female liver mitochondria are larger and produce more ROS (Justo *et al*, 2005; Valle *et al*, 2007). In this vein, it has been shown that female mitochondria, in brown adipose tissue, have an increased consumption of O_2 with higher production of ROS (Rodriguez-Cuenca *et al*, 2002). In our case, the increased TBARS levels in the adult female liver, comparing to male, are in accordance with Rikans *et al* (1991) and Gasbarrini *et al* (2001). Moreover, it has been shown that females also have increased levels of protein carbonyls (Langley-Evans and Sculley, 2005; Aydin *et al*, 2010) (Table 3.7). Anyway, the significant difference detected in adults was not found for the other age groups we studied.

It has been argued that oestrogens, especially estriol and oestradiol have an effective antioxidant action — by having a phenolic hydroxyl group, these substances can give a H^+ atom to a peroxyl radical, thus interfering with the beginning or propagation phase of LPO (Kireev *et al*, 2007). This is clear from a biochemical point of view and this effect was first shown *in vitro*, in model membranes (Sugioka *et al*, 1987). However, at physiological concentrations (*i.e.*, at the level of pg/ml as shown in Figure 2.19, in Chapter 2) it is very unlikely that they may act as such (Santanam *et al*, 1998; Viña *et al*, 2005). This also applies to oestradiol metabolites (that exist in high concentrations in the liver): when the hydroxyl group at the 3 position is blocked, as in 3-methoxyestradiol, the molecule loses its ability to inhibit or promote LPO (Santanam *et al*, 1998). Truly, antioxidant effects are only seen at supra-physiological concentrations (*i.e.*, μg levels), hundreds of fold higher than normal plasma levels. This may justify the results presented by some authors [*e.g.*, Hamden *et al* (2009) injected male rats with oestradiol at 1 μg/kg/daily (Table 3.7)].

Gender dimorphism can be related to oestrogens but also to growth hormone, which modulates GST as well as CYP enzymes (Mode *et al*, 1992). Growth hormone exerts effects in various genes during ageing and it appears to modulate antioxidant enzymes (Kireev *et al*, 2007). A dimorphic secretion pattern for this hormone has been shown for long (Eagon *et al*, 1985), and their levels tend to decrease with advanced age — the so-called somatopause. This phenomenon leads to a progressive attenuation of gender

dimorphism (Kireev *et al*, 2007). Other potential candidate for the gender dimorphism of the liver is melatonin. This hormone may also play a role, since it is a powerful scavenger of ROS, promoting endogenous antioxidant production. The administration of melatonin to ovariectomized rats is slightly more effective in inducing GPX and GST than oestrogens or growth hormone (Kireev *et al*, 2007). High levels of melatonin in the rat bile have been reported and this hormone is mostly catabolised in the liver (Tan *et al*, 2007). It has been shown that the first pass effect through the organ is much more marked in males (due to a higher CYP activity) and, contrary to oestrogens, melatonin metabolites (especially 6-hydroxymelatonin) are also powerful antioxidants (Tan *et al*, 2007).

In conclusion, we have shown that the liver is dimorphic in terms of oxidative stress and that this dimorphism tends to be progressively attenuated with ageing. Nevertheless, we found no evidence that the liver of females is *a priori* more protected. Although it is still possible that the antioxidant defences are differentially induced in pathological conditions (in which activated KC become important), it seems that other mechanisms apart from oxidative stress should explain the increased collagen deposition that we confirmed in normal conditions, in males, and the general dimorphic pattern of liver diseases (as abundantly illustrated in the literature and medical practice).

3.5- References

Ahmadi R, Oryan Sh (2008) Effects of ovariectomy or orchidectomy and estradiol valerate or testosterone enanthate replacement on serum insulin in rats. *Pakistan Journal of Biological Sciences* 15, 306-308.

Almeida JR, Oliveira C, Gravato C, Guilhermino L (2010) Linking behavioural alterations with biomarkers responses in the European seabass *Dicentrarchus labrax L*. exposed to the organophosphate pesticide fenitrothion. *Ecotoxicology* 19, 1369-1381.

Altunkaynak BZ, Ozbek E (2009) Overweight and structural alterations of the liver in female rats fed a high-fat diet: a stereological and histological study. *The Turkish Journal of Gastroenterology* 20, 93-103.

An CS, Petrovic LM, Reyter I, Tolmachoff T, Ferrell LD, Thung SN, Geller SA, Marchevsky AM (1997) The application of image analysis and neural network technology to the study of large-cell liver-cell dysplasia and hepatocellular carcinoma. *Hepatology* 26, 1224-1231.

Anatskaya OV, Vinogradov AE (2007) Genome multiplication as adaptation to tissue survival: evidence from gene expression in mammalian heart and liver. *Genomics* 89, 70-80.

Atchley WR, Wei R, Crenshaw P (2000) Cellular consequences in the brain and liver of age-specific selection for rate of development in mice. *Genetics* 155, 1347-1357.

Auvigne I, Pichard V, Aubert D, Robillard N, Ferry N (2002) *In vivo* cell lineage analysis in cyproterone acetate-treated rat liver using genetic labeling of hepatocytes. *Hepatology* 35, 281-288.

Aydin S, Atukeren P, Cakatay U, Uzun H, Altuğ T (2010) Gender-dependent oxidative variations in liver of aged rats. *Biogerontology* 11, 335-346.

Bannasch P (1976) Cytology and cytogenesis of neoplastic (hyperplastic) hepatic nodules. *Cancer Research* 36, 2555-2561.

Barter ZE, Bayliss MK, Beaune PH, Boobis AR, Carlile DJ, Edwards RJ, Houston JB, Lake BG, Lipscomb JC, Pelkonen OR, Tucker GT, Rostami-Hodjegan A (2007) Scaling factors for the extrapolation of *in vivo* metabolic drug clearance from *in vitro* data: reaching a consensus on values of human microsomal protein and hepatocellularity per gram of liver. *Current Drug Metabolism* 8, 33-45.

Barros RPA, Gustafsson JA (2011) Estrogen receptors and the metabolic network. *Cell Metabolism* 14, 289-299.

Bataller R, Brenner DA (2009) Hepatic fibrosis. In: *The liver: biology and pathobiology, 5th edition* (Arias IM, Alter HJ, Boyer JL, Cohen DE, Fausto N, Shafritz DA, Wolkoff AW eds), pp. 433-452. John Wiley & Sons Ltd.

Beckman KB, Ames BN (1998) The free radical theory of aging matures. *Physiology Reviews* 78, 547-581.

Belyaeva D, Ivleva TS (1979) Binuclear rat liver cells during reparative regeneration of the organ. *Bulletin of Experimental Biology and Medicine* 87, 355-357.

Biondo-Simões ML, Matias JE, Montibeller GR, Siqueira LC, Nunes E, Grassi CA (2006) Effect of aging on liver regeneration in rats. *Acta Cirurgica Brasileira* 21, 197-202.

Bioulac-Sage P, Dubuisson L, Bonjean P, Balabaud C (1984) L'analyse morphométrique du foie humain normal en microscopie électronique. *Gastroenterology Clinical Biology* 8, 856-860.

Bird RP, Draper HH (1984) Comparative studies on different methods of malonaldehyde determination. *Methods in Enzymology* 105, 299-305.

Blouin A, Bolender RP, Weibel ER (1977) Distribution of organelles and membranes between hepatocytes and nonhepatocytes in the rat liver parenchyma. A stereological study. *Journal of Cell Biology* 72, 441-455.

Borrás C, Sastre J, García-Sala D, Lloret A, Pallardó FV, Viña J (2003) Mitochondria from females exhibit higher antioxidant gene expression and lower oxidative damage than males. *Free Radical Biology & Medicine* 34, 546-552.

Boveris A, Chance B (1973) The mitochondrial generation of hydrogen peroxide. General properties and effect of hyperbaric oxygen. *The Biochemical Journal* 134, 707-716.

Bradford M (1976) A rapid and sensitive method for quantification of microgram quantities of protein utilizing the principle of protein-dye binding. *Analytical Biochemistry* 72, 248-254.

Bucher NL, Swaffield MN, Ditroia JF (1964) The influence of age upon the incorporation of Thymidine-2-C14 into the DNA of regenerating rat liver. *Cancer Research* 24, 509-512.

Burity CHF, Pissinatti A, Mandarim-de-Lacerda CA (2004) Stereology of the liver of three species of *Leontopithecus* (Lesson, 1840) *Callitrichidae* – Primates. *Anatomy Histology and Embryology* 33, 183–187.

Burns SP, Cohen RD, Iles RA, Germain JP, Going TC, Evans SJ, Royston P (1996) A method for determination *in situ* of variations within the hepatic lobule of hepatocyte function and metabolite concentrations. *Biochemical Journal* 319, 377-383.

Carlberg I, Mannervik B (1985) Glutathione reductase. *Methods in Enzymology* 113, 484-490.

Carlile DJ, Zomorodi K, Houston JB (1997) Scaling factors to relate drug metabolic clearance in hepatic microsomes, isolated hepatocytes, and the intact liver: studies with induced livers involving diazepam. *Drug Metabolism and Disposition* 25, 903-911.

Carthew P, Maronpot RR, Foley JF, Edwards RE, Nolan BM (1996) Method for determining whether the number of hepatocytes in rat liver is increased after treatment with the peroxisome proliferator Gembrozil. *Journal of Applied Toxicology* 17, 47-51.

Carthew P, Edwards RE, Nolan BM (1998a) New approaches to the quantitation of hypertrophy and hyperplasia in hepatomegaly. *Toxicology Letters* 102-103, 411-415.

Carthew P, Edwards RE, Nolan BM (1998b) The quantitative distinction of hyperplasia from hypertrophy in hepatomegaly induced in the rat liver by phenobarbital. *Toxicology Sciences* 44, 46-51.

Celton-Morizur S, Desdouets C (2010) Polyploidization of liver cells. *Advances in Experimental Medicine and Biology* 676, 123-135.

Clairborne A (1985) Catalase activity. In: *Handbook of methods in oxygen radical research* (Greenwald RA ed), pp. 283-284. CRC Press.

Cogger VC, Le Couteur DG (2009) Fenestrations in the Liver Sinusoidal Endothelial Cell. In: *The liver: biology and pathobiology, 5th edition* (Arias IM, Alter HJ, Boyer JL, Cohen DE, Fausto N, Shafritz DA, Wolkoff AW eds), pp. 389-406. John Wiley & Sons Ltd.

Da Costa CL, Sampaio de Freitas M, Sanchez Moura A (2004) Insulin secretion and GLUT-2 expression in undernourished neonate rats. *Journal of Nutritional Biochemistry* 15, 236-241.

Da Costa VMC, Moreira DG, Rosenthal D (2001) Thyroid function and aging: gender related differences. *Journal of Endocrinology* 171, 193-198.

David H (1985) The hepatocyte. Development, differentiation, and ageing. *Experimental Pathology Supplement*. 11, 1-148.

De Priester W, Van Manen R, Knook DL (1984) Lysosomal activity in the aging rat liver: II. Morphometry of acid phosphatase positive dense bodies. *Mechanisms of Ageing and Development* 26, 205-216.

Devasagayam TPA, Bolor KK, Ramasarma T (2003) Methods for estimating lipid peroxidation: an analysis of merits and demerits. *Indian Journal of Biochemistry & Biophysics* 40, 300-308.

Doğru-Abbasoğlu S, Tamer-Toptani S, Uğurnal B, Koçak-Toker N, Aykaç-Toker G, Uysal M (1997) Lipid peroxidation and antioxidant enzymes in livers and brains of aged rats. *Mechanisms of Ageing and Development* 98, 177-180.

Dorph-Petersen KA, Nyengaard JR, Gundersen HJ (2001) Tissue shrinkage and unbiased stereological estimation of particle number and size. *Journal of Microscopy* 204, 232–246.

Duncan AW, Taylor MH, Hickey RD, Hanlon Newell AE, Lenzi ML, Olson SB, Finegold MJ, Grompe M (2010) The ploidy conveyor of mature hepatocytes as a source of genetic variation. *Nature* 467, 707-710.

Duncan AW, Hanlon Newell AE, Smith L, Wilson EM, Olson SB, Thayer MJ, Strom SC, Grompe M (2012) Frequent aneuploidy among normal human hepatocytes. *Gastroenterology* 142, 25-28.

Dursun H, Albayrak F, Uyanik A, Keleş NO, Beyzagül P, Bayram E, Halici Z, Altunkaynak ZB, Süleyman H, Okçu N, Ünal B (2010) Effects of hypertension and ovariectomy on rat hepatocytes. Are amlodipine and lacidipine protective? A stereological and histological study. *The Turkish Journal of Gastroenterology* 21, 387-395.

Eagon PK, Porter LE, Francavilla A, DiLeo A, Van Thiel DH (1985) Estrogen and androgen receptors in liver: their role in liver disease and regeneration. *Seminars in Liver Disease* 5, 59-69.

Ekataksin W, Kaneda K (1999) Liver microvascular architecture: an insight into the pathophysiology of portal hypertension. *Seminars in Liver Disease* 19, 359-382.

El-Serag HB, Rudolph KL (2007) Hepatocellular carcinoma: epidemiology and molecular carcinogenesis. *Gastroenterology* 132, 2557-2576.

Epstein CJ (1967) Cell size, nuclear content, and the development of polyploidy in the Mammalian liver. *Proceedings of the National Academy of Sciences of the United States of America* 57, 327–334.

Espeland MA, Hogan PE, Fineberg SE, Howard G, Schrott H, Waclawiw MA, Bush TL (1998) Effect of postmenopausal hormone therapy on glucose and insulin concentrations. PEPI Investigators. Postmenopausal Estrogen/Progestin Interventions. *Diabetes Care* 21, 1589-1595.

Faggioli F, Vezzoni P, Montagna C (2011) Single-cell analysis of ploidy and centrosomes underscores the peculiarity of normal hepatocytes. *PLoS One* 6, e26080.

Falzone JA Jr, Barrows CH Jr, Shock NW (1959) Age and polyploidy of rat liver nuclei as measured by volume and DNA content. *Journal of Gerontology* 14, 2-8.

Fausto N, Campbell JS (2009) Liver regeneration. In: *The liver: biology and pathobiology*, *5th edition* (Arias IM, Alter HJ, Boyer JL, Cohen DE, Fausto N, Shafritz DA, Wolkoff AW eds), pp. 549-565. John Wiley & Sons Ltd.

Fawcett DH (1994) Liver and gallbladder. In: *Bloom and Fawcett. A textbook of Histology. 12th edition*, pp. 652-688. Chapman & Hall.

Fisher B, Gunduz N, Saffer EA, Zheng S (1984) Relation of estrogen and its receptor to rat liver growth and regulation. *Cancer Research* 44, 2410-2415.

Flohé L, Günzler WA (1984) Assays of glutathione peroxidase. *Methods in Enzymology* 105, 114–121.

Francavilla A, Eagon PK, DiLeo A, Polimeno L, Panella C, Aquilino AM, Ingrosso M, Van Thiel DH, Starzl TE (1986) Sex hormone-related functions in regenerating male rat liver. *Gastroenterology* 91, 1263-1270.

Fujii E, Karasawa Y, Kumano E, Sakurai T, Misawa Y, Mori T, Ito T, Suzuki M, Sugimoto T (2004) Nuclearity and BrdU labelling of rat hepatocytes in cytocentrifuge preparations of freshly isolated hepatocytes with cumulative labelling of bromodeoxyuridine. *Journal of Toxicological Pathology* 17, 43-49.

Funk-Keenan J, Haire F, Woolard S, Atchley WR (2008) Hepatic endopolyploidy as a cellular consequence of age-specific selection for rate of development in mice. *Journal Experimental Zoology [B]: Molecular and Developmental Evolution* 310, 385-397.

Gandillet A, Alexandre E, Holl V, Royer C, Bischoff P, Cinqualbre J, Wolf P, Jaeck D, Richert L (2003) Hepatocyte ploidy in the normal rat. *Comparative Biochemistry and Physiology [A]: Molecular & Integrative Physiology* 134, 665-673.

Gasbarrini A, Addolorato G, Di Campli C, Simoncini M, Montemagno S, Castagneto M, Padalino C, Pola P, Gasbarrini G (2001) Gender affects reperfusion injury in rat liver. *Digestive Diseases and Sciences* 46, 1305-1312.

Greengard O, Federman E, Knox WE (1972) Cytomorphometry of developing rat liver and its application to enzymic differentiation. *Journal of Cell Biology* 52, 261-272.

Grisham JW (2009) Organizational principles of the liver. In: *The liver: biology and pathobiology*, *5th edition* (Arias IM, Alter HJ, Boyer JL, Cohen DE, Fausto N, Shafritz DA, Wolkoff AW eds), pp. 3-15. John Wiley & Sons Ltd.

Grizzi F, Chiriva-Internati M (2007) Human binucleate hepatocytes: are they a defence during chronic liver diseases? *Medical Hypotheses* 69, 258-261.

Guidotti JE, Brégerie O, Robert A, Debey P, Brechot C, Desdouets C (2003) Liver cell polyploidization: a pivotal role for binuclear hepatocytes. *The Journal of Biological Chemistry* 278, 19095-19101.

Gundersen HJ (2002) The smooth fractionator. *Journal of Microscopy* 207, 191-210.

Gundersen HJG (1986) Stereology of arbitrary particles: a review of unbiased number and size estimators and the presentation of some new ones, in memory of William R. Thompson. *Journal of Microscopy* 143, 3-45.

Gupta S (2000) Hepatic polyploidy and liver growth control. *Seminars in Cancer Biology* 10, 161-171.

Guyot C, Lepreux S, Combe C, Doudnikoff E, Bioulac-Sage P, Balabaud C, Desmoulière A (2006) Hepatic fibrosis and cirrhosis: the (myo)fibroblastic cell subpopulations involved. *The International Journal of Biochemistry & Cell Biology* 38, 135-151.

Habig WH, Pabst MJ, Jakoby WB (1974) Glutathione-S-transferases, the first step in mercapturic acid formation. *The Journal of Biological Chemistry* 249, 7130-7139.

Hamden K, Carreau S, Ayadi F, Masmoudi H, El Feki A (2009) Inhibitory effect of estrogens, phytoestrogens, and caloric restriction on oxidative stress and hepato-toxicity in aged rats. *Biomedical and Environmental Sciences* 22, 381-387.

Harman D (1956) Aging: a theory based on free radical and radiation chemistry. *Journal of Gerontology* 11, 298-300.

Hayashi S, Fujii E, Kato A, Kimura K, Mizoguchi K, Suzuki M, Sugimoto T, Takanashi H, Itoh Z, Omura S, Wanibuchi H (2008) Characterization of multinuclear hepatocytes induced in rats by mitemcinal (GM-611), an erythromycin derivative. *Toxicologic Pathology* 36, 858-865.

Hilmer SN, Cogger VC, Fraser R, McLean AJ, Sullivan D, Le Couteur DG (2005) Age-related changes in the hepatic sinusoidal endothelium impede lipoprotein transfer in the rat. *Hepatology* 42, 1349-1354.

Hoehme S, Brulport M, Bauer A, Bedawy E, Schormann W, Hermes M, Puppe V, Gebhardt R, Zellmer S, Schwarz M, Bockamp E, Timmel T, Hengstler JG, Drasdo D (2010) Prediction and validation of cell alignment along microvessels as order principle to restore tissue architecture in liver regeneration. *Proceedings of the National Academy of Sciences of the United States of America* 107, 10371-10376.

Hoffman RP, Vicini P, Sivitz WI, Cobelli C (2000) Pubertal adolescent male-female differences in insulin sensitivity and glucose effectiveness determined by the compartment minimal model. *Pediatric Research* 48, 384-388.

Holt A, Smith A (2008) An introduction to the anatomy of the liver. In: *Drugs and the liver. A guide to drug handling in liver dysfunction* (North-Lewis P ed), pp. 49-72. Pharmaceutical Press.

Howard CV, Reed MG (2005) *Unbiased stereology. Three-dimensional measurements in microscopy*, *2nd edition*. Garland Science/Bios Scientific Publishers.

Hubbard AL, Wall DA, Ma A (1983) Isolation of rat hepatocyte plasma membranes. I. Presence of the three major domains. *The Journal of Cell Biology* 96, 217-229.

Igarashi T, Satoh T, Iwashita K, Ono S, Ueno K, Kitagawa H (1985) Sex difference in subunit composition of hepatic glutathione S-transferase in rats. *Journal of Biochemistry* 98, 117-123.

Iredale JP, Benyon RC, Pickering J, McCullen M, Northrop M, Pawley S, Hovell C, Arthur MJP (1998) Mechanisms of spontaneous resolution of rat liver fibrosis. *Journal of Clinical Investigation* 102, 538-549.

Ishibashi H, Nakamura M, Komori A, Migita K, Shimoda S (2009) Liver architecture, cell function, and disease. *Seminars in Immunopathology* 31, 399-409.

Jack EM, Bentley P, Bieri F, Muakkassah-Kelly SF, Stäubli W, Suter J, Waechter F, Cruz-Orive LM (1990) Increase in hepatocyte and nuclear volume and decrease in the

population of binucleated cells in preneoplastic foci of rat liver: a stereological study using the nucleator method. *Hepatology* 11, 286-297.

Janero DR (1990) Malondialdehyde and thiobarbituric acid-reactivity as diagnostic indices of lipid peroxidation and peroxidative tissue injury. *Free Radical Biology & Medicine* 9, 515-540.

Järveläinen HA, Lukkari TA, Heinaro S, Sippel H, Lindros KO (2001) The antiestrogen toremifene protects against alcoholic liver injury in female rats. *Journal of Hepatology* 35, 46-52.

Justo R, Boada J, Frontera M, Oliver J, Bermúdez J, Gianotti M (2005) Gender dimorphism in rat liver mitochondrial oxidative metabolism and biogenesis. *American Journal of Physiology. Cell Physiology* 289, 372-378.

Kalra M, Mayes J, Assefa S, Kaul AK, Kaul R (2008) Role of sex steroid receptors in pathobiology of hepatocellular carcinoma. *World Journal of Gastroenterology* 14, 5945-5961.

Kandilis AN, Koskinas J, Tiniakos DG, Nikiteas N, Perrea DN (2009) Liver regeneration: focus on cell types and topographic differences. *European Surgery Research* 44, 1-12.

Karbalay-Doust S, Noorafshan A (2009) Stereological study of the effects of nandrolone decanoate on the mouse liver. *Micron* 40, 471-475.

Kim H-G, Hong S-M, Kim, S-J, Park H-J, Jung H-I, Lee Y-Y, Moon J-S, Lim H-W, Park F-H, Lim C-J (2003) Age-related changes in the activity of antioxidant and redox enzymes in rats. *Molecules and Cells* 16, 278-284.

Kireev RA, Tresguerres AF, Vara E, Ariznavarreta C, Tresguerres JA (2007) Effect of chronic treatments with GH, melatonin, estrogens, and phytoestrogens on oxidative stress parameters in liver from aged rats. *Biogerontology* 8, 469-482.

Kitani K (1992) Liver and aging. *Gastroenterologia Japonica* 27, 276-285.

Kitani K (2007) What really declines with age? The Hayflick Lecture for 2006 35t^{h} American Aging Association. *Age* 29, 1-14.

Kmiec Z (2001) Cooperation of liver cells in health and disease. *Advances in Anatomy Embryology and Cell Biology* 161, 1-151.

Kolovou G, Damaskos D, Anagnostopoulou K, Cokkinos DV (2009) Apolipoprotein E gene polymorphism and gender. *Annals of Clinical and Laboratory Science* 39, 120-133.

Kondo F, Wada K, Kondo Y (1988) Morphometric analysis of hepatocellular carcinoma. *Virchows Archives [A]* 413, 425-430.

Kuiper GG, Carlsson B, Grandien K, Enmark E, Häggblad J, Nilsson S, Gustafsson JA (1997) Comparison of the ligand binding specificity and transcript tissue distribution of estrogen receptors alpha and beta. *Endocrinology* 138, 863-870.

Kwekel JC, Desai VG, Moland CL, Branham WS, Fuscoe JC (2010) Age and sex dependent changes in the liver gene expression during the life cycle of the rat. *BMC Genomics* 11, 675.

Lamas E, Chassoux D, Decaux JF, Brechot C, Debey P (2003) Quantitative fluorescence imaging approach for the study of polyploidization in hepatocytes. *Journal of Histochemistry & Cytochemistry* 51, 319-330.

Langley-Evans SC, Sculley DV (2005) Programming of hepatic antioxidant capacity and oxidative injury in the ageing rat. *Mechanisms of Ageing and Development* 126, 804-812.

Le Couteur DG, Fraser R, Cogger VC, McLean AJ (2002) Hepatic pseudocapillarisation and atherosclerosis in ageing. *Lancet* 4, 1612-1615.

Le Couteur DG, McLean AJ (1998) The aging liver. Drug clearance and an oxygen diffusion barrier hypothesis. *Clinical Pharmacokinetics* 34, 359-373.

Li Z, Tuteja G, Schug J, Kaestner KH (2012) Foxa1 and Foxa2 are essential for sexual dimorphism in liver cancer. *Cell* 148, 72-83.

Loud AV (1968) Quantitative stereological description of the ultrastructure of normal rat parenchymal cells. *Journal of Cell Biology* 37, 27-46.

Ma WL, Hsu CL, Wu MH, Wu CT, Wu CC, Lai JJ, Jou YS, Chen CW, Yeh S, Chang C (2008) Androgen receptor is a new potential therapeutic target for the treatment of hepatocellular carcinoma. *Gastroenterology* 135, 947-955.

Madra S, Styles J, Smith AG (1995) Perturbation of hepatocyte nuclear populations induced by iron and polychlorinated biphenyls in C57BL/10ScSn mice during carcinogenesis. *Carcinogenesis* 16, 719-727.

Malarkey DE, Johnson K, Ryan L, Boorman G, Maronpot RR (2005) New insights into functional aspects of liver morphology. *Toxicologic Pathology* 33, 27-34.

Manikonda PK, Jagota A (2012) Melatonin administration differentially affects age-induced alterations in daily rhythms of lipid peroxidation and antioxidant enzymes in male rat liver. *Biogerontology* 13, 511-524.

Marcos R, Monteiro RA, Rocha E (2004) Estimation of the number of stellate cells in a liver with the smooth fractionator. *Journal of Microscopy* 215, 174-182.

Marcos R, Monteiro RA, Rocha E (2006) Design-based stereological estimation of hepatocyte number, by combining the smooth optical fractionator and immunocytochemistry with anti-carcinoembryonic antigen polyclonal antibodies. *Liver International* 26, 116-124.

Marcos R, Rocha E, Monteiro RAF (2007) Determination of hepatocellularity. *Toxicology in Vitro* 21, 1692-1693.

Marcos R, Monteiro RA, Rocha E (2012) The use of design-based stereology to evaluate volumes and numbers in the liver: a review with practical guidelines. *Journal of Anatomy* 220, 303-317.

Martin G, Sewell RB, Yeomans ND, Smallwood RA (1992) Ageing has no effect on the volume density of hepatocytes, reticulo-endothelial cells or the extracellular space in livers of female Sprague-Dawley rats. *Clinical and Experimental Pharmacology and Physiology* 19, 537-539.

Mayol X, Neal GE, Davies R, Romero A, Domingo J (1992) Ethinyl estradiol-induced cell proliferation in the rat liver. Involvement of specific populations of hepatocytes. *Carcinogenesis* 13, 2381-2388.

McCuskey RS (2006) Anatomy of the liver. In: *Zakim and Boyer's hepatology. A textbook of liver disease, 5th edition* (Boyer TD, Wright TL, Manns MP eds), pp. 3-21. Saunders.

Medvedev ZA (1986) Age-related polyploidization of hepatocytes: the cause and possible role. A mini-review. *Experimental Gerontology* 21, 277-282.

Meihuizen SP, Blansjaar N (1980) Stereological analysis of liver parenchymal cells from young and old rats. *Mechanisms of Ageing and Development* 13, 111-118.

Melchiorri C, Bolondi L, Chieco P, Pagnoni M, Gramantieri L, Barbara L (1994) Diagnostic and prognostic value of DNA ploidy and cell nuclearity in ultrasound-guided liver biopsies. *Cancer* 74, 1713-1719.

Mode A, Tollet P, Ström A, Legraverend C, Liddle C, Gustafsson JA (1992) Growth hormone regulation of hepatic cytochrome P450 expression in the rat. *Advances in Enzyme Regulation* 32, 255-263.

Molodykh OP, Nepomnyashchikh LM, Lushnikova EL, Klinnikova MG (2000) Apoptosis: decrease of hepatocyte population in mice after hyperthermia. *Bulletin of Experimental Biology and Medicine* 130, 912-916.

Mossin L, Blankson H, Huitfeldt H, Seglen PO (1994) Ploidy-dependent growth and binucleation in cultured rat hepatocytes. *Experimental Cell Research* 214, 551-560.

Mugford CA, Kedderis GL (1998) Sex-dependent metabolism of xenobiotics. *Drug Metabolism Reviews* 30, 441-498.

Nadal C, Zajdela F (1966) Somatic polyploid cells in rat liver. I. The role of binuclear cells in the formation of the polyploid cells. *Experimental Cell Research* 42, 99-116.

Naugler WE, Sakurai T, Kim S, Maeda S, Kim K, Elsharkawy AM, Karin M (2007) Gender disparity in liver cancer due to sex differences in MyD88-dependent IL-6 production. *Science* 317, 121-124.

Navarro A, Boveris A (2004) Rat brain and liver mitochondria develop oxidative stress and lose enzymatic activities on aging. *American Journal of Physiology. Regulatory, Integrative and Comparative Physiology* 287, 1244-1249.

Odaci E, Bilen H, Hacimuftuoglu A, Keles ON, Can I, Bilici M (2009) Hepatocyte numbers in rats. A stereological and histopathological study. *Archives of Medical Research* 40, 139–145.

Ogou S, Yoshida-Noro C, Takeichi M (1983) Calcium-dependent cell-cell adhesion molecules common to hepatocytes and teratocarcinoma cells. *Journal of Cell Biology* 97, 944-948.

Ohkawa H (1979) Assay for lipid peroxides in animal tissues by thiobarbiturc acid reactions. *Analytical Biochemistry* 95, 351-358.

Ohtsubo K, Nomaguchi TA (1986) A flow cytofluorometric study on age-dependent ploidy class changes in mouse hepatocyte nuclei. *Mechanisms of Ageing and Development* 36, 125-131.

Papp V, Dezsö K, László V, Nagy P, Paku S (2009) Architectural changes during regenerative and ontogenic liver growth in the rat. *Liver Transplantation* 15, 177-183.

Parola M, Robino G (2001) Oxidative stress-related molecules and liver fibrosis. *Journal of Hepatology* 35, 297-306.

Pelletier G (2000) Localization of androgen and estrogen receptors in rat and primate tissues. *Histology and Histopathology* 15, 1261-1270.

Pfuhl W (1930) Untersuchungen über zweikernige zellen. I. Die berechnung der zweikernigen zellen nach der auszählung in mikroskopischen schnitt. *Zeitschrift für Mikroskopisch - Anatomische Forschung* 22, 557-578.

Pieri C, Nagy IZs, Mazzufferi G, Giuli C (1975) The aging of rat liver as revealed by electron microscopic morphometry — I. Basic parameters. *Experimental Gerontology* 10, 291-294.

Popper H (1985) Coming of age. *Hepatology* 5, 1224-1226.

Puviani AC, Ottolenghi C, Tassinari B, Pazzi P, Morsiani E (1998) An update on high-yield hepatocyte isolation methods and on the potential clinical use of isolated liver cells. *Comparative Biochemistry and Physiology* 121, 99-109.

Ramadori G, Ramadori P (2010) Hepatocytes. In: *Signaling Pathways in Liver Diseases* (Dufour J-F, Clavien P-A eds), pp. 3-24. Springer-Verlag.

Rikans LE, Ardinska V, Hornbrook KR (1997) Age-associated increase in ferritin content of male rat liver: implication for diquat-mediated oxidative injury. *Archives of Biochemistry and Biophysics* 344, 85-93.

Rikans LE, Moore DR, Snowden CD (1991) Sex-dependent differences in the effects of aging on antioxidant defences mechanisms of rat liver. *Biochemica et Biophysica Acta* 1074, 195-200.

Rikans LE, Snowden CD, Moore DR (1992) Effect of aging on enzymatic antioxidant defenses in rat liver mitochondria. *Gerontology* 38, 133-138.

Rodriguez-Cuenca S, Pujol E, Justo R, Frontera M, Oliver J, Gianotti M, Roca P (2002) Sex-dependent thermogenesis, differences in mitochondrial morphology and function, and adrenergic response in brown adipose tissue. *The Journal of Biological Chemistry* 277, 42958-42963.

Rohr HP, Lfithy J, Gudat F, Oberholzer M, Gysin C, Bianchi L (1976) Stereology of liver biopsies from healthy volunteers. *Virchows Arch [A]: Pathology, Anatomy and Histology* 371, 251-263.

Roskams T, Desmet VJ, Verslype C (2007) Development, structure and function of the liver. In: *MacSween's pathology of the liver, 5th edition* (Burt A, Portmann B, Ferrell L eds), pp. 1-73. Churchill Livingston.

Ruijter JM, Gieling RG, Markman MM, Hagoort J, Lamers WH (2004) Stereological measurement of porto-central gradients in gene expression in mouse liver. *Hepatology* 39, 343-352.

Santanam N, Shern-Brewer R, McClatchey R, Castellano PZ, Murphy AA, Voelkel S, Parthasarathy S (1998) Estradiol as an antioxidant: incompatible with its physiological concentrations and function. *Journal of Lipid Research* 39, 2111-2118.

Sanz N, Díez-Fernández C, Alvarez AM, Fernández-Simón L, Cascales M (1999) Age-related changes on parameters of experimentally-induced liver injury and regeneration. *Toxicology and Applied Pharmacology* 154, 40-49.

Sanz N, Díez-Fernández C, Andrés D, Cascales M (2002) Hepatotoxicity and aging: endogenous antioxidant systems in hepatocytes from 2-, 6-, 12-, 18- and 30-month-old rats following a necrogenic dose of thioacetamide. *Biochimica et Biophysica Acta* 1587, 12-20.

Sawada M, Carlson JC (1987) Changes in superoxide radical and lipid peroxide formation in the brain, heart and liver during the lifetime of the rat. *Mechanisms of Ageing and Development* 41, 125-137.

Schmitz C, Hof PR (2000) Recommendations for straightforward and rigorous methods of counting neurons based on a computer simulation approach. *Journal of Chemical Neuroanatomy* 20, 93-114.

Schmucker DL (1990) Hepatocyte fine structure during maturation and senescence. *Journal of Electron Microscopy Technique* 14, 106-125.

Schmucker DL (1998) Aging and the liver: an update. *Journal of Gerontology* 53, 315-320.

Schmucker DL (2001) Liver function and phase I drug metabolism in the elderly: a paradox. *Drugs Aging* 18, 837-851.

Schmucker DL, Jones AL (1975) Hepatic fine structure in young and aging rats treated with oxandrolone: a morphometric study. *The Journal of Lipid Research* 16, 143-150.

Schmucker DL, Mooney JS, Jones AL (1978) Stereological analysis of hepatic fine structure in the Fischer 344 rat. Influence of sublobular location and animal age. *Journal of Cell Biology* 78, 319-337.

Schmucker DL, Sanchez H (2011) Liver regeneration and aging: a current perspective. *Current Gerontology and Geriatrics Research* 2011, 526379.

Severin E, Willers R, Bettecken T (1984) Flow cytometric analysis of mouse hepatocyte ploidy. II. The development of polyploidy pattern in four mice strains with different life spans. *Cell and Tissue Research 238*, 649-652.

Shimizu I, Yasuda M, Mizobuchi Y, Ma YR, Liu F, Shiba M, Horie T, Ito S (1998) Suppressive effects of estradiol in chemical hepatocarcinogenesis in rats. *Gut* 42, 112-119.

Sirma H, Williams GM, Gebhardt R (1996) Strain- and sex-specific variations in hepatic glutamine synthetase activity and distribution in rats and mice. *Liver* 16, 166-173.

Smith R, Jones RD, Ballard PG, Griffiths HH (2008) Determination of microsome and hepatocyte scaling factors for in vitro/in vivo extrapolation in the rat and dog. *Xenobiotica* 38, 1386-1398.

Sohlenius-Sternbeck AK (2006) Determination of the hepatocellularity number for human, dog, rabbit, rat and mouse livers from protein concentration measurements. *Toxicology In Vitro* 20, 1582-1586.

Souza-Mello V, Mandarim-de-Lacerda CA, Aguila MB (2007) Hepatic structural alteration in adult programmed offspring (severe maternal protein restriction) is aggravated by postweaning high-fat diet. *British Journal of Nutrition* 98, 1159-1169.

St Aubin PM, Bucher NL (1952) A study of binucleate cell counts in resting and regenerating rat liver employing a mechanical method for the separation of liver cells. *The Anatomical Record* 112, 797-809.

Staffas L, Mankowitz L, Söderström M, Blanck A, Porsch-Hällström I, Sundberg C, Mannervik BB, Olin B, Rydström J, DePierre JW (1992) Further characterization of hormonal regulation of glutathione transferase in rat liver and adrenal glands. *Biochemical Journal* 286, 65-72.

Stocker E, Heine WD (1979) Regeneration of liver parenchyma under normal and pathological conditions. *Beiträge zur Pathologie* 144, 400-408.

Styles JA, Kelly M, Elcombe CR (1987) A cytological comparison between regeneration, hyperplasia and early neoplasia in the rat liver. *Carcinogenesis* 8, 391-399.

Styles JA (1990) Studies on the hyperplastic responsiveness of binucleated hepatocytes. *Carcinogenesis* 11, 1149-1152.

Styles JA, Kelly MD, Elcombe CR, Bybee A, Pritchard NR (1991) Recovery of hyperplastic responsiveness in the rat liver after dosing with the peroxisome proliferator methylclofenapate. *Carcinogenesis* 12, 2127-2133.

Styles JA (1993) Measurement of ploidy and cell proliferation in the rodent liver. *Environmental Health Perspectives* 101, 67-71.

Sugioka K, Shimosegawa Y, Nakano M (1987) Estrogens as natural antioxidants of membrane phospholipid peroxidation. *FEBS Letters* 210, 37-39.

Svenberg T, Hammarstrom S, Zeromski J (1979) Immunofluorescence studies on the occurrence and localization of the CEA-related biliary glycoprotein I (BGP I) in normal human gastrointestinal tissues. *Clinical Experimental Immunology* 36, 436-441.

Swartz F, Sams BF, Barton AG (1960) Polyploidization of rat liver following castration of males and females. *Experimental Cell Research* 20, 438-446.

Takahashi T (1970) Lobular structure of the human liver from the viewpoint of hepatic vascular architecture. *The Tohoku Journal of Experimental Medicine* 101, 119-140.

Tan DX, Manchester LC, Terron MP, Flores LJ, Reiter RJ (2007) One molecule, many derivatives: a never-ending interaction of melatonin with reactive oxygen and nitrogen species? *Journal of Pineal Research* 42, 28-42.

Teutsch HF (1984) Sex-specific regionality of liver metabolism during starvation; with special reference to the heterogeneity of the lobular periphery. *Histochemistry* 81, 87-92.

Teutsch HF, Schuerfeld D, Groezinger E (1999) Three-dimensional reconstruction of parenchymal units in the liver of the rat. *Hepatology* 29, 494-505.

Teutsch HF (2005) The modular microarchitecture of human liver. *Hepatology* 42, 317-325.

Tian L, Cai Q, Wei H (1998) Alterations of antioxidant enzymes and oxidative damage to macromolecules in different organs of rats during aging. *Free Radical Biology & Medicine* 24, 1477-1484.

Tillmann H, Plentz R, Begus-Nahrmann Y, Lechel A, Rudolph L (2009) Telomeres and ageing, cancer and hepatic fibrosis. In: *The liver: biology and pathobiology, 5th edition* (Arias IM, Alter HJ, Boyer JL, Cohen DE, Fausto N, Shafritz DA, Wolkoff AW eds), pp. 1105-1119. John Wiley & Sons Ltd.

Torres S, Díaz BP, Cabrera JJ, Díaz-Chico JC, Díaz-Chico BN, López-Guerra A (1999) Thyroid hormone regulation of rat hepatocyte proliferation and polyploidization. *American Journal of Physiology* 276, G155-163.

Torres-Lopez MI, Fernandez I, Fontana L, Gil A, Rios A (1996) Influence of dietary nucleotides on liver structural recovery and hepatocyte binuclearity in cirrhosis induced by thioacetamide. *Gut* 38, 260-264.

Trujillo E, Vásquez B, Del Sol M (2011) Stereologic characteristics of the liver of rats (*Rattus norvergicus*) submitted to ovariectomy-induced menopause. *International Journal of Morphology* 29, 1470-1478.

Valle A, Guevara R, García-Palmer FJ, Roca P, Oliver J (2007) Sexual dimorphism in liver mitochondrial oxidative capacity is conserved under caloric restriction conditions. *American Journal of Physiology. Cell Physiology* 293, 1302-1308.

Van Bezooijen CF (1984) Influence of age-related changes in rodent liver morphology and physiology on drug metabolism - a review. *Mechanisms of Ageing and Development* 25, 1-22.

Vana J, Murphy GP, Aronoff BL, Baker HW (1977) Primary liver tumors and oral contraceptives. Results of a survey. *The Journal of the American Medical Association* 238, 2154-2158.

Vickers AE, Lucier GW (1996) Estrogen receptor levels and occupancy in hepatic sinusoidal endothelial and Kupffer cells are enhanced by initiation with diethylnitrosamine and promotion with 17alpha-ethinylestradiol in rats. *Carcinogenesis* 17, 1235-1242.

Villa E (2008) Role of estrogen in liver cancer. *Womens Health* 4, 41-50.

Viña J, Borrás C, Gambini J, Sastre J, Pallardó FV (2005) Why females live longer than males? Importance of the upregulation of longevity-associated genes by oestrogenic compounds. *FEBS Letters* 579, 2541-2545.

Viña J, Borrás C, Miquel J (2007) Theories of ageing. *Life* 59, 249-254.

Vinogradov AE, Anatskaya OV, Kudryavtsev BN (2001) Relationship of hepatocyte ploidy levels with body size and growth rate in mammals. *Genome* 44, 350-360.

Vital P, Larrieta E, Hiriart M (2006) Sexual dimorphism in insulin sensitivity and susceptibility to develop diabetes in rats. *Journal of Endocrinology* 190, 425-432.

Vollmar B, Pradarutti S, Richter S, Menger MD (2002) *In vivo* quantification of ageing changes in the rat liver from early juvenile to senescent life. *Liver* 22, 330-341.

Von Bartheld CS (2002) Counting particles in tissue sections: choices of methods and importance of calibration to minimize biases. *Histology and Histopathology* 17, 639-648.

Wagenaar GT, Moorman AF, Chamuleau RA, Deutz NE, De Gier C, De Boer PA, Verbeek FJ, Lamers WH (1994) Vascular branching pattern and zonation of gene expression in the mammalian liver. A comparative study in rat, mouse, cynomolgus monkey, and pig. *The Anatomical Record* 239, 441-452.

Warren A, Chaberek S, Ostrowski K, Cogger VC, Hilmer SN, McCuskey RS, Fraser R, Le Couteur DG (2008) Effects of old age on vascular complexity and dispersion of the hepatic sinusoidal network. *Microcirculation* 15, 191-202.

Watanabe T, Tanaka Y (1982) Age-related alterations in the size of human hepatocytes. A study of mononuclear and binucleate cells. *Virchows Archives [B], Cell Pathology Including Molecular Pathology* 39, 9-20.

Weibel E, Stäubli W, Gnägi HR, Hess FA (1969) Correlated morphometric and biochemical studies on the liver cell. *The Journal of Cell Biology* 42, 68-91.

West MJ (1993) New stereological methods for counting neurons. *Neurobiology of Aging* 14, 275-285.

Wheatley DN (1972) Binucleation in the mammalian liver. *Experimental and Cell Research* 74, 455-465.

White IN, Green ML, Legg RF (1987) Fluorescence-activated sorting of rat hepatocytes based on their mixed function oxidase activities towards diethoxyfluorescein. *The Biochemical Journal* 247, 23-28.

Wynne HA, James OF (1990) The ageing liver. *Age Ageing* 19, 1-3.

Yamamoto R, Iishi H, Tatsuta M, Tsuji M, Terada N (1993) Suppressive effect of estrogen on hepatocellular tumorigenesis induced in mice by 3'-methyl-4-dimethylaminoazobenzene. *Experimental and Toxicologic Pathology* 45, 325-328.

Yang S, Lin HZ, Hwang J, Chacko VP, Diehl AM (2001) Hepatic hyperplasia in noncirrhotic fatty livers: is obesity-related hepatic steatosis a premalignant condition? *Cancer Research* 61, 5016-5023.

Yang X, Schadt EE, Wang S, Wang H, Arnold AP, Ingram-Drake L, Drake TA, Lusis AJ (2006) Tissue-specific expression and regulation of sexually dimorphic genes in mice. *Genome Research* 16, 995-1004.

Yokoyama Y, Nimura Y, Nagino M, Bland KI, Chaudry IH (2005) Current understanding of gender dimorphism in hepatic pathophysiology. *Journal of Surgical Research* 128, 147-156.

Yokoyama Y, Nagino M, Nimura Y (2007) Which gender is better positioned in the process of liver surgery? Male or female? *Surgery Today* 37, 823-830.

Zeeh J (2001) The aging liver: consequences for drug treatment in old age. *Archives of Gerontology and Geriatrics* 32, 255-263.

Zhou Y, Shimizu I, Lu G, Itonaga M, Okamura Y, Shono M, Honda H, Inoue S, Muramatsu M, Ito S (2001) Hepatic stellate cells contain the functional estrogen receptor beta but not the estrogen receptor alpha in male and female rats. *Biochemical and Biophysical Research Communications* 286, 1059-1065.

Chapter 4 – Kupffer cells

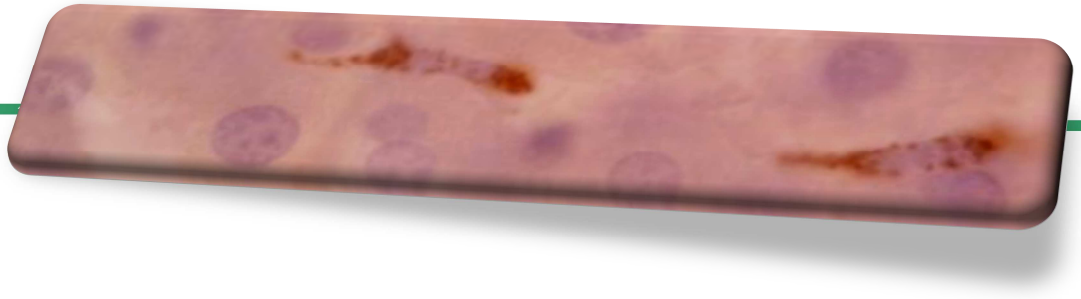

4 - Kupffer cells

4.1- Introduction

4.1.1- Quantification of KC

More than a century has passed since Karl von Kupffer observed phagocytosis of India ink and erythrocytes in cells that were named after him (Von Kupffer, 1899). These cells constitute the most abundant population of mononuclear phagocytes in the body, accounting for 80% to 90% of the resident macrophages (Kuiper *et al*, 1994; Steib and Gerbes, 2010). KC are often located at the junctions of sinusoids: a strategic position for removing particulate (*e.g.*, microorganisms and neoplastic cells) and soluble material from portal blood (*e.g.*, gut bacterial endotoxin) (McCuskey, 2007). In this vein, these cells are the main body scavengers in humans, rats and many species of mammals. [In some species, like pigs, goats and cattle (*i.e.*, of the family *Artiodactyla*) the blood-borne particulate material is not removed by KC, but by pulmonary intravascular macrophages (Haschek *et al*, 2010).] Besides this scavenger activity, KC also play a role in the initiation of immunological responses and, by producing several cytokines, have a functional cross-talk with both HEP and HSC in hepatic regeneration and fibrogenesis (Roskams *et al*, 2007). In these conditions, as well as in partial hepatectomy, after hepatic irradiation (Bouwens *et al*, 1992), or following the administration of macrophage stimulators — like glucan or zymosan (Naito *et al*, 1997) — the KC population expands, either due to the recruitment of monocyte derived cells or to proliferation of local cells. Under these conditions, it has been been reported that 75% of KC derive from the local pool (Kuiper *et al*, 1994; Roskams *et al*, 2007).

A common feature between HSC and KC is the activation process. Originally applied to describe macrophages with enhanced bactericidal properties, the term now includes all functions of stimulated cells (Kmiec, 2001). Of the many substances that can activate KC, the most important are gut bacterial endotoxins (lipopolysaccharides) that reach the liver through the portal vein system (Steib and Gerbes, 2010). However, other substances have been described and nowadays two activation pathways are considered. The “classical activation” occurs after exposure to bacteria (DNA or lipoproteins), parasites, pro-inflammatory cytokines, hypoxia and abnormal ECM, whereas the “alternative activation” occurs after a different set of stimuli including interleukins 4, 10, 13, as well as transforming growth factor-β and glucocorticoids (Duffield, 2003). Macrophages activated trough these pathways exert different functions, as follows: 1) the “classically activated” cells produce pro-inflammatory cytokines, being enrolled in ECM degradation and in phagocytosis of immune complexes, opsonised particles and bacterial products; 2) the

”alternatively activated” cells also phagocyte debris and apoptotic cells, but produce ECM and induce cell survival and proliferation (Duffield, 2003; Roskams et al, 2007). Moreover, they generate anti-inflammatory cytokines, suppress the pro-inflammatory ones and are resistant to re-activation (Duffield, 2003). Therefore, depending on the signals, different secretory (*in vivo* or *in vitro*) products may be released, including anti-inflammatory (*e.g.*, interleukins 4, 10, 13) as well as pro-inflammatory cytokines (*e.g.*, tumor necrosis factor-α) (Tsukamoto and Lin, 1997; Kmiec, 2001). Despite this thorough knowledge, and as earlier realized by Duffield (2003), there is no phenotypical marker of “classically” *versus* “alternatively activated” cells (Ramachandran and Iredale, 2012).

In a general view, the KC closely resembles other macrophages: they have bean-shaped nuclei and abundant cytoplasm, containing well developed heterogeneous lysosomes and pinocytotic vesicles (Kmiec, 2001). However, they have some characteristic features, like the vermiform processes, resulting from the fuzzy coat of membranous invaginations, or the *annulate lamellae*, which is thought to represent a particular arrangement of the rough endoplasmic reticulum (McCuskey, 2007). Additionally, the endogenous peroxidase staining of rough endoplasmic reticulum and perinuclear envelope is also characteristic of KC, namely in the rat (Wisse, 1974; Kmiec, 2001). In fact, peroxidase staining was one the first methods used for marking these cells, but in the last two decades, several monoclonal antibodies have been developed that allow a discrimination between KC and monocytes, like those against KCA1 (Sugihara *et al*, 1990) or ED2 (Dijkstra *et al*, 1985).

As above mentioned, KC are mostly located in the sinusoidal lumen: scanning electron microscopy has demonstrated that the cell body is mainly located inside sinusoids, being anchored by cytoplasmic processes — which often penetrate through endothelial *fenestrae* (Bouwens *et al*, 1992; Kuiper *et al*, 1994, McCuskey, 2008). Occasionally these cells are located in-between LSEC (McCuskey, 2007). Whatever the case, KC have intimate contact with HEP: ultrathin sections revealed that KC have microvilli intermingled over large distances with those of HEP (McCuskey, 2008). Because these cells are focally present in the space of Disse, they may also reach HSC — such contacts have been described as occasional (McCuskey, 2007; 2008) or rare (Senoo *et al*, 2010). Nevertheless, the juxtaposition of these two cells has never been evaluated systematically, to the best of our knowledge.

It is commonly accepted that KC predominate in periportal zones, a tactical distribution for their defence and clearance functions (McCuskey, 2008). In that location, KC are reported to be larger and more phagocytic, in contrast with pericentral cells, which are smaller, with stronger tumouricidal capacity (Roskams *et al*, 2007). Indeed, it is now established that diverse macrophage subpopulations coexist in the normal liver (Naito *et al*, 2004; Golbar *et al*, 2012; He *et al*, 2009). Differences in functional (*e.g.*, phagocytic and cytolytic

activity) and morphological (*e.g.*, size) features have been reported, either *in vivo* (Bouwens *et al*, 1992) or *in vitro* (Sleyster and Knook, 1982; Daemen *et al*, 1991; Hoedemakers *et al*, 1993; Bykov *et al*, 2004). This hepatic macrophage heterogeneity has also been studied by immunohistochemistry labelling (Gomes *et al*, 2004; Golbar *et al*, 2012). Two sets of cells have been described: 1) a less mature population, often called as small KC, which has been tagged by ED1; 2) a completely differentiated population, so-called large KC or simply as KC, recognised by ED2 monoclonal antibodies (Dijkstra *et al*, 1985; Barbé *et al*, 1990; Damoiseaux *et al*, 1994; Armbrust and Ramadori, 1996; Gomes *et al*, 2004; He *et al*, 2009). The $ED1^{+}ED2^{-}$ and $ED1^{+}ED2^{+}$ cell sets have been shown to participate, with a different timeline kinetics and quantitative expansion, in liver development (Golbar *et al*, 2012), as well as in pathological conditions, including acute liver injury (Johnson *et al*, 1992), cirrhosis (Hines *et al*, 1993; Ide *et al*, 2002) and experimental hepatocarcinogenesis (Johnson *et al*, 1998). More recently, it was even suggested that the imbalance of the two sets of macrophages may aggravate the liver inflammatory changes (Kumagai *et al*, 2007). Those cells may have an opposing role throughout the course of the disease, favouring the deposition of ECM during ongoing injury but enhancing their degradation in the recovery phase (Duffield *et al*, 2005; Ramachandran and Iredale, 2012). Moreover, it has been stressed that a description of the macrophage populations, *in vivo*, should form the basis of a rational and clinically relevant classification of the cell (Duffield *et al*, 2005).

Establishing appropriate quantification strategies, combined with a solid quantitative background in normal conditions (composed of unbiased estimates of liver cells) is relevant to disclose morphofunctional correlations and for monitoring the evolution of inflammatory and fibrotic liver conditions (Pinzani *et al*, 2005). In fact, even though advances in cell isolation and molecular biology have contributed significantly to the current understanding of the role of NHC in hepatic injury, the morphological examination, by providing visual assessments of the *in vivo* status, continues to be the most effective and powerful mean by which one can investigate the cellular interplay (Tsukamoto and Lin, 1997).

Regarding KC quantification, existing data are scarce: these cells have been estimated to represent between 10 to 15% of all the rat liver cells (Biozzi and Stiefel, 1965; Wisse, 1974), summing from $9x10^{6}$ (Blaner *et al*, 1985) to $20x10^{6}$ KC per gram of liver (Bouwens *et al*, 1986). In humans, $12x10^{6}$ KC per gram of liver has been reported (Fawcett, 1994). The KC population was calculated to occupy about 2.1% of the parenchymal volume (which is 50% more than HSC) (Blouin *et al*, 1977). Nevertheless, the cited values (except for the mentioned relative volume) were obtained with morphometrical or classical stereological techniques, known to be potentially biased by shape, size and distribution

assumptions (as mentioned in Chapter 1). Much more recently, Kiki *et al* (2007) determined the N and N_V of KC in rats fed with high fat diet using a combination of more modern stereological methods, namely the ratio-technique (depicted in Figure 1.10 in Chapter 1). Despite no exact figure was given, those authors reported an N of KC ≈ $70x10^3$ in normal adult female rats, using semithin sections but no specific identification of those cells (Kiki *et al*, 2007). Before our own research efforts, to the best of our knowledge, an unbiased quantification of KC using immunohistochemistry associated with cutting-edge "design-based" stereological tools has never been performed. Furthermore, the recognised subsets of liver macrophages, $ED1^+$ and $ED2^+$ cells have never been quantified *in vivo*.

4.1.2- Ageing, gender dimorphism and KC

Susceptibility to endotoxin induced hepatotoxicity is known to increase with ageing, presumably in accordance with changes in the properties of KC (Hendriks *et al*, 1987; Durham *et al*, 1990). Nevertheless, functional studies have produced conflictive results, since phagocytosis has been reported to be decreased (Martin *et al*, 1994), maintained (Vollmar *et al*, 2002) or increased (Hilmer *et al*, 2007), between 2 and 24 months rats. Moreover, it has been reported that the volume density of KC is maintained throughout ageing (Martin *et al*, 1992), being proposed that the volume expansion (in terms of total volume) of the KC population during ageing is either due to increased cell volume (Martin *et al*, 1994) or to an increased cell number (measured in "numbers per area") (Hilmer *et al*, 2007).

Regarding gender, it has been shown that exogenous oestrogen causes enlargement and proliferation of KC, enhancing their activity (Haschek *et al*, 2010). However, to the best of our knowledge, the N of KC has never been compared in rats of the opposite genders in a normal setting. Even so, this may have functional implications, not only in terms of differential fibrosis progression, but also in susceptibility to alcohol, which is greater in females (in humans, as well as in rats) (Colantoni *et al*, 2000; Eagon, 2010). Consequently, we may logically advance the hypothesis that males and females have baseline numerical differences regarding KC, which could help explaining the cited physiological and pathological implications.

To reinforce the fundamental knowledge in the rat model, and as for the HSC, our primary aim was to devise and apply a strategy to obtain an accurate and precise estimate of two known subsets of liver macrophages ($ED1^+$ and $ED2^+$ cells), estimating their N using a modern "design-based" stereological approach (combined with the immunohistochemical tagging of those phagocytes). Additionally, we aimed to evaluate whether gender and ageing differences existed regarding the N of KC (only of fully differentiated cells). Since

we hypothesised that a positive correlation between the N of HSC and KC existed, we wanted to see if this was mirrored morphologically, namely by an adjacent allocation of these cells. Finally, we sought after correlations between liver cells that could be important for regenerating and fibrotic responses — *i.e.*, HEP and HSC — estimated throughout ageing and gender in previous Chapters 2 and 3.

4.2- Materials and Methods

4.2.1- Baseline study: 1) Animals, tissue preparation and immunohistochemistry

For establishing the immunohistochemical and stereological protocol, we used the same material described in Chapter 2 (*i.e.*, 5 male Wistar rats with ≈ 3 months), and the procedure was similar to that previously described. In brief, a three-stage SUR sampling cascade was used, providing a mean of 5 fragments per liver. All fragments were processed for paraffin embedding (Histosech, Merck) and totally sectioned in a motorised rotary microtome (Leica RM2155), set to cut 30 µm thick sections. Two consecutive SUR sampled sections were collected (in every 30) and used for ED1 and ED2 immunohistochemistry.

After deparaffinising, antigen retrieval followed (set for 2 cycles of 4 minutes at 600W) and a streptavidin-biotin protocol was performed, using the Histostain-Plus kit (Zymed). Except for the primary antibody [(1:500 mouse monoclonal antibody ED1 or 1:100 mouse monoclonal antibody ED2 (Serotec, United Kingdom)], the protocol was similar to that described in Chapter 2. Negative controls were always included, in which the first antibody was omitted or replaced by non-immune serum (Dako).

The immunohistochemistry with the ED1 allows the recognition of a heavily glycosylated protein on the phagolysosome membrane of the mononuclear phagocyte system of cells; it recognises the cluster defined (CD)68 (Dijkstra *et al*, 1985; Damoiseaux *et al*, 1994). In contrast, the ED2 clone tags membrane antigens of resident macrophages, namely the completely differentiated KC of the liver; more specifically, it recognises CD163, an endocytic receptor for haemoglobin-haptoglobin complexes (Dijkstra *et al*, 1985; Barbé *et al*, 1990; Armbrust and Ramadori, 1996; Ide *et al*, 2002 Gomes *et al*, 2004; He *et al*, 2009).

4.2.1- Baseline study: 2) Stereological analysis

The N of $ED1^+$ and $ED2^+$ cells was estimated with the optical fractionator, following an established design for the rat liver (described in Chapters 2 and 3), with minor adaptations. The only differences reside in the stepwise movements of the stage in *x*- and *y*-directions ($step_{x,y}$ = 1500 µm) and in the area of the counting frame (1267 μm^2). The meander sampling and the counting procedures were implemented with the workstation CAST-Grid (Version 1.5, Olympus). The $ED1^+$ and $ED2^+$ cells were counted when the rim of nucleus was in perfect focus, at a plane below 4 µm and above or equal to 24 µm in the *z*-axis, and when, at the plane of focus, the nucleus was within the counting frame, or touching the inclusion lines, and not touching the forbidden lines or their extensions. It was always certified that the immunomarking extended beyond 24 µm, to assure that every $ED1^+$ and $ED2^+$ cells could be unambiguously recognised. The average thickness of the sections

was verified according to standardised procedures (Marcos *et al*, 2004; 2006). The use of the guard heights (4 µm and ≈ 6 µm at the upper and lower surfaces, respectively) was validated, after checking the distribution of particles in the z-axis (Annex 1). Counting was made on live images (final magnification of 4750x) captured with a 100x objective lens (NA = 1.35); this allowed a consistent and unambiguous recognition of all cells.

The N of $ED1^+$ and $ED2^+$ cells in the whole liver was estimated as:

$$N = (1/bsf) \times (1/ssf) \times (1/asf) \times (1/hsf) \times \Sigma Q^- \quad (4.1)$$

where ΣQ^- is the number $ED1^+$ or $ED2^+$ counted throughout the liver. The *bsf* is the block sampling fraction (*bsf* = 1/8), whereas *ssf* refers to the section sampling fraction (*ssf* = 1/30). The *asf* is the area sampling fraction, calculated by dividing the counting frame area, *a*, by the area associated with each *x*,*y* movement, *A* (*asf* = 1/1776). Finally, *hsf* is the height sampling fraction, being obtained by dividing the height of the disector, *h*, by the mean section thickness, *t* (*hsf* = 0.67).

Besides the N, the N/g of $ED1^+$ and of $ED2^+$, and the N_V of both these cells were also estimated. For the latter we used the formula:

$$N_V(KC, liver) = \Sigma Q^- / [h \times a(frame) \times \Sigma P] \quad (4.2)$$

where ΣQ^- is the number of cells counted in the sampled fields (either $ED1^+$ or $ED2^+$ cells), and *h* and *a* are the disector height and area of the counting frame, respectively, whereas ΣP refers to the number of accepted counting frames (*i.e.*, those that had no artificial liver edges within the counting frame or in its guard area, as detailed in Chapter 2).

The CE(N) of the estimates was computed by the formula [$CE(N) \cong 1/\sqrt{\Sigma Q^-}$] (Schmitz and Hof, 2000). For the estimations of both $ED1^+$ and $ED2^+$ cells we assessed the contribution of the CE(N) to the observed variance between animals, $OCV^2(N)$, that is basically due to the methodology plus the natural biological variance, BCV^2. For this we used the formula (Howard and Reed, 2005):

$$OCV^2(N) \cong BCV^2(N) + CE^2(N) \quad (4.3)$$

Finally, the numerical relations of $ED1^+$ and $ED2^+$ cells with total liver cells, HEP and HSC were determined, considering the data presented in Chapters 2 and 3. The KC index (KCI) was also estimated; it referred to the number of KC per 1000 HEP.

4.2.1- Baseline study: 3) Statistical analysis

The software Statistica 6.0 for Windows was used. After checking the normal distribution of data with the Shapiro-Wilk's test, a parametric correlation analysis was applied to find linear associations. After checking the homogeneity of variances with the Levene's test,

the Student's t-test for paired samples was used to compare the N of $ED1^+$ with the N of $ED2^+$ cells in the whole liver. Significance level was set at $p \leq 0.05$.

4.2.2- Age and gender study

4.2.2- Age and gender study: 1) Animals and immunohistochemistry for ED2

For this part of the study, we used the same material described in Chapter 2 [*i.e.*, 8 groups of young (2 months), adults (6 months), middle-aged (12 months), and old (18 months-old) animals]. The procedures have been detailed in Chapter 2 and above (in the baseline study). However, we did not use thin (immunostained) paraffin sections for point counting in the study of KC (as done with HSC in Chapter 2) and, in contrast with the baseline study, we only assessed herein the N, N/g and N_V and of fully differentiated KC (*i.e.*, $ED2^+$, which for the sake of simplification will be referred herein solely as KC). As previously mentioned, the immunohistochemistry protocol was standardised as much as possible (*e.g.*, same number of slides, defined container with the same level of buffer).

4.2.2- Age and gender study: 2) Double immunohistochemistry for ED2 and GFAP

Two random slides were used per animal. After deparaffinising, slides were placed in the microwave (three cycles of 4 minutes) immersed in citrate buffer (pH = 6.0). After blocking endogenous biotin and the endogenous peroxidase, the first streptavidin–biotin protocol then followed (Histostain Plus, Zymed). In this case, 10% non-immune goat serum was applied for 40 minutes, followed by incubation with 1:1500 rabbit polyclonal antibody against GFAP (Dako), for 4 days at 4ºC. After rinsing in PBS, the secondary antibody and the streptavidin–peroxidase complex were applied, for 40 minutes each. Then, after rinsing in PBS and TBS the slides were developed for 2 minutes in 0.05% 3, 3′-diaminobenzidine (Sigma) in TBS with 0.03% H_2O_2. A rinse in tap-water followed and sections were dipped in 50 mM glycine buffer (pH = 2.2) for 5 minutes, to strip off the antibodies of the first immunoreaction. The second streptavidin–biotin protocol was then continued. This was similar to that above described, except that sections were incubated with 1:100 mouse monoclonal antibody ED2 (Serotec), for another 4 days at 4ºC. For this reaction, slides were developed with aminoethylcarbazole (Dako) for 10 to 20 minutes (the final red colour was controlled by microscopic observation). Finally, the slides were mounted in Aquatex (Dako).

4.2.2- Age and gender study: 3) Stereological analysis

The procedure for the N estimation in the thick sections was similar to that described in the baseline study (except for the $step_{x,y}$ which was 1750 µm, instead of 1500 µm).

Regarding the co-localisation (*i.e.*, evaluation of the position of both HSC and KC), a SUR sampling was performed in the slides (using a $step_{x,y}$ similar to above described), and the whole thickness was evaluated. A minimum of 100 cells were evaluated per animal in order to estimate those that were in close vicinity (*i.e.*, HSC perikaryon next to KC nuclei).

4.2.2- Age and gender study: 4) Statistical analysis

Like in Chapters 2 and 3, the Shapiro-Wilk's test was performed to inspect the normality of the data. In all the cases, this was only met by a logarithmic transformation of the original variable. A parametric correlation analysis was applied for detecting linear associations between parameters. After checking the homogeneity of variances (Levene's test), a two-way ANOVA was performed, considering the effects of gender and ageing. When significant differences existed ($p \leq 0.05$), multiple comparisons were done using the post-hoc Tukey's test. The software SPSS18 (IBM) was used in the analysis.

4.3- Results

4.3.1- Qualitative findings

KC were clearly marked by ED1 and ED2 antibodies, commonly exhibiting either a spindle, or stellate shape, and, occasionally, a small round configuration (Figure 4.1). The first two morphologies predominated in sinusoids, especially in periportal areas, whereas the rounded macrophages appeared occasionally in sinusoids, but were more abundant in the portal and capsular areas. Those rounded cells were observed mostly with the ED1 immunomarking. In most KC, a stellate appearance was noted. However, comparing with HSC, the cytoplasmic processes were shorter and much thicker.

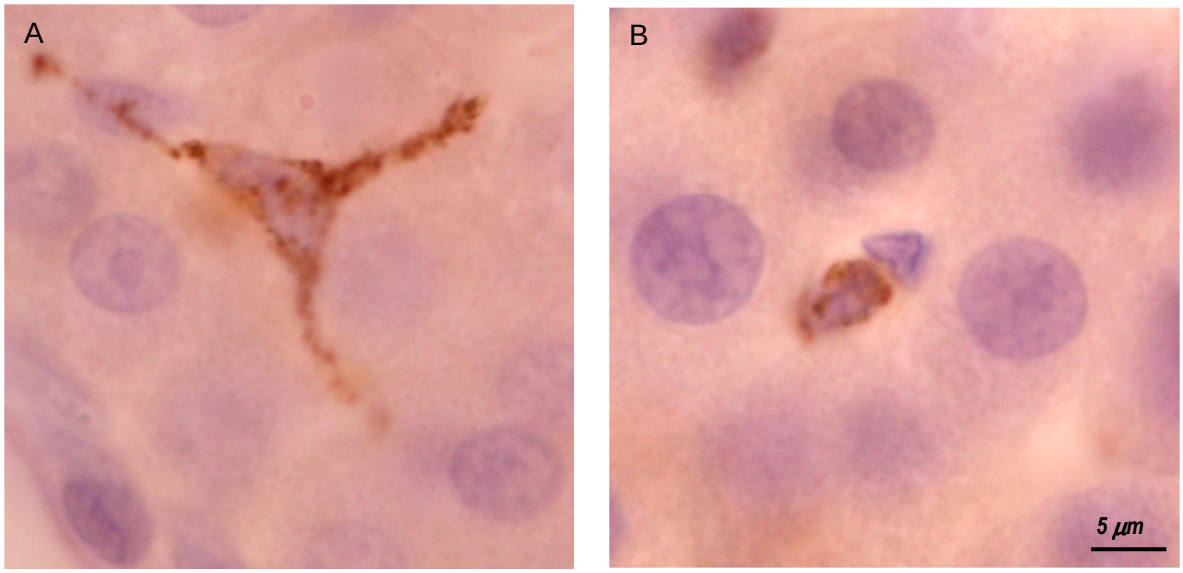

Figure 4.1 - Light micrograph taken from a 30 µm thick section. An $ED2^+$ Kupffer cell (A) stands out among hepatocytes (a less common localisation) and a rounded $ED1^+$ cell (B) is projected over the sinusoid. (Adapted from *Santos et al*, *Journal of Anatomy*, *2009.*)

In semithin sections, KC were readily identified within the sinusoids. Occasionally, these cells appeared in the vicinity of HSC (Figure 4.2); this feature was further studied using immunohistochemistry (see below). The nuclei of KC were commonly oval shaped, with a heterochromatin rim at the periphery and patches throughout the nuclei (Figure 4.3). In electron microscopy, we confirmed that lysosomal structures were the most prevalent cytoplasmic organelles, and that the cell membrane had a characteristical irregular appearance, with numerous *lamellipodia*. No morphological differences were noted throughout ageing and gender.

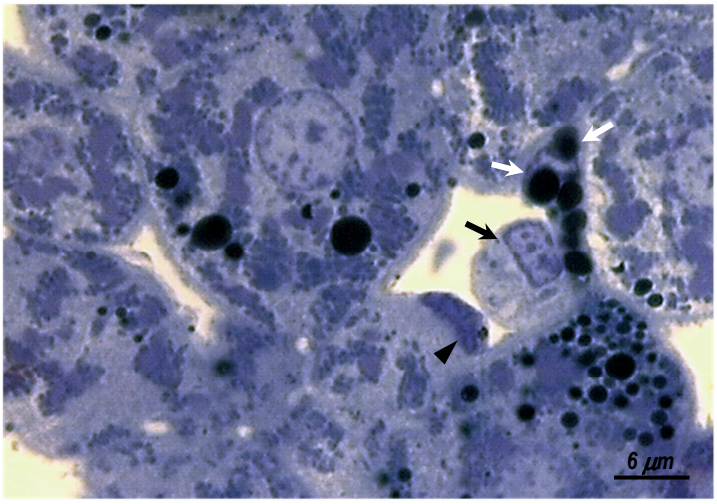

Figure 4.2 - Semithin section of the liver parenchyma. In the sinusoid, a close contact (co-localisation) is seen between a Kupffer cell (black arrow) and a hepatic stellate cell (white arrows), filled with lipid droplets; arrowhead: liver sinusoidal endothelial cell.

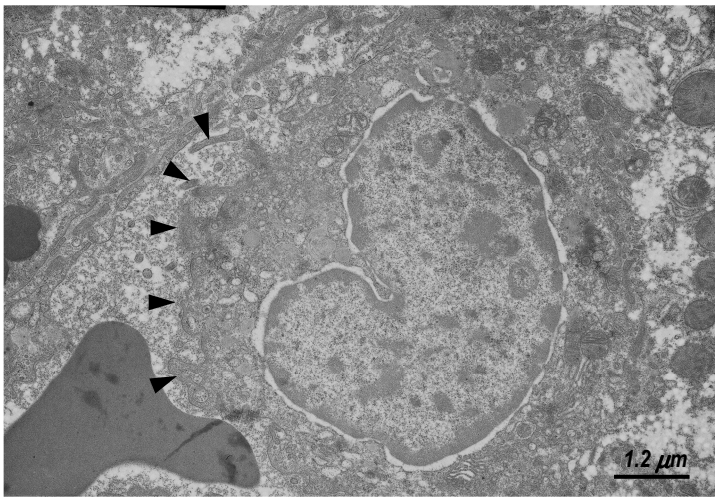

Figure 4.3 - Kupffer cell at transmission electron microscopy. The bean shaped nucleus has a heterochromatin rim. The cell membrane has the typical irregular appearance (arrowheads), with *lamellipodia*.

Co-localisation was evaluated in double-stained immunohistochemistry against GFAP and ED2, respectively for tagging HSC and KC (Figure 4.4). Throughout the thick section we could see the two cell types branching together, with their cell bodies positioned side-by-side.

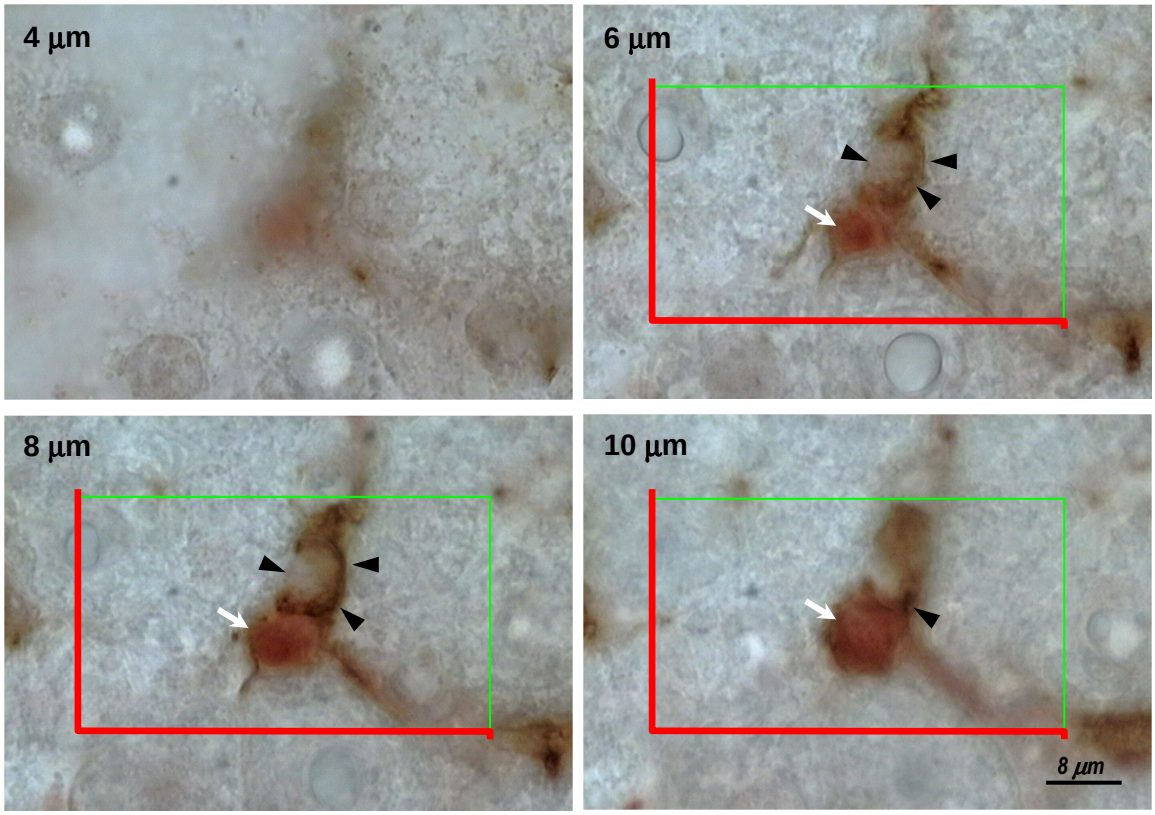

Figure 4.4 – Example of an optical disector, in which a hepatic stellate cell first appears in focus (arrowheads) immediately followed by a Kupffer cell (white arrow). The section depth (measured from the first plane of focus) is indicated in upper corner. The counting frame is depicted over the images for illustrative purposes.

4.3.2- Quantitative findings

4.3.2.1- Baseline study: *Total number, number per gram and numerical density of KC*

An average of 615 optical disectors were analysed per rat, counting 525 $ED1^+$ and 445 $ED2^+$ cells; in these disectors, the mean section thickness was 29.9 µm (CV = 0.03). The N and N/g of $ED1^+$and $ED2^+$cells from each rat are presented in Table 4.1, which also includes the estimates of the CE(N) per animal. For the estimates of the N of $ED1^+$ and $ED2^+$ cells, the sampling procedure was responsible for 6% and 7% of the total variance, meaning that the so-called "biological variance" was, by far, the most important component, as it contributed to more than 90% of the total variance. In accordance with the smooth fractionator, a dome-shape pattern was observed both in the N of $ED1^+$ and $ED2^+$ cells estimated per piece. As expected from the smooth arrange of liver pieces, the bigger and central ones presented more cells than the smaller and peripheral blocks (Figure 4.5).

Table 4.1 - Estimations of $ED1^+$ and $ED2^+$ number per gram (N/g) and total number (N) in the whole liver. CE is the coefficient of error, estimated according to Schmitz and Hof (2000). (Adapted from *Santos et al, Journal of Anatomy, 2009*.)

Parameters	N/g $ED1^+$	N $ED1^+$	CE(N_{ED1^+})	N/g $ED2^+$	N $ED2^+$	CE(N_{ED2^+})
Rat 1	$21.6x10^6$	$355x10^6$	0.04	$16.6x10^6$	$273x10^6$	0.05
2	$26.4x10^6$	$359x10^6$	0.04	$18.8x10^6$	$255x10^6$	0.05
3	$22.5x10^6$	$372x10^6$	0.04	$21.1x10^6$	$349x10^6$	0.04
4	$27.3x10^6$	$380x10^6$	0.04	$22.6x10^6$	$314x10^6$	0.04
5	$17.1x10^6$	$235x10^6$	0.05	$16.1x10^6$	$221x10^6$	0.05
Mean	$23.0x10^6$	$340x10^6$	0.04	$19.0x10^6$	$283x10^6$	0.05
CV	0.18	0.18	0.12	0.15	0.18	0.10

We conducted a correlation analysis between the data given in this Chapter and that displayed in Chapters 2 and 3 (in the "Baseline study" section). Still, no statistical correlations were observed between the different HEP, HSC and either $ED1^+$ or $ED2^+$ cells. The only (strong) significant correlation was between the numerical percentage of $ED2^+$ and the N_V of $ED1^+$ cells ($r = -0.93$; $p < 0.05$). Regarding the statistical analysis, it is opportune to mention that the N_V, N/g and N and of $ED1^+$ cells were significantly different from those of $ED2^+$ cells. A difference was also observed between the ratio of $ED1^+$/HSC and the $ED2^+$/HSC.

An average of 1.7 $ED1^+$ cells (CV = 0.28) existed per HSC. Regarding the $ED2^+$ cells, the ratio was 1.4 (CV = 0.18). Like for the HSCI (*i.e.*, number of HSC per 1000 HEP, as defined in Chapter 2), we calculated the KCI, which was 180 (CV = 0.26) and 148 (CV = 0.18) for $ED1^+$ and $ED2^+$ cells, respectively.

4.3.2.2- Age and gender study

Data for body weight, liver weight and liver-to-body weight ratio was showed in Chapter 2.

4.3.2.2- Age and gender study: *1) Total number, number per gram and numerical density of KC*

An average of 474 and 291 optical disectors were analysed in male and female rats, counting, respectively, 423 and 299 KC (*i.e.*, $ED2^+$ cells).

Regarding the N of KC, it presented the following moderate statistically significant correlations: 1) liver weight ($r = 0.67$, $p < 0.001$); 2) N of HSC ($r = 0.53$, $p < 0.01$); 3) N of HEP ($r = 0.5$, $p < 0.01$); and 4) percentage of BnHEP ($r = -0.5$, $p < 0.01$). The N of KC (Figure 4.6) was overall stable with ageing (no significant differences existed). In males it

varied between 270x10^6 KC (CV = 0.21) in young to 377x10^6 KC (CV = 0.12) in adults, whereas in females it varied less, from 293x10^6 KC (CV = 0.15) in young to 219x10^6 KC (CV = 0.17) in old animals. Statistical differences were noted under ANOVA for the gender factor ($p < 0.001$); these were mainly relevant for adults.

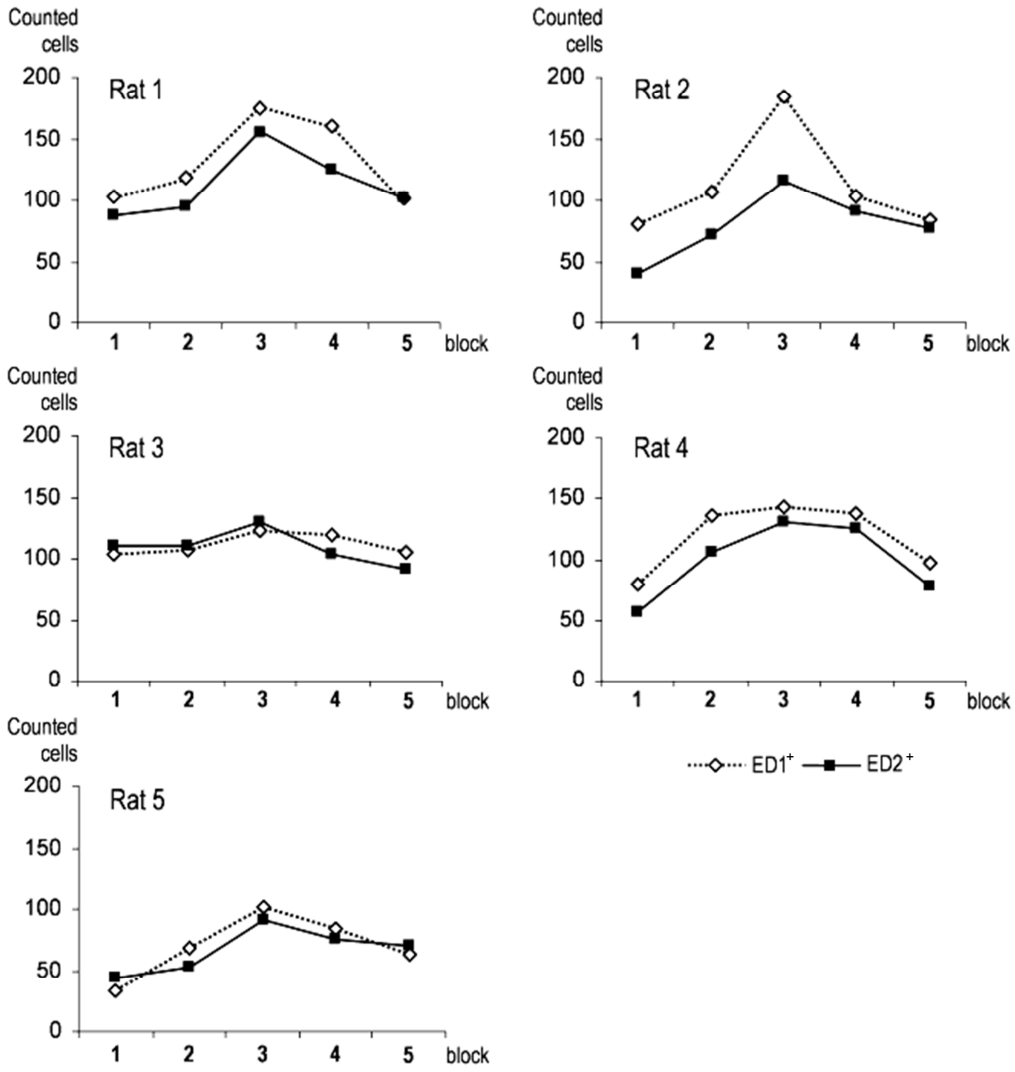

Figure 4.5 – Estimations of $ED1^+$ and $ED2^+$ cell number (N), per liver piece, in the 5 rats used in the baseline study. A dome-shaped pattern is evident. (Image published in *Santos et al*, *Journal of Anatomy,* 2009.)

The CE(N) was comprised between 0.05 and 0.07 for all the estimations of the N of KC. In the partition of the variance, the biological component was the most relevant, being responsible from 76% to 95% of the total observed variance (Figure 4.7).

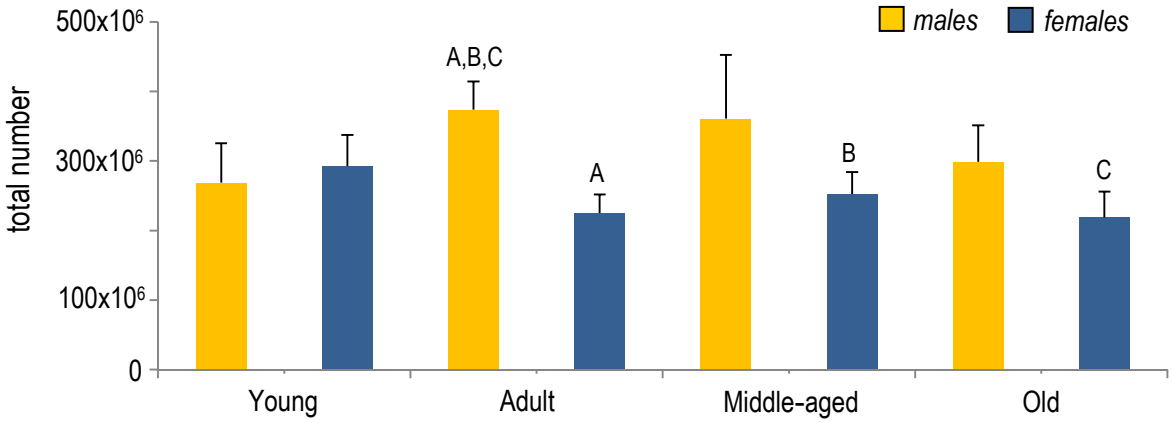

Figure 4.6 – Total number of Kupffer cells in male and female young (2 months), adult (6 months), middle-aged (12 months) and old (18 months) rats. Paired letters indicate significant differences (uppercase: across genders); data presented as mean + SD.

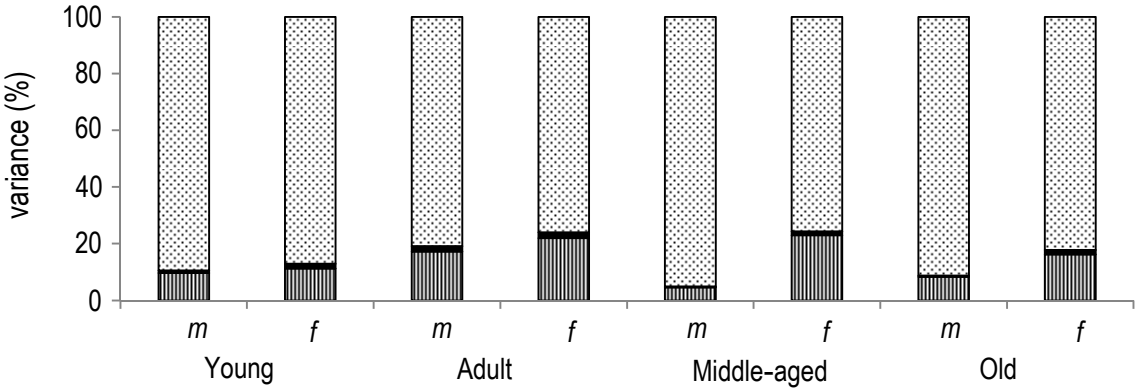

Figure 4.7 – Decomposition of the observed variance of the estimations of N of Kupffer cells (according to Equation 4.3) in male (m) and female (f) of young (2 months), adult (6 months), middle-aged (12 months) and old (18 months) rats; ⁘ = biological variance; ▮ = section thickness variance; ▩ = average sampling variance.

As to the N/g of KC, it presented a significant strong correlation with the N_V(KC, liver) ($r = 0.75$, $p < 0.001$). The latter parameter was stable in males [varied between 19×10^6 (CV = 0.15) KC/g in young males to 24×10^6 (CV = 0.15) KC/g in adults] as well as in females [in which it varied from 30×10^6 KC/g (CV = 0.20) in young to 21×10^6 KC/g (CV = 0.23) in middle-aged animals] (Figure 4.8). Despite no statistically significant differences were noted for ageing, minor differences existed for gender ($p < 0.05$); these were mainly at the cost of young animals (females with a greater value).

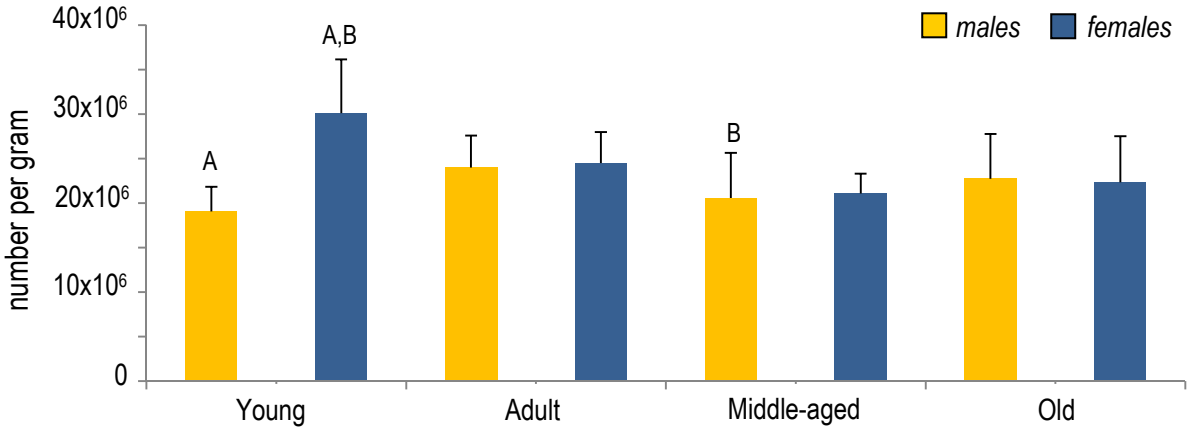

Figure 4.8 – Number per gram (N/g) of Kupffer cells in male and female young (2 months), adult (6 months), middle-aged (12 months) and old (18 months) rats. Paired letters indicate significant differences (uppercase: across genders); data expressed as mean + SD.

Apart from the above mentioned linear correlations, the N_V(KC, liver) was also moderately associated with the N_V(HEP, liver) (r = 0.63, $p < 0.001$). The N_V(KC, liver) presented significant differences for ageing ($p < 0.01$), as well as for gender ($p < 0.001$) (Figure 4.9). In females it decreased 28%, from 31.7x10^3 KC/mm^3 (CV = 0.12) in young to 24.7 x10^3 KC/mm^3 (CV = 0.16) in old females ($p < 0.01$). In males it tended to vary less [only young males were different from adults ($p < 0.05$)].

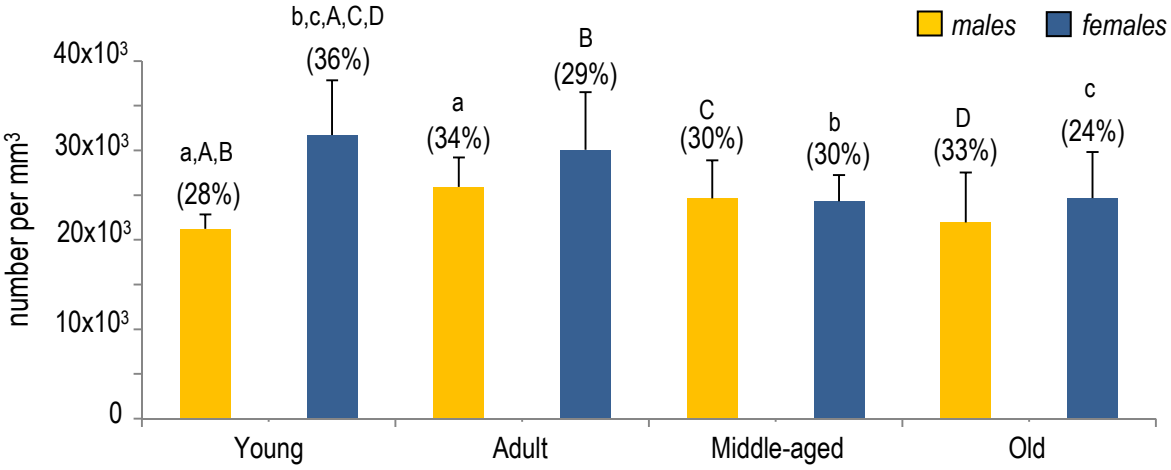

Figure 4.9 – Numerical density of Kupffer cells (per mm^3) in male and female young (2 months), adult (6 months), middle-aged (12 months) and old (18 months) rats; numbers in brackets correspond to the shrinkage. Paired letters indicate significant differences (lowercase: same gender; uppercase: across genders); data corrected for shrinkage and expressed as mean + SD.

4.3.2.2- Age and gender study: 2) Kupffer cell index

The KCI was rather constant: no ageing or gender differences existed (Figure 4.10). In males it varied from 134 in old (CV = 0.33) to 159 (CV = 0.33) in middle-aged rats,

whereas in females it varied from 120 (CV = 0.12) in middle-aged to 167 (CV = 0.17) in young animals.

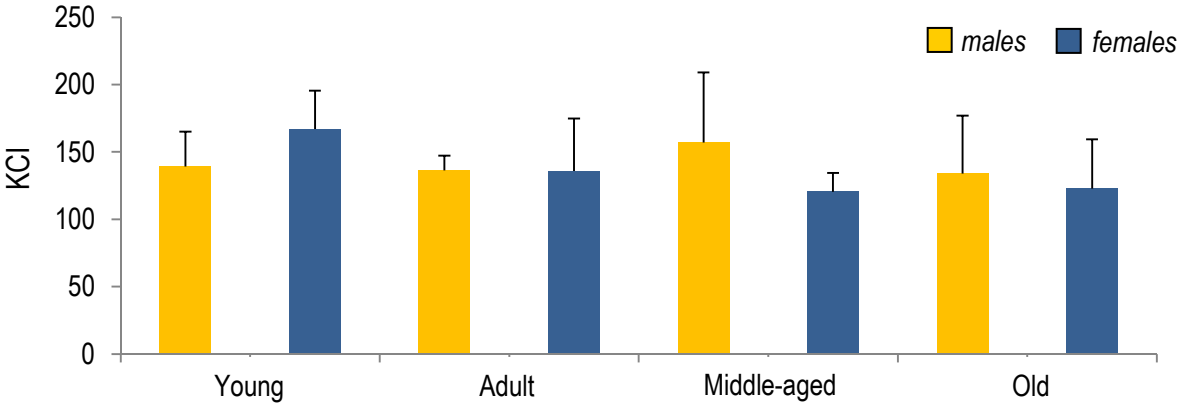

Figure 4.10 – Kupffer cell index (*i.e.*, number of Kupffer cells per 1000 hepatocytes) in male and female young (2 months), adult (6 months), middle-aged (12 months) and old (18 months) rats; data presented as mean + SD. No significant statistical differences existed.

4.3.2.2- Age and gender study: 3) Co-localisation of KC and HSC

Per animal we evaluated an average of 158 and 108 KC in males and females, respectively, in order to determine those that were in close contact with HSC. Approximately a fifth of KC was co-localised with HSC (Figure 4.11), or in other words, a third of HSC had KC as their neighbours. No ageing differences were noted in this vicinity, but gender differences existed ($p < 0.01$); these were mainly due to differences in young animals (less co-localisation in females). It is noteworthy that similar figures were obtained using GS as a marker for KC, as referred in Chapter 2 (data not shown).

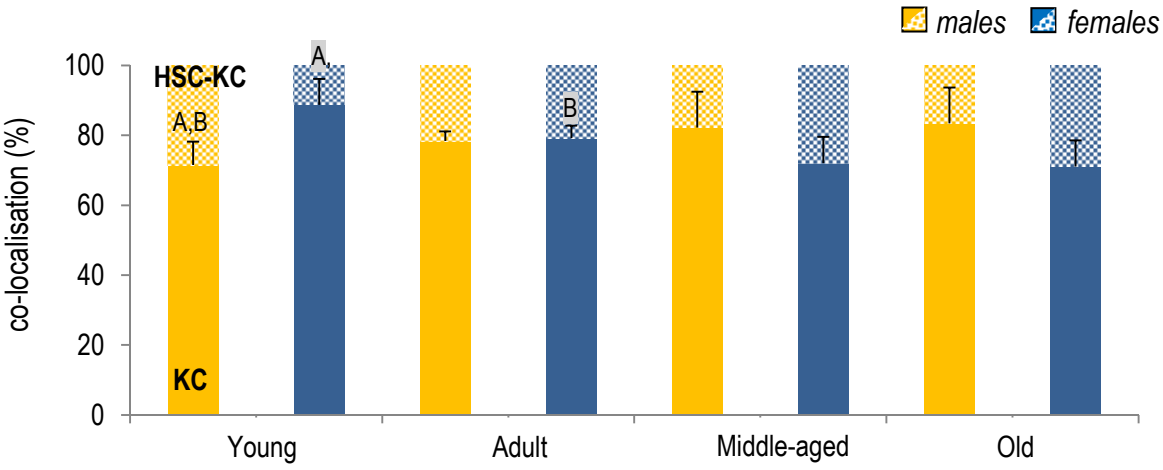

Figure 4.10 – Percentage of co-localisation of Kupffer cells (KC) and hepatic stellate cells (HSC) in male and female young (2 months), adult (6 months), middle-aged (12 months) and old (18 months) rats; data presented as mean + SD. Hatched part of columns: co-localised KC-HSC; full coloured: non co-localised KC. Paired letters indicate significant differences (uppercase: across genders).

4.4- Discussion

4.4.1- Baseline study

4.4.1- Baseline study: 1) KC quantification

In mammals, an accurate and permanent distinction of liver macrophages is not possible in routine histological sections, so we combined "design-based" stereological tools with immunohistochemistry for obtaining accurate and precise estimates of the N of $ED1^+$ and $ED2^+$ cells, the two main pools of hepatic macrophages (Dijkstra *et al*, 1985; Barbé *et al*, 1990; Hardonk *et al*, 1992; Damoiseaux *et al*, 1994; Armbrust and Ramadori, 1996; Gomes *et al*, 2004; Golbar *et al*, 2012). The heterogeneity of these cells has been recognised for more than 25 years, being generally accepted that the $ED1^+ED2^-$ and the $ED1^+ED2^+$ populations coexist (Dijkstra *et al*, 1985; Armbrust and Ramadori, 1996; Gomes *et al*, 2004), participating in liver responses to acute and chronic injuries (Johnson *et al*, 1992; 1998; Hines *et al*, 1993; Ide *et al*, 2002).

It was stated that KC occupy, in average, 2.1% of the rat liver volume, accounting for 2.5% of the liver protein (Blouin *et al*, 1977). Regarding the N of these cells only three classical studies and a more recent report focused their attention on this issue, estimating that KC comprise between 10% to 15% of all liver cells (Biozzi and Stiffel, 1965; Wisse, 1974), with a N/g between $14.2x10^6$ to $20.2x10^6$ (Bouwens *et al*, 1986) and a N close to $70x10^3$ (Kiki *et al*, 2007). Despite the proportion and N/g values were similar to our estimation of $ED2^+$ cells, major methodological differences exist between the estimations, as most previous authors (Biozzi and Stiffel, 1965; Wisse, 1974; Bouwens *et al*, 1986) used peroxidase staining coupled with the so-called "model-based" stereological techniques available at that time. Although valid for pure geometric forms, these classical tools are based on strict assumptions (as to cell size, shape and orientation), which seldom apply to the biological reality, thus inserting an unknown amount of bias in the estimates (Howard and Reed, 2005). Regarding KC tagging, it is noteworthy that immunohistochemistry has been more accepted as a marker of these cells (Armbrust and Ramadori, 1996; Yin *et al*, 1999), despite peroxidase continues to be recognised as a reliable marker of KC at the ultrastructural level (Bouwens *et al*, 1986; Kuiper *et al*, 1994). Moreover, liver macrophages negative for peroxidase have been described (Hoedemakers *et al*, 1995), being these cells considered as a heterogeneous population that may be derived from monocytes and resident macrophages (Naito and Takahashi, 1991). On the other hand, major methodological differences between our study and that of Bouwens *et al* (1986) include their reduced sampling, their assumption that KC have perfect ellipsoidal nuclei (which is not the case in many KC), and the estimation of the N/g based in "2D counts" (*i.e.*, number of cell profiles per area). The latter is undermined by uncontrolled bias due to the lost caps effect and to the heterogeneity of KC, regarding cell

shape and size (Sleyster and Knook, 1982; Hoedemakers *et al*, 1995), leading, for example, to an oversampling of larger KC. Further, regarding quantitative data on KC, it is opportune to mention that reported cell isolation yields range between 3 – 12x10^6 KC per gram of liver (Emeis and Planque, 1976; Sleyster and Knook, 1982; Heuff *et al*, 1993) or 80 – 120x10^6 KC per liver (Olynyk and Clarke, 1998; Valatas *et al*, 2003). These figures are lower, but of the same order of magnitude as the N/g and N here estimated.

As it has been emphasised in Chapter 1, numbers are zero-dimensional parameters that can be only accurately estimated using a 3D-probe, like the optical disector. "Design-based" stereological methods, namely the ratio-technique (illustrated in Figure 1.10 of Chapter 1), were applied by Kiki *et al* (2007) for estimating the N and N_V of KC; nevertheless, the reported values for female Sprague-Dawley rats were much lower than the ones we obtained. In this case, the differences could be related with the strain, gender and size of the rats used by Kiki *et al* (2007) and also with the absence of specific tag for KC, favouring underestimation. In fact, it has been emphasised that many KC may be missed in a direct observation of liver slides, without peroxidase cytochemistry or immunohistochemistry staining (Armbrust and Ramadori, 1996; Bouwens *et al*, 1986; Gomes *et al*, 2004). As to size, the organ volume reported by Kiki *et al* (2007) for controls denotes a liver weight of ≈ 10-11 g (the rat liver density is ≈ 1.07 according to our data), and so 30% lower than in our rats. Anyway, if by one hand a smaller liver weight could explain the lower N of KC, it can be easily derived that the N/g from Kiki *et al* (2007) is only ≈ 7x10^3, greatly contrasting with ours and other estimations (Emeis and Planque, 1976; Sleyster and Knook, 1982; Bouwens *et al*, 1986; Heuff *et al*, 1993). The facts point more to large underestimates due to the lack of specific tagging or to marked sex differences. (These latter appear to exist, at least in Wistar rats, according to our data of the age and gender study.)

In this baseline study, the N_V of $ED1^+$ and $ED2^+$ cells were directly derived from the optical disector. As such, the reported values are overestimations, owing to the shrinkage inherent to paraffin-embedding, serving only for comparative purposes. As we observed 38% of shrinkage (in the baseline study), the average corrected N_V is 21.0x10^3 $ED1^+$ cells/mm^3 and 17.7x10^3 $ED2^+$ cells/mm^3. The observed negative correlation between the percentage of $ED2^+$ and the N_V of $ED1^+$ cells is curious and may be explained by the process of cell maturation: since $ED1^+$ cells require about a week to become mature KC, acquiring ED2-positivity (Barbé *et al*, 1990), it seems logical that liver volumes bearing mostly mature KC, should have few of those $ED1^+$ $ED2^-$ immature cells.

4.4.1- Baseline study: 2) Subpopulations of liver macrophages

Regarding the N of $ED1^+ED2^-$ and $ED1^+ED2^+$ cells, no stereological estimations have been reported so far, to the best of our knowledge, and the existing "2D quantifications" are conflicting. In accordance with the two cited populations, some authors reported that $ED1^+$ cells are more abundant than $ED2^+$, like we observed, and that around 8% (Armbrust and Ramadori, 1996) or even more $ED1^+$ cells are $ED1^+ED2^-$ (Gomes *et al*, 2004). Considering that all $ED2^+$ cells are simultaneously $ED1^+$, in our case we estimated that $ED1^+ED2^-$ cells represent about 16% of all $ED1^+$ cells. In contrast, other authors reported that the $ED2^+$ cells are much more numerous than $ED1^+$ (Ide *et al*, 2002; Kono *et al*, 2002). These differences are possibly due to: 1) the immunohistochemistry — since the two latter studies did not use antigen retrieval methods, which are often needed to unmask antigens in paraffin embedded material (Shi *et al*, 2001); 2) the sampling, which was extremely small in both studies (only 5 fields studied per rat); 3) the section thickness (between 3 – 5 μm). The latter causes errors when counting, because $ED1^+$ cells are smaller than those $ED2^+$ (Armbrust and Ramadori, 1996), and thus they will have less probability of being sampled and counted in thin (3 – 7 μm) sections. In addition, smaller $ED1^+$ cells are more difficult to recognise when sectioned, especially if low magnifications are used for the counting, because they tend to have less lysosomes (Hoedemakers *et al*, 1995).

4.4.1- Baseline study: 3) Relation between KC and other liver cells

Regarding the numerical relations of $ED1^+$ and $ED2^+$ with HEP and HSC, no significant correlations were observed in this part of the study; one eventual reason for this may be the small number of rats sampled. Anyway, our data for the N of KC, combined with the data presented in the section "Baseline study" in Chapters 2 and 3 (Marcos *et al*, 2004; 2006), enabled us to compute the relative proportions of the hepatic cells involved in liver responses to injury. Indeed, the cross-talk between KC and HEP is extremely relevant in liver regeneration after partial hepatectomy (Takeishi *et al*, 1999) and in the mitigation of hepatic injury, either by releasing anti-inflammatory cytokines or by engulfing apoptotic bodies (Racanelli and Rehermann, 2006). In this vein, it seems useful that we offered an unbiased and precise estimation of the KCI (*i.e.*, the number of KC/1000 HEP), which has been recently used in the rat, even if it was not unbiasedly computed (Kumagai *et al*, 2007). This index may be relevant for hepatologists, since the recruitment, activation and proliferation of KC are features of many animal models of hepatic injury (Thompson *et al*, 1998; Steib and Gerbes, 2010). Likewise, the relation of HSC and HEP is quantitatively expressed in the HSCI and has been used in hepatology (and it was detailed in Chapter 2). The herein estimated 7:10 and 7:12 ratio of HSC:$ED2^+$ cells and HSC:$ED1^+$ cells,

respectively, “quantifies” the crosstalk between HSC and KC. These latter cells either have pro-fibrotic roles by stimulating the ECM synthesis, proliferation and activation of HSC (Pinzani *et al*, 2005; Friedman, 2008) or, as it was additionally shown, KC may also be anti-fibrotic during the resolution period of fibrosis, thus being essential for the recovery of the animal (Duffield *et al*, 2005; Xidakis *et al*, 2005; Ramachandran and Iredale, 2012).

In conclusion, in the baseline study we devised a strategy combining the use of immunomarking with $ED1^+$ and $ED2^+$ monoclonal antibodies and the optical fractionator. This allowed an accurate and precise estimate of the N of the two sets of liver macrophages in the rat. Herein, we offer a fundamental set of numerical reference data in healthy conditions in young Wistar rats, valuable for those studying rat models of liver regeneration, inflammation and fibrosis. Moreover, we also established sound methodological guidelines for the age and gender study.

4.4.2- Age and gender study

4.4.2- Age and gender study: 1) About the obtained data

In this part of the study we restricted the analysis to fully differentiated KC, *i.e.*, those $ED2^+$ cells because this population is more stable and long-lived [with a mean turnover of several weeks to months (Bouwens *et al*, 1986; Kuiper *et al*, 1994; Naito *et al*, 2004)]; in general, it is considered more relevant in liver responses. Accordingly, the number of these cells appears not to increase after a single dose of lipopolysaccharide (Kono *et al*, 2002), and $ED2^+$ KC have been reported to be more active in phagocytosis (Kono *et al*, 2002; Gomes *et al*, 2004) and in the secretion of tumour necrosis factor-α and ROS (Kono *et al*, 2002). As we stressed above, the kinetics of KC is still a matter of debate, but it is consensual that $ED2^+$ derive (at least partially) from $ED1^+$ cells (Naito *et al*, 2004) — in the baseline study we observed indirect evidences of that transition. It appears that the population of KC is in equilibrium, in which the loss of $ED2^+$ KC is coped by an influx of $ED1^+$ precursors (Gomes *et al*, 2004).

Our observation that a fifth of KC are co-localised, or in other words a third of HSC ($\approx$ 36% of in males and $\approx$ 32% in females) appear neighbouring KC, has never been reported in literature, to the best of our knowledge. We substantiated this using a double immunohistochemistry against GFAP and either ED2 (Dijkstra *et al*, 1985) and GS (Bode *et al*, 2000). The latter is not only a typical marker of centrilobular HEP (as detailed in Chapter 2 and 3), but has been shown to co-localise with ED2 *in vivo* and *in vitro* (Bode *et al*, 2000). However, we opted to use ED2 for the systematic evaluation of co-localisation because: 1) it is recognised as the best marker of fully differentiated KC (Dijkstra *et al*, 1985; Gomes *et al*, 2004; He *et al*, 2009); 2) it tends to mark more KC than GS, according

to our observations (data not shown) and the GS has been reported to produce a feeble spot-like marking in some cells (Bode *et al*, 2000) — which would be less suitable for assessing the co-localisation; 3) expression of GS has been shown in cultured HSC (Bode, 1988) — therefore, at least in theory, it could be argued that we were observing activated HSC instead of KC. The correlation we found between HSC and KC [even if moderate ($r = 0.53$, $p < 0.01$)] prompted us to evaluate this co-localisation, which we consider relevant, not only because it corresponds to a third of HSC, but also because it was consistent throughout ageing. It should be emphasised that this co-localisation also existed in semithin sections (as shown in Figure 4.2), but only in a minority of sections. In these, it is less likely to catch both KC and HSC in the thin (0.5 μm) section plane. In contrast, the thick sections, by encompassing the full size of both cells (including their major cytoplasmic processes), allowed an optimal cell recognition.

It can be argued that KC are movable cells within the sinusoids, and in this case, the co-localisation would be temporary and only incidental (despite the latter seems poorly or even not compatible with our reported consistency). Indeed, KC were traditionally defined as stationary tissue macrophages (Kuiper *et al*, 1994), but, more recently, pathology textbooks and reviews sustain that these cells are motile macrophages, patrolling the liver sinusoids both with and against the blood flow (Kmiec, 2001; Roskams *et al*, 2007). This "new concept" seems to have been based in a single *in vivo* video microscopy study that showed KC crawling along the liver sinusoids at several micrometers per minute (MacPhee *et al*, 1992). However, this study has been disputed (Frevert *et al*, 2007) and a similar *in vivo* video microscopy study using KC expressing green fluorescence protein failed to see any movement after several hours (Faust *et al*, 2000), thus suggesting that the traditional concept still prevails (Frevert *et al*, 2007). In this vein, KC (or at least a fifth of them) would reside for several days neighbouring HSC.

This close positioning should favour the crosstalk and paracrine/juxtacrine stimulation of HSC by KC. It is known for long that the conditioned medium of KC alone is able to stimulate proliferation, ECM synthesis and to promote activation of HSC (Friedman and Arthur, 1989; Meyer *et al*, 1990). The action of KC is mediated by a wide spectrum of mediators, like interleukin-1α, tumour necrosis factor-α, transforming growth factor-α and -β, which promotes ECM synthesis (Kmiec, 2001; Kuiper *et al*, 1994; Roskams *et al*, 2007). It is noteworthy that De Minicis *et al* (2007) showed that the gene expression profile of *in vitro* activated HSC differed substantially from the *in vivo* activation, but such differences were largely attenuated when HSC were co-cultured with KC.

Besides co-localisation, another new finding was the above mentioned correlation between KC and HSC in normal ageing conditions. Grinko *et al* (1995) studied biliary

fibrosis in young male Wistar rats using monoclonal antibodies against ED2 and desmin, respectively for KC and HSC. However, they failed to identify a correlation in normal controls, probably due to the low number of animals, to the sampled fields (the 30 fields per animal clearly contrasts with the 291 to 474 optical disectors we analysed), or to the biased nature of "numbers per area". Still, Grinko *et al* (1995) noted a significant correlation in pathological conditions: in biliary fibrosis, the number per area of KC was well correlated with that of periportal HSC. This bivalent kinetic of KC and HSC was also reported by other research groups, in that same model (Hines *et al*, 1993) and in the CCl_4 model of acute liver injury (Bouwens *et al*, 1986; Johnson *et al*, 1992). Moreover, it was also reported in liver regeneration studies (after a 70% partial hepatectomy), in which both cell types enter the DNA synthesis at 24 hours after HEP, having their peak activity at 48 hours (Budny *et al*, 2007). Interestingly, a strong ($r = 0.89$) correlation between KC and HSC number is also present in humans after moderate to severe (but not mild) paracetamol-induced liver necrosis (Mathew *et al*, 1994).

4.4.2- Age and gender study: 2) Ageing and KC

It is often difficult to correctly and unequivocally correlate functional assays with structural numerical information. For instance, increased phagocytosis can be due to an increased activity of the existing cell population, and/or to an expansion of the population of phagocytes. So far, conflicting results have been generated regarding phagocytosis *in vivo* for rats between 2 and 24 months of age. It has been reported to decrease (Nashat *et al*, 1985; Martin *et al*, 1994; Videla *et al*, 2001), be maintained (Vollmar *et al*, 2002), or increase (Yamano *et al*, 2000; Hilmer *et al*, 2007) with ageing. Data from *in vitro* studies points to a reduced endocytosis by KC (Brouwer *et al*, 1985). Most of these studies were based in the fraction of recovery of injected particles and the type of these may justify some discrepancy. It is generally accepted that particles under 100 nm pass through endothelial *fenestrae*, those between 100-500 nm are taken by LSEC, whereas those over 500 nm are phagocyted by KC (Dan and Wake, 1985). In the case of colloidal carbon injection (Nashat *et al*, 1985; Yamano *et al*, 2000; Videla *et al*, 2001), the contribution of LSEC should be considered, even if the scavenger activity of these cells has been reported to be reduced with ageing, at least in mice (Ito *et al*, 2006). Discrepancy may also result from strain differences or from gender: for instance Martin *et al* (1994) used female Sprague-Dawley rats, whilst all other studies used males (Sprague-Dawley or Fischer). In our study, with Wistar rats, we did not reveal very different ageing patterns between genders, namely when considering the N/g of KC, which did not vary with ageing. Despite in females the latter parameter seemed to decrease with ageing (for up to

26%), whereas in males it appeared to increase (19%), such trends were not statistically significant. (Eventually, our study had no power to achieve the statistical significance.)

To the best of our knowledge, the N of KC has never been evaluated throughout ageing. Martin *et al* (1992; 1994), reported that the V_V(KC, liver) is maintained in female Sprague-Dawley rats, hypothesising that the increased V_{KC} (*i.e.*, total volume of the KC compartment) is either due to increased cell size or increased cell numbers (note that the liver of old Sprague-Dawley rats is significantly larger than that of young ones). Apart from strain differences, our data favours the first hypothesis (*i.e.*, boosts of phagocytosis by a numerically stable KC population). The degradation of particles is said to occur more slowly in aged KC (Martin el al, 1994), so it is possible that cells would appear larger due to the accumulation of non-functional material in their cytoplasm. More recently, Hilmer *et al* (2007) reported a 3-fold increase in the number of KC with ageing, measured in "numbers per area", and using thin paraffin sections stained by haematoxylin-eosin. Those authors further reported a parallel increased in KC phagocytic activity with ageing. Major technical concerns can also be evoked to explain the differences: not only is the use of haematoxylin-eosin for quantification purposes is undoubtedly inadequate, causing uncontrolled bias in the counts, but also size differences (the larger KC in old animals) may (quite likely) lead to overestimations when using "numbers per area".

4.4.2- Age and gender study: 3) Gender and KC

Sexual dimorphism in KC function has been studied for long: peaks of phagocytic activity and proliferation of cells have been correlated with elevated oestrogen levels in the oestrous cycle of mice (Nicol *et al*, 1965). The same phenomenon occurs in rats: ethinylestradiol, a major component of numerous oral contraceptives, has been shown to induce a 5-fold increase in the proliferation of KC *in vitro* (Vickers and Lucier, 1996). These facts are not exactly in accordance to our data, because, for the same age, we only observed a greater N/g of KC in females at young age (increased $\approx$ 60% in females). (Significant differences in the N of KC existed, but these were mainly due to the scaling factor, *i.e.*, larger liver of male adult rats.) In any case, KC respond less to oestrogen when compared with HEP, because these cells have lower levels of ER (Vickers and Lucier, 1996, Eagon, 2010). Both cells have the two types of ER (α and β) (Vickers and Lucier, 1996; Shimizu *et al*, 2008), but they are different regarding androgen and progesterone receptors, which are absent in females (Spitzer, 1997).

Oestrogen appears to exert actions against both inflammation and oxidative stress, by inhibiting the production of pro-inflammatory tumour necrosis factor-α, interleukin-1β and -6 (Huang *et al*, 2008). Accordingly, data from *in vitro* studies has shown that oestrogen inhibits the synthesis and signal transduction of multiple cytokines (Straub, 2007) and

menopause is associated with spontaneous increases in the above mentioned cytokines in women (Pfeilschifter *et al*, 2002). Hospital records show that the severity and incidence of sepsis and post-surgery infections is reduced in women (Yokoyama et al, 2007) and animal studies have underlined gender dimorphism in trauma-haemorrhage models, with androgens being responsive for immunosuppression and oestrogens for protection properties in the liver (Choudhry *et al*, 2005; Shimizu *et al*, 2008). Although none of those studies quantified the (total or relative) number of KC, a recent study showed that female Wistar rats (as well as C57BL/6 mice) have ≈ 50% more macrophages in their pleural and peritoneal cavities (Scotland *et al*, 2011). Moreover, these authors demonstrated that female macrophages have more toll-like receptors, being more efficient in phagocytosis (these cells were associated with an increased population of resident T lymphocytes that prevented the excessive production of macrophage derived cytokines) (Scotland *et al*, 2011). Considering the classical data of Nicol *et al* (1965) (*i.e.*, an increased phagocytosis in oestrous) and ours, we may hypothesise that the periteoneal scenario also stands for the rat liver. Nevertheless, additional research is needed, in order to disclose differences in the cytokine profile (and in the population of lymphocytes). The next step in research should include an evaluation of gender differences in the population of $ED2^+$ KC, since a recent study by He *et al* (2009) showed that this population is functionally heterogeneous. Using fluorescence activated cell sorting, these authors revealed that some cells were highly phagocytic KC, producing interleukin-1β, MMP-9, and had an increased content of toll-like receptors, while another part of $ED2^+$ cells was formed by smaller and less phagocytic cells, which produced TIMP-1 (He *et al*, 2009).

It is also compelling to relate this gender dimorphism with the increased severity of alcohol liver disease in females. Using an enteric feeding model, Thurman (1998) showed that young female rats had an increased pathology score, more marked infiltration by neutrophils and higher endotoxin levels, which ultimately was responsible for a higher activation of KC, when compared with males (Thurman, 1998). These findings were confirmed by several research groups, that further showed an increased production of tumour necrosis factor-α and ROS in KC isolated from females fed a liquid diet with ethanol (Colantoni *et al*, 2000, Eagon, 2010). A classical study by McCuskey *et al* (1984) demonstrated a significant strong correlation ($r \approx 0.97$) between endotoxin sensitivity and the number of KC in various species, including rats. Several factors have been proposed for explaining the gender dimorphic response to alcohol, namely the hormonal dysfunction, the mitochondrial injury and oxidative stress, the altered enzyme activities (*e.g.* of CYP2E1) and the differences in gut permeability (Eagon, 2010). According to our

data, it is likely that quantitative differences in KC (at least at the young age) may also take part in this complex and intriguing equation.

In conclusion, in this Chapter we showed hitherto unknown features of KC, like their correlation with other liver cells throughout ageing, their co-localisation with HSC and their gender dimorphism in the N/g (at young age). However, we found no differences in quantitative parameters in the groups that presented the increased collagen deposition (*i.e.*, adults and old males). Overall, we are still far from a full understanding as to how and when gender matters regarding the KC fine structural and functional details.

4.5- References

Armbrust T, Ramadori G (1996) Functional characterization of two different Kupffer cell populations of normal rat liver. *Journal of Hepatology* 25: 518-528.

Barbé E, Damoiseaux JGMC, Döpp EA, Dijkstra CD (1990) Characterization and expression of the antigen present on resident rat macrophages recognized by monoclonal antibody ED2. *Immunobiology* 182, 88-99.

Biozzi G, Stiffel C (1965) The physiopathology of the reticuloendothelial cells of the liver and the spleen. In: *Progress in Liver Diseases*, *Volume 2* (Popper H, Scaffner F eds), pp. 166. Grune and Stratton.

Blaner WS, Hendriks HF, Brouwer A, De Leeuw A, Knook DL, Goodman DS (1985) Retinoids, retinoid-binding proteins, and retinyl palmitate hydrolase distributions in different types of rat liver cells. *Journal of Lipid Research* 26, 1241-1251.

Blouin A, Bolender RP, Weibel ER (1977) Distribution of organelles and membranes between hepatocytes and nonhepatocytes in rat liver parenchyma - A stereological study. *Journal of Cell Biology* 72, 441-455.

Bode JG, Peters-Regehr T, Gressner AM, Häussinger D (1998) De novo expression of glutamine synthetase during transformation of hepatic stellate cells into myofibroblast-like cells. *The Biochemical Journal* 335, 697-700.

Bode JG, Peters-Regehr T, Kubitz R, Häussinger D (2000) Expression of glutamine synthetase in macrophages. *Journal of Histochemistry & Cytochemistry* 48, 415-422.

Bouwens I, De Bleser P, Vanderkerken K, Geerts B, Wisse E (1992) Liver cell heterogeneity: functions of non-parenchymal cells. *Enzyme* 46, 155-168.

Bouwens L, Baekeland M, De Zanger R, Wisse E (1986) Quantification, tissue distribution and proliferation kinetics of Kupffer cells in normal rat liver. *Hepatology* 6, 718-722.

Brouwer A, Barelds RJ, Knook DL (1985) Age-related changes in the endocytic capacity of rat liver Kupffer and endothelial cells. *Hepatology* 5, 362-366.

Budny T, Palçmes D, Stratmann U, Minin E, Herbst H, Spiegl HU (2007) Morphological features in the regenerating liver – a comparative intravital, light microscopical and ultrastructural analysis with focus in hepatic stellate cells. *Virchows Archives* 451, 781-791.

Bykov I, Ylipaasto P, Eerola L, LIndros KO (2004) Functional differences between periportal and perivenous Kupffer cells isolated by digitonin-collagenase perfusion. *Comparative Hepatology* 3, S34.

Choudhry MA, Schwacha MG, Hubbard WJ, Kerby JD, Rue LW, Bland KI (2005) Gender differences in acute response to trauma-hemorrhage. *Shock* 24, 101-106.

Colantoni A, Paglia N, De Maria N, Emanuele MA, Emanuele NV, Idilman R, Harig J, Van Thiel DH (2000) Influence of sex hormonal status on alcohol-induced oxidative injury in male and female rat liver. *Alcoholism: Clinical and Experimental Research* 24, 1467-1473.

Daemen T, Veninga A, Regts J, Scherphof GL (1991) Maintenance of tumoricidal activity and susceptibility to reactivation of subpopulations of rat liver macrophages. *Journal of Immunotherapy* 10, 200-206.

Damoiseaux JGMC, Döpp EA, Calame W, Chao D, MacPherson GG, Dijkstra CD (1994) Rat macrophage lysosomal membrane antigen recognized by monoclonal antibody ED1. *Immunology* 83, 140-147.

Dan C, Wake K (1985) Modes of endocytosis of latex particles in sinusoidal endothelial and Kupffer cells of normal and perfused rat liver. *Experimental Cell Research* 158, 75-85.

De Minicis S, Seki E, Uchinami H, Kluwe J, Zhang Y, Brenner DA, Schwabe RF (2007) Gene expression profiles during hepatic stellate cell activation in culture and *in vivo*. *Gastroenterology* 132, 1937-1946.

Dijkstra CD, Döpp EA, Joling P, Kraal G (1985) The heterogeneity of mononuclear phagocytes in lymphoid organs: distinct macrophage subpopulations in the rat recognized by monoclonal antibodies ED1, ED2 and ED3. *Immunology* 54, 589-599.

Duffield JS (2003) The inflammatory macrophage: a story of Jekyll and Hyde. *Clinical Science* 104, 27-38.

Duffield JS, Forbes SJ, Constandinou CM, Clay S, Partolina M, Vuthoori S, Wu S, Lang R, Iredale JP (2005) Selective depletion of macrophages reveals distinct, opposing roles during liver injury and repair. *Journal of Clinical Investigation* 115, 56-65.

Durham SK, Brouwer A, Barelds RJ, Horan MA, Knook DL (1990) Comparative endotoxin-induced hepatic injury in young and aged rats. *The Journal of Pathology* 162, 341-349.

Eagon PK (2010) Alcoholic liver injury: influence of gender and hormones. *World Journal of Gastroenterology* 16, 1377-1384.

Emeis JJ, Planque B (1976) Heterogeneity of cells isolated from rat liver by pronase digestion: ultrastructure, cytochemistry and cell culture. *Journal of the Reticuloendothelial Society* 20, 11-29.

Faust N, Varas F, Kelly LM (2000) Insertion of green fluorescent protein into the lysozyme gene creates mice with green fluorescent granulocytes and macrophages. *Blood* 96, 719-726.

Fawcett DH (1994) Liver and gallbladder. In: *Bloom and Fawcett. A textbook of Histology, 12th edition*, pp. 652-688. Chapman and Hall.

Frevert U, Usynin I, Baer K, Klotz C (2007) Liver: Plasmodium sprozoite passage across the sinusoidal cell Layer. In: *Molecular Mechanisms of Parasite Invasion* (Burleigh B, Soldati D eds), pp. 3-16. Landes Bioscience.

Friedman SL, Arthur MJ (1989) Activation of cultured rat hepatic lipocytes by Kupffer cell conditioned medium. Direct enhancement of matrix synthesis and stimulation of cell proliferation via induction of platelet-derived growth factor receptors. *The Journal of Clinical Investigation* 86, 1780-1785.

Friedman SL (2008) Hepatic stellate cells: protean, multifunctional, and enigmatic cells of the liver. *Physiological Reviews* 88, 125-172.

Golbar HM, Izawa T, Murai F, Kuwamura M, Yamate J (2012) Immunohistochemical analyses of the kinetics and distribution of macrophages, hepatic stellate cells and bile duct epithelia in the developing rat liver. *Experimental and Toxicologic Pathology* 64, 1-8.

Gomes LF, Lorente S, Simon-Giavarotti KA, Areco KN, Araújo-peres C, Videla LA (2004) Tri-iodothyronine differentially induces Kupffer cell ED1/ED2 subpopulations. *Molecular Aspects in Medicine* 25, 183-190.

Grinko I, Geerts A, Wisse E (1995) Experimental biliary fibrosis correlates with increased numbers of fat-storing and Kupffer cells, and portal endotoxemia. *Journal of Hepatology* 23, 449-458.

Hardonk MJ, Dijkhuis FW, Hulstaert CE, Koudstaal J (1992) Heterogeneity of rat liver and spleen macrophages in gadolinium chloride-induced elimination and repopulation. *Journal of Leukocyte Biology* 52, 296-302.

Haschek WM, Rousseaux CG, Wallig MA (2010) The liver. In: *Fundamentals of Toxicologic Pathology, 2nd edition,* pp. 197-235. Academic Press.

Hendriks H, Horan M, Durham S, Earnest D, Brouwer A, Hollander C, Knook D (1987) Endotoxin-induced liver injury in aged and subacutely hypervitaminotic A rats. *Mechanisms of Ageing and Development* 41, 241-250.

He Y, Sadahiro T, Noh S-I, Wang H, Todo T, Chai N, Klein AS, Wu GD (2009) Flow cytometric isolation and phenotypic characterization of two subsets of $ED2^+$ (CD163) hepatic macrophages in rats. *Hepatology Research* 39, 1208-1218.

Heuff G, Steenbergen JJ, Van de Loosdrecht AA, Sirovich I, Dijkstra CD, Meyer S, Beelen RH (1993) Isolation of cytotoxic Kupffer cells by a modified enzymatic assay: a methodological study. *Journal of Immunology Methods* 159, 115-123.

Hilmer SN, Cogger VC, Le Couteur DG (2007) Basal activity of Kupffer cells increases with old age. *Journal of Gerontology series A, Biological Sciences and Medical Sciences* 62, 973-978.

Hines JE, Johnson SJ, Burt AD (1992) *In vivo* responses of macrophages and perisinusoidal cells to cholestatic liver injury. *American Journal of Pathology* 142, 511-518.

Hoedemakers RMJ, Vossebeld PJM, Daemen T, Scherphof GL (1993) Functional characteristics of the rat liver macrophage population after a single intravenous injection of liposome-encapsulated muramyl peptides. *Journal of Immunotherapy* 13, 252-260.

Hoedemakers RMJ, Atmosoerdjo-Briggs JA, Morselt HWM, Daemen T, Scherpof GL, Hardonk MJ (1995) Histochemical and electron microscopic characterization of hepatic macrophage subfractions isolated from normal and liposomal muramyl dipeptide treated rats. *Liver* 15, 113-120.

Howard CV, Reed MG (2005) Number estimation. In: *Unbiased Stereology. Three-dimensional measurement in microscopy*, *2nd edition*, pp. 65-99. Garland Science/Bios Scientific Publishers.

Huang H, He J, Yuan Y, Aoyagi E, Takenaka H, Itagaki T, Sannomiya K, Tamaki K, Harada N, Shono M, Shimizu I, Takayama T (2008) Opposing effects of estradiol and progesterone on the oxidative stress-induced production of chemokine and proinflammatory cytokines in murine peritoneal macrophages. *Journal of Medical Investigation* 55, 133-141.

Ide M, Yamate J, Machida Y (2002) Macrophage populations, myofibroblastic cells, and extracelular matrix accumulation in chronically-developing rat liver cirrhosis induced by repeated injection of thioacetamide. *Journal of Toxicological Pathology* 15, 19-29.

Ito Y, Sørensen KK, Bethea NW, Svistounov D, McCuskey MK, Smedsrød BH, McCuskey RS (2006) Anatomy of the liver. In: *Zakim and Boyer's Hepatology. A textbook of liver disease, 5th edition* (Boyer TD, Wright TL, Manns MP eds), pp. 3-21. Saunders.

Johnson SJ, Hines JE, Burt AD (1992) Phenotypic modulation of perisinusoidal cells following acute liver injury: a quantitative analysis. *International Journal of Experimental Pathology* 73, 765-772.

Johnson SJ, Burr AW, Toole K, Dack CL, Mathew J, Burt AD (1998) Macrophage and hepatic stellate responses during hepatocarcinogenesis. *Journal of Gastroenterology and Hepatology* 13, 145-151.

Kiki I, Altunkaynak B Z, Altunkaynak M E, Vuraler O, Unal D, Kaplan S (2007) Effect of high fat diet on the volume of liver and quantitative features of Kupffer cells in the female rat: a stereological and ultrastructural study. *Obesity Surgery* 17, 1381-1388.

Kmiec Z (2001) Cooperation of liver cells in health and disease. *Advances in Anatomy, Embryology and Cell Biology* 161, 1-151.

Kono H, Fujii H, Asakawa M (2002) Functional heterogeneity of the Kupffer cells population is involved in the mechanism of gadolinium chloride in rats administered endotoxin. *Journal of Surgery Research* 106, 179-187.

Kuiper J, Brouwer A, Knook DL, Van Berkel TJ (1994) Kupffer and sinusoidal endothelial cells. In: *The liver: biology and pathobiology, 3rd edition* (Arias IM, Boyer JL,

Fausto N, Jakoby WB, Schachter DA, Shafritz DA eds), pp. 791-809. Raven Press Ltd.
Kumagai K, Kiyosawa N, Ito K, Yamoto T, Teranishi M, Nakayama H, Manabe S (2007) Influence of Kupffer cell inactivation on cycloheximide-induced hepatic injury. *Toxicology* 241, 106-118.
MacPhee PJ, Schmidt EE, Groom AC (1992) Evidence for Kupffer cell migration along liver sinusoids, from high-resolution *in vivo* microscopy. *American Journal of Physiology* 263, G17-23.
Marcos R, Monteiro R A F, Rocha E (2004) Estimation of the number of stellate cells in a liver with the smooth fractionator. *Journal of Microscopy* 215, 174-182.
Marcos R, Monteiro RA, Rocha E (2006) Design-based stereological estimation of hepatocyte number, by combining the smooth optical fractionator and immunocytochemistry with anti-carcinoembryonic antigen polyclonal antibodies. *Liver International* 26, 116-124.
Martin G, Sewell RB, Yeomans ND, Morgan DJ, Smallwood RA (1994) Hepatic Kupffer cell function: the efficiency of uptake and intracellular degradation of 14C-labelled mitochondria is reduced in aged rats. *Mechanisms of Ageing and Development* 73, 157-168.
Mathew J, Hines JE, James OFW, Burt AD (1994) Non-parenchymal cell responses in paracetamol (acetaminophen) induced liver injury. *Journal of Hepatology* 20, 537-541.
McCuskey RS, McCuskey PA, Urbaschek R, Urbaschek B (1984) Species differences in Kupffer cells and endotoxin sensitivity. *Infection and Immunity* 45, 278-280.
McCuskey RS (2007) Age-related changes in the hepatic microcirculation in mice. *Experimental Gerontology* 42, 789-797.
McCuskey (2008) The hepatic microvascular system in health and in response to toxicants. *The Anatomical Record* 291, 661-671.
Meyer DH, Bachem MG, Gressner AM (1990) Transformed fat storing cells inhibit the proliferation of cultured hepatocytes by secretion of transforming growth factor beta. *Journal of Hepatology* 11, 86-91.
Naito M, Hasegawa G, Ebe Y, Yamamoto T (2004) Differentiation and function of Kupffer cells. *Medical Electron Microscopy* 37, 16-28.
Naito M, Takahashi K (1991) The role of Kupffer cells in glucan-induced granuloma formation in the liver of mice depleted of blood monocytes by administration of strontium-89. *Laboratory Investigation* 64, 664-674.
Nashat KH, Slater DN, Underwood JC, Triger DR, Woods HF (1985) Phagocytic function in the isolated perfused rat liver. An experimental model. *Journal of Hepatology* 1, 153-166.

Nicol T, Veron-Roberts B (1965) The influence of the estrus cycle, pregnancy and ovariectomy on RES Activity. *Journal of the Reticuloendothelial Society* 60, 15-29.

Olynyk JK, Clarke SL (1998) Isolation and primary culture of rat Kupffer cells. *Journal of Gastroenterology and Hepatology* 13, 842-845.

Pfeilschifter J, Köditz R, Pfohl M, Schatz H (2002) Changes in proinflammatory cytokine activity after menopause. *Endocrine Reviews* 23, 90-119.

Pinzani M, Rombouts K, Colagrande S (2005) Fibrosis in chronic liver diseases: diagnosis and management. *Journal of Hepatology* 42, S22-S36.

Racanelli V, Rehermann B (2006) The liver as an immunological organ. *Hepatology* 43, S54-S62.

Ramachandran P, Iredale JP (2012) Macrophages: central regulators of hepatic fibrogenesis and fibrosis resolution. *Journal of Hepatology* 56, 1417-1419.

Roskams T, Desmet VJ, Verslype C (2007) Development, structure and function of the liver. In: *MacSween's pathology of the liver, 5th edition* (Burt A, Portmann B, Ferrell L eds), pp 1-73. Churchill Livingstone.

Santos M, Marcos R, Santos N, Malhão F, Monteiro RAF, Rocha E (2009) An unbiased stereological study on subpopulations of rat liver macrophages and on their numerical relation with the hepatocytes and stellate cells. *Journal of Anatomy* 214, 744-751.

Schmitz C, Hof PR (2000) Recommendations for straightforward and rigorous methods of counting neurons based on a computer simulation approach. *Journal of Chemical Neuroanatomy* 20, 93-114.

Scotland RS, Stables MJ, Madalli S, Watson P, Gilroy DW (2011) Sex differences in resident immune cell phenotype underlie more efficient acute inflammatory responses in female mice. *Blood* 118, 5918-5927.

Senoo H, Yoshikawa K, Morii M, Miura M, Imai K, Mezaki Y (2010) Hepatic stellate cell (vitamin A-storing cell) and its relative — past, present and future. *Cell Biology International* 34, 1247-1272.

Shi SR, Cote RJ, Taylor CR (2001) Antigen retrieval techniques: current perspectives. *Journal of Histochemistry & Cytochemistry* 49, 931-937.

Shimizu T, Suzuki T, Yu HP, Yokoyama Y, Choudhry MA, Bland KI, Chaudry IH (2008) The role of estrogen receptor subtypes on hepatic neutrophil accumulation following trauma-hemorrhage: direct modulation of CINC-1 production by Kupffer cells. *Cytokine* 43, 88-92.

Sleyster EC, Knook DL (1982) Relation between localization and function of rat liver Kupffer cells. *Laboratory Investigation* 47, 484-490.

Spitzer JA (1997) Ceramide inhibits nitric oxide production in alveolar macrophages of endotoxin and ethanol plus endotoxin-treated rats. *Biochemical and Biophysical Research Communications* 234, 738-741.

Steib CJ, Gerbes AL (2010) Signaling pathways in liver diseases Kupffer cells. In: *Signaling Pathways in liver diseases* (Dufour J-F, Clavien P-A eds), pp. 69-78. Springer-Verlag.

Sugihara S, Martin SR, Hsuing CK, Maruiwa M, Bloch KJ, Mosciki RA, Bhan AK (1990) Monoclonal antibodies to rat Kupffer cells. Anti-KCA-1 distinguishes Kupffer cells from other macrophages. *American Journal of Pathology* 136, 345-355.

Takeishi T, Hirano K, Kobayashi T, Hasegawa G, Hatakeyama K, Naito M (1999) The role of Kupffer cells in liver regeneration. *Archives of Histology and Cytology* 62, 413-422.

Thompson K C, Trowern A, Fowell A, Marathe M, Haycock C, Arthur MJ, Sheron N (1998) Primary rat and mouse hepatic stellate cells express the macrophage inhibitor cytokine interleukin-10 during the course of activation in vitro. *Hepatology* 28, 1518-1524.

Thurman RG (1998) Alcoholic liver injury involves activation of Kupffer cells by endotoxin. *American Journal of Physiology* 275, G605-G611.

Tsukamoto H, Lin M (1997) The role of Kupffer cells in liver injury. In: *Cells of the hepatic sinusoid, Volume 6* (Wisse E, Knook DL, Balabaud C eds), pp. 244-250. Kupffer Cell Foundation.

Valatas V, Xidakis C, Roumpaki H, Kolios G, Kouroumalis EA (2003) Isolation of rat Kupffer cells: a combined methodology for highly purified primary cultures. *Cell Biology International* 27, 67-73.

Vickers AE, Lucier GW (1996) Estrogen receptor levels and occupancy in hepatic sinusoidal endothelial and Kupffer cells are enhanced by initiation with diethylnitrosamine and promotion with 17 alpha-ethinylestradiol in rats. *Carcinogenesis* 17, 1235-1242.

Videla LA, Tapia G, Fernández V (2001) Influence of aging on Kupffer cell respiratory activity in relation to particle phagocytosis and oxidative stress parameters in mouse liver. *Redox Report: Communications in Free Radical Research* 6, 155-159.

Vollmar B, Pradarutti S, Richter S, Menger MD (2002) *In vivo* quantification of ageing changes in the rat liver from early juvenile to senescent life. *Liver* 22, 330-341.

Von Kupffer C (1899) Ueber die sogennanten Sternzellen der Säugethierleber. *Archives Mikroscopie und Anatomie* 54, 254-288.

Wisse E (1974) Observations on the fine structure and peroxidase cytochemistry of normal rat liver Kupffer cells. *Journal of Ultrastructure Research* 46, 393-426.

Xidakis C, Ljumovic D, Manousou P Notas G, Valatas V, Kolios G, Kouroumalis E (2005) Production of pro- and anti-fibrotic agents by rat Kupffer cells; the effect of octreotide. *Digestive Diseases Sciences* 50, 935-941.

Yamano T, DeCicco LA, Rikans LE (2000) Attenuation of cadmium-induced liver injury in senescent male Fischer 344 rats: role of Kupffer cells and inflammatory cytokines. *Toxicology and Applied Pharmacology* 162, 68-75.

Yin L, Lynch D, Sell S (1999) Participation of different cell types in the restituitive response of the rat liver to periportal injury induced by allyl alcohol. *Journal of Hepatology* 31, 497-507.

Yokoyama Y, Nagino M, Nimura Y (2007) Which gender is better positioned in the process of liver surgery? Male or female? *Surgery Today* 37, 823-830.

Chapter 5 – Conclusions and future perspectives

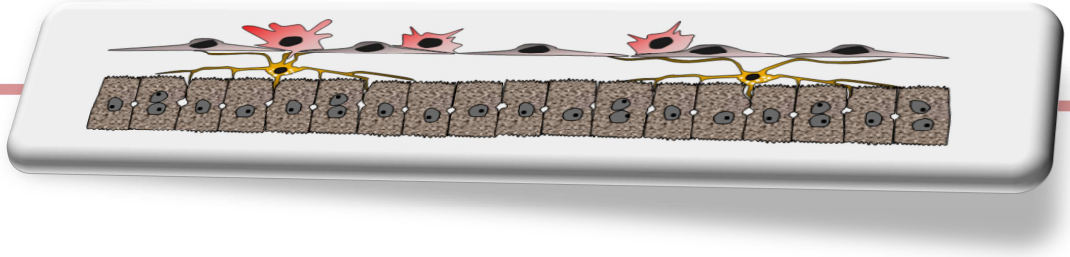

5- Conclusions and future perspectives

5.1- Overview of cell populations and summary of the data

The numerical proportions of HSC, HEP (MnHEP and BnHEP) and KC, remained stable throughout the studied ageing period (Figure 5.1). Females tended to have more HEP and BnHEP (as detailed in Chapter 3, this difference was statistically significant in young animals), as well as an increase number of KC (differences also in young animals, as stressed in Chapter 4). On the contrary, HSC were equally abundant throughout ageing and gender (Chapter 2).

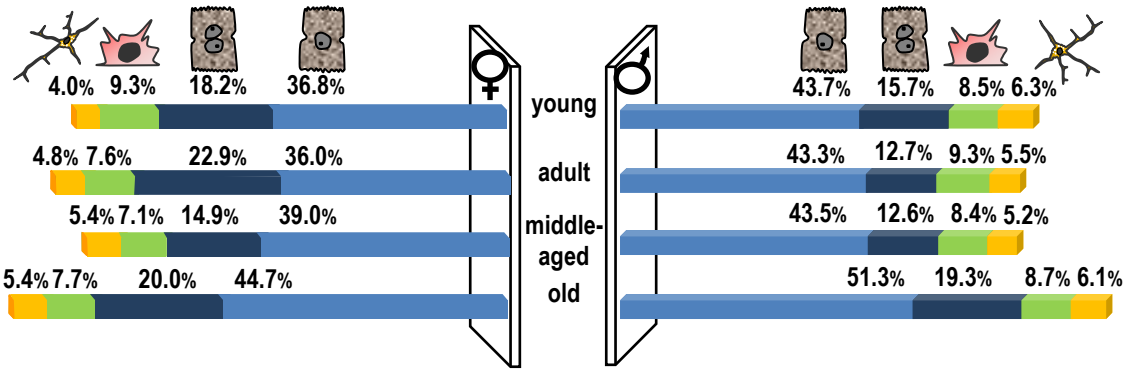

Figure 5.1 – Percentages (in relation to the total number of liver cells) of hepatocytes [mononucleated (■) and binucleated (■)], Kupffer cells (■), and hepatic stellate cells (■), in male and female young (2 months), adult (6 months), middle-aged (12 months), and old (18 months) rats. The remaining part of 100% corresponds to liver sinusoidal endothelial cells, as well as stromal cells.

It is curious that gender differences existed mostly in young animals. This was the case for HEP and KC, in a lesser extent, but not for HSC. This can be due, at least partially, to differences in the ER of each cell: for instance, HEP and KC have ER-α, whereas HSC only have ER-β, namely in young male and female rats (Zhou *et al*, 2001). This research group showed cytoprotective effects, due to the over-expression of Bcl-2 and apoptosis prevention, as well as anti-proliferative actions of oestradiol *in vitro* (Yasuda *et al*, 1999; Zhou *et al*, 2001). Our finding that the N/g of HSC is highly stable throughout ageing, and between genders, is suggestive that those anti-proliferative actions are conserved during the lifespan of rodents. As detailed in Chapter 2, the facts contradicted our initial hypothesis that gender and ageing differences would exist in those cells. It is interesting and biologically challenging that the normal ageing process did not elicit either activation or sustained proliferative responses in HSC. Nevertheless, ageing was mirrored in collagen deposition — with unexpected gender differences in this regard. As expressed in Chapter 3, we first hypothesised that these could be due to a higher generation of ROS in

aged males. Again, this was only partially verified: if it is true that older animals generate more ROS, females seemed to have a greater production. In future studies we will explore another hypothesis: that males have a decreased activity of MMP and/or an increase action of their inhibitors (TIMP).

Another surprising finding was that ageing attenuated most cytological differences in liver cells: for instance, the HSCI, the N/g and the cell $\overline{v}_N$ of HEP, the N/g and percentage of BnHEP, as well as the N/g of KC. In order to strength this conclusion, and to further put forward the parameters truly influenced by ageing (Table 5.1), we plan to analyse 24 months animals, both males and females. (These are currently being aged and will be collected in March of 2013.) To the best of our knowledge, such a gender approximation trend has never been revealed by quantitative methods, but it actually follows a well characterised pattern for enzymatic activities (Kitani, 2007). It has been known for long that CYP has a higher activity in males and that a “feminization” occurs with ageing: the activity in male liver is completely overlapped with that of old (24 months) female Fischer rats (Kitani, 1992). More recently, an exhaustive micro-array gene expression study with that rat strain highlighted a similar trend, because gene differences occurred mostly between young and adults — by middle-aged they decreased and were completely abolished in old animals (Kwekel *et al*, 2010).

The reason for this attenuation in the liver is as obscure as the mechanism behind gender dimorphism itself (Yokoyama *et al*, 2007; Villa, 2008). Two leading actors have been pointed and eventually they can share the stage. Growth hormone is one and it is known for long that the levels of this hormone decline with ageing, resulting in the somatopause of various mammals, including rats (Sonntag *et al*, 1980; Bartke, 2008). More recently, it was shown that levels of insuline-like growth factor-1 (the efector mollecule of growth hormone) were reduced in the plasma of old males, but not in females (Castillo *et al*, 2004). The other actor is oestrogen; their levels tend to be maintained in rats: a certain degree of secretion exists until latter life of females (Vom Saal *et al*, 1994) — as we observed in our set of rats (Figure 2.19, in Chapter 2). This does not mean that oestrogen has no role, since a variation in ER throuhout ageing has been proposed (Eagon *et al*, 1985), but never evaluated in detail. Some controversy still exists regarding the content and location of ER in males *versus* females (Eagon *et al*, 1985; Villa, 2008). By its intrinsic unbiased nature, “design-based” stereology would be the tool of choice to evaluate this.

It would also be interesting to include ovariectomised females in that analysis (in this vein, we plan to focus our attention in the study of ER and in the dimorphic parameters here highlighted). Indeed, because ovariectomised rats have been used extensively to withstand oestrogenic actions (which are almost absent in those animals, being repaired

with oestrogenic supplementation), we should explain why such models were not included herein in the first place. Castrated animals were rarely studied by stereology: to the best of our knowledge only two papers focused this issue, but reaching to opposite conclusions (Dursun *et al*, 2010; Trujillo *et al*, 2011). So, it would be logical to first gather data in normal conditions, knowing which parameters were dimorphic, before going to the castration model. Moreover, ER have been reported to increase substantially (both in cytosol and nuclei) in castrated animals, meaning that these animals have an enhanced response to oestrogen supplementation (Eagon *et al*, 1985). As far as we know, data about ER and stereological parameters were never compared between normal males and females *versus* castrated animals.

Table 5.1- Overview of the structural and functional parameters that were significantly influenced by gender and ageing factors in the studied rats (each isolated factor was considered as significant when $p < 0.05$, under the two-way ANOVA analysis).

	Gender influences	Ageing influences
Liver 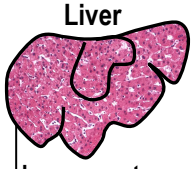	Body weight Liver weight	Body weight Liver weight Liver-body ratio
homogenates →	Reactive oxygen species and antioxidant activity (catalase, glutathione peroxidase, glutathione-S-transferase).	Reactive oxygen species and antioxidant activity (catalase, glutathione-S-transferase).
histological slides →	Collagen deposition	Collagen deposition
Hepatic stellate cells 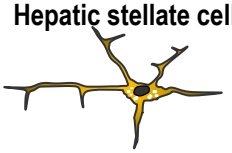	Total number Total volume Hepatic stellate cell index	Relative volume of perikaryon Lobular distribution
Hepatocytes 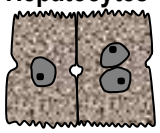	Total number Number per gram Numerical density Mean number-weighted cell volume Percentage of binuclear cells	Increased polyploidy Number per gram Mean volume-weighted cell volume
Kupffer cells 	Total number Number per gram Numerical density Co-localisation with hepatic stellate cells	Numerical density

As we stressed throughout this Thesis, the approach to reveal morphological ageing differences should be as quantitative and unbiased as possible, because the qualitative descriptive morphology alone may overlook some important structural features. Overall, the data summarised in Table 5.1, substantiates the notion that the liver ages fairly well. Even so, we should emphasise some features that occurred in our set of rats: 1) The increase of polyploidy in HEP — this is a well known age related change of the liver of rodents (Roskams *et al*, 2007). 2) The rise in the N/g of HEP, namely in males, is a new finding, that has never been reported, to the best of our knowledge. 3) The enlargement of HSC perikaryon with ageing has been previously suggested (Martin *et al*, 1992) but never proved; herein we established that it occurred in males and females. 4) The increase of liver collagen has already been shown in aged males (Porta *et al*, 1981; Gagliano *et al*, 2002), but it has never been demonstrated to be a dimorphic characteristic. 5) The shift in the lobular distribution of HSC in males and females is another hitherto unknown feature.

Although liver cells look homogeneous at light microscopy, they are functionally heterogeneous, according to their lobular position. The study of lobular heterogeneity has more than an academic relevance, because different properties of liver cells can help explaining the regional distribution of lesions and susceptibility to hepatotoxicants (Malarkey *et al*, 2005) and the loss of zonal heterogeneity has been recognised for long as a first step in the malignant transformation to hepatocellular carcinoma (Jungermann and Katz, 1982). As detailed in Chapter 2, lobular heterogeneity of HSC has never been highlighted, nor evaluated throughout ageing. In future studies we will establish if it is due a lower content of GFAP (qualitatively this seems unlikely, since the relative volume assessed by GFAP was relatively constant throughout ageing), or if it really takes place in both genders. In this vein, we plan to use molecular biology techniques (western blots and/or reverse-transcriptase polymerase chain reaction) to exclude the eventual loss of GFAP. Afterwards, we will explore two other hypotheses detailed in the Chapter 2, *i.e.*, that HSC are proliferating in periportal areas or that cells are moving due to changes in ECM composition.

5.2- Gender dimorphism: the Prometheus wife

The Promethean myth is mandatory in lectures on liver regeneration, and people continue to be fascinated by the tale of a giant and mighty eagle that daily, or on alternate days, tore out and devoured the liver of Prometheus, defenceless chained to a crag in the Caucasus Mountains. Since the organ regenerated overnight, the punishment for stealing fire from gods was deemed to be eternal; if it was not the case that Hercules, 30000 years later, killed the eagle and released Prometheus from the chains. Twenty-seven centuries later, Higgins and Anderson (1931) published the first experimental model on liver

regeneration, confirming the forecasts of ancient mythographers: after removing two-thirds of the liver in rodents, the organ reached full size by 3 days. Although there is yet no convincing evidence that ancient Greeks had any specific knowledge about liver regeneration, the tale is remarkably precise. It was even calculated that the eagle could indeed live from the ingested calories of Prometheus liver (Reuben, 2004; Tiniakos *et al*, 2010)! Taking the (extreme) audacity of adulterating that classical tale, and the high risk of extrapolating data from rodents to humans, our work globally suggests that an alternative version of the Promethean myth starred by Hesione (Prometheus wife according to Greek tragedy of Aeschylus) could also take place, and could even be more accurate. Even before the continuous insult by the eagle, Hesione's liver would have less collagen (and lower amounts would be deposited during the chronic injury). By having an increased number of HEP, with more diploid particles, her liver would regenerate faster. Finally, by having more KC, her liver would respond better to the recurring bacterial infection caused by the eagle's beak.

In this Thesis, we highlighted gender differences in a triumvirate of liver cells responsible for collagen deposition, regeneration and phagocytic responses. In Chapter 2 we established that female rats present less collagen deposition, eventually due to a lower expression of TIMP-1. This will be further studied by us, using molecular biology techniques. In Chapter 3 we highlighted differences in the N/g of HEP, in the size of MnHEP, in the N of BnHEP (that can rapidly divide to form diploid MnHEP) and in the diploid nuclei of young females, facts that, hypothetically, could be traduced in a more rapid and efficient liver regeneration. Finally, in Chapter 4 we disclosed differences in KC, which were more abundant in young females, which, again hypothetically, could provide a stronger and/or more prompt phagocytic immune reaction.

According to our data it is possible to differentiate the liver of young males and females at the microscope, using stereological tools. Even if this may look an out of the box issue, it has been recognised that there is a lack of knowledge regarding gender differences of rodents and even when a disease is predominant in females, biomedical research is made mainly in male animals (Kim *et al*, 2010). It is often assumed that no organ differences exist, but according to our data this is not the case for the liver. Our finding that young females have more HEP and KC has functional relevance, and this gender dimorphism should be considered in biomedical and pharmaceutical research (especially in drug development).

Our work suggests that some of the potential mechanisms of action of oestrogens, known to attenuate hepatic stress induced changes (Yokoyama *et al*, 2005), may also take place in the normal non-stressful conditions of ageing (Figure 5.2). At a first glance, our data regarding oxidative stress may seem contradictory, but it should be noted that we only

studied liver homogenates, and not isolated cells. So the contribution of ROS by more abundant and active female HEP does not exclude that oestradiol may reduce the ROS generation by KC. Additionally, it is possible that such a reduction does not take place in normal ageing conditions, being only relevant in a pathological setting, in which ROS generation by KC is of uttermost importance.

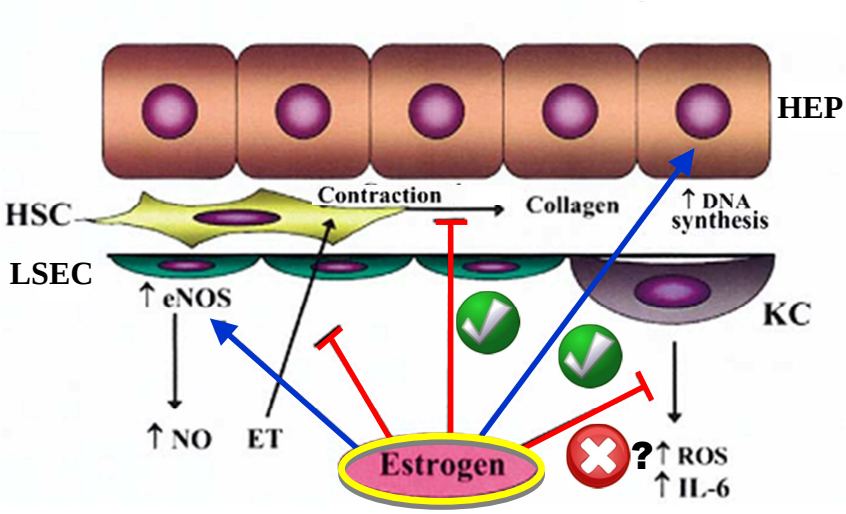

Figure 5.2- Potential mechanisms of oestrogenic stimulus in attenuating the hepatic stress-induced changes and correspondence with data gathered in this study. Blue and red arrows refer to promotional and blocking effects, respectively. Data from the present study is placed next to the arrows (☑ in accordance, ☒ partially contradictory?). HSC: hepatic stellate cells; HEP: hepatocytes; LSEC: liver sinusoidal endothelial cells; KC: Kupffer cells; ET: endothelin; NO: Nitric oxide; NOS: NO synthase; ROS: reactive oxygen species; IL-6: interleukin-6. [Adapted from Yokoyama *et al* (2005), with the author's permission.]

As stressed above, it is risky to extrapolate data from rats to humans, *i.e.*, from a species recognised as highly dimorphic to a lower dimorphic one. Therefore, it would be relevant to evaluate if the dimorphic parameters we observed (*e.g.*, collagen deposition, theoretical higher regeneration potential of HEP) are also valid for the normal ageing process of humans — even if ethical constrains and scarcity of material then become major issues. The existing data in humans seems to favour the extrapolation, since liver stiffness, measured by transient elastography, in normal healthy persons (between 18 and 79 years) was higher in men than in women (Corpechot *et al*, 2006), thus suggesting an higher collagen content of the male liver. Moreover, clinical studies have shown that men have reduced lobe hypertrophy (of the non-embolised lobe) and increased complications after portal vein embolization (Imamura *et al*, 1999; Yokoyama *et al*, 2008).

5.3- Is there a functional liver lobule?

As mentioned in Chapter 1, and despite it may be viewed as an overstatement, the liver has been considered second only to brain in its functional complexity (Malarkey *et al*,

2005), not only because of the plethora of organ functions but because its cells are intimately related: several factors synthesised by sinusoidal cells, including HSC and KC, exert profound effects on themselves (autocrine action) and in neighbouring cells (either by releasing soluble factors, paracrine effects, or by acting through cell contacts, juxtacrine effects). This has been elucidated in a great detail by experimental models of liver injury, research in bioartificial liver systems, and *in vitro* studies. These have emphasised the crosstalk between the triumvirate of cell types we studied here. For instance, it has been shown that HEP functions are better maintained in a culture with direct contacts with NHC and that a heterogeneous population of these produce better results than a single cell type of NHC (Ries *et al*, 2000; Krause *et al*, 2009). Moreover, the proliferation of HEP is induced by different cells: HSC account for about half of the stimulus *in vitro* (Tateno *et al*, 2000) and KC are also implicated, at least by secreting the hepatocyte growth factor (Masumoto and Yamamoto, 1993). More recently, an elegant study in liver regeneration proved that HEP cell alignment is determined by the existing endothelial tubes (Hoehme *et al*, 2010).

Paradoxically, the role of cell interactions under normal conditions is far less understood than in the pathological setting, probably because precise methods for the investigation of normal liver cell function and architecture have been lacking (Kmiec, 2001; Rojkind *et al*, 2011). In this vein, it is noteworthy that the N of the different liver cells studied by us was significantly correlated under normal conditions — this has never been reported, to the best of our knowledge. (In the baseline study we failed to reach a level of significance, as the correlations were restricted just to 5 rats, but in the age and gender study these were revealed.) In our study, we have estimated that the porto-central axis is composed of 16-18 HEP and that these are related with a defined number of HSC and KC (Figure 5.3).

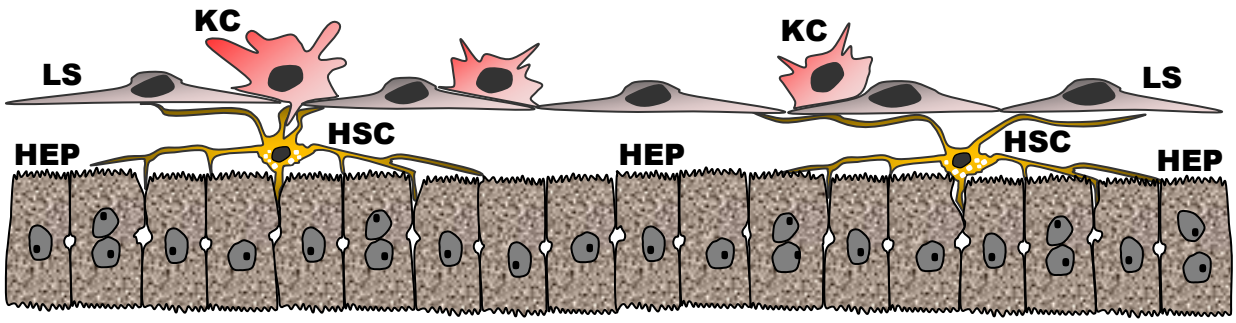

Figure 5.3 - Proposed microarchitecture of a liver cord and respective sinusoid (only half is represented). Except for liver sinusoidal endothelial cells (LSEC) (not quantified herein), all the cells are represented according to the proportions observed in the young male [cell cord composed of 18 hepatocytes (HEP)]. HSC: hepatic stellate cells; KC: Kupffer cells.

The cell-to-cell correlations support the existence of functional hepatic lobules, which are maintained throughout ageing and gender. As expressed in Chapter 1, the primary lobule proposed thirty years ago has gained acceptance as a functional unit in the liver (Matsumoto and Kawakami, 1982; Roskams *et al*, 2007; McCuskey, 2008; Vollmar and Menger, 2009). These primary lobules were renamed as “hepatic microvascular subunits”, since it was demonstrated that they consist of a group of sinusoids supplied by a single inlet venule, and have a terminal branch of the hepatic arteriole (McCuskey, 2008). Recently, it was hypothesised that functional liver units, with defined cell ratios of HEP and liver sinusoidal cells may exist in the liver (Rojkind *et al*, 2011). Our study definitively supports the existence of such units, and, instead of the “hepatic microvascular subunits”, we propose a new concept: the “hepatic microvascular cell plate subunits”. This concept emphasises that cells surrounding LSEC are strictly related, having established juxtacrine effects and defined cell ratios (Figure 5.3). We have not quantified their number, but it is likely that they would be as correlated with HEP as HSC are. [HEP and HSC presented one of the tightest correlation of our study ($r = 0.73$) — which was only supplanted by the correlation of body and liver weight.] As we previously mentioned, a recent study showed that LSEC are determinants for liver cell microarchitecture (Hoehme *et al*, 2010). According to our data, the proposed “hepatic microvascular cell plate subunits” should behave like a “melodious orchestra”, having a bandmaster and a first violin, respectively LSEC and HSC in this metaphor, and a defined number of cord and metal instruments (HEP and KC). As long as the fundamental structure is maintained (like in the remnant liver lobules after partial hepatectomy), the LSEC conserved, and the cell ratios between HSC and HEP preserved within certain limits, a melodious symphony is played — *i.e.*, regeneration will still take place without significant fibrosis. In contrast, when cell ratios are markedly altered or LSEC destroyed, the orchestra will be tuneless and scar formation will prevail.

In conclusion, we expanded the meagre knowledge about the microarchitecture and general organisation of liver lobules of the rat throughout ageing and gender. Our quantitative structural data supports the existence of a morphofunctional organisation, with a cell-chain unit that may play an important role in the intercellular cross talk. This organisation is maintained throughout ageing, but gender differences exist in the normal organ; these should be taken in account in various pathological conditions. Overall, this stereology based approach has opened new avenues that will be followed by us in future studies, for instance using molecular biology strategies. Besides shedding a new light over the liver ageing, the quantitative data here gathered will also be relevant to better interpret the evolution of liver fibrosis, hepatic regeneration and alcoholic liver disease. In

this context, it was stressed that it is imperative to perceive whether the gender dimorphic pattern here established in the rat also takes place in the human liver.

5.4 - References

Bartke A (2008) Growth hormone and aging: a challenging controversy. *Clinical Interventions in Aging* 3, 659-665.

Castillo C, Salazar V, Ariznavarreta C, Vara E, Tresguerres JA (2004) Effect of recombinant human growth hormone on age-related hepatocyte changes in old male and female Wistar rats. *Endocrine* 25, 33-39.

Corpechot C, El Naggar A, Poupon R (2006) Gender and the liver: is the liver stiffness weaker in the weaker sex? *Hepatology* 44, 513-514.

Eagon PK, Porter LE, Francavilla A, DiLeo A, Van Thiel DH (1985) Estrogen and androgen receptors in liver: their role in liver disease and regeneration. *Seminars in Liver Disease* 5, 59-69.

Gagliano N, Arosio B, Grizzi F, Masson S, Tagliabue J, Dioguardi N, Vergani C, Annoni G (2002) Reduced collagenolytic activity of matrix metalloproteinases and development of liver fibrosis in the ageing rat. *Mechanisms of Ageing and Development* 123, 413-425.

Dursun H, Albayrak F, Uyanik A, Keleş NO, Beyzagül P, Bayram E, Halici Z, Altunkaynak ZB, Süleyman H, Okçu N, Ünal B (2010) Effects of hypertension and ovariectomy on rat hepatocytes. Are amlodipine and lacidipine protective? (A stereological and histological study). *The Turkish Journal of Gastroenterology* 21, 387-395.

Higgins JM, Anderson RM (1931) Experimental pathology of the liver. I. Restoration of the liver of the white rat following partial surgical removal. *Archives of Pathology* 12, 186–202.

Hoehme S, Brulport M, Bauer A, Bedawy E, Schormann W, Hermes M, Puppe V, Gebhardt R, Zellmer S, Schwarz M, Bockamp E, Timmel T, Hengstler JG, Drasdo D (2010) Prediction and validation of cell alignment along microvessels as order principle to restore tissue architecture in liver regeneration. *Proceedings of the National Academy of Sciences of the United States of America* 107, 10371-10376.

Imamura H, Shimada R, Kubota M, Matsuyama Y, Nakayama A, Miyagawa S, Makuuchi M, Kawasaki S (1999) Preoperative portal vein embolization: an audit of 84 patients. *Hepatology* 29, 1099-1105.

Jungermann K, Katz N (1982) Functional hepatocellular heterogeneity. *Hepatology* 2, 385-395.

Kim AM, Tingen CM, Woodruff TK (2010) Sex bias in trials and treatment must end. *Nature* 465, 688-689.

Kitani K (1992) Liver and aging. *Gastroenterologia Japonica* 27, 276-285.

Kitani K (2007) What really declines with age? The Hayflick Lecture for 2006 35th American Aging Association. *Age* 29, 1-14.

Kmiec Z (2001) Cooperation of liver cells in health and disease. *Advances in Anatomy, Embryology and Cell Biology* 161, 1-151.

Krause P, Saghatolislam F, Koenig S, Unthan-Fechner K, Probst I (2009) Maintaining hepatocyte differentiation in vitro through co-culture with hepatic stellate cells. *In Vitro Cellular & Developmental Biology. Animal* 45, 205-212.

Kwekel JC, Desai VG, Moland CL, Branham WS, Fuscoe JC (2010) Age and sex dependent changes in liver gene expression during the life cycle of the rat. *BMC Genomics* 11, 675.

Malarkey DE, Johnson K, Ryan L, Boorman G, Maronpot RR (2005) New insights into functional aspects of liver morphology. *Toxicological Pathology* 33, 27–34.

Martin G, Sewell RB, Yeomans ND, Smallwood RA (1992) Ageing has no effect on the volume density of hepatocytes, reticulo-endothelial cells or the extracellular space in livers of female Sprague-Dawley rats. *Clinical and Experimental Pharmacology & Physiology* 19, 537-539.

Masumoto A, Yamamoto N (1993) Characterization of a hepatocyte growth factor derived from nonparenchymal liver cells. *Cell Structure and Function* 18, 87-94.

Matsumoto T, Kawakami M (1982) The unit-concept of the hepatic parenchyma — a re-examination based on angioarchitectural studies. *Acta Pathologica Japonica* 32, 285-314.

McCuskey (2008) The hepatic microvascular system in health and in response to toxicants. *The Anatomical Record* 291, 661-671.

Porta E, Keopuhiwa L, Joun N, Nitta R (1981) Effects of the type on dietary fat at two levels of vitamin E in Wistar male rats during development and ageing. III. Biochemical and morphometric parameters of the liver. *Mechanisms of Ageing and Development* 15, 297-335.

Reuben A (2004) Prometheus and Pandora - together again. *Hepatology* 39, 1460-1463.

Ries K, Krause P, Solsbacher M, Schwartz P, Unthan-Fechner K, Christ B, Markus PM, Probst I (2000) Elevated expression of hormone-regulated rat hepatocyte functions in a new serum-free hepatocyte-stromal cell coculture model. *In Vitro Cellular & Developmental Biology. Animal* 36, 502-512.

Rojkind M, Philips G, Diehl AM (2011) Microarchitecture of the liver: a jigsaw puzzle. *Journal of Hepatology* 54, 187-188.

Roskams T, Desmet VJ, Verslype C (2007) Development, structure and function of the liver. In: *MacSween's Pathology of the liver, 5th edition* (Burt A, Portmann B, Ferrell L eds), pp. 1-74. Churchill Livingstone Elsevier.

Sonntag EW, Steger RW, Forman JL (1980) Decreased pulsate release of growth hormone in old male rats. *Endocrinology* 107, 1875-1879.

Tateno C, Takai-Kajihara K, Yamasaki C, Sato H, Yoshizato K (2000) Heterogeneity of growth potential of adult rat hepatocytes in vitro. *Hepatology* 31, 65-74.

Tiniakos DG, Kandilis A, Geller SA (2010) Tityus: a forgotten myth of liver regeneration. *Journal of Hepatology* 53, 357-361.

Trujillo E, Vasquez B, Del Sol M (2011) Stereologic characteristics of the liver of rats (*Rattus norvergicus*) submitted to ovariectomy-induced menopause. *International Journal of Morphology* 29, 1470-8.

Villa E (2008) Role of estrogen in liver cancer. *Women's Health* 4, 41-50.

Vollmar B, Menger MD (2009) The hepatic microcirculation: mechanistic contributions and therapeutic targets in liver injury and repair. *Physiology Reviews* 89, 1269-1339.

Vom Saal FS, Finch CE and Nelson JF (1994) Natural history and mechanisms of reproductive aging in humans, laboratory rodents, and other selected vertebrates. In: *Physiology of Reproduction* (Knobil E, Neill JD eds), pp. 1213–1314. Raven Press.

Yasuda M, Shimizu I, Shiba M, Ito S (1999) Suppressive effects of estradiol on dimethylnitrosamine-induced fibrosis of the liver in rats. *Hepatology* 19, 719-727.

Yokoyama Y, Nimura Y, Nagino M, Bland KI, Chaudry IH (2005) Current understanding of gender dimorphism in hepatic pathophysiology. *Journal of Surgical Research* 128, 147-156.

Yokoyama Y, Nagino M, Nimura Y (2007) Which gender is better positioned in the process of liver surgery? Male or female? *Surgery Today* 37, 823-830.

Yokoyama Y, Nagino M, Oda K, Nishio H, Ebata T, Abe T, Igami T, Nimura Y (2008) Sex dimorphism in the outcome of preoperative right portal vein embolization. *Archives of Surgery* 143, 254-259.

Zhou Y, Shimizu I, Lu G, Itonaga M, Okamura Y, Shono M, Honda H, Inoue S, Muramatsu M, Ito S (2001) Hepatic stellate cells contain the functional estrogen receptor beta but not the estrogen receptor alpha in male and female rats. *Biochemical and Biophysical Research Communications* 286, 1059-1065.

Annex 1

For each age group, 3 slides of one animal were randomly selected, in order to determine the distribution of nuclei along the z-axis. For this task, HEP nuclei were counted (*i.e.*, without differentiating MnHEP from BnHEP). In each case, the position in the z-axis was recorded and after counting 1000-1500 nuclei the percentage of nuclei per thickness bin (*i.e*., per fraction of the section thickness) was determined. Considering that the mean section thickness in our material varied from 30.2 μm (CV = 0.02) to 37.4 μm (CV = 0.03), we established eight bins of 4 μm (Figure 6.1). It could be seen that the shallow (0 - 4 μm) and deeper parts (24 - 32 μm) of the sections exhibited less nuclei and this was statistically significant (chi-square test). Therefore, guard heights could be safely applied, and should be used, when counting or sampling liver cells with the optical disector.

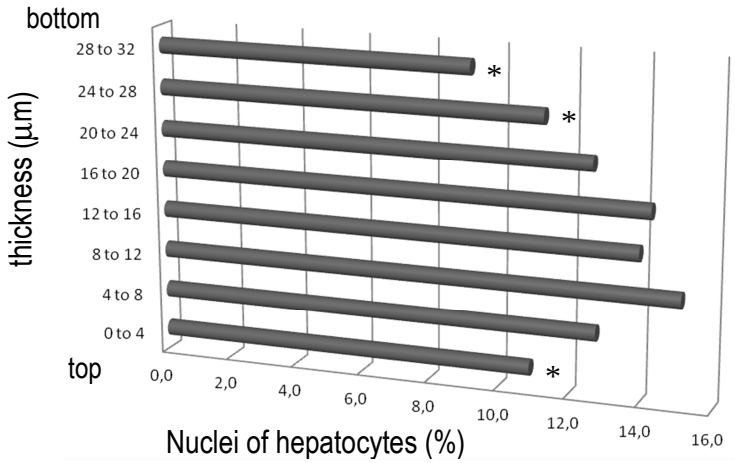

Figure 6.1 – Distribution of the nuclei of hepatocytes along the z-axis in thick paraffin sections of rat liver; (*) $p < 0.05$. (Adapted from *Marcos et al, Journal of Anatomy, 2012.)*

As above mentioned, we opted to evaluate the z-axis distribution of HEP nuclei as a proxy for HSC and KC distribution, because counting 1500 HEP nuclei is much less laborious and faster than counting sinusoidal cells. From our qualitative observations, and our in-house trials, it seems reasonable to extend the conclusions drawn from HEP to other liver cell types (namely to HSC and KC).